

UNIVERSITY OF ALBERTA LIBRARY



0 0000 2548 964

EXTENDED ABSTRACTS

OF PAPERS

INTERNATIONAL CONFERENCE ON KIMBERLITES

University of Cape Town

Rondebosch, Cape

South Africa

16th Sept. — 8th Oct. 1973

Ex LIBRIS
UNIVERSITATIS
ALBERTAEANAE





Digitized by the Internet Archive
in 2018 with funding from
University of Alberta Libraries

<https://archive.org/details/internationalcon01inte>

EXTENDED ABSTRACTS

OF PAPERS

INTERNATIONAL CONFERENCE ON KIMBERLITES

Editorial Committee

Prof L.H. Ahrens
Dr. J.B. Dawson
Dr. A.R. Duncan

Dr. A.J. Erlank



C O N T E N T S

Authors are listed alphabetically:

	<i>Page</i>
AKIMOTO, S and SATO, Y.	1
ALLSOPP, H.L. and WELKE, H.J.	5
ANDERSON, O.L. and PERKINS, P.C.	7
ANDREWS, J.R. and EMELEUS, C.H.	11
BARDET, M.G.	15
BARRETT, D.R.	19
BARRETT, D.R. and ALLSOPP, H.L.	23
BARRETT, D.R. and BERG, W.	27
BERG, W. and O'HARA, M.J.	31
BOETTCHER, A.L., MYSEN, B.O. and MODRESKI, P.J.	35
BORLEY, G.D. and SUDDABY, P.	39
BOULLIER, A. and NICOLAS, A.	43
BOYD, J.R. and NIXON, P.H. (1)	47
BOYD, J.R. and NIXON, P.H. (2)	51
BRAVO, M.S. and O'HARA, M.J.	55
CARSWELL, D.A.	59
CLARKE, D.B. and MITCHELL, R.H.	63
CLEMENT, C.R.	67
CORNELISSEN, A.K. and VERWOERD, W.J.	71
COX, G., GURNEY, J.J. and HARTE, B.	75
DANCHIN, R.V., FERGUSON, J., McIVER, J.R. and NIXON, P.H.	77
DAWSON, J.B. and SMITH, J.V. (1)	81
DAWSON, J.B. and SMITH, J.V. (2)	83
DEINES, P. and GOLD, D.P.	85
DICKEY, J.S. and OBATA, M.	89
DONALDSON, C., REID, A.M., RIDLEY, W.I., BROWN, R.W. and DAWSON, J.B.	93
EGGLER, D.H.	95
EMELEUS, C.H. and ANDREWS, J.R.	99
ERLANK, A.J.	103
FERGUSON, J., MARTIN, H., NICOLAYSEN, L.O. and DANCHIN, R.V.	107
FESQ, H.W., BIBBY, D.M., ERASMUS, C.S., KABLE, E.J.D. and SELLSCOP, J.P.F.	111
FESQ, H.W., KABLE, E.J.D. and GURNEY, J.J.	115

FRICK, C.	119
GERINGER, G.J.	123
GITTINS, J., HEWINS, R.H. and LAURIN, A.F.	127
GOLD, D.P.	131
GRIFFIN, W.L. and TAYLOR, P.N.	135
GURNEY, J.J., HARTE, B. and COX, K.G.	139
GURNEY, J.J. and HOBBS, J.B.M.	143
HAGGERTY, S.E.	147
HARRIS, J.W., HAWTHORNE, J.B., OOSTERVELD, M.M. and WEHMEYER, E.	150
HARTE, B., COX, K.G. and GURNEY, J.J.	155
HARTE, B. and GURNEY, J.J.	159
HAWTHORNE, J.B.	163
HEARN, B.C. and BOYD, F.R.	167
HELMSTAEDT, H. and DOIG, R.	171
HOWELLS, S., BEGG, C. and O'HARA, M.J.	173
JANSE, A.J.A.	177
JOHNSTON, J.L.	181
KABLE, E.J.D., FESQ, H.W. and GURNEY, J.J.	185
KLEEMAN, J.D. and LOVERING, J.F.	189
KRESTON, P.	191
LAPPIN, M.A. and DAWSON, J.B.	195
LLOYD, F.E. and BAILEY, D.K.	199
LORENZ, V.	203
MacGREGOR, I.D.	207
MATHUR, S.M.	211
McCALLISTER, R.H., MEYER, H.O.A. and BROOKINS, D.G.	213
McCALLUM, M.E., EGGLER, D.H. and BURNS, L.K.	217
McFADDEN, P.L.	221
MEYER, H.O.A. and SVISERO, D.P.	225
MILASHEV, V.A.	229
MITCHELL, R.H.	231
MITCHELL, R.H. and BRUNFELT, A.O.	235
MOORE, A.E.	239
NIXON, P.H. and BOYD, F.R.	243
O'HARA, M.J. (1)	247
O'HARA, M.J. (2)	251
O'HARA, M.J. (3)	255

O'HARA, M.J., SAUNDERS, M.J. and MERCY, E.L.P.	259
O'HARA, M.J., SAUNDERS, M.J. and MERCY, E.L.P.	263
PRINZ, M., MANSON, D.V., HLAVA, P.F. and KEIL, K.	267
REID, A.M., BROWN, R.W., DAWSON, J.B., WHITFIELD, G.G. and SIEBERT, T.C.	271
REID, A.M., RIDLEY, W.I., DONALDSON, C., BROWN, R.W. and DAWSON, J.B.	273
RHODES, J.M. and DAWSON, J.B.	275
RIDLEY, W.I. and DAWSON, J.B.	277
ROBINSON, D.N.	279
SHEPPARD, S.M.F. and DAWSON, J.B.	283
SHIMIZU, N.	287
SMITH, J.V., DAWSON, J.B. and BISHOP, F.C.	291
SUDDABY, P.	295
SUWA, K., OANA, S., WADA, H. and OSAKI, S.	297
SUWA, K., YUSA, Y., and KISHIDA, N.	301
WATSON, K.D.	305
WHITE, A.J.R. and TAYLOR, S.R.	309
WHITFIELD, G.G. (1)	313
WHITFIELD, G.G. (2)	317
WILSHIRE, H.G. and SHERVAIS, J.W.	321
WOOLSEY, T.S., McCALLUM, M.E. and SCHUMM, S.A.	325
YODER, H.S.	329

VERIFICATION OF THE STABILITY OF THE MODIFIED
SPINEL BY MEANS OF HIGH-PRESSURE AND HIGH-
TEMPERATURE X-RAY ANALYSIS

Syun-iti AKIMOTO and Yosiko SATO

Institute for Solid State Physics,
University of Tokyo, Tokyo 106

Modified spinel (β -phase), a high-pressure polymorph of olivine, has hitherto been found in Mn_2GeO_4 (1), Co_2SiO_4 (2), Zn_2SiO_4 (3) as well as in the magnesium rich side of the Mg_2SiO_4 - Fe_2SiO_4 system(4), (5). Since $(Mg,Fe)_2SiO_4$ olivine is believed to be the most abundant minerals in the upper mantle, the stability of the modified spinel phase is greatly relevant to the phase changes in the mantle.

Structure analysis(6) carried out on the single crystals of βMn_2GeO_4 and βCo_2SiO_4 revealed that the oxygen atoms in the modified spinel are approximately in cubic close packing as in normal spinel. The modified spinel, however, partly violates Pauling's electrostatic valence rule : Two GeO_4 or SiO_4 tetrahedra, which would be isolated in the normal spinel structure, share one of their oxygen atoms resulting in a Ge_2O_7 or Si_2O_7 group and an oxygen atom not bonded to any Ge or Si atom. It was further shown that the structure of the modified spinel phase of Co_2SiO_4 could be derived from the normal spinel structure of γCo_2SiO_4 by displacing four Si and four Co atoms out of the eight Si and sixteen Co atoms in the cell. These particularities of the crystal structure aroused much discussion on the stability of the modified spinel. Since all the modified spinel phases have been obtained as quench products, the possibility of the metastable phase, which would be produced during quenching of an original normal spinel, has not yet been completely denied.

In the present investigation, stability of the modified spinel was examined *in situ* by a high-pressure and high-temperature X-ray diffraction technique. A cubic anvil type of high pressure apparatus was used. The pressure cell attached to the 250-ton uniaxial hydraulic ram is designed so as to converge the six cemented tungsten carbide anvils with square face of 4mm edge length towards the center of the cubic pressure medium. Amorphous boron mixed with polyester resin in the ratio of boron/resin = 1/2 (in weight) was used as a pressure medium.

Powder samples of αMn_2GeO_4 with olivine structure was shaped into a thin plate with thickness of 0.1 - 0.2 mm and sandwiched by boron nitride blocks and settled into the center hole of the pressure medium with 6 mm edge length. A pair of stainless steel disk heater 0.05 mm in thickness and 2.5 mm in diameter was used as a high-temperature furnace. D. C. power was supplied to the heater through Au electrodes which were faced to one pair of cubic anvils. Temperature was measured with Pt/Pt-Rh13% thermocouple which was placed in the upper part of the furnace not to screen the X-ray path.

Thermocouple leads were brought out to the faces of another pair of anvils, which were insulated electrically from the anvil pair used for D.C. power supply.

Samples in the pressure medium were first subjected to the desired pressure and then heated to the desired temperature. Pressure values are calibrated at room temperature on the basis of the volume change of NaCl using the same pressure medium. Phase change of the sample was detected by the X-ray diffraction method.

A finely collimated molybdenum X-ray beam was entered through the gap of the two cubic anvils, and the X-ray diffracted by the sample was passed through the opposite gap of the anvils. The diffracted X-rays were measured in fixed-time step-scanning method using a scintillation counter. The angle width of one step was 0.1° and the fixed time for one-step was controlled in the range from 40 seconds to 200 seconds depending upon the gap width of anvils.

Examples of the X-ray diffraction pattern obtained in the present investigation are shown in Figs.1 and 2. Fig.1 shows the diffraction pattern of $\alpha\text{Mn}_2\text{GeO}_4$ at 45 kbar and at room temperature. The very strong peak of the (002) line of boron nitride masked the (130) line of $\alpha\text{Mn}_2\text{GeO}_4$ with olivine structure. 2θ angles of $\alpha\text{-Mn}_2\text{GeO}_4$ at atmospheric pressure and at room temperature are shown by black arrows. No diffraction peaks assigned to the modified spinel were observed. Fig.2 shows the diffraction pattern at 45 kbar and at 780°C . The diffraction line (002) of boron nitride moved remarkably to the lower angle side owing to the effect of the thermal expansion. White arrows in the figure indicate the 2θ angle to be observed on the $\beta\text{-Mn}_2\text{GeO}_4$ with the modified spinel structure at atmospheric pressure and at room temperature. Diffraction peaks assigned to the modified spinel structure are easily distinguished in the figure.

Akimoto, and Sato

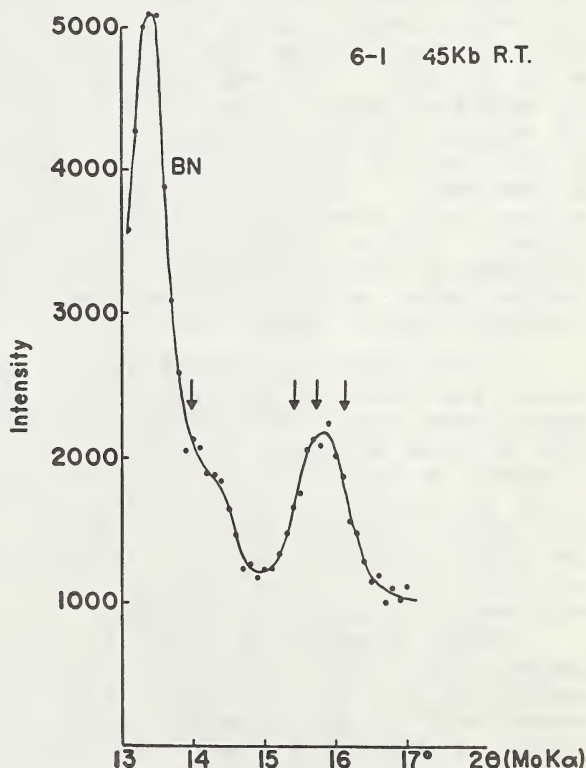


Fig. 1
X-ray diffraction pattern of Mn_2GeO_4 at 45 kbar and at room temperature.

The appearance of the diffraction line (112) of $\beta\text{Mn}_2\text{GeO}_4$ is most remarkable. Comparing Fig.1 with Fig.2, we can surely say that the $\beta\text{Mn}_2\text{GeO}_4$ with the modified spinel structure really exists as a stable phase at 45 kbar and at 780°C. The present results harmonize well with a previous study of the high-pressure and high-temperature stability diagram (Fig.3) of Mn_2GeO_4 which was determined using the usual quenching method.(1)

It was established through the present investigation that the modified spinel structure can exist stably as a high-pressure and high-temperature phase of olivine. It is plausible to conclude that in the earth's mantle the $(\text{Mg}, \text{Fe})_2\text{SiO}_4$ olivine transforms to the modified spinel phase in the first step of its phase change and this phase transformation corresponds to the rapid increase of seismic wave velocities at a depth near 400 km.

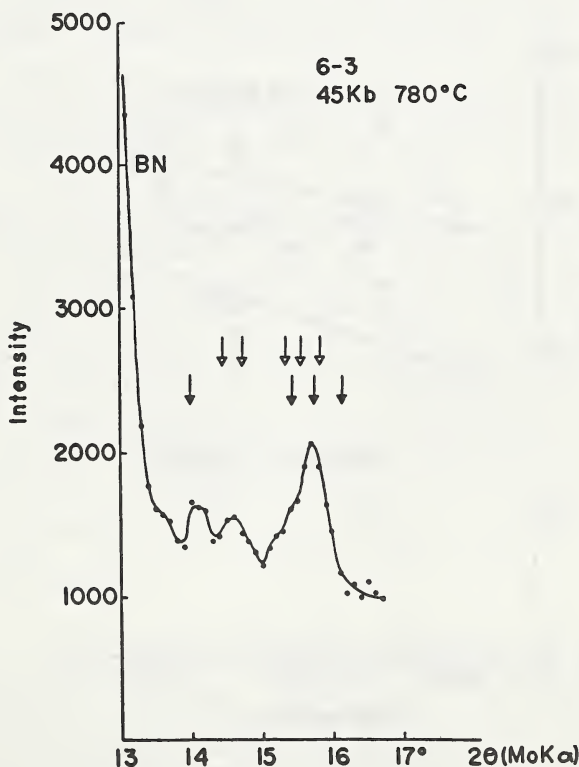


Fig. 2
X-ray diffraction pattern of Mn_2GeO_4
at 45 kbar and at 780°C.

References

- (1) Akimoto,S. (1970) Phys. Earth Planet. Interiors 3, 189.
- (2) Akimoto,S. and Y.Sato (1968) Phys. Earth Planet. Interiors 1, 498.
- (3) Syono, Y., S.Akimoto, and Y.Matsui (1971) J. Sol. State Chem. 3, 369.
- (4) Ringwood,A.E. and A.Major (1970) Phys. Earth Planet. Interiors 3, 89.
- (5) Akimoto,S. (1972) Tectonophys., 13, 161.
- (6) Morimoto,N., S.Akimoto, K.Koto and M.Tokonami (1970) Phys. Earth Planet. Interiors 3, 161.

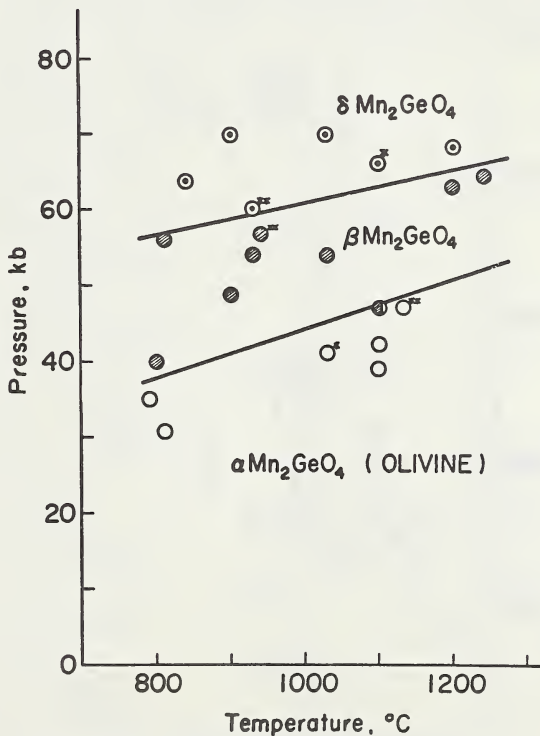


Fig. 3

Stability diagram for the high-pressure and high-temperature transformations of Mn_2GeO_4 (1)

K, RB, U, SR AND PB IN DIAMONDS CONTAINING INCLUSIONS

H.L. Allsopp and H.J. Welke

Bernard Price Institute of Geophysical Research,
University of the Witwatersrand, Johannesburg.

The determinations of the Pb- and Sr-isotopic compositions of syn-genetic inclusions contained in diamonds is potentially useful because:

- (i) the masking effect of crustal contamination (which is a serious limitation in the study of kimberlites and nodules) can be overcome by preliminary strong acid treatment of the diamonds.
- (ii) diamonds containing significant amounts of Pb (e.g. those with sulphide inclusions) should have Pb-isotopic compositions lying on a primary Pb growth curve. Should this be the case it will be possible to test the accuracy of assumed U/Pb (μ) ratios for the mantle, and to estimate the age of particular diamonds.
- (iii) diamonds containing significant amounts of Sr (e.g. those with diopside inclusions) will allow of a better assessment of Sr-isotopic evolution models for the mantle-crust system.

With a view to assessing the feasibility of such measurements three batches of diamonds were obtained. The first (with mainly graphite inclusions) was used to test the method, and no results are reported. The second and third batches, both from the Premier Mine, contained green (mainly diopside) and black (mainly graphite and sulphide) inclusions respectively. The weights of the diamonds were 0.27 and 0.32 gm. respectively, and the stones ranged in size from 1 - 2 mm. The diamonds were placed in a covered quartz crucible and burnt at $\sim 850^{\circ}\text{C}$ in an oxygen atmosphere. The residues were dissolved in a teflon autoclave, and the resulting solutions aliquoted for the separate analyses. Concentrations of K, Rb, Sr, U and Pb were measured by isotope dilution, and special reagents were prepared to ensure that the blank concentration for these elements (except K) was in the sub-nanogram range. Pb- and Sr-isotopic compositions were measured on tracer-free aliquots.

In the results summarised below the weights are given in nanograms (gm. $\times 10^{-9}$), and the figures in brackets are the blanks expressed as percentages of the total. The $\text{Sr}^{87}/\text{Sr}^{86}$, $\text{Pb}^{206}/\text{Pb}^{204}$ and $\text{Pb}^{207}/\text{Pb}^{204}$ ratios are initial ratios, i.e. correction has been made for the radiogenic component using an assumed age of 1250 m.y. Correction has also been made for mass-spectrometer fractionation and blanks.

"Green" diamonds

<u>K</u>	<u>Rb</u>	<u>K/Rb</u>	<u>Sr</u>	<u>Sr</u> ⁸⁷ / <u>Sr</u> ⁸⁶
599 (6.8%)	2.87 (4.1%)	204	59.9 (0.9%)	0.7029 \pm .0007

"Black" diamonds

<u>Pb</u>	<u>U</u>	<u>Pb</u> ²⁰⁶ <u>Pb</u> ²⁰⁴	<u>Pb</u> ²⁰⁷ <u>Pb</u> ²⁰⁴
40.2 (32.0%)	1.53 (25%)	16.32 \pm .06	15.58 \pm .05

The accuracy of the concentration measurements is limited by the level of the blanks. The effect of the reagent-blank, as distinct from the full experiment blank, was small in all cases except U, for which the inclusion concentration was very low. The Pb experiment blank was particularly large; the source of the contamination is unknown, but is thought to be the quartz crucible.

The accuracy of the isotopic ratio measurements was severely limited by mass-spectrometer sensitivity. In the case of Pb, for which there is a large blank correction, an approximate measurement was made of the isotopic composition of the contaminating Pb.

The Pb isotopic composition indicates a μ value of the source region of about 9.0 and a Pb-model age in reasonable agreement with the age of the Premier pipe. The Sr isotopic composition falls on the same trend as that of fresh kimberlites, and the K/Rb ratio of ~ 200 is approximately the same as that for peridotite nodule diopsides, but much lower than that of eclogite nodule omphacites.

The main purpose of this work was to establish the levels of concentration of the above elements in diamonds with inclusions, and to make a preliminary estimate of the Sr- and Pb-isotope ratios. It is concluded that with improved apparatus it will be possible to make precise measurements of the parameters discussed.

A PLATE TECTONICS MODEL INVOLVING NON-LAMINAR ASTHENOSPHERIC FLOW TO ACCOUNT FOR CERTAIN KIMBERLITE PIPES

Orson L. Anderson
Priscilla C. Perkins

Institute of Geophysics and Planetary Physics
University of California, Los Angeles 90024

The Colorado Plateau is an anomalous region of uplift in the North American Plate which is pierced by Cenozoic kimberlite pipes containing eclogites which do not correspond to the eclogites normally found in kimberlite pipes (Helmstaedt et al., 1972). The cause of uplift of the Plateau and the pattern of magmatism exposed there have remained unexplained by the theory of plate tectonics. Also unexplained is the mechanism for concentration of volatiles in the mantle which is generally agreed to have been a necessary prerequisite for kimberlite and carbonatite eruption of material from the deeper mantle beneath the Plateau (Watson, 1967; McGetchin, 1968). McGetchin et al. (1973, p.1867) state that "the ultimate source of these volatiles is both unknown and of great significance...The details of the occurrence and the mobility of the mantle volatiles are important and interesting questions because they bear on the outgassing of the earth, petrogenesis of basalt and kimberlite, and the physical state of the upper mantle."

In this paper we introduce an extension of plate tectonics theory to account for the almost random nature of magmatism in this region (which greatly contrasts with a simple pattern of magmatic transgression in time which would have been predicted as a consequence of overriding of the Pacific Plate in Mesozoic and Cenozoic time). The mechanism represents a means by which deep material can be brought from considerable depths in the mantle to higher levels where accumulation of volatiles could trigger kimberlite eruptions.

Gilluly (1970) has emphasized the difficulties in explaining the structural and magmatic history of the southwestern United States by a conventional plate tectonics model. As he indicates, "it can be safely inferred from the distribution of Cenozoic volcanism that there are great local variations in temperature, and hence, plasticity, of both crust and mantle" (Gilluly, 1970, p. 53) in the western United States. He notes that in this region, "the continental crust varies dramatically in thickness and elastic properties from place to place...The upper mantle, too, varies greatly in elastic properties" (Gilluly, 1970, p. 67).

Sbar and Sykes (1973, p. 1878) report that at the present time, the Colorado Plateau is "a region of east-west compressional stress" between two regions of extension, the Rio Grande Graben and the Intermountain Seismic Belt. The presence of an uplifted plateau in compression, surrounded by zones of extension, has been attributed to "convective flow in the asthenosphere in which upwelling occurs beneath two zones of extension" or, alternatively, to "a number of mantle plumes as proposed by Morgan (1972), or a single major current" (Sbar and Sykes, 1973, p. 1878). Wilson (1972, p. 91) also postulated the existence of a mantle plume beneath the Colorado Plateau.

Gilluly (1973, p. 509) suggested that "differences in depth and configuration of the decoupling zone beneath the drifting continent would tend to cause flowage within the crust and upper mantle, first in one direction and then in another." He notes that "the youngest magmatism has been in the western Cordillera, not the eastern... while tectonism has indeed migrated eastward in the eastern Cordillera, it migrated westward in the western part and is now most active there" (Gilluly, 1973, p. 507).

Radiometric ages of igneous rocks plotted by Armstrong and Higgins (1973, Figs. 2-3) and Armstrong and Suppe 1973, Fig. 2) show irregular patterns in time for magmatic activity in the western United States. The distribution of volcanism and plutonism during the Cretaceous, and the existence of paired metamorphic belts in the western part of the plate are more easily explained by plate tectonics theory. The onset of anomalous magmatic patterns may have coincided with the cessation of subduction of the Farallon Plate and the overriding of a Pacific ridge system.

The regional geology is difficult to reconcile with fluid dynamic models of mantle motion for regions in the neighborhood of Benioff zones. The geological evidence demands a process which produced random effects in time and space in the lithospheric plates which resulted from some irregularities imposed on steady laminar flow in the asthenosphere.

While the value for viscosity for mantle material is not agreed upon, it is generally recognized that the Reynolds number must be very small so that laminar flow would be expected. Laminar and highly viscous flow imply that flow streamlines would be expected to conform faithfully to the geometry of lithospheric boundaries. Induced flow from the downgoing slab might possibly cause stress variations along the lithospheric boundaries, or eddies away from the boundaries, but it is difficult to predict from fluid dynamic theories any variations in motion "first in one direction and then in another" as suggested by Gilluly (1973, p. 509). It is likely that volatiles rising through a moving

mantle would have a large component of drift in the direction of flow near the lithosphere-asthenosphere boundary.

The irregular flow patterns deduced from southwest U.S. and Colorado Plateau regional geology are at odds with regular unidirectional patterns expected from fluid dynamics in the context of plate tectonics. We propose a solution to this discrepancy by consideration of a special case of fluid dynamic flow near plate boundaries. The required dynamic mechanism must produce irregular patterns in the surface manifestations of the flow proceeding in the corner between the overriding plate and the downgoing slab. The flow mechanism must account for several features: irregular distribution of magmatic activity in space and time; the presence of alternating zones of compression and extension in the lithosphere (uplift in one region, crustal thinning and extension in an adjacent region); great irregularities in plate thickness; and great areal variations in gravity and mechanical properties of the plate. This desired special fluid dynamic mechanism need not be invoked at most plate boundaries where magmatism and tectonism are in harmony with anticipated flow patterns in the asthenosphere.

It seems to us that the geology of the southwestern U.S. implies that there have been several regions of reverse flow near the lithosphere-asthenosphere boundary. In fluid dynamic theory, reverse flow at a boundary is often correlated with the onset of turbulence which produces eddies, but we are not suggesting the existence of turbulence in the mantle. The mechanism of reverse flow is produced by changes in the pressure gradient along the boundary; we believe that reverse flow occurs where the pressure gradient along the boundary is such that there is a pressure increase in the direction of flow of sufficient magnitude to overcome inertial and viscous forces. We propose that the overriding of a ridge system and the establishment of the San Andreas fault boundary for the North American plate (Atwater, 1970) caused a pressure gradient to be created in early Mesozoic time. We postulate that the pressure gradient was positive from east to west and that it caused several regions of reverse flow to develop near the lithosphere-asthenosphere boundary under what is now the southwestern U.S. This phenomenon caused surges of mantle material which not only induced regions of reversed flow along the boundary, but also promoted upwelling of material drawn from deep within the asthenosphere under the Colorado Plateau. This mechanism could provide an alternative to the plume under the Plateau proposed by Wilson (1972, p. 91). With this model, we can account for the movement of material upward from the deeper mantle to give rise to kimberlite and carbonatite intrusion. Several regions of reverse flow could also account for the complicated structural and magmatic patterns described by Gilluly.

The relaxation time of flow in the mantle material is

apparently so large that this flow probably persisted millions of years after the Farallon Plate was consumed. An upward surge could be responsible, in our view, for the existence of the "crust-mantle mix" of Cook (1962) as well as the surface manifestations summarized by Gilluly and by Armstrong. The surge could be responsible for the transport of source material for the kimberlite pipes in southern Utah and northern Arizona.

The idea for the existence of surges of mantle material came from examination of the flow streamlines in photographs of the Susitna and Malaspina Glaciers of Alaska (Post and LaChapelle, 1971). Glacier ice has a very high viscosity (10^{13} poise) and a very low Reynolds number. The creep law of ice (Weertman, 1973, p.292, Eq.10) has a relationship between strain rate and stress which functionally resembles the creep law for dunite (Stocker and Ashby, 1973, p. 405, Fig.5) and presumably the creep laws for other mantle material. Experiments under the physical conditions presently achieved show that glacier ice and olivine both greatly depart from Newtonian creep. It seems reasonable, therefore, that if reverse flow can occasionally occur at the boundaries of glaciers, it should be possible for reverse flow to occur occasionally near the boundary between the lithosphere and the asthenosphere. Reverse flow in the mantle would be a rare phenomenon because establishment of an adverse pressure gradient would only be the product of unusual circumstances.

ARMSTRONG and HIGGINS, 1973, Bull. Geol. Soc. Amer. 84, 1095-1100.

ARMSTRONG and SUPPE, 1973, Bull. Geol. Soc. Amer. 84, 1375-1393.

ATWATER, 1970, Bull. Geol. Soc. Amer. 81, 3513-3536.

COOK, 1962, in Advances in Geophysics, 9, 295-360.

GILLULY, 1970, in The Megatectonics of Continents and Oceans, 47-73.

GILLULY, 1973, Bull. Geol. Soc. Amer. 84, 499-514.

HELMSTAEDT, ANDERSON, and GAVASCI, 1972, J. Geophys. Res. 77, 4350-4365.

McGETCHIN, 1968, The Moses Rock Dike, Ph.D. Dissertation, Caltech, 405p.

McGETCHIN, NIKHANJ, and CHODOS, 1973, J. Geophys. Res. 78, 1854-1869.

MORGAN, 1972, Bull. Am. Assoc. Pet. Geol. 56, 203-213.

POST and LaCHAPELLE, 1971, Glacier Ice, 111p.

SBAR and SYKES, 1973, Bull. Geol. Soc. Amer. 84, 1861-1882.

STOCKER and ASHBY, 1973, Rev. Geophys. 11, 391-426.

WATSON, 1967, in Ultramafic and Related Rocks, 261-268.

WEERTMAN, 1972, Rev. Geophys. 10, 287-333.

WILSON, 1972, in The Upper Mantle, 73-94.

STRUCTURAL ASPECTS OF KIMBERLITE DYKE AND SHEET INTRUSION
IN SOUTH-WEST GREENLAND.

by

James R. Andrews¹ & C.H. Emeleus²

1 - Department of Geology, University College, Belfield,
Dublin 4, Ireland

2 - Department of Geological Sciences, University of Durham,
South Road, Durham DH1 3LE.

Field relationships of kimberlites have been extensively examined since their first reported occurrence (Andrews & Emeleus, 1971). Three localities, Nigerdlikasik, Midtneraes and Pyramidefjeld, were revisited in Summer 1971 and approximately 20 km (along strike) of outcrop remapped.

Field Relationships

(a) Nigerdlikasik. Kimberlite intrusion as a narrow dyke of rather constant thickness and trend took place at an oblique angle to a strong regional fabric in inhomogeneous Archaean gneisses. Throughout a total length of outcrop exceeding 3000 m en - echelon replacement takes place at 700 - 800 m intervals with a consistent dextral offset of 20 - 50 m. Closely spaced parallel jointing is a conspicuous feature of the host rock over a zone commonly 5 - 10 m wide, about ten times the width of the dyke. Selective erosion has developed shallow gullies commonly filled with rubbly pieces of grandioritic gneiss, obscuring the kimberlite which may occupy anywhere between the axial zone and margins and frequently lies along one margin.

(b) Pyramidefjeld. Kimberlite sheets occupy parts of the Precambrian Pyramidefjeld granite complex at various levels between 400 and 900 m, sometimes extending beyond the granite contact into the host Archaean gneisses. Three distinct systems of interconnected sills can be outlined by stratum contours in the north (Vestvoldgrav - Østvoldgrav), north-central (Safirsø - Blokpas) and south-east (Grydesø) areas of granite. Sheets overlooking Vestvoldgrav and Østvoldgrav dip north at 10 - 20 degrees outcropping between 700 and 800 m. Sheets on the south-east side of Safirsø dip gently south-east and outcrop at a lower level along the north-east side of Blokpas, a valley running between the two granites which make up the complex. Around Grydesø at least five different levels with 20 - 50 m intervals are developed with gentle northerly dips which bring the highest level underground at the northern end of the lake. The lowest level extends at least 1 km beyond the granite contact. The granite around most sheets is invariably well jointed parallel to the intrusion margins in the manner of the Nigerdlikasik dyke. The tendency for the sheets to erode into the granite giving rise to small caves and rock shelters has resulted in large collapse structures, especially where the jointing is very closely spaced. Ice action has exaggerated the effect by producing bench features sometimes 20 - 30 m wide. Not all shatter zones and bench features are accompanied by kimberlite and some contain sheets

only 10 mm thick. En - echelon relationships are so common that it is rarely able to follow one intrusion more than 100 m before it dies out and some sheets expand and contract rapidly to give the bodies a very laccolithic profile.

(c) Midternaes. Kimberlite sheets generally dip westward rising from sea level at Sioralik glacier to almost 600 m in the high ground to the north-east. The intrusion pass upwards through Archaean gneisses and across an unconformity into a Proterozoic supracrustal succession. The planar foliation in the gneisses and well developed bedding surfaces in the supracrustal rocks have little or no influence on the attitude of the sheets which higher in the succession cut across bedding at very acute angles. The massive basement gneisses and supracrustal rocks where they are tightly folded and indurated develop the characteristic well jointed or shattered aspect familiar in the Pyramidefjeld complex.

Mechanism of intrusion

Kimberlites in all three localities were intruded along zones of pronounced platy jointing. Similar features have also been noted in granite host rock to the Kisirisills in Tanzania (Williams, 1939) though they have evidently not been readily recognised in association with other kimberlite sills (Hawthorne, 1968). As the zones occur only in association with kimberlites, development of the jointing must have immediately preceeded the kimberlite magma: the sheets themselves are massive and occasionally follow irregular paths through the shattered rocks. Internal calcite-filled fractures developed as the magma consolidated and are a consequence of shrinkage accompanying crystallisation. The volatile rich nature of kimberlites suggests that the magma was accompanied by massive gas emanations which preceeded the magma and were instrumental in leading to the brittle failure of the host rocks. These gases are thought to have passed along those parts of well jointed zones which are barren or almost barren of kimberlite for short distances along strike. Evidence of volatile activity occurs on Midternaes where metasomatism from kimberlitic fluids has completely calcified a siltstone member of the supracrustal succession for up to 2 m from the contact. The process is confined to a zone beneath a thick gabbro sill indicating that the massive impermeable sheet has acted as a confining cap rock. Along strike where the kimberlite cuts the lower part of the gabbro the latter is anastomized by a network of calcite veins.

Once the way had been opened by brittle failure of the host rocks emplacement of the kimberlite magma took place very rapidly, though not explosively as very few xenoliths of local rock types have been found. Though thermal contact effects are virtually absent there has been small scale mechanical shattering of the granite and gneisses extending only for a few millimetres. Nodules with high-pressure pyrope-garnet are preserved in many places and rounded lower-crustal xenoliths with pyroxene-granulite facies mineralogy have not been recrystallised. Rapid lateral movement of magma carried the dense peridotite xenoliths to most parts of the sheet systems. Xenocryst-bearing kimberlite penetrates the finest channels with some nodules lodged in passages barely wider than the nodule diameters. When the magma stopped moving, peridotite xenoliths in the sheets sank to the bottom resulting in dense concentrations of nodules

superficially resembling conglomerates. Later pulses of magma followed along or within the first sheets which accumulated up to two or three layers of sedimented xenoliths. Rarely the later kimberlite takes a different path and becomes separated from the earlier sheets by thin screens of host rock. These features together with some size sorting of crystals suggest a very fluid magma with little variation in magma viscosity. There is no evidence of any pipes or other forms of blowout to suggest that the kimberlites ever reached the open surface.

Structural control of dyke and sill intrusion

The overall pattern of kimberlite intrusion reveals a complete disregard for preferential planes of weakness in gneisses and supracrustal rocks, splendidly displayed on Midternaes. Structural control is ascribed not to pre-existing inhomogeneties in the host rocks but to the prevailing external stress field. Following Anderson (1951) sills are intruded under conditions of horizontal compression and dykes under horizontal tension. Theoretically the alternating stress conditions necessary to explain both kimberlite dykes and sills can be brought about by major crustal flexures (Sanford, 1959) such that sills intrusion would occur within regions of downward displacement and dyke intrusion within regions of elevation. These conditions were probably realised at the time of kimberlite emplacement, at some time during the early Mesozoic (Andrews & Emeleus, 1971), since the early stages of continental rifting between Greenland and Canada were then taking place. Graben formation in northern West Greenland during the Cretaceous is documented by Rozenkrantz and Pulvertaft (1969) and probably followed a period of updoming similar to that over the East African rift system. Conditions would be created for dyke intrusion on the margins. A coast - parallel Jurassic dolerite dyke swarm flanking the coastal strip of S.W. Greenland (Watt, 1969) supports the early development of axial doming: fringe members of this swarm straddle the Nigerdlikasik dyke. Dolerite dykes do not extend as far inland as Pyramidefjeld and Midternaes, areas marginal to the Inland Ice, and kimberlite sill intrusion took place under horizontal compression.

References

Anderson, E.M., 1951 The dynamics of faulting. 2nd ed. Oliver & Boyd, Edinb.

Andrews, J.R. & Emeleus, C.H. 1971 Rept Grønlands geol.Unders., 31.

Hawthorne, J.B. 1968 Trans.geol.Soc. S.Africa, LXXI, 291-311.

Rozenkrantz, A. & Pulvertaft, T.C.R. 1969 Mem.Amer.Assoc.Petroleum Geologists, 12, 883-898.

Sanford, A.R. 1959 Bull. geol. Soc. Amer., 70, 19-.

Watt, W.S., 1969 Can.J.Earth. Sci., 6, 1320-1321.

Williams, G.J., 1939 The kimberlite province and associated diamond deposits of Tanganyika Territory. Dpt. of Land and Mines, Geol. div., Tanganyika Govt. Printer, Dar-es-Salaam, 41p.

M E T A K I M B E R L I T E S

M.G. BARDET

Consulting Geologist, BRGM

26, rue Jean Giraudoux - PARIS - 16e

The petrographic features of all Kimberlites are the same all over the world, and independantly of their age : Precambrian Premier kimberlite, Paleozoic ones from Yakutia or the Cretaceous kimberlites from everywhere are similar. Yet, during the last years, some rather deceiving Precambrian kimberlites had been found near Seguela (Ivory Coast), and Mitzic, (Gabon), which I propose to call "Metakimberlites" to distinguish them, for their unusual features, from the "classic" kimberlites. Their macroscopic aspect is different as they often look like talcschists or micaschists. They occur always in the form of dykes and are completely devoid of picroilmenite and pyrope, though diamond-bearing and sometimes very rich. One particularity is the relative abundance of spinels : ferromagnesian or chrome spinels at Seguela, chromite spinel in Gabon. They mineralize the alluvia in their vicinity and the subordinate drainage. Autometasomatism and perhaps dynamometamorphism in Gabon had completely transformed the original lamprophyric kimberlites into a kind of micaceous soapstone, and a late highly potassic phase is obvious at Seguela where fenitization occurs in the granitic walls, and sometimes a strange association with rare fitzroyite leucite rocks.

Seguela "metakimberlites"

In the center of Ivory Coast, the Seguela alluvial diamond field which produced about 2 M ct derives from two main dykes systems, Toubabouko and Bobi.

The Toubabouko dyke, about one meter wide with a general N or NNW strike (a Precambrian direction) is more or less known along several kilometers and is intrusive in a Precambrian (1900 m.y) granite. The kimberlitic fabric of the soft rock is hardly seen as the olivine nodules are completely transformed into talc, with some calcite, and serpentine quite subordinate. There is much phlogopite ; picroilmenite and pyrope are absent or the former has been leucoxenized and very fine. Apatite, zircon, magnetite can be seen, and an unusual Mn-Illmenite (Pyrophanite), with traces of galena, sphalerite and scheelite, and.. diamond. Sometimes there is a marked fenitization of the granitic wall which, over a foot or more is transformed into a hyperalcaline syenite with high K₂O. Chloritization, epidotization and hematization penetrates some meters deeper. At depth chloritization is more pronounced, but I do not think like KNOPF that this transformation result from the action of meteoric water but of metasomatism.

Bobi dykes

Ten miles to the East the thin, but very rich, Bobi dykes are inti-

mately associated with lodes of a barren lamproïte, which is more exactly a fitzroyite. Those very peculiar and rare leucitic volcanic rocks were described by WADE & PRIDER (1929) in Western Australia and are kin to the wyomingites of USA and jumillites of Spain. They are rich in Ba, Sr, Zr (sometimes Nb) like kimberlites, and Ti, K₂O (10 %), with low Na₂O. According to a study by the Overseas Geolo. Survey the Bobi lamproïte contains, in 37 % groundmass (phlogopite, leucite, chlorite and SiO₂), 19 % of altered leucite crystals, 24 % of phlogopite, 10 % of anatase, 4 % of apatite etc. Chemical analysis is very close to that of PRIDER fitzroyite. It is interesting to note that this geologist had proposed a similar origin for kimberlites and fitzroyites, from a micaceous peridotitic magma, enriched in minor elements, K₂O and SiO₂ by the separation of olivine. In the lamproïtes this evolution was probably carried on for too long, under too low P/T conditions, for the preservation of the magma diamonds. On the contrary, at Bobi, the contiguous kimberlite was kept very rich (up to 30 ct/m³!). A same very rare association of kimberlite and lamproïte had been found recently in the explosive structure of Mt Abbott (W. Australia), and confirms PRIDER hypothesis. Seguela kimberlites had been dated by BARDET & VACHETTE at 1429 m.y by the Rb-Sr method.

Mitzic Metakimberlites

Near Mitzic (NW Gabon) many kimberlitic dykes had been recently discovered, and the possibility of a wider province from Equatorial Guinea to Brazzaville Congo (with the small Komono deposit) cannot be dismissed. Those mineralized dykes have a general NW trend following conspicuous fractures in the basement. The kimberlite, more schistose than at Séguela and which seems to have been crushed, is formed by 80 % of talc, with relics of altered mica, some chlorite and prisms of tremolite-actinote, and contains many very small octahedrons of diamond. The nodular structure appears to result from dynamic deformations, and olivine relics are not recognizable. There is no ilmenite nor pyrope, but chromite is rather abundant and, found in the alluvia with diamonds, behaves as a good tracer. Like at Seguela the chemistry is quite characteristic of a kimberlite, with high Ba, Sr, V etc., elements which are absent from the Gabon M'Bigou Soapstones, in spite of some similarity with these rocks of a quite different origin. The age of Mitzic kimberlites is not known, but is obviously Precambrian and probably older than the base of Francevillian (1900 m.y. or less ?) which contains diamonds.

Conclusion

Direct transformation of olivine into talc without serpentization had been described by BOWEN, and some "talc-kimberlites" mentioned in Soviet literature, but not as a source of diamonds. In some regions of the world, diamond alluvial deposits occur which carry no specific kimberlitic minerals. To be sure, ilmenite and pyrope could have been completely destroyed mechanically and chemically during the long processes of erosion and transportation. But sometimes this evidence is lacking, and one could question the possibility of a "metakimberlitic" origin, especially when more resistant spinels are systematically associated with the diamonds. For example in some isolated Sierra-Leone diamond fields HALL (1970)suspected the existence of such an aberrant

source, but did not succeed in proving it. Possibly in some Precambrian areas, diamond fields have been missed owing to the absence of the "classic" kimberlitic tracers and some intriguing problems could be reexamined with this point of view. This abnormal type of kimberlite deserves a better and deeper study.

Analysis (BRGM - Orléans)

Metakimberlite						
Seguela, Toubabouko - Mitzic, Amié - Lamproïte Bobi-Fitzroyite						
SiO ₂	57.80	56.40	-	54.60	-	50.3
Al ₂ O ₃	0.80	1.50	-	2.95	-	8.2
Fe ₂ O ₃	1.90	2.60	-	5.40	-	7.4
FeO	2.90	3.10	-	2.50	-	0.2
TiO ₂	1.45	1.60	-	0.93	-	5.7
CaO	1.30	1.80	-	0.60	-	2
MgO	25.90	26.10	-	26.85	-	9.8
Na ₂ O	0.20	0.15	-	0.10	-	0.2
K ₂ O	0.45	0.55	-	0.30	-	10
P ₂ O ₅	0.30	0.40	-	0.30	-	2
H ₂ O	1.50	1.20	-	0.25	-	0.45
H ₂ O ⁺	2.80	4.50	-	5.40	-	1.85
Ni ppm			1500		NiO	0.03
Cr			1150			
Co			80			
Ba			460	BaO	0.70	BaO
Sr			15	SrO	0.20	1.19
Sc			19			
V			170			
Pb			96			
Zn			250			
				ZrO ₂	0.3	
				F	0.7	

Bibliography

BARDET M.G. - 1973 - "Géologie du Diamant". BRGM PARIS - Under Press.

BARDET M.G. & VACHETTE M. - 1970 - "Détermination d'âges de kimberlites de l'Ouest Africain" 3e Colloque de Géologie Africaine, Bruxelles-Tervuren.

HALL P.K. - 1970 - "The Diamond Fields of S. Leone". SL Geol. Surv. Bull. n° 5.

KNOPF D. - 1970 - "Les kimberlites et roches apparentées de Côte d'Ivoire" SODEMI - Abidjan - & Thèse Lausanne.

PRIDER R.T. - 1960 - "The leucite lamproïtes of the Fitzroy Basin W.A" Jl Geol. Sty Australia v. 6, Pt 2 1960.

WADE A. & PRIDER R.T - 1939 - "The leucite-bearing rocks of the West Kimberleys Area-Western Australia" Quat. Jl Geol. Sty V XCVI Pt 1.

THE GENESIS OF KIMBERLITE AND ASSOCIATED ROCKS:
STRONTIUM ISOTOPIC EVIDENCE

D. R. Barrett, Bernard Price Institute of Geophysical Research,
University of the Witwatersrand, Johannesburg.

Strontium isotopic tracer techniques have been applied in the investigation of materials from kimberlite pipes. Studies were made on 13 samples of fresh kimberlite, 20 samples of peridotite-, eclogite-, phlogopite-, and diopside nodules, and mineral concentrates from kimberlite groundmass and nodules (42 micas, 21 other samples, mainly clinopyroxenes). This work was complemented by K, Rb and Sr concentration determinations (employing isotope dilution) and petrographic, electron-probe and contamination studies (including acid leaching and ground-water analyses).

Sr-isotopic compositions were mostly determined on tracer-free samples. They are in general accurate to $\pm 0,0003$ (1σ). The accuracy of concentration data was $\sim 0,5\%$. $\text{Sr}^{87}/\text{Sr}^{86}$ refers to the strontium ratio ~ 100 m.y. ago (i.e. at pipe emplacement).

RESULTS

1. Assessment of samples: The significance of the results hinges on whether the samples represent uncontaminated material. Although it is widely thought that kimberlite inclusions have suffered contamination, the evidence presented below indicates that in the carefully selected samples studied this is minimal, and has not significantly affected the purified minerals.

Leaching of nodular samples with cold dilute HCl showed two distinguishable "contaminants". Contaminant "A" (observed only in peridotite diopsides and one Wesselton eclogite total rock), is similar to fresh kimberlite with $\text{Sr}^{87}/\text{Sr}^{86} \sim 0,705$, K/Rb ~ 120 and relatively high Rb and Sr contents. This gives rise to the effect that unleached diopsides have lower $\text{Sr}^{87}/\text{Sr}^{86}$ than leached samples. Contaminant "B" (found in eclogite- and diopside-nodules) has high $\text{Sr}^{87}/\text{Sr}^{86}$ ($\sim 0,710$), high K/Rb (~ 1000) and low Rb and Sr contents. Such material could be an alteration product (e.g. zeolite and kelyphite) formed by percolating ground waters ($\text{Sr}^{87}/\text{Sr}^{86} \sim 0,712 - 0,720$). Leached and unleached omphacites do not show significant differences in $\text{Sr}^{87}/\text{Sr}^{86}$ values indicating that these are not dominated by this contaminant. Leach solutions from peridotite whole rocks showed intermediate character.

Petrographic assessment of the eclogites revealed, in some cases, that phlogopitisation occurred before kelyphitisation. The latter is envisaged as occurring at about the time of, or since, emplacement (Kramers 1973). Some peridotite mica was considered primary with lesser amounts of secondary mica. Petrographic assessment of the selected nodular samples showed limited serpentinisation and other alteration.

Also relevant are the following points:

- i) Although crustal contamination of whole rocks is possible, it appears that contaminating Sr has not had a serious effect on the purified mineral concentrates since juxtaposed samples of the

types studied, all of which would be expected to be similarly affected, retain distinct and individual ranges in $\text{Sr}^{87}/\text{Sr}^{86}$ ratios.

- ii) The peridotite mica and diopside were probably in isotopic equilibrium with each other (and ~ with the whole rock) at the time of emplacement, implying minimal contamination.
- iii) Leaching experiments show that ground-water type material could have affected the nodules (particularly eclogites). Ground water would be expected to raise the $\text{Sr}^{87}/\text{Sr}^{86}$ ratios: there is, however, no relationship between $\text{Sr}^{87}/\text{Sr}^{86}$ ratio and degree of freshness. The contaminant appears to be similar to that which has affected fresh kimberlite (see companion Barrett-Berg paper).
- iv) In view of the consistent age data of most micas (see companion Barrett-Allsopp paper) it would seem that any alteration occurred mainly about the time of pipe formation.

2. (a) Nodular Inclusion and Kimberlite Data (See Figure): The most striking results obtained are the generally significant differences in $\text{Sr}^{87}/\text{Sr}^{86}$ of kimberlite and of well-purified clinopyroxenes from different hosts. They increase in the following order: diopside nodule diopsides (0,703 - 0,704); the freshest kimberlite (0,704 - 0,705); eclogite omphacite (0,7047 - 0,7062); peridotite diopsides (0,7060 - 0,7075).

All the freshest eclogite total rocks and the pyroxenes lie to the left of G with Rb/Sr ratios too low to account for their observed $\text{Sr}^{87}/\text{Sr}^{86}$ values. They cannot therefore be primary mantle material. In contrast, similar reasoning shows that peridotite nodule total rocks, lying to the right of G, could be undifferentiated mantle.

K/Rb ranges tend to overlap: fresh kimberlite (90 - 210); micas (95 - 380); peridotite total rocks (~200); peridotite diopsides (~235); eclogite total rocks (~200 - 500); eclogite omphacites (250 - 5,000); diopside nodule diopsides (850 - 970). The contrasting clinopyroxene values are noteworthy.

These results substantiate and extend the work of Allsopp et al. (1969) and Berg and Allsopp (1972).

2. (b) Eclogite: The eclogite minerals were not in isotopic equilibrium at pipe emplacement time. Eclogite mica has $\text{Sr}^{87}/\text{Sr}^{86}$ ~0,7082 whereas omphacite has $\text{Sr}^{87}/\text{Sr}^{86}$ ~0,7055. It follows that much of the eclogite mica is not primary.

Relationships between eclogite and basalt have been previously suggested. For instance Allsopp et al. (1969) theorised about the possibility of an ideal eclogite (i.e. omphacite and garnet only) which might be parental to oceanic tholeiite. The $\text{Sr}^{87}/\text{Sr}^{86}$ values now obtained for omphacite are too high to be consistent with such a model.

A possible relationship between eclogite and Stormberg basalts is suggested by the similarity in K/Rb , K , Rb , Sr and Rb/Sr values if the freshest eclogites are considered. On the other hand, assuming a mean Rb/Sr ratio, $\text{Sr}^{87}/\text{Sr}^{87}$ values (200 m.y. ago) of the freshest eclogite total rocks are too high to conform with the implied simple relationship; the similarity of most of the data would appear to be fortuitous.

Only "ideal" eclogite (omphacite, garnet and possible primary mica) could be comagmatic with the basalts, in which case even the freshest eclogite total rocks must have been subsequently contaminated by a high $\text{Sr}^{87}/\text{Sr}^{86}$ component. The Roberts Victor eclogite micas indicate an age of ~ 126 m.y. but the data are more scattered than those of micas from other sources. The kelyphitisation of eclogites may be the responsible factor; from this aspect too it would appear that the eclogites have been contaminated. Berg (1968) considers that phlogopite may result from alteration involving addition of alkalis from kimberlite whilst still in a fluid state. Contrasting $\text{Sr}^{87}/\text{Sr}^{86}$ values for fresh kimberlite and mica (this work) suggest that such a model is untenable.

2. (c) Peridotite: In contrast to the eclogite mica-pryoxene pair, peridotite micas and diopsides have very similar $\text{Sr}^{87}/\text{Sr}^{86}$ values ($\sim 0,707$). Possibly there was isotopic equilibrium between these minerals until pipe emplacement. Assuming a $\text{Sr}^{87}/\text{Sr}^{86}$ value of $\sim 0,702$ for the source of these peridotite nodules and an average mica Rb/Sr ratio (and that the increase in this ratio to 0,707 has been a result of Sr^{87*} production in the mica only) then a lengthy association (~ 800 m.y.) of the two minerals is implied.

2. (d) Origin of Nodules: Eclogite omphacites having lower $\text{Sr}^{87}/\text{Sr}^{86}$ values than the garnet peridotite cannot have been derived from such material (by a process such as suggested by O'Hara and Yoder 1967). Since a cumulate origin for eclogite is consistent with other data, it is possible that garnet peridotite of another type with low $\text{Sr}^{87}/\text{Sr}^{86}$ values yields picritic partial melts. Eclogite (and basalt) could be derived from this melt. The peridotites possibly represent xenoliths of mica bearing mantle zones.

2. (e) Kimberlite: Fresh kimberlite with lower $\text{Sr}^{87}/\text{Sr}^{86}$ ratios than its eclogite and peridotite inclusions cannot be derived from such material. The nodules are xenolithic. Only diopside nodules ($\text{Sr}^{87}/\text{Sr}^{86} < 0,704$) could be representative of parental material. Alternatively they could be early cumulates from a "kimberlite" melt or merely accidental inclusions.

It is suggested that kimberlite has a deep origin, possibly in undepleted low $\text{Sr}^{87}/\text{Sr}^{86}$, garnet peridotite regions. Small degrees of partial melting give rise to a melt with carbonatitic affinities. Note that carbonatites have $\text{Sr}^{87}/\text{Sr}^{86}$ values of 0,702 - 0,705 and K/Rb ratios of 90 - 200, very similar to fresh kimberlite. Differentiation within a rapidly ascending magma concentrates Rb relative to K, giving rise to the observed $\text{K}/\text{Rb} \sim 140$. The melt intercepts and incorporates pre-existing garnet peridotite (probably micaceous) with $\text{Sr}^{87}/\text{Sr}^{86} \sim 0,707$, and possibly phlogopite with $\text{Sr}^{87}/\text{Sr}^{86} \sim 0,710 - 0,714$. (Phlogopite nodules are believed to be of mantle origin, Clement 1973.) This mechanism could, together with percolating ground-water (see companion Barrett-Berg paper) give rise to the higher $\text{Sr}^{87}/\text{Sr}^{86}$ values of typical kimberlite and also account for the abundance of peridotite minerals and mica. Eclogite, where present, is incorporated too. If eclogite (or ideal eclogite) is related to basalt genesis the prevalence of eclogite at Roberts Victor may be due to the kimberlite having ascended along a Stormberg volcanic conduit which contains remnant eclogite.

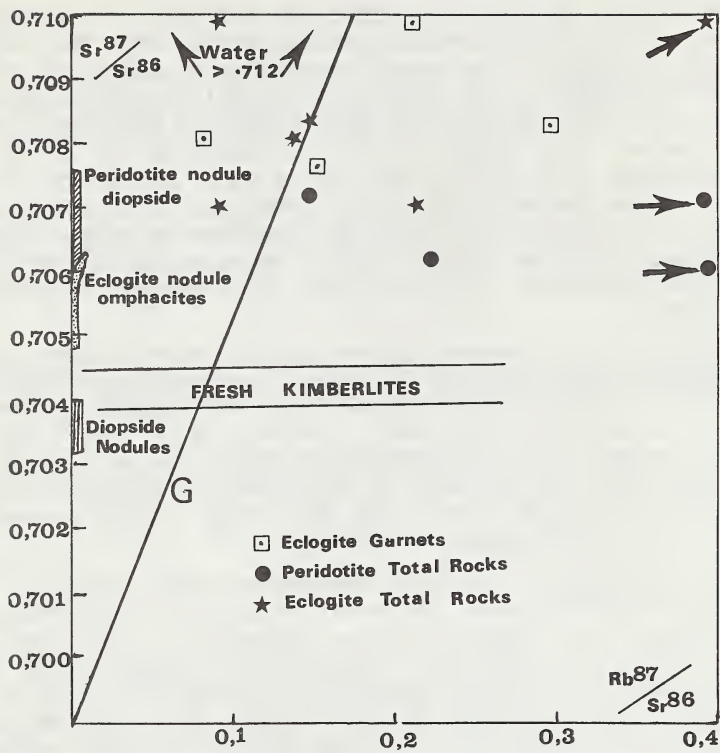


Figure: Sketch of Isochron Diagram

All points on the generating line 'G' have $\text{Rb}^{87}/\text{Sr}^{86}$ ratios sufficient to account for their observed $\text{Sr}^{87}/\text{Sr}^{86}$ ratios over a period of 4,6 b.y.

REFERENCES

Allsopp, H.L., Nicolaysen, L.O., and Hahn-Weinheimer, P. 1969. *Earth & Planet. Sci. Letters*, 5, 231-244.

Berg, G.W. 1968. *Amer. Mineral.* 53, 1336-1346.

Berg, G.W., and Allsopp, H.L. 1972. *Earth & Planet. Sci. Letters*, 16, 27-30.

Clement, R. 1973. (Personal communication)

Kramers, J. 1973. (Personal communication)

O'Hara, M.J., and Yoder (Jr.) H.S. 1967. *Scott. J. Geol.* 3(1), 67-117.

RUBIDIUM-STRONTIUM AGE DETERMINATIONS ON SOUTH AFRICAN KIMBERLITE PIPES

D.R. Barrett and H.L. Allsopp

Bernard Price Institute of Geophysical Research,
University of the Witwatersrand, Johannesburg.

Although kimberlite pipes are common in South Africa relatively few isotopic age measurements have been made on samples from these pipes. Lovering and Richards (1964) reported K-Ar measurements on mica and pyroxene from eclogite inclusions in the Roberts Victor pipe but obtained inconsistent results. Allsopp et al. (1969) reported Rb-Sr ages on three mica samples: two Roberts Victor eclogite micas indicated an age of 105 ± 20 m.y., and one Du Toitspan peridotite mica indicated an age of approximately 80 m.y. Allsopp et al. (1967) used Rb-Sr biotite measurements to establish a definite minimum age of 1115 ± 15 m.y. for the Premier pipe, and galena data suggested that the pipe might be as old as 1750 ± 100 m.y.

The present study was undertaken to establish to what extent reliable ages could be obtained by the Rb-Sr isochron method on phlogopite micas from kimberlite and its associated inclusions, and to establish whether significant age differences exist between various pipes. The Table below summarises the results obtained from nine different kimberlite pipes.

Primary mica (i.e. mica crystallised prior to pipe emplacement) would be expected to yield the age of pipe emplacement since temperatures in the source region are almost certainly high enough to maintain isotopic equilibrium prior to that time. Secondary mica, if associated with pipe emplacement, would be expected to yield the same age. In both cases, however, variations in the primary $\text{Sr}^{87}/\text{Sr}^{86}$ ratio might occur, and samples of the two types, and also micas from different types of inclusion, may not define a single linear isochron. As a test of this the Wesselton pipe was subjected to detailed study, micas from the kimberlite groundmass, from peridotite nodules and from phlogopite nodules all being studied. Two significantly different isochrons (ages 118 ± 6 and 78 ± 3 m.y.) were obtained, one defined by the phlogopite nodules and the other by the other two types. (A minority of samples were rejected due to the data lying more than five standard deviations from the mean line, and the same procedure was adopted with the data from other pipes. Such scatter could be due to experimental error, but it is more likely to be the result of post-emplacement alteration.) The most significant result is that a linear isochron was obtained for samples of a given type, and according to isochron theory, it is most probable that the indicated ages are valid.

As noted above the micas from the phlogopite nodules indicate a different age from those from peridotite nodules and from kimberlite groundmass. Radiogenic Sr retention in the presumed primary phlogopite nodules is one possible explanation of this anomaly. This is considered unlikely since in such a case the degree of retention would vary

depending on sample size and other factors, thereby giving rise to a non-linear isochron; in fact an excellent isochron was obtained for the phlogopite nodules. A simpler explanation is that there were different periods of kimberlite intrusion in the Wesselton pipe, with the phlogopite nodules being largely or entirely confined to one particular intrusion, and the peridotite nodules to another. Observations in the mine clearly show that there have been different periods of intrusion, but no information is available as to the distribution of different types of nodule. No definite conclusion can be reached on the fundamental question of whether the isochron method yields reliable ages for kimberlites, and the distribution of nodules at Wesselton should be investigated with a view to clarifying this issue.

Reference to the table shows that ages in the range 147 to 78 m.y. are indicated for all pipes apart from Premier. The prima facie evidence, therefore, is that there has been an extended period of kimberlite formation during Jurassic to lower Cretaceous times, with different intrusions sometimes following earlier ones up the same pipe.

A completely different approach was adopted in the dating of the Premier pipe. In this pipe at least four types of kimberlite have been mapped, and a sequence of intrusions has been suggested. The situation is, however, complicated by the intrusion of a diabase sill that post-dates both the pipe and the country rock. The heating effect of the sill would be expected to "re-set" the ages of micas situated close to the sill, and to affect micas further from the sill to a lesser extent. Local variations in the temperature distribution (associated with minor diabase intrusions) and the formation of secondary mica as a direct result of diabase-induced metamorphism could be expected to effect departures from the simple pattern indicated. Nevertheless six samples of Type 1 kimberlite yield results of the expected pattern (see Figure); one additional sample is discrepant and this sample is from an area in which minor intrusions have been observed. From these data it is concluded that the age of the Type 1 kimberlite is close to 1250 m.y. Data for the Type 4 kimberlite is widely scattered, with ages both older and younger than 1250 m.y. being indicated. No definite conclusions can be reached, but it is possible that the Type 4 is a mixture of the Types 1, 2 and 3. Of these Type 2 is considered to be the oldest and Type 3 the youngest; mixture of these could account for the observed scatter, and very tentatively ages of \sim 1400 m.y. and \sim 1200 m.y. are assigned to Types 2 and 3 respectively.

REFERENCES

Lovering, J.F., and Richards, J.R. J. Geophys. Res. 69 (1964) 4895.

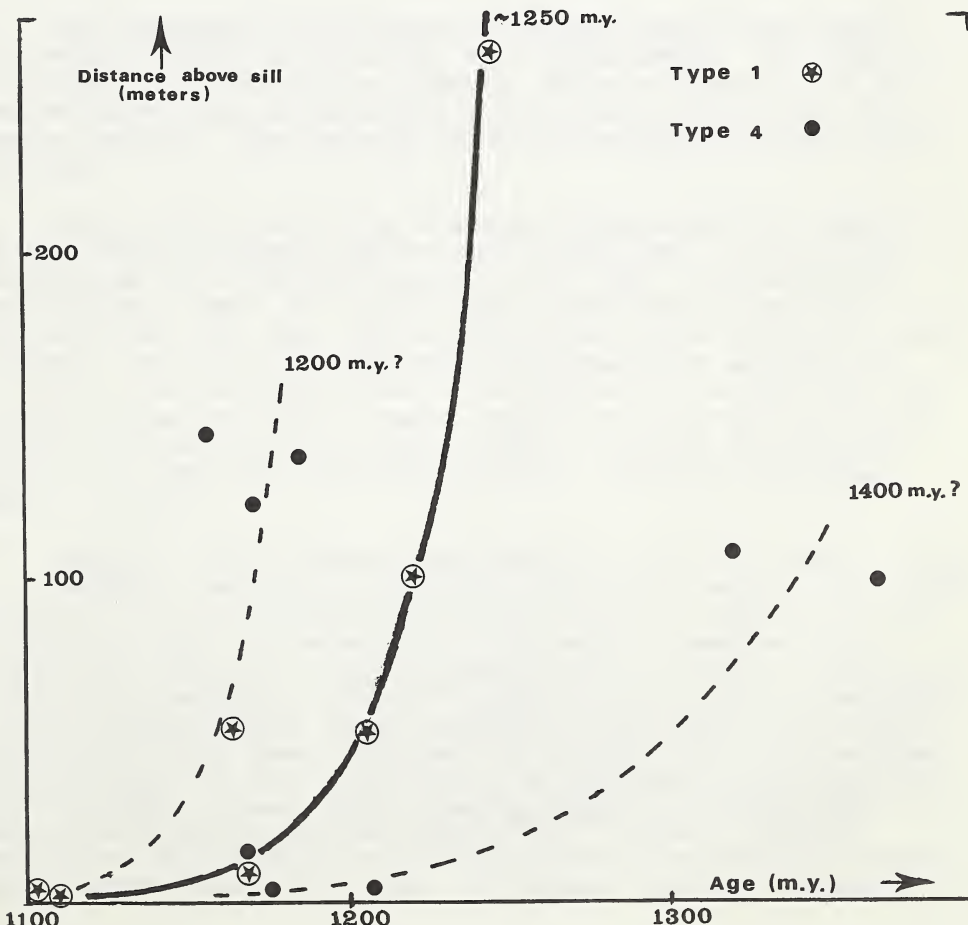
Allsopp, H.L., Nicolaysen, L.O. and Hahn-Weinheimer, P. Earth & Plan. Sci. Letters, 5 (1969) 231.

Allsopp, H.L., Burger, A.J., and van Zyl, C. Earth & Plan. Sci. Letters, 3 (1967) 161.

SUMMARY OF RB-SR AGE-DETERMINATIONS ON S. AFRICAN KIMBERLITE MICAS

Type	Age (m.y.)	$\text{Sr}^{87}/\text{Sr}^{86}$ %
Wesselton peridotite nodules	77 ± 2	$0.7101 \pm .0014$
Wesselton groundmass	80 ± 4	$0.7074 \pm .0016$
Wesselton phlogopite nodules	118 ± 6	$0.7096 \pm .0005$
Kimberley area (excl. Wesselton) peridotite nodules	89 ± 2	$0.7073 \pm .0007$
Roberts Victor eclogite nodules	126 ± 4	$0.7082 \pm .0012$
Monastery groundmass	90 ± 3	$0.7050 \pm .0011$
Gross Brukkaros groundmass	~ 84	~ 0.7041
Swartruggens groundmass	147 ± 2	$0.7067 \pm .0009$
Premier groundmass Type 1	$\sim 1250^*$	-

* Note that both older and younger ages are indicated by Type 4.



COMPLEMENTARY PETROGRAPHIC AND STRONTIUM-ISOTOPE RATIO-
STUDIES OF SOUTH AFRICAN KIMBERLITES

D.R. Barrett, Bernard Price Institute of Geophysical Research,
University of the Witwatersrand, Johannesburg.

and G.W. Berg, Grant Institute for Geology, Edinburgh, U.K.

The Cretaceous kimberlites of South Africa might be expected to have primary $\text{Sr}^{87}/\text{Sr}^{86}$ ratios comparable with that of the mantle - less than about 0,704. Most kimberlites however have $\text{Sr}^{87}/\text{Sr}^{86}$ ratios in the range 0,706 - 0,715 (Mitchell and Crocket 1971). These authors consider such ratios to be characteristic. Berg and Allsopp (1972) recently showed that lower ratios of ~0,704 do occur in kimberlites that are exceptionally fresh, but their study included only three fresh samples. The present work was undertaken to extend the preliminary findings of Berg and Allsopp. A total of 13 fresh kimberlites from many pipes were analysed. Detailed petrographic descriptions of the samples were made and the K, Rb, Sr concentrations and $\text{Sr}^{87}/\text{Sr}^{86}$ ratios were also measured.

The freshness of the samples was assessed quite independently, i.e. without access to the isotope ratio measurements. The criteria of freshness include relative hardness, degree and appearance of serpentinisation, apparent permeability and porosity, colouration and general geology. These criteria are illustrated by reference to thin sections.

Most of the K, Rb and Sr abundance determinations were made by isotope dilution although XRF was used in some cases. The accuracy obtained was ~0,5% (isotope dilution) to 5% (XRF) in the kimberlite and wall-rock samples but in the case of water samples (very low abundance) was 10% - 50%. The isotope ratios were measured on unspiked samples. The precision (including the ground-water samples) was $\sim \pm 0,0003$ (68% confidence limit). The accuracy of the data was established by regular Eimer and Amend standard determinations which gave $\text{Sr}^{87}/\text{Sr}^{86}$ values $\sim 0,7081 \pm 0,0003$. Primary strontium isotope ratios ($\text{Sr}^{87}/\text{Sr}^{86}$) have been calculated assuming a kimberlite emplacement age of 100⁰m.y.

RESULTS: Representative data obtained are given in Table 1. The samples considered to be freshest have ratios varying from 0,7039 to 0,7046 which substantiate the previous results of Berg and Allsopp (1972), and which are compatible with the autolith samples ratios reported by Ferguson et al. in a companion paper. There is substantial evidence for assigning a $\text{Sr}^{87}/\text{Sr}^{86}$ ratio of ~0,704 to fresh kimberlite. Slightly altered samples give intermediate ratios whilst more altered samples (including those of Mitchell and Crocket (1971), thin sections of which one of us (W.B.) has examined and assessed as being altered), all have higher ratios. Fresh micaceous samples containing small inclusions of granite also had high $\text{Sr}^{87}/\text{Sr}^{86}$ ratios. Thus the correlation between freshness (in inclusion-free samples) and strontium isotope ratio is seen to be good. In contrast there is no apparent

relationship between K, Rb, Sr abundances and K/Rb or Rb/Sr ratios with $\text{Sr}^{87}/\text{Sr}^{86}$.

SIGNIFICANCE OF LOW RATIOS: Carbonatites are thought to be genetically related to kimberlites (e.g. Brookins 1970, Dawson 1971). Carbonatites have a high Sr content 1000 ppm - 10,000 ppm (with a mean of ~ 3500 ppm) and $\text{Sr}^{87}/\text{Sr}^{86}$ values of 0,702 - 0,705 are reported by Brookins (1967). Fresh kimberlite $\text{Sr}^{87}/\text{Sr}^{86}$ ratios obtained in this work lend support to the proposed relationship. The average Sr abundance is considerably lower in kimberlite than in carbonatite, as would be expected if kimberlite is a mixture of carbonatitic material and other mantle rocks (for instance garnet peridotite). Further carbonatite-kimberlite similarities occur in K/Rb ratios which both range from ~ 90 - 200.

HIGHER STRONTIUM RATIOS IN AVERAGE KIMBERLITE: There are a number of possible mechanisms for enhancing the strontium isotope ratios of fresh kimberlite.

i) Assimilation: Wall Rock and Mantle derived Xenoliths: Mitchell and Crocket (1971) calculated that bulk assimilation of typical basement material was most unlikely to account for the high $\text{Sr}^{87}/\text{Sr}^{86}$ values in kimberlite. Similar calculations using data obtained for actual pipe wall rocks support this conclusion. However certain micaeucos kimberlites containing small granitic inclusions have high $\text{Sr}^{87}/\text{Sr}^{86}$ values. The $\text{Sr}^{87}/\text{Sr}^{86}$ ratios and strontium content of wall-rock are such that they may influence the kimberlite value locally. The mica, if cognetic with fresh kimberlite, would not raise the $\text{Sr}^{87}/\text{Sr}^{86}$ value. However if the mica is xenolithic being incorporated in ascending kimberlite magma from the breakup of mantle garnet-mica peridotite ($\text{Sr}^{87}/\text{Sr}^{86} \sim 0,707$) & phlogopite ($\text{Sr}^{87}/\text{Sr}^{86} \sim 0,710$ to 0,714) (ratios as reported by Barrett in a companion paper) then it would be expected to raise the kimberlite ratios. Dawson (1971) advocates such a process and contends that it adequately explains the enhanced kimberlite $\text{Sr}^{87}/\text{Sr}^{86}$ ratios of typical kimberlite. Both this mechanism and (iii) below could explain the lack of correlation of elemental abundances and ratios with the $\text{Sr}^{87}/\text{Sr}^{86}$ ratios.

ii) Diffusion: Isotopic exchange by diffusion between kimberlite material and country rock would occur only if high magma temperatures were maintained for long periods (Hart et al). The temperature of kimberlite emplacement (at least at depths currently accessible) is considered to have been low; Brookins (1970) suggests temperatures $\sim 200^\circ\text{C}$. That low temperatures are involved is supported by wall rock studies undertaken in this work.

Wall rock studies in this work show that muscovite samples from 0,5 m to 120 m from the pipe contact are colinear on an isochron diagram. The age corresponding to the slope of this line is that of the basement rocks, indicating that no net Rb or Sr concentration nor $\text{Sr}^{87}/\text{Sr}^{86}$ changes have occurred in these rocks for 2,9 b.y. at these levels. Thus the effect of diffusive processes has been minimal, and low temperatures are implied for pipe emplacement.

iii) Percolating Ground Water: Ion-exchange of Sr between the kimberlite and ground-water was suggested by Berg and Allsopp (1972) as a mechanism whereby the ratio of kimberlite could be raised after pipe emplacement. To assess the possible influence of ground-water, samples of water were collected underground on the mines and from surface in the vicinity of Kimberley. The $\text{Sr}^{87}/\text{Sr}^{86}$ value of the water was found to be high: 0,712 - 0,720. This, combined with the observation that the freshest kimberlites have the lowest ratios, does support the suggested mechanism. Leaching with cold dilute HCl removed over 80% of the kimberlite Sr. Assuming that this readily soluble component is mainly calcite (and zeolite), it is probable that exchange with ground-water can readily occur and that the ground-water hypothesis is plausible to this extent. The low total strontium content of the waters (0,06 - 1,7 ppm) coupled with the high content in kimberlite (~1500 ppm) implies a much higher permeability of fresh kimberlite than for average crustal rocks. Whether or not this is so is unknown.

CONCLUSION

The results of this study indicate that ground-water mechanisms alone could account for the high $\text{Sr}^{87}/\text{Sr}^{86}$ values of typical kimberlite. However incorporation of xenolithic high $\text{Sr}^{87}/\text{Sr}^{86}$ material (particularly mica) from the mantle into rising kimberlitic magmas could be an important additional process.

Table 1

Some Typical Strontium Isotopic and Elemental Ratios
in Kimberlites, Wall Rocks and Ground Waters

Brief Assessment of Samples	Sr Total (ppm)	$\text{Sr}^{87}/\text{Sr}^{86}$	Rb/Sr	K/Rb
Most fresh	700 to 1900	0,7039 to 0,7046	0,003 to 0,09	120 to 200
Similar to above but slightly altered	1400	0,7058	0,004	120
Mica kimberlite (fresh & serpentinised) and kimberlite containing small granitic inclusions	800 to 1700	0,7062 to 0,7084	0,06 to 0,1	90 to 210
Basement granite - gneiss wall rock	88,0 to 463,0	0,706 to 0,879	0,02 to 1,5	-
Surface and under- ground Kimberley area waters	0,06 to 1,7	0,712 to 0,720	<0,1	-

REFERENCES

Berg, G.W., and Allsopp, H.L. (1972). *Earth & Planet. Sci. Letters*, 16, 27-30.

Brookins, D.G. (1967). *Earth & Planet. Sci. Letters*, 2, 235-240.

Brookins, D.G. (1970). *State Geological Survey of Kansas Bull.* 199 part 4 and Bull. 200.

Dawson, J.B. (1971). *Earth-Sci. Rev.* 7, 187-214.

Mitchell, R.H. and Crocket, J.H. (1971). *Contrib. Mineral. and Petrol.* 30, 277-290.

Watson, K.D. (1968). *Ultramafic and Related Rocks*, Ed. by Wyllie, 1968.

SOURCE MANTLE, RESIDUUM AND PARTIAL MELT COMPOSITIONS DEDUCED FROM THE KIMBERLITE RECORD

W. Berg and M.J. O'Hara

After consideration of phase equilibria and petrographic characters (O'Hara 1973a,b) compositions have been selected as representing best available estimates of undepleted source rock and depleted residuum in the upper mantle sampled by kimberlite diatremes from data presented or cited by Berg (1973), O'Hara *et al* (1973). Compositions based on the data of Berg (1973) are systematically slightly richer in MgO than those based on data of O'Hara *et al* (1973).

I One method of interpreting these results, and its conclusions are discussed by O'Hara *et al* (1973) involving use of a best fit to observed rock types.

II An alternative approach is to select chemical analyses of garnet-lherzolite and either garnet-harzburgite or harzburgite, and to calculate the composition of the liquid which must be extracted from garnet-harzburgite in any particular amount in order to obtain the observed residuum. The spread of 'average' analyses creates large uncertainties in this calculation. An 'acceptable' fit is shown in table 1A and in fig 1 in relation to the maximum possible spread consistent with both sets of average compositions. Low silica and extremely high MgO and FeO characterise all such solutions, pointing to ultrabasic liquids as the only plausible extracts. Knowing the Fe/Mg ratio of the residue and applying the empirical Fe/Mg distribution coefficient derived by Roeder and Emslie (1971), it is possible to choose within the linear range of table 1A those compositions yielding the best fit. This criterion suggests that a composition with close to 32% MgO constituting a 12-20% partial melt will provide an internally consistent model.

Table 1A Compositions of plausible liquid extracts (primary magmas) to cause observed variation in ultrabasic nodules from kimberlite.

	(a)	(b)	(c)	(d)	(e)
SiO ₂	45	44	42.5	41.5	40.5
Al ₂ O ₃	3	4.5	6	7	8
FeO	8.5	10	11.5	13.5	15
MgO	38	34	30	26	22
CaO	2.6	3.8	4.7	6	7
Na ₂ O	.4	.8	1.2	1.6	2

Table 1B Approximate percentage of source garnet-lherzolite converted to liquid in each case using average garnet-lherzolite of Berg 1973 (1) or O'Hara *et al* (2).

(1)	21	14	10	8	7
(2)	37.5	23	17	13	11

A liquid intermediate in composition between columns (b) and (c) satisfies the equilibrium Mg:Fe distribution coefficient (see fig 1).

III Alternatively the same calculations can be made using individual selected analyses of garnet-peridotite and garnet-harzburgite or harzburgite from the published data tables. The subjective element and the consequences of sampling errors tend to become dominant, even though this technique offers the possibility of choosing individual rocks free from alteration or contamination.

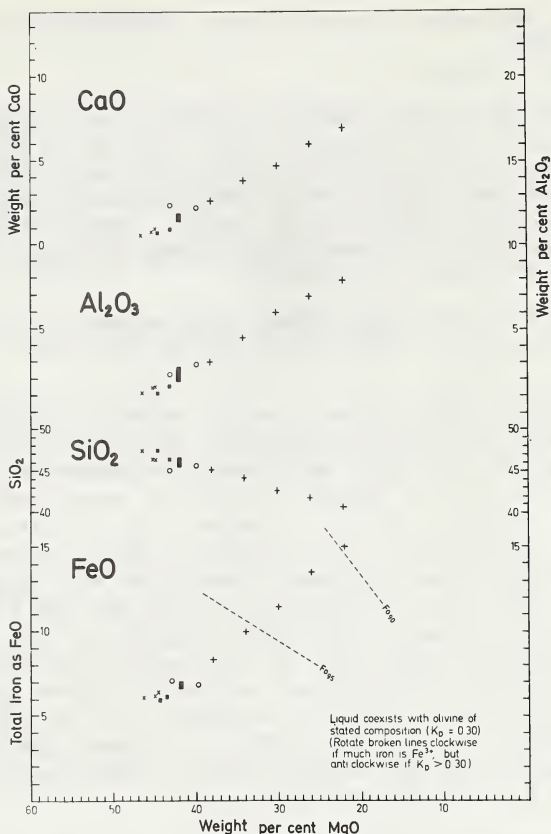


Fig 1 Oxide plot v. MgO (volatile free) showing average harzburgite, garnet lherzolite from Berg (1973; X-symbols) and O'Hara *et al* (1973 fig 1, filled boxes). Two open circles represent two relatively fertile garnet-lherzolites (Berg 1973) which nevertheless are very much less fertile than 1032 (MF) of O'Hara *et al* (1973 fig 1). Large + symbols indicate tabulated selected liquid compositions (table 1).

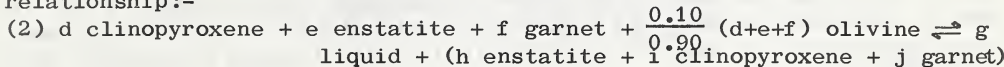
Methods I, II, III described above lead to identification of the composition and amount of primary magma which was actually produced during the partial melting events which most profoundly affected the upper mantle sampled by kimberlite. Significantly, the pressure required to stabilize the required phase equilibria is high and the deduced liquid product very scarce at the earth's surface, particularly in recent geological times.

The next method attempts to calculate the liquid composition which will be produced by partial melting of garnet-lherzolite under some known or assumed form of the phase equilibria, starting from the composition of the coexisting minerals.

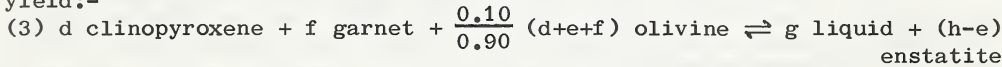
IV In partial melting of garnet-lherzolite, the change is expressed by the relationship (derived from O'Hara and Yoder, 1967):-

(1) $a \text{ clinopyroxene}_{\text{ss}} + b \text{ garnet}_{\text{ss}} + (1-a-b) \text{ olivine} = c \text{ liquid} + (1-c) \text{ enstatite}_{\text{ss}}$
 quantities a, b, c (weight fractions) are not precisely known, and vary with pressure. Moreover, the compositions of the clinopyroxene

undergoes major changes in the content of potential garnet and enstatite with both P,T. Nevertheless, this relationship offers the possibility of obtaining an approximate linear solution for the compositions of the liquids which might be produced in partial melting of a particular garnet peridotite. Data from O'Hara and Yoder (1967) and Davis and Schairer (1965) indicate that the quantity $(1-a-b)$ is of the order of 0.10 at 30-40 kb. The liquid composition produced when all garnet and clinopyroxene have been consumed in partial melting may then be obtained from the relationship:-



where clinopyroxene, enstatite, etc. are the analysed compositions of these minerals in the low temperature subsolidus assemblage of the garnet peridotite, and d , e , $.....j$ are absolute weight fractions in the peridotite, d and f being known from the mode. For the purpose of this approximate calculation, the quantities i , j , representing solid solution components in the enstatite are assumed to be small, and the extra enstatite dissolved in the clinopyroxene at the solidus (e) may be transferred, to yield:-



and this has been solved for the trial cases where $0.10 (d+e+f)/0.90=0.10 (d+f)$ and $0.20 (d+f)$ respectively, and $(h-e)$ ranges from $+0.20$ to -0.20 . The amounts, (g of equation III) and compositions of the calculated 'liquids' are presented , these analyses and percentages representing linear ranges within a possible primary magma might be. The nature of the calculation is displayed diagrammatically in fig 2.

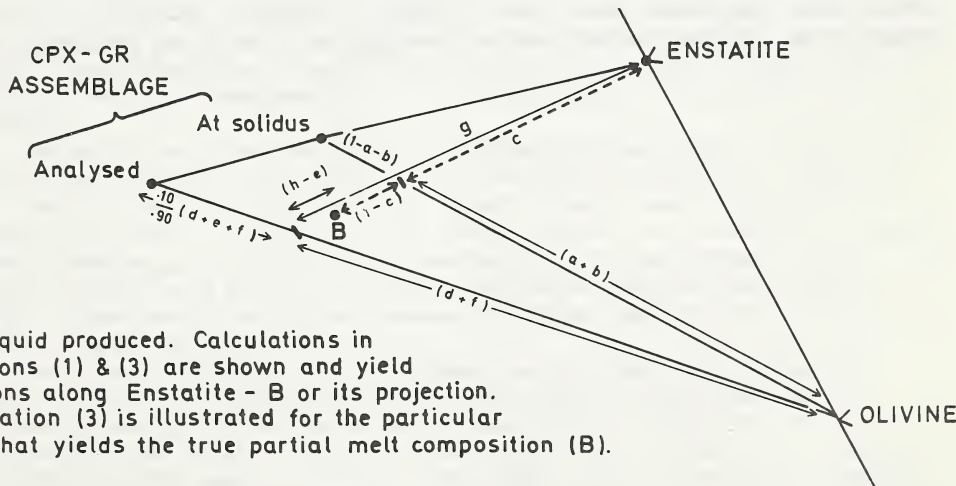


Fig 2

The obvious falacy in this first trial calculation is that it assumes that all end-member components in each mineral solid solution contribute equally to the liquid product. This is not true, conspicuously so in the case of the Na and Ca clinopyroxene components, the Cr and Al pyroxene

and garnet components, the Fe and Mg components of all minerals, and the Ni component of olivine. The liquids, therefore, should have higher values of Na_2O , Al_2O_3 and FeO than calculated from (3) and lower values of MgO , NiO .

A correction procedure has been adopted for FeO and MgO , based upon the Roeder and Emslie (1970) relationship and an indicated $\text{Mg}/(\text{Mg}+\text{Fe}) = 0.95$ in the residual minerals (from petrography of residual harzburgites). While retaining the same total number ($\text{N}'\text{FeO} + \text{N}'\text{MgO}$) of molecules of FeO and MgO in the compositions, the number to be calculated as FeO ($\text{N}'\text{FeO}$) has been increased, and that to be calculated as MgO ($\text{N}'\text{MgO}$) decreased, until

$$\frac{5}{95} \frac{\text{N}'\text{MgO}}{\text{N}'\text{FeO}} = 0.3.$$

The weights of FeO , MgO corresponding to $\text{N}'\text{FeO}$, $\text{N}'\text{MgO}$ have then been calculated, reinserted in the original compositions and the totals rescaled to 100%. The results represent an approximate linear series of solutions which should include the composition of the primary magma which might be formed by partial melting of natural garnet lherzolite at 30-40 kb pressure (90-120 km depth).

References

Berg, W. 1973 this volume.
 Davis, B.T.C. and Schairer, J.F. 1965. Carnegie Instn. Wash. Yearb. 64, 123-127.
 O'Hara, M.J. a 1973 this volume. Subsolidus mineral assemblages etc,
 O'Hara, M.J. b 1973 this volume. Phase equilibria principles etc.
 O'Hara, M.J. et al 1973 this volume. Chemistry of ultramafic nodules
 from kimberlite etc.
 O'Hara, M.J. and Yoder, H.S. 1967. Scott. J. Geol. 3, 67-117.
 Roeder, P.L. and Emslie, R.F. 1970. Contrib. Min. Pet. 29, 275-289.

PHASE RELATIONSHIPS IN NATURAL AND SYNTHETIC PERIDOTITE-H₂O AND
PERIDOTITE-H₂O-CO₂ SYSTEMS AT HIGH PRESSURES

A. L. Boettcher
Bjorn O. Mysen
*P. J. Modreski

Department of Geosciences
The Pennsylvania State University
University Park, PA 16802
U.S.A.

Phase relationships to about 30 kbars and 1200°C have been determined in the presence of H₂O and H₂O-CO₂ vapors with controlled a_{O₂} and a_{H₂O} for four peridotite nodules (including one from the Wesselton Mine) and a garnet websterite nodule. Their compositions (Rocks A-E, respectively) are SiO₂ = 45.7 (wt %), 43.7, 45.10, 44.82, 45.58; Al₂O₃ = 1.6, 4.0, 3.92, 8.21, 13.69; CaO = 0.70, 3.50, 2.66, 8.12, 11.78; Na₂O = 0.09, 0.38, 0.27, 0.89, 1.27; K₂O = 0.04, 0.01, 0.02, 0.03, 0.02; Mg/(Mg + Fe²⁺) = 0.94, 0.89, 0.90, 0.85, 0.88. Additional data to 1350°C and 35 kbars were obtained from experiments on synthetic phlogopite-bearing peridotites in the system K₂O-MgO-CaO-Al₂O₃-SiO₂-H₂O at conditions of P_{H₂O} ~ P_T and P_{H₂O} << P_T.

Temperatures of the vapor-saturated solidii for the nodules with a mol fraction of H₂O in vapor (X_{H₂O}^V) ~ 1 are shown in Fig. 1. Lowering the a_{H₂O} by the addition of CO₂ to the vapor raises the temperature of the beginning of melting, as shown for rock B in Fig. 2.

The stable crystalline assemblages at all of the vapor-saturated solidii include O1 (absent in nodule E), Cpx, Opx, and Amph. Amphiboles are stable on the solidii of the nodules for values of X_{H₂O}^V as low as 0.25. These amphiboles range from pargasitic [CaO/(CaO + Na₂O + K₂O) ~ 0.80] at 800°C to tschermakitic (~ 0.93) at 1100°C for nodule D + H₂O at 15 kbars.

Micas do not occur except in a series of experiments in which the nodules were spiked with 3 to 10 wt % synthetic phlogopite. However, for the synthetic peridotites with larger proportions of phlogopite components, mica is stable to high temperatures. For example, the assemblage diopside_{ss} + phlogopite_{ss} + enstatite_{ss} + forsterite + pyrope begins to melt at 1350°C at 35 kbars (Modreski and Boettcher, 1972; 1973). Experiments at higher pressures suggest that phlogopite may persist to depths as great as 175 km.

As shown in Fig. 3, liquids formed as much as 150°C above the solidii of the peridotites are SiO₂-rich (quartz normative) to the highest pressures investigated under conditions of X_{H₂O}^V of 1.0 to 0.6. At lower values (higher a_{CO₂} and lower a_{H₂O}), the liquids are undersaturated in SiO₂ and rich in CaO and Al₂O₃; they may represent models of CO₂-charged kimberlite magmas. This phenomena is in part related to the change from the congruent melting of enstatite at high pressures under anhydrous conditions (Boyd *et al.*, 1964) to incongruent melting (to a SiO₂-rich liquid) at high a_{H₂O} (Kushiro *et al.*, 1968). It also results in part from a reduction in the proportion of amphibole as a_{H₂O}

*Present address: AFWL/LRT, Kirtland A.F.B., New Mexico 87117

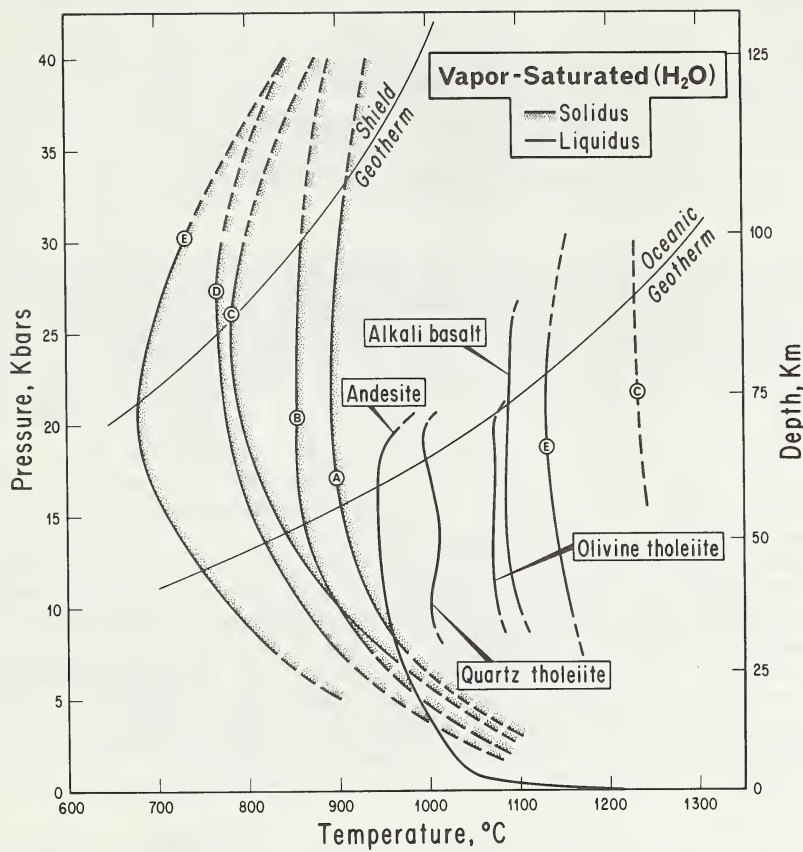


Fig. 1 P-T projection of the vapor-saturated ($X_{H_2O}^V \sim 1$) solidii for nodules A-E. Also shown are the vapor-saturated liquidii ($X_{H_2O}^V \sim 1$) for andesite, quartz tholeiite, olivine tholeiite, and alkali basalt (all from Allen *et al.*, 1972) and for nodules E and C (this work). The continental geotherm is from Clark and Ringwood (1964). The oceanic geotherm is from Ringwood *et al.* (1964).

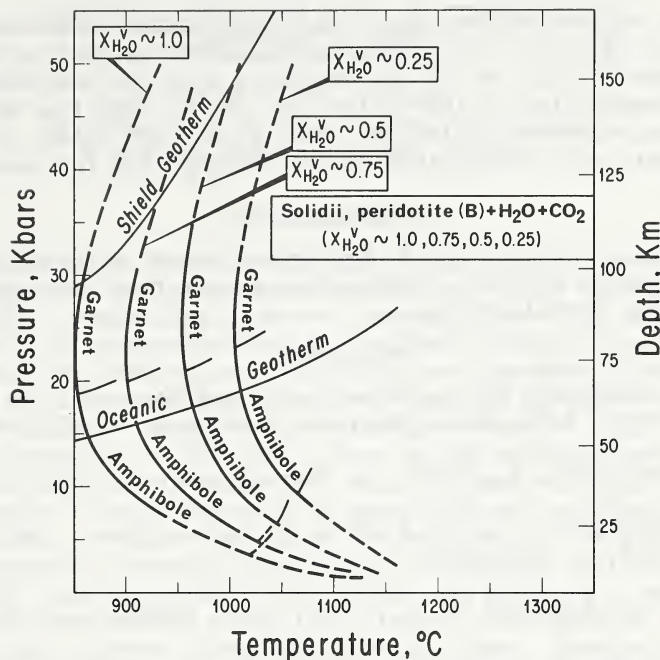


Fig. 2 P-T projection showing vapor-saturated solidi, garnet stability, and amphibole stability for nodule B with $X_{\text{H}_2\text{O}}^{\text{V}} \sim 1.0, 0.75, 0.50, \text{ and } 0.25$. See also Fig. 1.

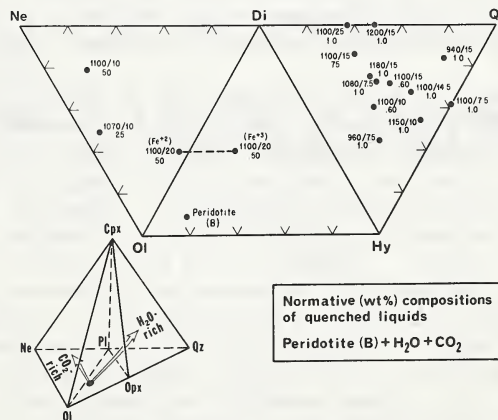


Fig. 3 Compositions of quenched liquids for nodule $B + H_2O + CO_2$. 1080/7.5 indicates 1080°C at 7.5 kbars with $X_{H_2O}^V = 1.0$. All Fe was calculated as Fe^{+2} . The effect of calculating all Fe as Fe^{+3} is shown for one point.

is lowered by decreasing the $X_{H_2O}^V$. Our data indicate that under conditions of, say, $X_{H_2O}^V$ of ~ 0.25 to 0.50 , melting of peridotite would begin at depths of 100 to 175 km, depending upon the geothermal gradient and the composition of the peridotite. This range lies athwart the diamond \rightleftharpoons graphite equilibrium curve (Berman and Simon, 1955), and it is in concert with the minimum depths proposed for the genesis of kimberlites.

Acknowledgments

I thank E. D. Jackson, D. A. Pretorius, and R. W. White for providing the valuable nodules. This work was supported by National Science Foundation Grant NSF GA-12737.

References

Allen, J. C., Modreski, P. J., Haygood, C., and Boettcher, A. L., 1972: Twenty Fourth Intl. Geol. Congress, Section 2, p. 231-240.

Berman, R., and Simon, F., 1955: Z. Elektrochemie, V. 59, p. 333-338.

Boyd, F. R., England, J. L., and Davis, B. T. C., 1964: Jour. Geophys. Res., V. 69, p. 2101-2109.

Clark, S. P., and Ringwood, A. E., 1964: Rev. Geophys., V. 2, p. 35-88.

Kushiro, I., Yoder, H. S., Jr., and Nishikawa, M., 1968: Geol. Soc. America Bull., V. 79, p. 1685-1692.

Modreski, P. J., and Boettcher, A. L., 1972: Am. J. Sci., V. 272, p. 852-869.

Modreski, P. J., and Boettcher, A. L., 1973: Am. J. Sci., V. 273, p. 385-414.

Ringwood, A. E., MacGregor, I. D., and Boyd, F. R., 1964: Carnegie Inst. Washington Yearbook 63, p. 147-152.

PYROXENITE XENOLITHS FROM THE KIMBERLITE OF
JAGERSFONTEIN MINE

G.D. Borley and P. Suddaby
Department of Geology, Imperial College
of Science and Technology, London,
S.W.7., U.K.

Two xenoliths from the Williams' collection are referred to as diallage rock and pyroxenite respectively (1). Hand and petrographic examination suggests, however, that they are both varieties of a pyroxenite that has suffered variable degrees of deformation, exsolution, alteration, and recrystallisation.

The diallage consists of coarse, lamellar diopside crystals $> 10\text{cm}$ long that have kinked and broken every 4 - 5cm. Thin sections cut parallel to the (001) plane of the clinopyroxene show exsolution lamellae of enstatite which is almost totally altered to serpentine. Small crystals of pyrope garnet are also aligned along the lamellae. Sections cut along (010) planes of the pyroxene show more interesting features than those cut parallel to (001). In particular they demonstrate that stress has produced a parting plane in the pyroxene that is slightly oblique to the plane of exsolution, and slip has occurred along this parting plane. Tension cracks have developed along the length of the pyroxene lamellae at right angles to the apparent direction of the parting plane; occasionally the tension cracks have a near-sigmoidal shape, and they also appear to have acted as channels for serpentinising solutions. In this orientation, the garnet is seen frequently to lie along the parting plane as elongate crystals, which suggests that it formed at a late stage under stress conditions, and not during the initial stages of pyroxene unmixing.

In the kink bands of the xenolith there has been recrystallisation of the pyroxene to give large, irregularly shaped grains which contain scattered, small grains of garnet. Garnet is also present in the form of stringers of grains along the grain boundaries of the recrystallised pyroxene. Considerable serpentinisation of the pyroxene has occurred in the kink bands and randomly oriented grains of secondary phlogopite are also abundant. Except for small grains in some highly serpentinised areas of the lamellar pyroxene, the phlogopite appears to be restricted to the kink bands.

The pyroxenite xenolith also consists of lamellar pyroxene, but the lamellar texture has been distorted by crushing and is partly replaced by a finely granular pyroxene mosaic. In coarser grains, deformation twin lamellae appear to be present but they have not been verified as such. Phlogopite and serpentine are generally absent.

Mineral compositions were determined by electron microprobe

analysis, using the method described by Borley et al. (2). Compositionally (Table 1) the diopside has the higher Mg:Fe of the two pyroxenes, as might be expected, but both pyroxenes are poor in Al, Ti and Mn.

Table 1
Mineral analyses

	<u>Diopside</u>	<u>Enstatite</u>	<u>Pyrope</u>
SiO ₂	54.7	57.7	41.5
TiO ₂	0.02	0.02	-
Al ₂ O ₃	0.79	0.37	22.0
FeO	1.93	6.9	11.7
MnO	0.04	0.12	0.69
MgO	17.1	34.8	17.8
CaO	23.4	0.31	5.03
Na ₂ O	0.65	-	-
Cr ₂ O ₃	0.33	0.03	0.93
NiO	0.12	0.15	-
V ₂ O ₅	0.08	0.02	0.04
Totals	<u>99.16</u>	<u>100.40</u>	<u>99.69</u>

Substitution of Al for Si and the entry of Cr into the diopside lattice has probably been responsible for the entry of Na to maintain charge balance, though in part the entry of Na must have been determined by the presence of the large M2 site in the clinopyroxene. In the initial absence of olivine, Ni has entered the pyroxene and the partition of this element is now approximately equal between diopside and enstatite. Partition of Cr is pyrope > diopside > enstatite. Compared with many reported analyses of diopside from xenoliths in kimberlite, the diopside of these xenoliths is low in Cr. The phlogopite is a low iron variety.

The origin of these nodules is uncertain. They would appear to have formed, perhaps as settling phases, at high temperature (the diopside-enstatite equilibrium is temperature rather than pressure controlled), and have been deformed and altered during decreasing temperature, possibly under directional stress.

References

Williams, A.F. 1932. The Genesis of the Diamond. Vol. 2. E. Benn, London.

Borley, G.D., Suddaby, P., and Scott, P.W. 1971. Contr.
Mineral. Petrol. v. 31, p102-114.

TEXTURES AND FABRICS OF PERIDOTITE NODULES FROM KIMBERLITE
AT MOTHAE, THABA PUTSOA AND KIMBERLEY

Anne-Marie BOULLIER and Adolphe NICOLAS

Laboratoire de Géologie Structurale, BP 1044, 44037 NANTES CEDEX

INTRODUCTION

The present report is the result of a preliminary examination of 25 ultramafic xenoliths, brought up by the kimberlite intrusions Thaba Putsoa and Mothae (Lesotho) and Kimberley (Republic of South Africa). The rocks studied, viz., harzburgites, garnet-harzburgites, lherzolites, garnet and/or spinel-lherzolites are often serpentinized. It is a complement of the data of Mercier (1972), Nicolas et al. (1971) on the peridotite xenoliths in basalts and on Alpine-type peridotite massifs both of which probably originated in more superficial levels of the upper-mantle. On the basis of texture and fabric of olivine and enstatite, the samples have been grouped in a provisional classification providing a clue to the textures of the layers of the mantle where these xenoliths originated. Some textural types can be readily interpreted in terms of flow processes in view of recent theoretical and experimental research (Ave Lallement, Carter, 1970; Carter et al., 1972; Nicolas et al., 1971, 1972 in press; Mercier, 1972).

MAIN TEXTURES

- 1- The "coarse-grained" texture is characterized by:
 - a single generation of coarse-grained crystals (6mm);
 - neither foliation nor lineation;
 - straight or curved mineral boundaries;
 - a weak orthorhombic olivine fabric, even weaker in enstatite; (fig 1)
- 2- The "tabular olivine and enstatite" texture is characterized by:
 - a single generation of generally undeformed crystals;
 - a medium grain size and a good foliation defined by tabular olivine and enstatite crystals ($L/W = 5/2$ mm);
 - a strong olivine fabric and a weaker but unusual enstatite fabric (Xen normal to the foliation). (fig 2)
- 3- The porphyroclastic texture is characterized by:
 - two generations of crystals: strongly deformed large porphyroclasts and undeformed smaller neoblasts;
 - an excellent foliation and a good lineation;
 - a characteristic olivine fabric and enstatite fabric; (fig 3)
- 4- The "mosaic" texture is characterized by:
 - a single generation of small olivine neoblasts (0.3mm) constraining with two generations of enstatite porphyroclasts locally recrystallizing into neoblasts;
 - a good foliation and an excellent lineation;
 - an insignificant olivine fabric, but strong local subfabric pointing to the former existence of large porphyroclasts. (fig 4)

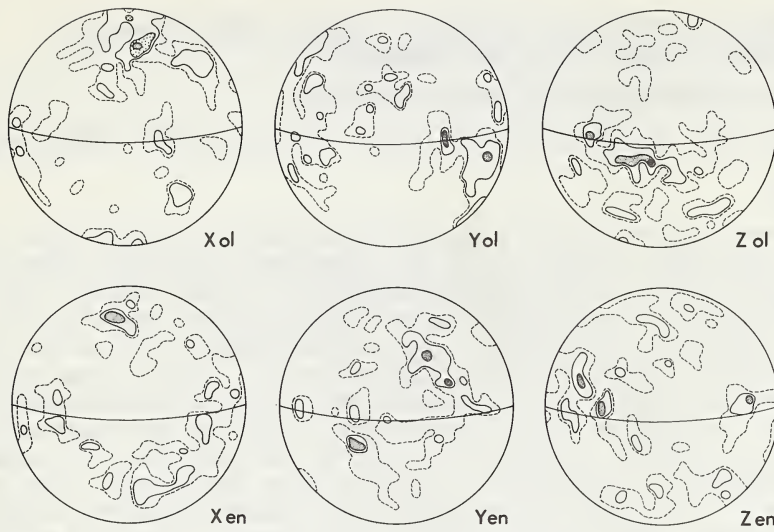


Fig 1

Fabric of the "coarse-grained" texture

Ol = Olivine

En = Enstatite

line : measured plane of crystals flattening

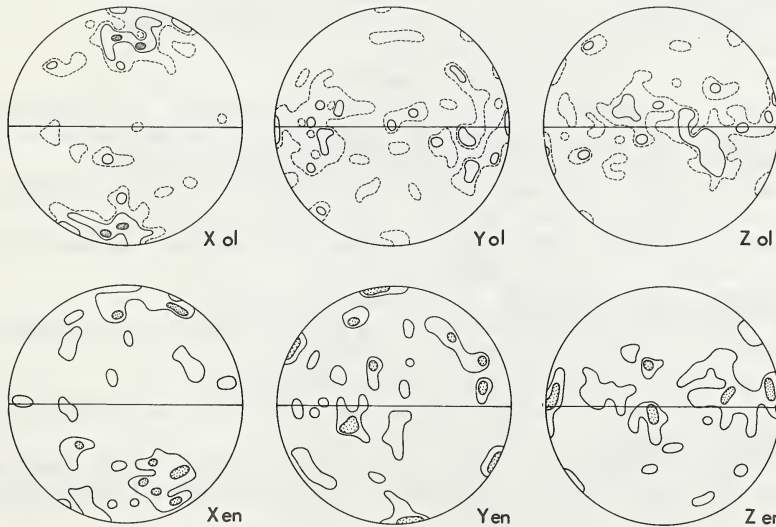


Fig 2

Fabric of the "tabular olivine and enstatite" texture

Ol = Olivine

En = Enstatite

line : foliation plane observed on sample.

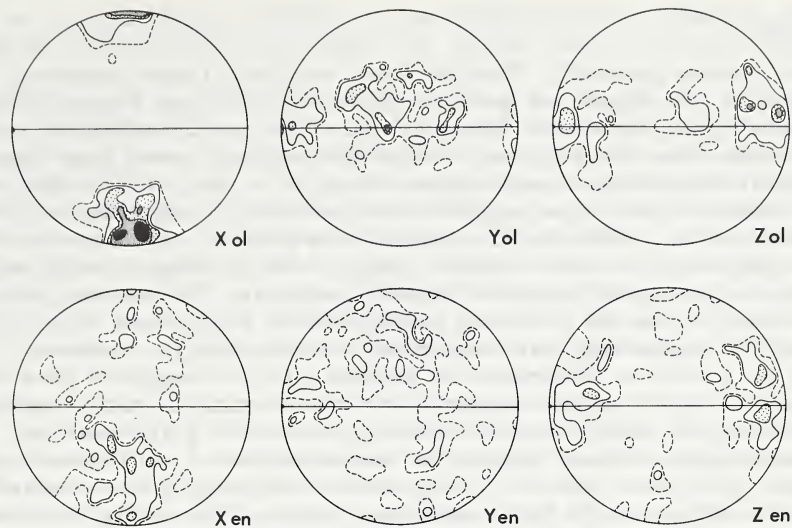


Fig 3 Fabric of the porphyroclastic texture
 Ol : olivine porphyroclasts; En : enstatite porphyroclasts.
 Horizontal line and point : respectively foliation and mineral linea-
 tion observed on sample

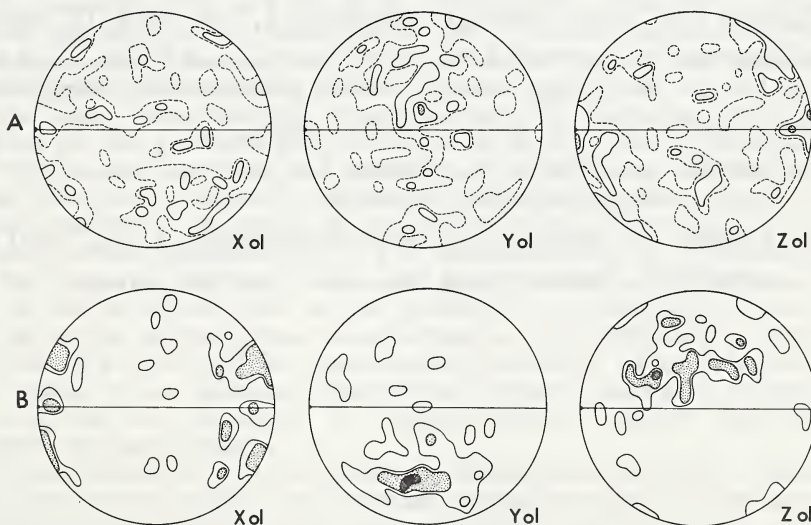


Fig 4 Fabric of the "mosaic" texture
 A- olivine general fabric
 B- olivine local subfabric
 Horizontal line and point : respectively foliation and mineral
 lineation observed on sample.

DISCUSSION

The "coarse-grained", "tabular" and porphyroclastic textural groups correspond to the "granular group" defined by Boyd and Nixon (1972) and our "mosaic" group to their "sheared" one. The porphyroclastic and mosaic textures have already been described in basalt xenoliths (Mercier, 1972) and in Alpine type peridotites (Nicolas et al., 1971, 1972). They were interpreted, with the support of experimental comparisons (Avé Lallement and Carter, 1970; Nicolas et al., in press), as formed by plastic flow (porphyroclastic texture) with progressive passage to syntectonic and annealing recrystallization (mosaic texture). The coarse-grained texture can be compared with the protogranular texture of basalt xenoliths, but no equivalent has been found for the tabular texture.

The existence of intermediate textural facies suggests that the coarse-grained and tabular textures are transformed to porphyroclastic and ultimately to mosaic textures through increasing deformation. The discrepancy between their respective temperatures of equilibration (Boyd and Nixon, 1972) is tentatively explained admitting that the mosaic textured lherzolites result from mechanical mixing of formerly interlayered pyroxenites and harzburgites with a coarse-grained texture.

REFERENCES

AVE LALLEMANT H.G., CARTER N.L. (1970)-*Geol. Soc. Am. Bull.*, 81, 2203-2220.
 BOYD F.R., NIXON P.H. (1972)-*Carnegie Institution, Year Book* 71, 362-373.
 CARTER N.L., BAKER D.W., GEORGE R.P. (1972)-In *Flow and Fracture of Rocks-The Griggs volume* - A.G.U., WASHINGTON, 167-190.
 MERCIER J.C. (1972)-*Thèse 3^o cycle*, NANTES, 229 p.
 NICOLAS A., BOUCHEZ J.L., BOUDIER F., MERCIER J.C. (1971)
 Tectonophysics, 12, 55-86.
 NICOLAS A., BOUCHEZ J.L., BOUDIER F. (1972)-*Tectonophysics*, 14, 143-171.
 NICOLAS A., BOUDIER F., BOULLIER A.M.-*Am. Jour. Sc.* (In press).

ORIGIN OF THE LHERZOLITE NODULES IN THE KIMBERLITES OF NORTHERN LESOTHO
 F. R. Boyd, Geophysical Lab., and P. H. Nixon, Dept. of Mines, Maseru

Estimates of equilibration temperatures and pressures for lherzolite nodules from kimberlites can be made through consideration of experimentally determined phase studies and mineral compositions determined by electron microprobe analysis. It is necessary that a sample have equilibrated with the assemblage Ca-rich pyroxene+Ca-poor pyroxene+garnet for the equilibration conditions to be estimated. At present, it is also necessary that these phases be poor in FeO. The diopside solvus (Davis and Boyd, 1966) is used to estimate the equilibration temperature. Once this temperature is known, the equilibration pressure can be estimated from the Al_2O_3 content of enstatite using the data of MacGregor (1973). This procedure is discussed in more detail by Boyd (1973).

Figure 1 shows plots of estimated equilibration temperatures and depths for a group of lherzolite nodules from northern Lesotho. These estimates are subject to substantial uncertainties, but it appears likely that the broad stratigraphic relations will not be changed by subsequent refinement. In Fig. 1 the "raw" percentages of Al_2O_3 in the enstatites were used to estimate the equilibration pressures. These data appear to define an inflected geotherm in which the points on the shallow limb plot close to the predicted geotherm of Clark and Ringwood (1964). In Fig. 2 the estimated equilibration pressures have been corrected for the presence of minor amounts of FeO in the natural enstatites and garnets using a method developed by Wood and Banno (in press). This correction shifts the points to more shallow depths. Corrections can also be applied for sodium, assuming that all the Na in the natural enstatite is present as jadeite ($NaAlSi_2O_6$), or combining Al and Cr before subtracting Na. Such corrections shift the points on the inflected limb of the geotherm to somewhat greater depths but do not appreciably affect the points on the shallow limb. Nevertheless, regardless of the correction made, the overall form of the geotherm and the order of points remain the same.

The lherzolites from the kimberlites of northern Lesotho form two groups that differ markedly in texture, mineralogy, bulk composition, and mineral chemistry. A group whose equilibration points fall on the shallow limb of the geotherm (Fig. 1) is characterized by a coarse-grained (2-4 mm) granular texture. A second group, whose equilibration points fall on the inflected limb of the geotherm, is intensely sheared. Lherzolites in the second group contain coarse porphyroblasts of garnet and diopside in a fine-grained, granulated groundmass of olivine and enstatite. Some of the granular lherzolites contain accessory phlogopite, chromite, and rare graphite, but these minerals have not been found in the sheared lherzolites.

It is unlikely that the geotherm illustrated in Fig. 1 describes a steady-state situation. For a steady-state geotherm to have such an inflection would require that the rocks above and below the inflection have markedly different thermal properties. There are compositional and textural differences between the sheared lherzolites on the inflected limb of the geotherm and the granular lherzolites on the shallower limb, but it seems unlikely that these differences would affect the thermal properties to a significant degree. It appears more likely that the geotherm in Fig. 1 was perturbed. In other words, it appears that in a period prior to the eruption of the kimberlites a steady-state geotherm was established in the mantle beneath Lesotho with a slope rather like the "shield geotherm" of Clark and Ringwood (1964). This primitive geo-

therm was then perturbed by an event that caused major heating in the depth range 150-200 km. Possibly the postulated heating was related to the intense shearing of the lherzolites that define the inflected limb of the geotherm and possibly that shearing resulted from the plate movements that occurred during the break-up and dispersal of Gondwanaland.

Briden (1967) has compiled paleomagnetic data for the southern hemisphere and found evidence for four episodes of drift since the Cambrian separated by quasi-static intervals. The principal episode of drift occurred when Gondwanaland broke up in Late Triassic and Jurassic time after a quasi-static interval lasting for approximately 200 m.y. Smith and Hallam (1970) concluded that the initial rifting of Gondwanaland began in the Late Jurassic and Early Cretaceous, but that much of the dispersal occurred in Late Cretaceous and Tertiary times. Most of the kimberlites in Lesotho and South Africa are believed to have been erupted in the Late Cretaceous (e.g., Wagner, 1914; although there are as yet few radiometric dates. Dr. T. E. Krogh (personal communication) has obtained an age of 90-110 m.y. for a crystal of zircon from one of the pipes in the Kimberley area. Thus the African plate was in motion after a long quasi-static period when the kimberlites were erupted. The data in Fig. 1 suggest that the sheared lherzolites of deepest origin may have been stress-heated by as much as 300°C above their ambient, preshearing temperature.

Phlogopite is commonly found in the granular lherzolites, but no phlogopite has been found in any of the sheared lherzolites of deep origin (Fig. 2). Sample 1582, a sheared dunite from Thaba Putsoa, has the highest equilibration temperature of any of the phlogopite-bearing nodules--it is estimated to have crystallized at 1115°C. This temperature is well below the melting curve found for pure phlogopite in the presence of enstatite by Modreski (Fig. 2). However, the natural phlogopites contain substantial amounts of FeO and TiO₂, which would be expected to reduce their stability at high temperatures.

The occurrence of phlogopite in these lherzolites is complicated because it is possible that some of the phlogopite has been introduced at a late stage in their eruption. For example, phlogopite is often found mantling the kelyphite rims on the garnet in the granular lherzolites. Nevertheless it is possible that some of the phlogopite was introduced at depth in the mantle, prior to the incorporation of the nodules in kimberlite. Lambert and Wyllie (1968) have suggested that H₂O is largely stored in hydrous minerals in the lithosphere, whereas in the upper part of the asthenosphere it is dissolved in small amounts of interstitial silicate liquids. Possibly the occurrence of phlogopite in these nodules reflects such a relationship.

Experimental studies of the solidi of peridotites at high pressures show that H₂O produces an extremely large decrease in the temperature range for the beginning of melting. The data of Mysen and Boettcher (1972) suggest that small amounts of melting would be expected in the depth range from which the sheared lherzolites have come, provided small amounts of H₂O were present. Nevertheless, there would be no melting in the absence of H₂O.

Various lines of evidence suggest that the point of inflection in the geotherm (Fig. 1) might have been the top of the low-velocity zone in Late Cretaceous time. The sheared lherzolites have probably been erupted intact because they were dry. Most of the sheared lherzolites show some degree of depletion relative to pyrolite. Thus they may have undergone small degrees of partial fusion, and the liquids with dis-

solved H_2O may have been kneaded out by the shearing process. Weertman (1972) has emphasized the importance of shearing stresses in causing the coalescence of dispersed liquids in mantle rocks.

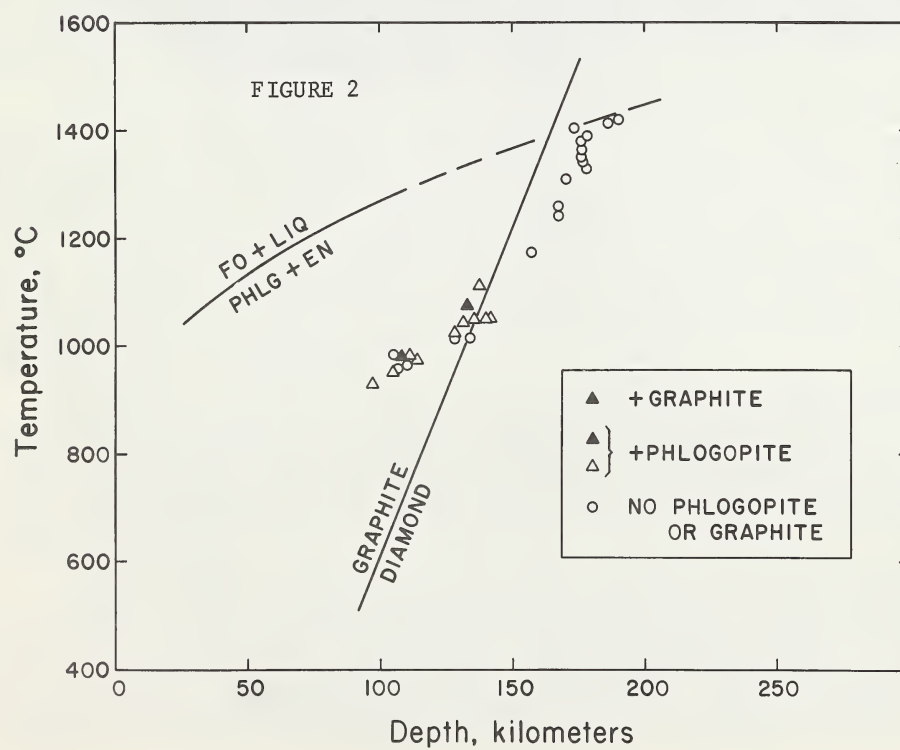
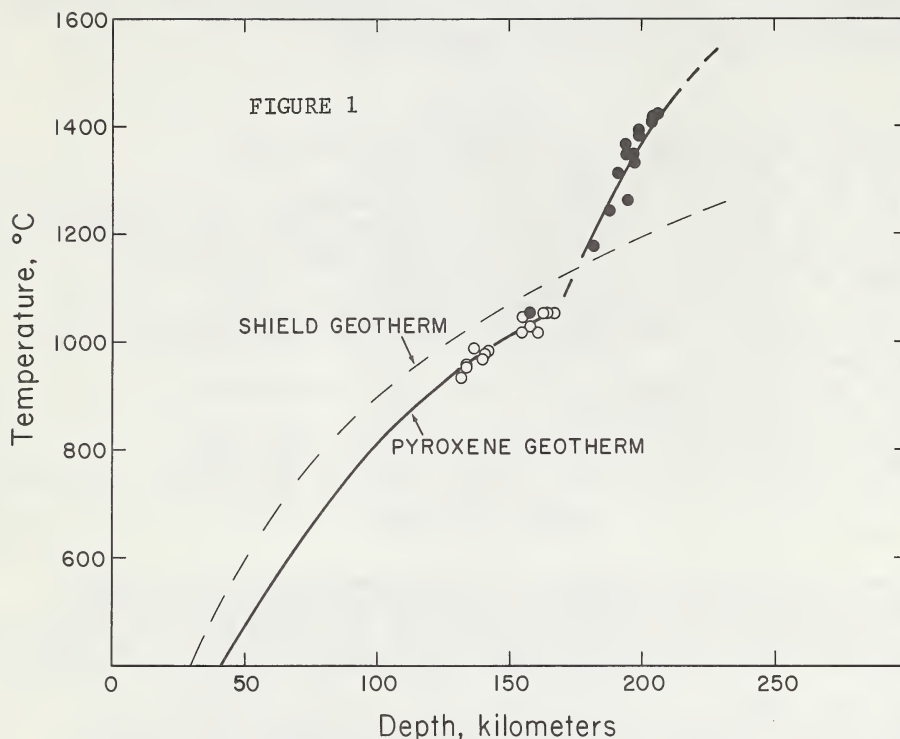
References

Boyd, F. R., 1973, *Geochim. et Cosmochim. Acta*, in press.
 Briden, J. C., 1967, *Nature* 215, p. 1334-1339.
 Clark, S. P., and A. E. Ringwood, 1964, *Rev. Geophys.* 2, p. 35-88.
 Davis, B.T.C., and F. R. Boyd, 1966, *J. Geophys. Res.* 71, p. 3567-3576.
 Lambert, I. B., and P. J. Wyllie, 1968, *Nature* 219, p. 1240-1241.
 MacGregor, I. D., 1973, *Amer. Min.*, in press.
 Modreski, P. J., 1972, *Carnegie Inst. Wash. Year Book* 71, p. 392-396.
 Mysen, B.O., and A.L. Boettcher, 1972, *Geol. Soc. Amer. Abstracts with Programs* 4, p. 608.
 Smith, A. G., and A. Hallam, 1970, *Nature* 225, p. 139-144.
 Wagner, P. A., 1971, *Cape Town*.
 Weertman, J., 1972, *Geol. Soc. Amer. Bull.* 83, p. 3531-3532.
 Wood, B. J., and S. Banno, 1973, *Contrib. Mineral. and Petrol.*, in press.

Figure Legends

Fig. 1: Temperature-depth points for lherzolite nodules from northern Lesotho compared with the shield geotherm (Clark and Ringwood, 1964). Open points are granular lherzolites and solid points are sheared lherzolites. Equilibration pressures calculated by "raw Al_2O_3 " method.

Fig. 2: Temperature-depth points for lherzolite nodules from northern Lesotho compared with the graphite \rightleftharpoons diamond curve and the curve for the melting of pure phlogopite + enstatite (Modreski, 1972). Equilibration pressures calculated by the Wood-Banno method.



ORIGIN OF THE DISCRETE NODULES IN THE KIMBERLITES OF NORTHERN LESOTHO
 F. R. Boyd, Geophysical Lab., and P. H. Nixon, Dept. of Mines, Maseru

Coarse, single crystals of garnet, pyroxene and ilmenite are abundantly developed in the kimberlites of northern Lesotho and of the neighboring Monastery Pipe, O. F. S. Commonly these crystals form rounded nodules several centimeters in diameter and occasionally they attain a diameter of 10-20 centimeters. Intergrowths are rare, but a variety have been studied in this investigation. Inclusions in discrete nodules consist of garnet, pyroxene, ilmenite and olivine, but chromite and phlogopite are not included. Among the intergrowths are the much-studied diopside-ilmenite lamellar intergrowths and similar crystals in which enstatite and ilmenite are interlaminated.

Compositions of garnet megacrysts (Fig. 1) are distinguished from those of the garnets in compound, lherzolite nodules because the former have a wide range in $Mg/(Mg + Fe)$ and restricted range in Ca (average 10.5 mole per cent Ca). The lherzolite garnets show a range in Ca and are predominantly more magnesian than the discrete nodule garnets. The most Fe-rich garnets are sometimes intergrown with ilmenite in a host or inclusion relationship.

Enstatite megacrysts also show a range in $Mg/(Mg + Fe)$ and these relationships are believed to be due to an igneous fractionation which has not been experienced by the phases in the compound nodules.

Diopside discrete nodules (Fig. 2) are uniformly more Fe-rich than the diopsides in the lherzolites and they are also usually subcalcic. Diopside-ilmenite megacrysts are distinctive in that they appear to have formed in a lower temperature range than their more magnesian, ilmenite-free counterparts.

Compositions of intergrown phases in discrete nodules and the relatively restricted ranges of composition of the minerals involved suggest that the discrete nodules crystallized as a part of the assemblage diopside + enstatite + garnet + olivine \pm ilmenite, but that the original associations were usually fragmented during eruption. If this assemblage is assumed to have existed, it becomes possible to make estimates of the equilibration conditions of the pyroxene discrete nodules.

Equilibration temperatures of the enstatite nodules can be estimated from a curve which relates $Ca/(Ca + Mg)$ in the lherzolite enstatites to the equilibration temperatures of their associated diopsides. Equilibration pressures of the enstatite discrete nodules can be estimated from their Al_2O_3 contents, making a Wood-Banno correction (1973) with the aid of a curve which relates $Mg/(Mg + Fe)$ in enstatites to $Mg/(Mg + Fe)$ in coexisting garnets.

Temperature-depth points for twenty-two enstatite discrete nodules cluster along the sheared limb of the lherzolite geotherm (Fig. 3). This consistent relationship would not have been obtained if the original assumption that the enstatite nodules crystallized in equilibrium with diopside and garnet were not true. Moreover the range of equilibration temperature obtained for the diopside discrete nodules spans the range found for the sheared lherzolites (Fig. 3). Thus it appears that the discrete nodules have come from the same depth range in the mantle as have the sheared lherzolites.

Crystals of pyroxene and olivine as coarse-grained as the discrete nodules have been found in pegmatitic zones and metasomatic rocks in other kinds of ultramafic intrusions. Irvine (1973) has described occurrences of such rocks in the Duke Island ultramafic complex and

attributed their origin to the action of volatiles emanating from crystallizing interstitial liquids. The action of volatiles alone would not appear to explain the strong fractionation in $Mg/(Mg + Fe)$ shown by the discrete nodules (e.g., Fig. 1). But it is possible that crystallization in the presence of an H_2O -rich melt over a long period of time might produce ultracoarse crystals and might also provide an environment in which fractionation could occur.

The idea that the discrete nodules might be phenocrysts in the magmas that initiated the kimberlite eruptions (e.g., Nixon, *et al.* 1963) now seems improbable because of the large ranges in equilibration temperature exhibited by suites of discrete pyroxene nodules from individual kimberlite pipes. For example, fourteen bronzite nodules from Letseng-La-Terai have equilibration temperatures ranging from 1170° to $1360^\circ C$ and five diopside nodules from Monastery (including diopside-ilmenite varieties) have a range of equilibration temperatures of 1200° - $1365^\circ C$.

Nevertheless, the large range in equilibration temperature found for the discrete nodules could be explained by a model in which the discrete nodules are taken to be megacrysts in large volumes of H_2O -bearing, crystal-mush magmas in the low-velocity zone. Moreover, such a model appears to be consistent with the occurrence of phlogopite in the lherzolites and with experimental studies of the lherzolite solidus in the presence of H_2O (Mysen and Boettcher, 1972). Thus we suggest that the point of inflection of the geotherm, which occurs at a depth of about 140 km, might have been the top of the low-velocity zone in Late Cretaceous time.

Ilmenite-bearing discrete nodules appear to be confined to shallow depths in the low-velocity zone (Fig. 3) where they are associated with ilmenite-bearing rocks and granular aggregates (Boyd and Nixon, 1973). Green (1971) has suggested that magmas in the low-velocity zone may initially contain less than about 5% liquid. If such liquids gradually seep and ooze upward through large volumes of crystal-mush, following a P-T path along the geotherm, some crystallization must occur as they cool. The effect of such a process over a long period of time might be to enrich the upper portion of the asthenosphere in Fe and Ti and also in certain trace elements (Green, 1971). The concentration of ilmenite-bearing rocks and magmas (?) near the top of the low-velocity zone might be caused by such enrichment.

If the interpretation of the discrete nodules as megacrysts in crystal-mush magmas is correct, it appears inescapable that erupting kimberlites would pick up and include the interstitial liquids as well as the crystalline grains. If so, the liquid phase in a kimberlite eruption may be hybrid. Various authors, including Dawson and Hawthorne (1973), have suggested a genetic relationship between carbonatites and kimberlites. It is interesting to speculate that kimberlite magmas might be carbonatite/silicate hybrids.

Boyd, F. R., and P. H. Nixon, 1973, in Lesotho Kimberlites, Cape Town, in press; Dawson, J. B., and J. B. Hawthorne, 1973, *J. Geol. Soc. London* 129, p. 61-85; Green, D. H., 1971, *Phil. Trans. Royal Soc. London, Ser. A* 268, p. 707-725; Irvine, T. N., 1973, *Geol. Soc. Amer. Mem.* 138, in press; Mysen, B. O., and A. L. Boettcher, 1972, *Geol. Soc. Amer. Abs. with Programs* 4, p. 608; Nixon, P. H., O. von Knorring, and J. M. Rooke, 1963, *Amer. Min.* 48, p. 1090-1132; Wood, B. J., and S. Banno, 1973, *Contrib. Min. and Pet.*, in press.

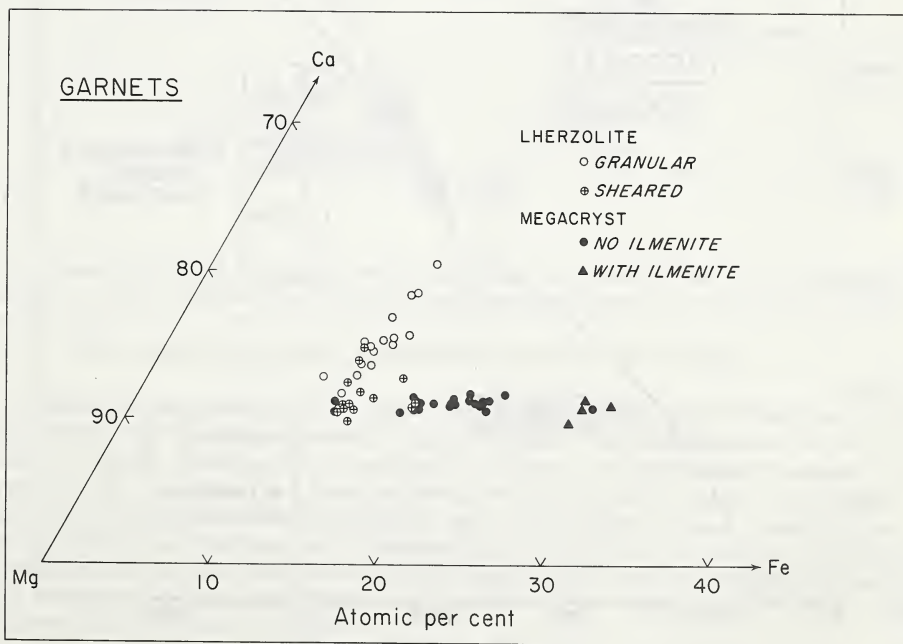
Figure Legends

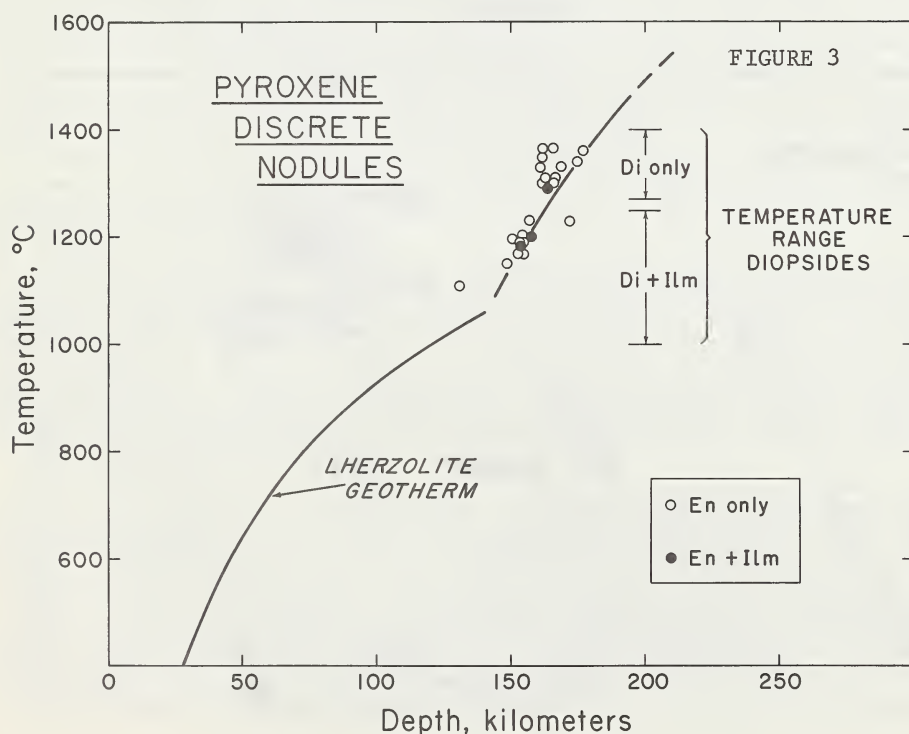
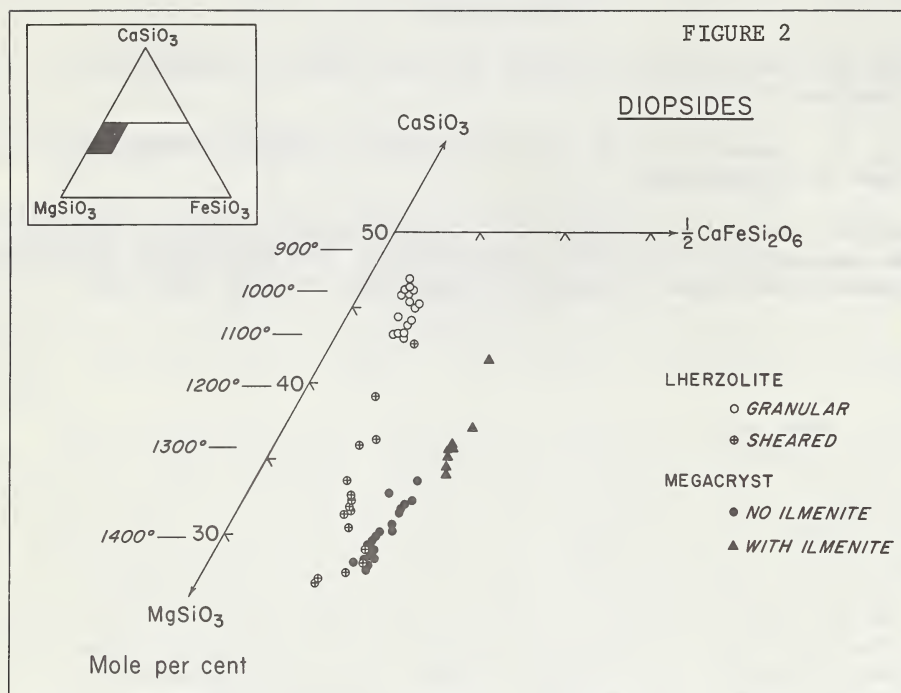
Fig. 1: Compositions of garnet discrete nodules compared with those from the lherzolites.

Fig. 2: Compositions of diopside discrete nodules compared with those from the lherzolites.

Fig. 3: Estimated equilibration conditions for pyroxene discrete nodules compared with the lherzolite geotherm. The calculated equilibration pressures have been corrected by the method of Wood and Banno.

FIGURE 1





PARTIAL MELTING OF PHLOGOPITE-BEARING SYNTHETIC SPINEL- AND GARNET-LHERZOLITES

M.S. Bravo, University of Luanda, Angola, and M.J. O'Hara, Grant Institute of Geology, University of Edinburgh.

The principal mineral phases of phlogopite-garnet or spinel-lherzolite appear in the six component model system $\text{CaO}-\text{K}_2\text{O}-\text{MgO}-\text{Al}_2\text{O}_3-\text{SiO}_2-\text{H}_2\text{O}$ (CKMASH) as phlogopite, spinel, pyrope-rich garnet, spinel, forsterite, enstatite and diopside.

An interpretation of results at 15 kb is presented in fig 1 which is a projection of starting compositions into the system $\text{CaO}-\text{Al}_2\text{O}_3-\text{K}_2\text{O}$ (CAK) from MgO , SiO_2 and H_2O (forsterite, enstatite and vapour) showing the nature of the additional crystalline phases (diopside, phlogopite or spinel) which will crystallize from the starting compositions, forsterite, enstatite and vapour already being present. Boundaries between the fields where diopside, phlogopite or spinel is the additional crystalline phase are shown, with an indication of the uncertainty in their location. The compositions studied are indicated. The unique liquid which is in simultaneous equilibrium with forsterite, enstatite, diopside, spinel, phlogopite and water-rich vapour has been located and its proportions of $\text{CaO}:\text{Al}_2\text{O}_3:\text{K}_2\text{O}$ read from the diagram (table 1, row 1). The geometric average composition from the uncertainty triangle is quoted.

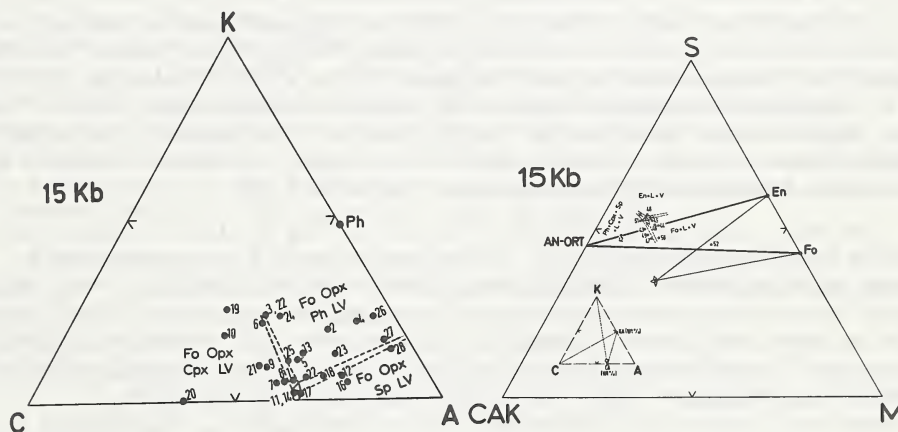


Fig 1. $\text{CaO}-\text{Al}_2\text{O}_3-\text{K}_2\text{O}$ diagram (wt%) showing projection of the forsterite, enstatite and vapour saturated liquidus surfaces in the system CKMASH at 15 kb.

Fig 2. $(\text{CaO}_{33.4}\text{Al}_2\text{O}_{36.6}\text{K}_2\text{O}_{3.0})-\text{MgO}-\text{SiO}_2$ system at 15 kb.

Compositions were synthesised using the appropriate C:A:K proportions (from fig 1) in a system (C:A:K). M.S. The boundaries of the fields in which forsterite, enstatite or diopside+phlogopite+spinel appear at the liquidus in the presence of water-rich vapour in this system were then determined (fig 2) and the unique liquid composition in simultaneous equilibrium with forsterite, enstatite, diopside, phlogopite, spinel and water-rich vapour read off (table 1, row 3) and converted to oxide weight percentages (table 1, row 5). The CIPW norm of this liquid is presented in table 2, row 1.

Table 1

Compositions (wt% proportions, water-free) of liquids in isobaric invariant equilibria with phlogopite-bearing spinel- or garnet-lherzolite in the presence of water-rich vapour.

		CaO	Al ₂ O ₃	K ₂ O	MgO	SiO ₂
1)	15 kb	980 \pm 10°C	33.4	63.6	3.0	
2)	30 kb	1080 \pm 10°C	33.2	54.5	12.3	
3)	15 kb	980 \pm 10°C		35.5		11.5
4)	30 kb	1080 \pm 10°C		29.5		18.0
5)	15 kb	980 \pm 10°C	11.9	22.6	1.0	11.5
6)	30 kb	1080 \pm 10°C	9.8	16.1	3.6	18.0
						53.0
						52.5
						53.0
						52.5

Table 2

CIPW norms of isobaric invariant liquids in equilibrium with water-rich vapour and phlogopite-bearing spinel or garnet lherzolite.

		Qz	Or	An	Di	Hy	Ol
1)	15 kb	980 \pm 10°C	6.5	6.3	58.5	0.2	28.5
2)	30 kb	1080 \pm 10°C	-	21.5	33.1	12.0	19.5
							13.8

In fig 2 the heavy triangle links the compositions of enstatite and forsterite to the point on the SiO₂-(CaO+K₂O+Al₂O₃) join where the CIPW norm of the composition is just saturated with silica (labelled An-Ort in fig 2; negligible diopside appears in this particular CAK ratio). The inset figure shows that the CAK proportions of the isobaric invariant liquid (small circle) are such that it is almost corundum-normative and far remote from peralkaline character (because K < A).

The more lightly delineated triangle in fig 2 links forsterite, enstatite and the piercing point in this section of the join diopside (CaMgSi₂O₆)-phlogopite(K₂Mg₆Al₂Si₆O₂₀(OH)₄)-spinel(MgAl₂O₄). The area inside this triangle represents the intersection with this composition plane of the subsolidus phlogopite-spinel-lherzolite mineral assemblage. The unique liquid with which it coexists at 15 kb has a composition lying outside this region. There will be a reaction relationship:-

forsterite+liquid = enstatite+diopside+phlogopite+spinel+vapour - I in the isobaric invariant equilibrium. If a phlogopite-spinel-lherzolite containing excess water vapour were to be partly melted at 15 kb, the initial liquid, if isolated and fractionally crystallized, would precipitate mineral assemblages resembling phlogopite-spinel websterite, containing no forsterite, and the residual liquids would become yet richer in normative quartz.

The initial liquid composition produced by partial melting has affinities with andesitic and high alumina basalt melts particularly in high quartz, anorthite and low diopside in the CIPW norm (table 2).

Results at 30 kb are presented in figs 3 and 4 and in tables 1 (rows 2, 4 and 6) and table 2 (row 2). The isobaric invariant liquid in equilibrium with phlogopite+garnet+diopside+enstatite+forsterite+vapour at 30 kb, although relatively rich in SiO₂, has higher MgO than at 15 kb, and there is substantial olivine, diopside and orthoclase in the CIPW norm. The liquid is far from being critically undersaturated in silica or peralkaline in character.

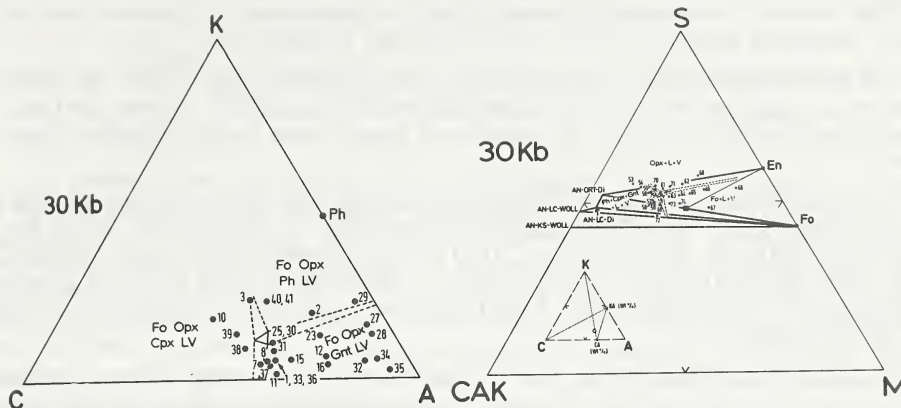


Fig 3. $\text{CaO}-\text{Al}_2\text{O}_3-\text{K}_2\text{O}$ diagram (wt%) showing projection of the forsterite, enstatite and vapour saturated liquidus surfaces in the system CKMASH at 15 kb.

Fig.4. $(\text{CaO}_{33.2}\text{Al}_2\text{O}_{354.5}\text{K}_2\text{O}_{12.3})-\text{MgO}-\text{SiO}_2$ system at 30 kb.

In fig 4 the heavy lines connect forsterite to the compositions within the system whose CIPW norms contain anorthite, orthoclase and diopside only (An-Ort-Di); anorthite-leucite-diopside (An-Lc-Di); anorthite-leucite-wollastonite (An-Lc-Woll) and anorthite-kalsilite-wollastonite (An-Ks-Woll). Enstatite is connected to the first of these piercing points and the heavily outlined triangles depict the compatibility assemblages in the CIPW norm as bulk compositions become increasingly undersaturated in silica within this system.

Also shown, and linked to enstatite and forsterite by light lines, is the piercing point in this section of diopside ($\text{CaMgSi}_2\text{O}_6$)-pyrope ($\text{Mg}_3\text{Al}_2\text{Si}_3\text{O}_{12}$)-phlogopite ($\text{K}_2\text{Mg}_6\text{Al}_2\text{Si}_6\text{O}_{20}(\text{OH})_4$). The area within this triangle represents the intersection with this composition section of the subsolidus phlogopite-garnet-lherzolite mineral assemblage. The unique liquid with which it coexists at 30 kb under water saturated conditions has a composition lying outside this region and there will be a reaction relationship:-

forsterite+liquid = enstatite+diopside+phlogopite+garnet+vapour - II in the isobaric invariant equilibrium.

If a phlogopite-garnet-lherzolite containing excess water vapour were to be partly melted at 30 kb, the initial liquid, if isolated and fractionally crystallized, would precipitate mineral assemblages resembling phlogopite-enstatite-eclogite or phlogopite-eclogite and the residual liquids would trend towards oversaturation in silica.

The initial liquid composition produced by partial melting at 30 kb has no affinities with common eruptive magmas, and like the liquid formed at 15 kb, it bears no resemblance to any suggested kimberlite fluid.

If kimberlite fluids are small scale partial melting products of phlogopite-bearing peridotites, the process must be assigned to greater pressures than 30 kb, or postulated to occur in the absence of a vapour phase, or in the presence of a vapour phase containing substantial

amounts of CO_2 etc.

The extract required to modify the 30 kb liquid to become the 15 kb liquid consists essentially of diopside and phlogopite.

In the presence of a water-rich vapour, enstatite is not in equilibrium with liquids critically undersaturated in silica in the system $\text{CaO-K}_2\text{O-MgO-Al}_2\text{O}_3-\text{SiO}_2-\text{H}_2\text{O}$ at pressures below some value greater than 30 kb.

In the K_2O free system CMASH the temperature of beginning of melting of water-saturated spinel- or garnet-lherzolite is $1000^\circ \pm 10^\circ\text{C}$ at 10 kb (Yoder and Chinner, 1960; Yoder, 1971; Ford unpublished), and $1000^\circ \pm 5^\circ\text{C}$ at 15 kb (new determination, Bravo 1973). Addition of K_2O to this alumina oversaturated system has very little effect upon the temperature of beginning of melting.

Unlike the situation in dry systems where garnet-pyroxene assemblages constitute a thermal divide between olivine-saturated and quartz-saturated liquids, fig 4, and reaction relationship II show that phlogopite-bearing eclogites with excess water melt 'incongruently', yielding olivine-bearing residua. The complementary liquids do not of course resemble kimberlite.

References

Yoder, H.S., Jr. 1971. Yb. Carnegie Inst. Wash., 69, 176-181.

Yoder, H.S., Jr. and Chinner, G.A. 1960. Yb. Carnegie Inst. Wash. 59, 78-81.

PRIMARY AND SECONDARY PHLOGOPITES AND CLINOPYROXENES
IN GARNET LHERZOLITE XENOLITHS

D. A. CARSWELL, Department of Geology, University of Sheffield,
Mappin Street, Sheffield S1 3JD, U.K.

As garnet lherzolites are the most common ultramafic xenolith type in the majority of kimberlite pipes (Mathias et al 1970), they appear to represent the predominant rock type in the regions of the upper mantle from which kimberlite originates or through which it passes during its emplacement into the crust. It is thus a reasonable proposition that the primitive upper mantle material, from which basalt magmas are derived, has a mineral and overall chemical composition largely similar to the standard garnet lherzolite xenoliths of the type previously analysed and described by Carswell and Dawson (1970).

Whilst the major element chemistry of the postulated primitive upper mantle material has now been fairly well established, whole rock analyses of garnet lherzolite xenoliths do not provide reliable figures of K_2O and H_2O due to the growth of secondary phlogopite, amphibole, and serpentine. It is therefore necessary to deduce the likely K_2O and H_2O values from a consideration of the primary mineralogy and mineral chemistry of these xenoliths.

Although phlogopite is only present as a minor phase in garnet lherzolite xenoliths, petrographic examination suggests the common presence of two generations of phlogopite growth. On the one hand it forms rare, large discrete plates, showing no apparent textural evidence of being in disequilibrium with the other primary minerals and hence thought itself to be primary. In addition it forms generally narrow rims around some garnets, where it is undoubtedly of secondary growth.

The phlogopites in six South African garnet lherzolite xenoliths were therefore analysed with an electron microprobe to see if significant chemical distinctions exist between the postulated primary and secondary phlogopites, and the analyses are presented in Tables 1 and 2.

Each of the analyses listed is an average of from two to six analyses of appropriate phlogopite grains in the xenolith in question. In the majority of cases the internal variation in the group of analyses averaged was strikingly small, and in fact it is apparent that there is little variation in composition within the groups of primary and secondary phlogopites from the different xenoliths. However, the primary phlogopites as a group have significantly lower TiO_2 , Cr_2O_3 and Al_2O_3 contents, lower Fe^{2+}/Mg^{2+} and Na^+/K^+ ratios, and higher SiO_2 contents than the secondary phlogopites. They also have much lower TiO_2 contents and Fe^{2+}/Mg^{2+} ratios than the previously postulated primary upper mantle phlogopites from a Lashaine garnet lherzolite xenolith (Dawson et al 1970) and from Jan Mayen alkali basalts (Flower 1971). They are therefore thought more likely to represent a primary phase in equilibrium with the four phase garnet lherzolite assemblage in the upper mantle than the Lashaine and Jan Mayen phlogopites.

Recent experimental data (Yoder and Kushiro 1969; Modreski and Boettcher 1972) has indicated that the stability field of phlogopite is likely to extend down into the upper mantle - perhaps to depths as great as 150-200 kms. in continental regions with low geothermal gradient.

The presence of on average 1% by volume of primary phlogopite in the garnet lherzolite xenoliths studied, thought to have originated from depths of 100-150 kms., suggests that the primitive upper mantle material at such depths may contain on average about 0.10 wt.% K_2O and 0.03 wt. % H_2O .

An interesting petrographic feature of the clinopyroxenes in all six xenoliths studied, except CB6, is the existence in most grains of rather cloudy 'porous' outer zones around clear pale green cores. These 'porous' rims are variable in width even in the same grain and in places cut right across the grains and almost completely replace the original clinopyroxene.

Both the clear primary clinopyroxene cores and the cloudy 'porous' clinopyroxene rims have been analysed by electron microprobe and the critical chemical features are summarised in Tables 3 and 4.

By far the most striking difference in composition between the clear clinopyroxene cores and the cloudy margins is the decrease in the Al_2O_3 and Na_2O contents in the latter, reflected in the much lower percentage of jadeite molecule. On the other hand differences in Cr_2O_3 are negligible and in $Ca/Ca+Mg$ ratio only minimal - corresponding to equilibrium temperatures only some 20-80°C lower for the rims than the cores, on the basis of the solid solution limits in the synthetic diopside-enstatite system at 30 kbs. pressure (Davis and Boyd 1966).

No additional Na_2O and Al_2O_3 rich phase such as plagioclase was detected to be associated with the jadeite depleted clinopyroxene rims, at least in amounts resolvable with the microprobe. It seems most likely that the Na_2O and Al_2O_3 released, possibly as a consequence of the pressure decrease during kimberlite emplacement, has been taken up in both the secondary phlogopite and amphibole. It is noteworthy that the secondary phlogopites have higher Na^+/K^+ ratios than the primary phlogopites.

References:

CARSWELL, D.A. and DAWSON, J.B. 1970. *Contr. Mineral. Petrol.* 25, 163-184.
 DAVIS, B.T.C. and BOYD, F.R. 1966. *J. Geophys. Res.* 71, 3567-3576.
 DAWSON, J.B. et al. 1970. *J. Petrology* 11, 519-548.
 FLOWER, M.P.J. 1971. *Contr. Mineral. Petrol.* 32, 126-137.
 MATHIAS, M. et al. 1970. *Contr. Mineral. Petrol.* 26, 75-123.
 MODRESKI, P.J. and BOETTCHER, A.L. 1972. *Am. J. Sci.* 272, 852-869.
 YODER, H.S. and KUSHIRO, I. 1969. *Am. J. Sci.* 267-A, 558-582.

TABLE 1 - Primary Phlogopites

Wt.%	CK1	CK2	CK3	CK4	CB6
SiO ₂	40.73	41.24	41.10	41.54	41.67
TiO ₂	00.28	00.22	00.15	00.26	00.68
Al ₂ O ₃	12.81	12.39	13.24	12.47	12.20
Cr ₂ O ₃	00.86	00.70	00.60	00.75	00.61
*FeO	02.63	02.64	02.56	02.52	02.78
MnO	00.01	00.05	00.01	00.03	00.02
MgO	26.52	26.55	27.87	26.53	26.49
CaO	00.02	00.02	00.02	00.01	00.01
Na ₂ O	00.75	00.76	00.99	00.91	00.31
K ₂ O	09.31	09.32	08.78	09.16	10.21
TOTAL	93.92	93.89	95.32	94.16	94.98
Fe ²⁺ /Mg ²⁺	0.056	0.056	0.051	0.053	0.059
Na ⁺ /K ⁺	0.123	0.124	0.172	0.151	0.046

*FeO - Total Iron as FeO

TABLE 2 - Secondary Phlogopites

Wt.%	CK1	CK3	CK4	CB4	CB6
SiO ₂	39.69	39.04	39.22	39.06	39.33
TiO ₂	01.45	00.45	00.86	01.36	01.41
Al ₂ O ₃	13.93	16.06	14.54	15.13	14.81
Cr ₂ O ₃	01.60	01.51	01.36	01.57	01.50
*FeO	03.12	03.15	03.17	02.95	02.90
MnO	00.10	00.02	00.14	00.05	00.02
MgO	24.83	25.27	24.48	25.10	24.67
CaO	00.03	00.02	00.03	00.02	00.03
Na ₂ O	00.92	01.41	01.82	01.05	00.92
K ₂ O	09.06	07.87	07.38	08.41	09.14
TOTAL	94.73	94.80	93.00	94.70	94.73
Fe ²⁺ /Mg ²⁺	0.070	0.070	0.073	0.066	0.066
Na ⁺ /K ⁺	0.154	0.272	0.376	0.189	0.153

*FeO - Total Iron as FeO

TABLE 3 - Primary Clinopyroxene Cores

Wt.%	CK1	CK2	CK3	CK4	CB4	CB6
Al ₂ O ₃	3.37	3.48	3.39	2.30	4.63	2.54
Cr ₂ O ₃	1.89	1.64	1.85	1.61	2.69	1.62
Na ₂ O	2.74	3.12	3.09	2.08	4.02	2.33
%Jadeite	9.0	13.5	8.8	4.7	13.8	3.6
Ca/Ca+Mg	0.471	0.462	0.472	0.477	0.477	0.458

TABLE 4 - Cloudy Clinopyroxene Rims

Wt.%	CK1	CK2	CK3	CK4	CB4
Al ₂ O ₃	2.31	1.43	2.30	1.26	3.44
Cr ₂ O ₃	1.76	1.82	1.82	1.60	2.65
Na ₂ O	2.24	1.76	2.19	0.96	2.29
%Jadeite	2.6	4.1	3.5	0.3	6.5
Ca/Ca+Mg	0.482	0.471	0.477	0.501	0.470

MINERALOGY, PETROLOGY AND PETROGENESIS OF THE KIMBERLITE
FROM SOMERSET ISLAND, N.W.T., CANADA

D.B. Clarke, Dalhousie University, Halifax, N.S., Canada
R.H. Mitchell, Lakehead University, Thunder Bay, Ont., Canada

Mitchell and Fritz (1973) have given the first general description of the location, tectonic setting and mineralogy of the Somerset Island kimberlite. This paper deals with the mineralogy and texture in detail, interprets the crystallization history and speculates on the petrogenetic evolution of this occurrence of kimberlite.

The primary crystallization products are tabulated below:

<u>Name</u>	<u>Approx. Mode</u>	<u>Pheno- cryst</u>	<u>Ground- mass</u>	<u>Composition or Compositional Range</u>
Olivine	35	X	X	Fo ₉₀ -Fo ₈₈
Garnet	1	X		Gr ₁₂ Py ₆₅ Al ₁₅ Sp ₁ Uv ₇
Phlogopite	1	X	X	Phl ₈₉ Ann ₁₁
Ilmenite	<1	X		Ilm ₅₃ Geik ₄₇ -Ilm ₁₀₀
Chromite	2	X	X	Chr ₇₅ Sp ₂₅
Red Chrome Spinel	<1	X		Chr ₆₀ Sp ₄₀
'Magnetite'	<1	X		Mt ₉₈ Usp ₂ -Mt ₆₀ Usp ₄₀
Perovskite	2		X	FeO 1.5%, Nb ₂ O ₅ 0.3-0.9%
Rutile	1	X	X	
Pyrite	<1		X	Ni 0-7%
Heazlewoodite	<1		X	Fe 1-2%
Chalcopyrite	<<1		X	
'Native Silver'	<<1		X	Ag 91%, Co 0.01% Ni 0.1%, Fe 1%
Carbonate Groundmass	15		X	MgO = 17%, FeO 3%
Silicate Groundmass	35		X	

Secondary minerals include serpentine, chlorite and minor magnetite. In addition, there are single crystals of enstatite-bronzite and clinopyroxene which may be xenocrysts and a long list of xenoliths including monomineralic phlogopite aggregates, highly altered eclogite(?), lherzolite and many other assemblages including various combinations of phlogopite, clinopyroxene, serpentine, chlorite, oxides, sulphides, carbonate and apatite. Also, there are at least three distinctly different types of Palaeozoic sedimentary carbonate xenoliths.

There is considerable textural evidence for the formation of an immiscible carbonate liquid at some intermediate stage in the crystallization of the kimberlite. There is intimate mixing of carbonate and microcrystalline silicates in the groundmass ranging from isolated blebs of carbonate in the silicate groundmass to isolated blebs of silicate in the carbonate groundmass. The carbonate groundmass is not believed, on compositional or on textural grounds, to be in any way related to the xenoliths of sedimentary carbonate rocks, all of which show sharp contacts with both the silicate and carbonate groundmasses.

The most striking textural feature is the wide variety of epitaxial zoning displayed by the late-stage primary minerals where rapid rates of crystallization have prevailed. These zonations include the following sequences (core to rim):

- 1) olivine - perovskite + serpentine - rutile
- 2) magnesian ilmenite - serpentine + rutile - perovskite - rutile*
- 3) chromite - carbonate - perovskite - rutile -
(+heazlewoodite)
- 4) chromite - "spinel" - perovskite*
- 5) magnetite - ulvöspinel - ilmenite*
- 6) red spinel - opaque - carbonate - rutile
- 7) heazlewoodite - pyrite

(*Chemical analyses are given in Table 1 for parts of sequences indicated above.)

Except for the sulphides, all zonations are towards increasing TiO_2 and must reflect a late-stage concentration of titanium in the silicate liquid.

The sequence of crystallization may be generalized as follows: Pre-Fluidization - red spinel, phlogopite, garnet, olivine, possibly some of the large rounded chromites, and the extensive reaction rims of the phlogopites and garnets.

Post-Fluidization - all other minerals listed above as groundmass, including the euhedral groundmass chromites with epitaxial zoning. The one important mineral not easily assigned to a position in the crystallization sequence is the magnesian ilmenite. The continuous zoning from a highly magnesian central region outwards to a lower magnesian edge suggests that these crystals grew in an environment of high but rapidly decreasing pO_2 , or high but rapidly decreasing MgO , or both. The restricted occurrence of magnesian ilmenite in the silicate groundmass, its variable composition and the apparent late-stage concentration of TiO_2 in the silicate groundmass, all suggest a Post-Fluidization origin for these grains. However, the crystals are anhedral and do not have their magnesian 'core' in the centre of the grains. This might indicate a Pre-Fluidization origin followed by magmatic corrosion and mantling by such Post-Fluidization minerals as perovskite and rutile.

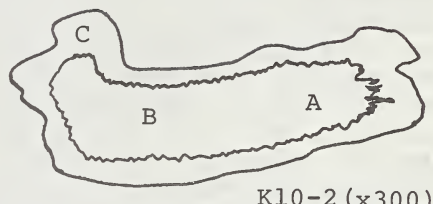
Two of the most important problems still to be resolved are the very late-stage concentration of nickel, as evidenced by the epitaxial zones of heazlewoodite on the chrome spinels, and the enigmatic existence of native silver which occurs as common isolated grains in the silicate groundmass.

Reference: Mitchell, R.H. and Fritz, P.
Canadian J. Earth Sci. 10, 384-393, 1973.

(Table 1 overleaf)

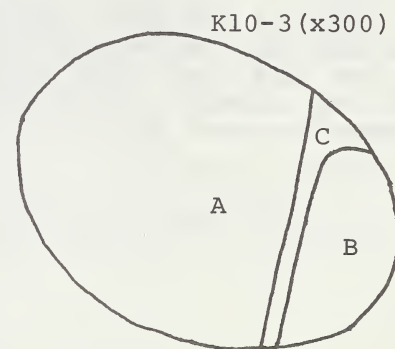
ZONED MAGNESIAN ILMENITE-PEROVSKITE

	<u>K10-2A</u>	<u>K10-2B</u>	<u>K10-2C</u>
Ti ₀ ²	58.45	57.45	54.93
Zr ₀ ²	0.00	0.00	0.08
Al ₀ ⁰	0.06	0.06	0.44
Cr ₂ ⁰ ₃	0.02	0.03	0.00
Fe ₀ ² ₃	26.17	30.88	1.39
Mn ₀	0.65	0.58	0.00
Mg ₀	13.46	10.66	0.14
Ni ₀	0.05	0.04	0.01
Ca ₀	0.29	0.30	35.00
Nb ₂ ⁰ ₅	0.10	0.10	0.71
	<u>99.25</u>	<u>100.10</u>	<u>92.70</u>



ZONED MAGNETITE-ULVOSPINEL-ILMENITE

	<u>K10-3A</u>	<u>K10-3C</u>	<u>K10-3B</u>
Si ₀ ²	-	0.31	-
Ti ₀ ²	1.16	19.41	53.42
Zr ₀ ²	0.03	-	0.00
Al ₀ ⁰	0.45	1.37	0.08
Cr ₂ ⁰ ₃	0.11	0.02	0.01
Fe ₀ ² ₃	66.05	27.66	1.39
Fe ₀ ³	31.14	44.49	41.41
Mn ₀	0.24	0.75	1.29
Mg ₀	0.34	1.97	3.60
Ni ₀	0.10	-	0.02
Ca ₀	0.17	0.25	0.17
Nb ₂ ⁰ ₅	0.02	-	0.05
	<u>99.81</u>	<u>96.23</u>	<u>101.44</u>



ZONED CHROME SPINEL- "SPINEL"-PEROVSKITE

	<u>K10-4C</u>	<u>K10-4A</u>	<u>K10-4B</u>
Ti ₀ ²	5.10	13.25	55.35
Zr ₀ ²	-	0.00	0.09
Al ₀ ⁰	11.29	9.72	0.42
Cr ₂ ⁰ ₃	43.77	0.19	0.00
Fe ₂ ⁰ ₃	7.44	38.33	-
Fe ₀ ² ₃	18.66	21.54	1.71
Mn ₀	0.34	0.43	0.00
Mg ₀	12.64	13.94	0.13
Ni ₀	-	0.13	0.03
Ca ₀	0.10	0.95	37.06
Nb ₂ ⁰ ₅	-	0.00	0.89
	<u>99.34</u>	<u>98.48</u>	<u>95.68</u>

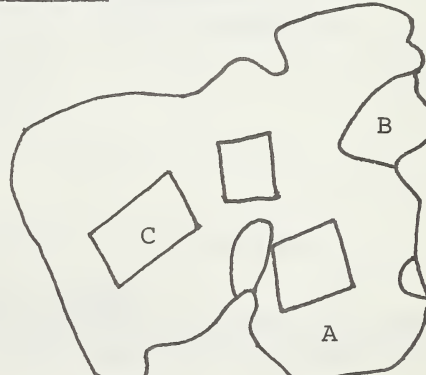


Table 1

THE EMPLACEMENT OF SOME DIATREME-FACIES KIMBERLITES

C.R. Clement

Geology Department, De Beers Consolidated Mines Ltd., Kimberley. S.A.

Intrusive kimberlite breccias from several South African pipes or pipe-like enlargements on dykes contain abundant fragments of country rock (mainly derived from Karroo strata) including huge, often brecciated, xenolithic masses ("floating reefs") which are located at positions well below their original stratigraphic levels. The fragments have been metasomatically altered but show no pyrometamorphic effects indicative of relatively high temperatures during or subsequent to their incorporation in the kimberlite. Tuffaceous kimberlites with xenolith contents similar to these intrusive breccias have been ascribed to explosive boring (Wagner, 1914) or gas-solid fluidised intrusion (Dawson, 1962). The origin of these intrusive breccias cannot, however, be attributed to either of these processes since the rocks lack the essentially fragmental textures characteristic of the tuffaceous varieties.

A striking petrographic feature of the intrusive breccias is the presence of numerous, frequently highly micaceous, globular or pellet-like segregations (0,1mm to 8 cms in diameter) which are set, together with scattered megacrysts and country rock xenoliths in a matrix of calcite and serpentine. In some examples sheaf-like aggregates of slender apatite crystals, considered to result from quenching (Wyllie, Cox & Biggar, 1962), are associated with the matrix calcite.

This texture is particularly well displayed by kimberlite from the Finsch pipe in which the segregations exhibit the following features: Many are spherical or ellipsoidal but others have irregularly curved shapes and lobate protrusions. The more irregular shapes are often the result of coalescence of two or more individuals. Sometimes clear separation of segregations is absent, the material forming web-like patches with lobate margins against the enclosing and interstitial calcite-serpentine matrix. Commonly individual segregations contain more or less centrally located kernels. Most kernels consist of single grains of olivine (often pseudomorphously replaced, mainly by serpentine). The two generations of olivine common to many kimberlites (Dawson, 1971) are represented among the kernel population. Megacrysts of phlogopite and garnet and rare peridotitic and dunitic fragments also occur as kernels as do metasomatically altered country rock fragments. Some segregations are, however, devoid of kernels. The fine-grained or crypto-crystalline material around the kernels or forming the bulk of kernel-free segregations consists mainly of reddish-brown slightly pleochroic phlogopite and a little colourless serpentine. Set in this groundmass are microphenocrysts (up to 0,4mm) of pale brown phlogopite and serpentinised olivine together with minute grains of perovskite, magnetite, and chromite. Elongate micro-phenocrysts are commonly oriented tangentially to the outer surfaces of the segregations.

The relative proportions of calcite and serpentine in the matrix surrounding the segregations vary considerably. In some instances calcite is restricted to scattered irregular grains, shreds and aggregates within serpentine but elsewhere the matrix consists almost entirely of calcite. The amount of calcite present depends on the degree to which it has been replaced by serpentine. Evidence of this replacement includes: Isolated rafts of calcite in serpentine which

are optically continuous and show identical cleavage orientations, highly irregular replacement-type boundaries of many calcite grains against serpentine; pronounced embayments of serpentine in calcite, often with rhombohedrally stepped margins reflecting original calcite cleavages; pseudomorphous replacement of individual calcite aggregates by serpentine; and areas of serpentine containing numerous minute residual shreds of calcite where replacement has been incomplete. In view of this evidence it is concluded that the interstitial material between the segregations originally consisted largely of calcite. This conclusion is supported by the abundance of calcite in much of the kimberlite, by the poikilitic enclosure of small segregations in calcite and by the presence, even where the matrix is mainly serpentine, of residual aggregates of calcite which locally completely fill interstitial areas between segregations.

Kimberlites texturally similar to the Finsch material are present at the Monteleo, Andriesfontein, Muldersvlei, Dutoitspan, Wesselton, Koffyfontein and Klipfontein occurrences although the textural relationships are not always as clearly revealed. All these kimberlites do, however, contain segregations (similar to those of the Finsch kimberlite) which are set in serpentine-calcite matrices.

Several features of the matrix calcite in these kimberlites are interpreted as evidence that it is a late-crystallising primary mineral. These include the abundance of calcite (where massive replacement by serpentine has not occurred); the lack of gradational relationships between calcite and other minerals (except later serpentine); its occurrence as anhedral fine to medium sized grains (0,1 to 0,7mm), its poikilitic enclosure of other minerals and small phlogopitic segregations.

The clear separation of the carbonate and silicate phases, resulting in the emulsion-like textures described, is attributed to the development, during emplacement of the kimberlites, of late-stage, low temperature, immiscible K-rich silicate and carbonatitic liquids. Globular segregations of the silicate phase within the carbonate phase are ascribed to the greater viscosity of the former, the likelihood that it started to crystallise prior to the carbonatitic liquid, and the original abundance of the carbonatitic liquid which probably acted as a transporting medium during intrusion. Under these conditions it might be expected that solid material already present would provide nucleating centres around which the silicate fraction would tend to crystallise thereby accounting for the presence of kernels and the spherical shapes of many segregations. The carbonatitic liquid would be extremely fluid (Wyllie, 1966) and would crystallise in an interstitial relationship to the silicate segregations.

The following model for the development of the immiscibility relationships and emplacement of the kimberlites is proposed:

After the crystallisation of early phenocrysts the residual ascending kimberlite magma (carrying xenocrysts, phenocrysts and some xenoliths) differentiates, at relatively high crustal levels, into K-rich silicate and carbonatitic liquids, accompanied by a coexisting gaseous phase. Continued intrusion is accompanied by the separation of the gaseous phase and its accumulation at the head of the magma column where it forms a gas cap or aureole. Upon further uprise a stage is reached where the internal gas pressure exceeds the lithostatic load and the diatreme is formed by explosive breaching of the cap rocks. The rapid pressure drop resulting from break-through is accompanied by the upsurge of partly degassed magma fractions which incorporate explosively

disrupted cap rock fragments and material which slumps from the walls of the diatreme. The presence of large "floating reefs" and smaller xenoliths at positions well below their original stratigraphic levels presents few difficulties if they are considered to have sunk through a low density, essentially carbonatitic liquid. The low temperatures envisaged, which are consistent with experimental results (eg. Wyllie, 1966; Franz and Wyllie 1967; Seifert and Schreyer, 1968), explain the absence of thermal metamorphic effects on xenoliths and wallrocks.

Franz and Wyllie (1967) suggested on experimental grounds that the fluid involved during the fluidised intrusion of some kimberlites may be a carbonatitic liquid rather than a dense gas phase; a concept which appears very similar to the final stages of emplacement proposed here. Postulation of an essentially carbonatitic transporting fluid (Watson, 1967; Franz and Wyllie, 1967 and this paper) overcomes many of the objections to high level magmatic activity within kimberlite diatremes.

REFERENCES

Dawson, J.B.	(1962)	Geol. Soc. Am. Bull., 73: 545-560
	(1971)	Earth-Sci. Rev., 7: 187-214
Franz, G.W. and	(1967)	In. P.J. Wyllie (Editor), Ultramafic and
Wyllie, P.J.		Related Rocks, Wiley, New York, N.Y.,
		323-326.
Seifert, Von F. and	(1968)	Geologische Rundschau, 57: 349-362.
Schreyer, W.		
Wagner, P.F.	(1914)	The Diamond Fields of Southern Africa. The Transvaal Leader, Johannesburg.
Watson, K.D.	(1967)	In. P.J. Wyllie (Editor), Ultramafic and Related Rocks, Wiley, New York, N.Y.,
		312-323.
Wyllie, P.J.	(1966)	In Tuttle, O.F. and Gittens, J. (Editors), Carbonatites. Intersci. Publishers, New York. 311-352.
	(1962)	Jour. Petrology, 1: 1-46
Cox, K.G. and Biggar,		
G.M.		

THE BUSHMANLAND KIMBERLITES

by

A.K. Cornelissen* and W.J. Verwoerd**

*19 Josling Street, Upington, South Africa

**University of Stellenbosch, South Africa

The Bushmanland plateau is situated south of the Orange River and approximately 100 km inland, adjoining a highly dissected portion of the Western Escarpment of South Africa. Kimberlite was first reported from this area by Reuning (1931) who sought to establish the source of the coastal diamonds at the mouth of the Buffels River (Kleinsee). He claimed the discovery of a kimberlite dyke and seven pipes, including a diamondiferous one on the farm Burtonsputs. Subsequently Du Toit (1939) stated that a small diamond had been found in a pipe on the boundary between the farms Gamoep and Koppies-kraal. On chemical grounds he considered this occurrence to be intermediate between kimberlite and melilite basalt.

Between 1928 and 1961 the Namaqualand-Bushmanland area was closed to diamond prospecting with the result that it remained one of the least known kimberlite provinces in South Africa. An intensive prospecting campaign followed during the years 1961 - 1966. At least 151 pipe-like features were drilled to depths ranging from 20m to 279m and kimberlitic material was encountered in 77 of them. It is the purpose of this paper to present some of the geological information that were brought to light. Grateful acknowledgement is due to the three mining companies concerned (De Beers, Rand Mines and the O'okiep Copper Company) for access to plans, logs and reports which were formerly considered as confidential.

Distribution: Some 270 pipe-like bodies are known to occur in an area of approximately 8 400 sq. km from the vicinity of Platbakkies in the south to Aggeneys in the north. Without any doubt many more remain to be discovered. Only about two-thirds of this area was held under option and properly prospected. In the dissected country the pipes generally show up on aerial photographs as hills or circular depressions among gneiss outcrops but towards the east they are covered by calcrete which reaches a thickness of 1 - 2m on the pipes. Magnetometer traverses proved useful in locating some pipes and in delineating their boundaries. An aeromagnetic map by the Geological Survey shows hundreds of small circular anomalies but these could not be correlated successfully with individual pipes. It seems likely that the Bushmanland Province consists of several clusters in which pipes are more closely spaced; outliers which may or may not belong here are found as far afield as Bitterfontein and Pofadder.

The regional structure of the gneisses appears to have exerted no influence on the emplacement of the pipes but prominent vertical joints trending N15°W, N60°W and N55°E are responsible for the alignment of some of them. Joint directions can only be established in the dissected area west of the plateau. Attention is also drawn to the fact that several other manifestations of volcanic activity of the type usually associated with cratonic upwarp are located along a zone parallel to the west coast of the continent: trachyte, carbonatite and olivine-melilitite near Sutherland, carbonate-rich diatremes in the Great Karasberge, phonolite in the Klinghardt Mountains, kimberlitic rocks near Gibeon, carbonatitic diatremes around Brukkaros and plugs of trachyte and phonolite between Windhoek and Rehoboth. The warping probably preceded the separation of Africa and South America during the Cretaceous.

Description: The pipes fall in three categories: (a) Melilite and melilite-nepheline basalts (olivine melilitite) that are clearly distinguishable from the others. They form conspicuous brown rubble-strewn hills. The rocks are perfectly fresh. They were first described by Rogers (1911) and genetically linked with kimberlite by Taljaard (1937) and are at present being studied by Mr. A. Moore in the Department of Geochemistry, University of Cape Town.

(b) Sediment and breccia-filled diatremes. This description applies to the majority of occurrences. They range from 50m to 500m in diameter and are occupied by shale, sandstone, grit, arkose and conglomerate showing graded bedding. The sediments are often disturbed by great blocks of country rock that collapsed into the crater. The latter may be adjoined by a volcanic neck (as on Riembreek and Kap-Kap), consisting wholly of angular blocks of gneiss measuring up to several metres across and testifying to repeated explosive eruptions. More tranquil crater-filling conditions and a temperate climate are reflected elsewhere by deposits of carbonaceous shale, dysodile and mudstone with calcareous intercalations. These contain fossil frogs and dicotyledonous leaf impressions (Haughton 1931, Rennie 1931, Kirchheimer 1934). Drilling has proved that such sediments extend down to depths of 250m (Koppieskraal no. 5) and more than 266m (Hoendersvlei). In many cases e.g. Burtonspits, Gamoep no. 1 and Koppieskraal no. 5 the shales were found to have intercalations of blue-green tuffaceous kimberlite towards the base (cf. chemical analysis by Reuning, 1934) and eventually to overlie solid blue-ground resembling kimberlite breccia. The prospecting programme thus strengthened the opinion that the diatremes and sediment-filled depressions are surface expressions of deep-seated pipes with kimberlitic affinities.

A peculiar feature of the sediment-filled pipes is the presence of late-stage silicification around their margins:

ferruginous opal, veins of opaque white silicified kaolin and sometimes manganese oxide encrustations afford excellent indications of the proximity of a pipe. In a semi-arid area such as this the pipes are of considerable importance as aquifers.

(c) A few bodies (some of them dyke-like rather than pipe-like) are known where weathered kimberlitic rock are exposed at the surface. The best-known occurrence is the one (Gamoep no. 1) referred to by Du Toit (1939) where an off-shoot from the sediment-filled pipe consists of "hardebank." It contains nodules of an earlier kimberlite(?) in which chrome-diopside appears to be concentrated. No undoubtedly eclogite or peridotite inclusions have been found. The only known occurrence with a large amount of biotite in a weathered serpentinous groundmass is the one on the boundary between Papkuilsfontein and Couragiefontein. A heavy residue from a similar decomposed kimberlite(?) on Kap-Kap yielded ilmenite but no garnet.

Age: The Bushmanland pipes cannot be dated too closely yet.

The fossil evidence from the crater deposits indicate an Upper Cretaceous or Eocene age. Detailed investigation of fossils collected during the prospecting activities are still in progress.

Composition and Mineralogy: The results of the prospecting were not only disappointing, but it actually failed to yield a single diamond from any of these pipes, despite the fact that several thousand loads were treated in washing plants. Consequently some doubt has arisen about the validity of their identification as kimberlites and the older reports have come to be regarded with skepticism.

Unfortunately most bore-hole samples have been destroyed and complete analyses of Bushmanland kimberlites are not available. Partial analyses for SiO_2 , Al_2O_3 , FeO and MgO have been carried out on 512 samples and these results led one of us (A.K.C.) to the conclusion that only a few pipes (e.g. Gamoep no. 1, Klein Katvlei no. 1, Koppieskraal no. 18, Vermeulens Rust no. 1) contain classical kimberlite; the rest are deficient in magnesia.

In thin section the kimberlitic rocks present the usual intensely altered appearance. The following minerals were identified in heavy concentrates from the bore-holes: ilmenite (ubiquitous), garnet (purple, red and brown), chrome-diopside, enstatite (En_{80-85}), zircon, biotite, pyrite, magnetite and barite. Olivine and perovskite are sometimes present, undoubtedly derived from melilite basalt. In addition to pyrope with $n=1.74 - 1.76$ and $a=11.55\text{A}$, more almandite-rich garnets (from gneiss?) were also found. The ilmenite shows a variable composition and variable magnetic properties.

Picroilmenite with 10,20% MgO and 57,00% TiO₂, was recovered from Banke no. 3 but several other analysed samples contain less than 6% MgO and are low in titania. Indications are that strongly magnetic ilmenite or titaniferous magnetite is associated with the "low-magnesia kimberlites" and that chrome-diopside is absent from them. The real affinities of this rock type appears to be problematic. Hydrothermally altered melilite-bearing rocks may have been confused with kimberlite. However, the presence of typical "indicator minerals" in at least some of the pipes would seem to confirm the existence of true kimberlite in this province.

Conclusion: The Bushmanland pipes attracted the attention of geologists mainly for three reasons:

(a) They were considered to be the most likely source of the alluvial diamonds along the lower and upper reaches of the Buffels River to the west and the Koa River valley to the east (eg. on Galputs and Bosluispan). This problem has not been solved. In Tanzania over 200 kimberlite occurrences were found during a R4 million prospecting campaign, yet nearly all of them are barren and the Mwadui mine remains the only one of economic importance. (Edwards and Howkins 1966). Thus there is still a possibility that a diamondiferous pipe may be discovered in Bushmanland. The two provinces have many features in common.

(b) The former existence of craters 250m deep and their subsequent filling by lacustrine sediments represent aspects of the emplacement of kimberlite that are unknown elsewhere in South Africa. Does this imply a difference in erosion level, age or eruptive mechanism?

(c) The age-old question whether kimberlite and melilite basalt are genetically related may possibly be answered here. It has been claimed that both rock types are found together in the pipes on Tauseb and Klein Katvlei and that the kimberlite pipe on Kamiebees contains inclusions of melilite basalt. Geological relationships are not sufficiently clear to confirm this.

From the above it should be clear that a detailed study of the Bushmanland pipes promises to elucidate many intriguing problems of kimberlite geology.

References

1. Du Toit, A.L. 1939. The Geology of South Africa. 2nd.Ed.
2. Edwards, C.B. and J.B. Howkins 1966. Econ. Geol. 61, 537-554.
3. Haughton, S.H. 1931. Trans. roy. Soc. S. Afr. 19, 233-249.
4. Kirchheimer, F. 1934. Trans. roy. Soc. S. Afr. 21, 41-50.
5. Rennie, J.V.L. 1931. Trans. roy. Soc. S. Afr. 19, 251-253.
6. Reuning, E. 1931. Trans. roy. Soc. S. Afr. 19, 215-232.
7. Reuning, E. 1934. Trans. roy. Soc. S. Afr. 21, 33-39.
8. Rogers, A.W. 1911. Ann. Rep. Geol. Comm. Cape of Good Hope, 16, 7-84.
9. Taljaard, M.S. 1937. Trans. geol. Soc. S. Afr. 39, 291-316.

BULK COMPOSITIONS OF ULTRAMAFIC NODULES FROM THE MATSOKU PIPE AND THEIR
RELATION TO KARROO BASALTS

By

K.G. Cox, J.J. Gurney and B. Harte

Studies have been carried out to determine whether any simple relationships exist between the bulk compositions of peridotitic nodules from the Matsoku Pipe and the Karroo basalts, which the pipe cuts. A small proportion of the nodules is comparatively rich in garnet and clinopyroxene and thus has more basaltic compositions than the majority, which is clinopyroxene- and garnet-poor ilherzolite. However none of the garnet-clinopyroxene-rich samples has a bulk composition which can give rise to Karroo basalt by any simple crystal-liquid fractionation process (e.g. removal of olivine, orthopyroxene or both). Thus at present the proposition that such nodules might represent trapped Karroo liquids can not be proved.

An alternative hypothesis, that the garnet-clinopyroxene-rich nodules, many of which show coarse mineralogical banding, are variably sorted crystal cumulates associated with the extraction of basaltic liquids is perhaps more attractive. Only major element characters have so far been studied and amongst these the behaviour of Na seems to place considerable restraints on the types of relationship which may be postulated. Na is enriched in Karroo basalts by a factor of about 15 relative to the garnet-clinopyroxene-rich nodules. Even allowing for modest amounts of olivine fractionation at low pressures in the basalt magma this still leaves a ten-fold enrichment to be accounted for. Experimental melting of the nodules is clearly required to ascertain whether their partial melts have the required characteristics.

THE PETROCHEMISTRY OF KIMBERLITE
AUTOLITHS

R.V. Danchin*, John Ferguson[†], J.R. McIver[†]
and P.H. Nixon^f

* Anglo American Research Laboratories

+ University of the Witwatersrand

f Department of Mines, Lesotho.

Diatreme facies of kimberlite frequently contain nucleated spheroidal bodies varying in size from a few millimetres to 70 millimetres in diameter. These autoliths consist of rock or mineral fragment nuclei which usually make up only a small volume percentage, encased in fine-grained kimberlitic material. It is thought that autoliths represent crystallisation of kimberlitic magma around a nucleus so that these bodies are more likely to reveal the matrix composition of kimberlites than the normally chaotic host kimberlite with its attendant xenolithic and xenocrystic material (Ferguson *et al.* in press). The nuclei of the autoliths comprise both mantle and crustal derived fragments. Olivine is the dominant mineral of the autoliths occurring as euhedral to subhedral phenocrysts 0.15 to 0.80 mm in diameter and having compositional range of $_{90-94}$ FO. Other possible primary phases include apatite, calcite and dolomite. Alteration reaction and minor accidental products include serpentine, ilmenite, phlogopite, spinels, perovskite and rutile.

Major element compositions were determined for a total of 26 autoliths from Wesselton Mine and various localities in Lesotho, and a cluster analysis program was used to compare the chemistry of these autoliths with 96 kimberlites and alkaline ultramafic rocks associated in space and time. It was found that the major element chemistry of the autoliths did not offer any unique composition but grouped with two of five varieties of kimberlite. Relative to the major kimberlite groups not clustering with autoliths the latter are enriched in TiO_2 , P_2O_5 , K_2O and MnO and impoverished in MgO . Further confirmation of the similarities between autoliths and kimberlites is given by their low $K:Rb$ and $Sr^{87}:Sr^{86}$ values. The $Sr^{87}:Sr^{86}$ ratio for Lesotho autoliths gives values between 0.7040 and 0.7045 (Hugh Allsopp, personal communication), which are comparable to the lowest values yet recorded for kimberlites (Berg and Allsopp, 1972).

On the CMAS tetrahedron (O'Hara, 1968) kimberlites lie on a well-defined olivine control line trending sub-parallel to the CAM plane consistent with melting of a four-phase garnet lherzolite mantle rock at depths equivalent to more than 40 Kb. Autoliths have compositions which plot near the extremity of the main kimberlite trend showing no major differences to most kimberlite other than having fractionated more olivine than the more primitive varieties. This supports the contention that the autoliths represent kimberlite magma which has only undergone olivine fractionation and has erupted from depth equivalents

of greater than 40Kb. The alkaline ultramafic rocks that are associated in space and time with the kimberlites plot at the extremity of the kimberlitic trend with some degree of overlap indicating possible consanguinity (Ferguson *et al.*, in press).

PICROILMENITES IN THE AUTOLITHS

Major element compositions have been determined in the electron microprobe for a total of 70 ilmenites included in the autoliths, and five autolith nuclei. The results of these analyses are summarized in Table 1, where they are compared with other relevant ilmenite analyses from the literature.

TABLE 1
COMPOSITIONS OF MAGNESIAN ILMENITES FROM AUTOLITHS, KIMBERLITE,
AND ILMENITE-SILICATE NODULES (%)

	1	2	3	4	5	6	7	8
TiO ₂	52.24	53.98	50.98	47.27	52.63	56.40	56.80	53.01
Cr ₂ O ₃	1.20	2.13	1.02	1.67	1.42	1.13	2.27	5.04
*Fe ₂ O ₃	9.20	6.81	10.26	14.41	0.33	1.91	0.57	5.20
FeO	22.41	20.61	26.76	28.97	32.17	19.90	27.09	19.42
MgO	13.64	15.10	10.71	7.60	12.02	20.23	13.19	15.74

* Calculated from the mineral formula

1. Average Wesselton pipe and dyke ilmenite (Mitchell, 1973)
2. Average Wesselton autolith ilmenite
3. Average Lesotho autolith ilmenite
4. Average autolith nucleus
5. Primary Lighobong ilmenite (Haggerty, In Press)
6. Secondary Lighobong ilmenite (Haggerty, In Press)
7. Secondary ilmenite in garnet lherzolite (Boyd and Nixon)
8. Ilmenite inclusion in euhedral olivine crystal from kimberlite, Isonville, Kentucky, U.S.A. (Boyd and Nixon, In Press).

The MgO contents of the autolith ilmenites are, with few exceptions, greater than ten weight per cent, and inspection of the data in Table 1 shows that these ilmenites contain significantly more magnesia and less ferric iron than ilmenites occurring as autholith nuclei. The ilmenites from the Lesotho autoliths appear to be transitional between the nucleus ilmenites, and those from the Wesselton autoliths, both with respect to MgO and Fe³⁺. The chrome contents of the autolith ilmenites are generally high, and values in excess of 3.0 per cent Cr₂O₃ are not uncommon. Also of interest is a fairly well developed inverse relationship between Cr and Fe³⁺, a trend also noted by Boyd and Nixon (In Press) for ilmenites intergrown with various silicate minerals.

Of particular importance, however, is the marked similarity in composition between the autolith ilmenites and secondary ilmenites from the Lighobong kimberlite (Haggerty, In Press) and from a garnet

lherzolite from Monastery Mine (Boyd and Nixon, In Press) (Table 1).

Haggerty (op. cit.) has described mantled sequences of ilmenite and spinel on picroilmenite in the Lighobong kimberlite, and he has shown that the zoning with respect to Mg/Mg + Fe in these sequences is inverted, and that secondary ilmenites thus produced are conspicuously more magnesian than the primary ilmenites from which they were derived. Like the autolith ilmenites, these secondary ilmenites appear to be enriched in Cr, and depleted in Fe³⁺ relative to ilmenites intergrown with various silicate minerals (Boyd and Nixon, op. cit.).

These observations support Boyd and Nixon's suggestion that these magnesian ilmenites are of a later generation than the more Fe-rich variety, of which the autolith nuclei are excellent examples. From the work of Boyd and Nixon (op. cit.) and Mitchell (1973) it is evident that much of the ilmenite now found in kimberlite was formed at great depth, possibly in the low-velocity zone (Boyd and Nixon, op. cit.), and possibly also before the generation of diamond (Mitchell, op. cit.).

Clearly, therefore, kimberlitic ilmenites have formed over wide ranges of pressure, temperature and oxygen fugacity. It is also evident that although the autoliths contain occasional low-magnesian ilmenites, the majority are the more magnesian variety, and the abundance of these ilmenites, together with secondary spinels in the autoliths provide strong evidence for the existence of highly reactive kimberlite liquids prior to and during kimberlite eruption.

It is concluded that autoliths represent kimberlite matrix having precipitated around solid nuclei during pipe development of kimberlite intrusions. They have only been subjected to olivine fractionation and have erupted from depths in excess of 100 km.

REFERENCES

Berg, G.W., and Allsopp, H.L. (1972) Earth Planet. Sci. Letts. 16, 27-30.

Boyd, F.R. and Nixon, P.H. (In Press) In : Lesotho Kimberlites (Ed. P.H. Nixon).

Ferguson, J., Martin, H., Nicolaysen, L.O. and Danchin, R.V. This Volume.

Ferguson, J., Danchin, R.V. and Nixon, P.H. (In Press) In : Lesotho Kimberlites (Ed. P. H. Nixon).

Haggerty, S.E. (In Press) In : Lesotho Kimberlites (Ed. P.H. Nixon).

Mitchell, R.H. (1973) Jour. Geol. 81, 301-311.

O'Hara, M.J. (1968) Earth Sci. Revs. 4, 69-133.

GARNET EXSOLUTION FROM STRESSED ORTHOPYROXENE IN GARNET LHERZOLITE
FROM THE MONASTERY MINE

J.B. Dawson¹ and J.V. Smith²

1) Dept. of Geology, University of St. Andrews, Fife, Scotland.
2) Dept. of Geophysical Sciences, University of Chicago,
Illinois 60637, U.S.A.

In a specimen of garnet lherzolite from the kimberlite of the Monastery Mine, O.F.S., South Africa, megacrysts of orthopyroxene up to 2 cm long are set in a finer-grained mosaic of olivine, clinopyroxene and garnet. The orthopyroxene crystals have been deformed, being bent along their C axes and exhibiting undulose extinction. Blebs, rods and platelets of garnet occur on (100) planes, generally at the point of maximum curvature, and very fine lamellae of ?clinopyroxene occur ubiquitously on (100) planes. Some more severely deformed orthopyroxene crystals are kinked on {100}[101] and garnet blebs along the kink junctions have coalesced to form continuous stringers of garnet (Fig. 1). A complete sequence can be traced from minute blebs appearing along minor dislocations to the continuous stringers of garnet, some of which separate thin rotated slices of the host pyroxene. The garnet appears to have exsolved from the orthopyroxene, and the occurrence of the garnet along dislocations suggests that this sub-solidus exsolution was induced by deformation of the host pyroxene in a non-isotropic stress field. This is similar to the origin proposed for garnet lamellae ("lamellae de démixtion") exsolved from tectonically-emplaced ultramafic rocks in the Bois des Feuilles, France (LASNIER, 1972) but differs from the garnet and clinopyroxene exsolved from orthopyroxene in garnet pyroxenites from Salt Lake Crater, Oahu, the origin of which is attributed to sub-solidus unmixing due to a drop in temperature (BEESON and JACKSON, 1970).

It should be noted that, in the Monastery Mine lherzolite, the composition of the exsolved garnet (MgO 20.9 - 21.4, CaO 4.7 - 5.1, Cr₂O₃ 2.1 - 2.8 wt. %) is the same as that in the surrounding, finer-grained matrix. The composition of the host orthopyroxene (En₉₄, Al₂O₃ 0.85, Cr₂O₃ 0.22 wt. %) is not noticeably different from values previously reported for orthopyroxenes from garnet lherzolites.

The other phases in the peridotite are olivine (Fo₉₂, diopside (Na₂O 1.45, Al₂O₃ 1.98, Cr₂O₃ 1.47 wt. %), and picrochromite (MgO 12.9, FeO 17.3, Al₂O₃ 15.2, Cr₂O₃ 52.0 wt. %).

References

BEESON, M.H. and JACKSON, E.D. Min. Soc. America, Special Paper 3, 95 - 112, 1970.
LASNIER, B. Contr. Min. Petrol. 34, 29-42, 1972.

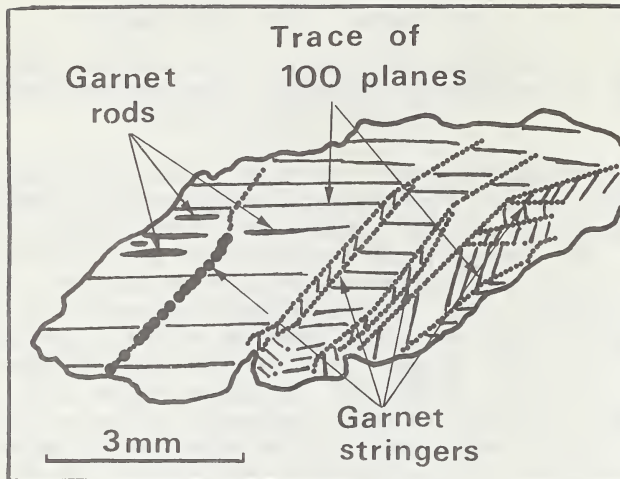


Fig. 1 - Sketch of kinked orthopyroxene in lherzolite BD1366 from the Monastery Mine, showing exsolved rods and coalescing stringers of garnet, and curvature and re-orientation of (100) planes.

CHEMISTRY OF OPAQUE MINERALS FROM PERIDOTITE AND ECLOGITE XENOLITHS

J.B. Dawson¹ and J.V. Smith²

- 1) Dept. of Geology, University of St. Andrews, Fife, Scotland.
- 2) Dept. of Geophysical Sciences, University of Chicago,
Illinois 60637, U.S.A.

Opaque phases in a variety of peridotite and eclogite xenoliths from South African kimberlites and in peridotites from the Lashaine volcano have been analysed with the electron microprobe. When plotted on a $Mg Cr_2O_4$ - $Mg Al_2O_4$ - FeO diagram, chrome-rich spinels from eleven garnet lherzolites, spinel lherzolites and spinel harzburgites, together with eleven analyses from the literature, show a trend mainly from $Mg Cr_2O_4$ to $Mg Al_2O_4$ with relatively little Fe_2O_3 in solid solution. There is a weak tendency for the chromium-rich spinels to occur in lherzolites, and some of the lherzolite specimens plot close to the magnesian chromite inclusions found in diamond. The whole suite overlaps the range found by IRVINE (1967) for chromites from ultramafic rocks. There is a good positive correlation between $Cr/(Cr + Al)$ for co-existing spinels and pyroxenes. When rutile is a co-existing phase, Ti is also high in the spinel.

Picrochromites from a dunite and a glimmerite contain, respectively, MgO 6.7, Cr_2O_3 1.6 and MgO 11.0, Cr_2O_3 1.5 wt. %. In the dunite the ilmenites coexist with relatively iron-rich olivine (Fo_{85}) and is a new paragenesis, possibly analogous to the pyroxene-ilmenite and garnet-ilmenite intergrowths reported by BOYD and DAWSON (1972).

Rutiles from eclogites have low (0.0 wt. %) Cr_2O_3 , whereas those from lherzolites and a glimmerite contain between 1.6 and 7.2 wt. %. One rutile grain in a spinel lherzolite from the Bultfontein Mine is zoned from a core with Cr_2O_3 7.2, FeO 0.6, MgO 0.1 to a rim of composition Cr_2O_3 7.0, FeO 2.3, MgO 8.9 wt. %; the rim contains minute needle-like lamellae of picrochromite.

References

BOYD, F.R. and DAWSON, J.B. Carnegie Inst. Washington Year Book 71, 373-378, 1972.

IRVINE, N. Can. Jour. Earth Sci. 4, 71-103, 1967.

THE CARBON ISOTOPIC COMPOSITION OF CARBONATITES, KIMBERLITES, AND DIAMONDS

P. Deines, and D.P. Gold, Department of Geosciences, The Pennsylvania State University, University Park, Pa. 16802

The carbon and oxygen isotopic composition of carbonates from 14 carbonatite complexes and 11 kimberlites have been measured, and additional occurrences from Canada, East Africa, Greenland, and Australia are being processed.

While there is some overlap in carbon and oxygen isotopic composition of carbonate species, e.g., dolomite (rauhaugites), ankerite and siderite (rodbergites), are enriched in C^{13} by about 2.2, 2.0, and 3.5‰ respectively with respect to calcite (sovites). Other intrinsic variable are indicated in carbonatite processes by the range in mean carbon isotopic composition of some well known carbonatites (Table 1), and the spatial and temporal relationships with the rift valleys in the East African carbonatites (Table 2). Likewise there is a spread in isotopic composition of seven Canadian carbonatites from $\delta\text{C}^{13} = -2.4\text{\textperthousand}$, $\delta\text{O}^{18} = 10.7\text{\textperthousand}$ for St. Andre, Quebec to $\delta\text{C}^{13} = -7\text{\textperthousand}$, $\delta\text{O}^{18} = 7\text{\textperthousand}$ for Lackner Lake, Ontario.

The clustering of values of certain carbonatite complexes in δC^{13} - δO^{18} space (Figure 1), separates into groups of (a) deep-seated or hyperbysal carbonatites with restricted fields, and (b) a near surface "volcanic-subvolcanic association" carbonatite with much greater fields. The larger oxygen isotopic composition range extending towards higher O^{18} contents for carbonatites of shallower levels may be due to: (1) a loss of isotopically light-water during pressure reduction at the time of emplacement; (2) an equilibration of some of the carbonates with magmatic carbonatite waters to low temperatures; (3) an influx of meteoritic water. In

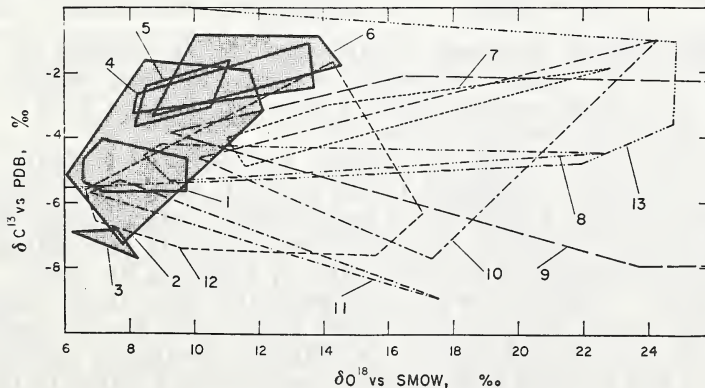


Fig. 1. The carbon and oxygen isotopic composition ranges of carbonatite complexes.

1. Oka;
2. Alnö;
3. Laacher See;
4. Sukulu Hill;
5. Tororo Hill;
6. St. André;
7. Homa Mountain;
8. Albany Forks;
9. Ruri;
10. Rangwa;
11. Magnet Cove;
12. Kaiserstuhl;
13. Mbey.

The Oka field is restricted to multiple readings only.

Table 1. The carbon isotopic composition of selected carbonatites

Location	Mean $\delta^{13}\text{C}$	Rock type	Source
1. Complexes for which a large number of analyses have been carried out.			
St. Honoré	-4.7	all rocks	This work
Oka	-5.0	all rocks	DEINES (1970a)
2. Complexes for which few isotopic composition analyses are available, showing a restricted carbon and oxygen isotopic composition range			
St. André	-2.6	rauhaugites	This work
Tororo	-2.7	sövites	This work
Sukulu	-2.7	sövites	This work
Mbeya	-3.4	sövites, rauhaugites	SUWA <i>et al.</i> (1969)
Alnö	-5.5	sövites	TAYLOR <i>et al.</i> (1967), BAERTSCHI (1957) ECKERMANN <i>et al.</i> (1952)
Magnet Cove	-5.5	sövites	CONWAY and TAYLOR (1969), This work
Oldoinyo Lengai	-5.8	natro-carbonate lava	DENAHEYER (1970), VINOGRADOV <i>et al</i> (1970) O'NEIL (1971)
Kaiserstuhl	-6.2	sövites	GONFIANTINI and TONGIORGI (1964)
Laacher See	-7.1	sövites	TAYLOR <i>et al.</i> (1967)
3. Complexes for which only carbon isotopic composition measurements have been reported (four analyses and more)			
Chadobets	-3.4	ankerite sövite	BAGDASAROV <i>et al.</i> (1969)
Potvornyy	-5.2	sövites	VINOGRADOV <i>et al.</i> (1967)
Ozerny	-5.6	sövites	VINOGRADOV <i>et al.</i> (1967)
Kerimasi	-5.8	sövites	VINOGRADOV <i>et al.</i> (1970)
Sanskiy	-6.3	sövites	VINOGRADOV <i>et al.</i> (1967)
4. Individual analyses of carbonatite carbonates with oxygen isotopic compositions between 6 and 8‰ vs SMOW			
Spitzkop	-5.3	sövite	BAERTSCHI (1957)
Cripple Creek	-5.4	olivine syenite	TAYLOR <i>et al.</i> (1967)
Iron Hill	-5.6	sövite, rauhaugite	TAYLOR <i>et al.</i> (1967), BAERTSCHI (1957)
Lueshe	-5.9	sövite	DENAHEYER (1970)
Nemegosenda Lake	-6.5	sövite	This work
Lackner Lake	-7.0	sövite	This work

the latter case any isotope exchange would have to be limited to below 250°C, because at higher temperatures an exchange with ordinary surface or ground waters ($\delta\text{O}^{18} < 0\text{\textperthousand}$) would lead to a depletion in O^{18} in the carbonate below 6‰.

We conclude that the spread in carbon and oxygen isotopic composition in carbonatite complexes is due not only to the carbonate species present, but also is a function of geographic locality, depth of emplacement. By analysing rocks only with like minerals and taking the mean of a large population of samples, and by applying an "emplacement level" filter to include only those analyses lying in the range $\delta\text{O}^{18} = 6$ to 8‰ (the range for feldspars from ultramafic rocks, which by analogy should be the range for primary, high temperature carbonates) we believe we are looking at geographic variations related to the source material. Table 1 represents a compilation of filtered results, with a mean carbon isotopic composition of -5.1‰, and a standard deviation of $\pm 1.4\text{\textperthousand}$, vs PDB.

Because diamonds, kimberlite carbonates and carbonatites are thought to derive their carbon from similar depths, we can ponder the question of how uniform the isotopic composition of carbon might be in the mantle. A review of the available data on the carbon isotopic

Table 2. Spatial and temporal isotopic composition relationships of carbon in East African carbonatites

Approximate age relation	Location			
	W. Rift	Lake Victoria	Lake Malawi (Nyasa)	Lake Chilwa
Recent Rift	-5.7 to -7.9			
volcanism				-5.9
Mt. Elgon		-2.4		-5.8 to -7.4
volcanism				
Kavirondo rift				
volcanism		-3.3 to -4.4		
Tororo				
intrusions		-2.7 to -2.9		
Mbeya			-3.4	
carbonatite				
Chilwa intrusive				-2.3 to -3.2
series, Cretaceous				

composition ranges of carbonatite and kimberlite carbonates shows that they are similar and overlap that of diamonds except for the anomalously light ($\delta\text{C}^{13} = -27.8$ to -28.4) carbonados. The mean for 22 selected carbonatite complexes ($-5.1\text{\textperthousand}$, $s = +1.4\text{\textperthousand}$ vs PDB) is indistinguishable from that of 13 kimberlite pipes ($-4.7\text{\textperthousand}$, $S = +1.2\text{\textperthousand}$) as well as that of 60 individual diamond analyses ($-5.8\text{\textperthousand}$, $s = \pm 1.8\text{\textperthousand}$). The oxygen isotopic compositions of kimberlite carbonates (10.5 to $15.5\text{\textperthousand}$), however, are enriched in O^{18} by several permil with respect to those of carbonates from the subvolcanic type of carbonatite.

The data suggest that not all carbonatite, kimberlite (1.6 to 9.0 \textperthousand) and diamond occurrences have the same average carbon isotopic composition and that significant difference exist between them. The available diamond analyses are plotted in Figure 2 and compared with those of the kimberlite carbonates. Diamonds from the Kimberley pipes are enriched in C^{13} (mean $\delta\text{C}^{13} = -2.9$) with respect to the Zairian pipes of Tshaba (-6.6), and Disele (-6.8) and the Mir pipe (-7.5) in Siberia.

If the filtered analyses of sylvites of subvolcanic carbonatites are adequate to represent the carbon isotopic composition of the total carbon in a carbonatite, and that no major losses of carbon have occurred in the formation of carbonatites, one is led to the conclusion that the carbon isotopic composition of the original carbonatite magmas differed. This might be due either to isotopic inhomogeneities in the source of the carbonatite carbon, or to isotope effects in the derivation of the carbonatite magma from its ultimate source. In this connection it would be interesting to study the carbon isotopic composition difference between diamonds and carbonate in kimberlites, because such isotope effects should be different for reduced and oxidized forms of carbon. Theoretical computations suggest that even at 1000°C considerable isotopic composition differences should exist between diamond, carbon dioxide and carbonate. At this temperature diamond would be expected to be $4.4\text{\textperthousand}$ lighter and calcium carbonate about 2\textperthousand lighter than carbon dioxide, so that diamond would be depleted in C^{13} about 2\textperthousand compared to calcite at isotopic equilibrium. A general

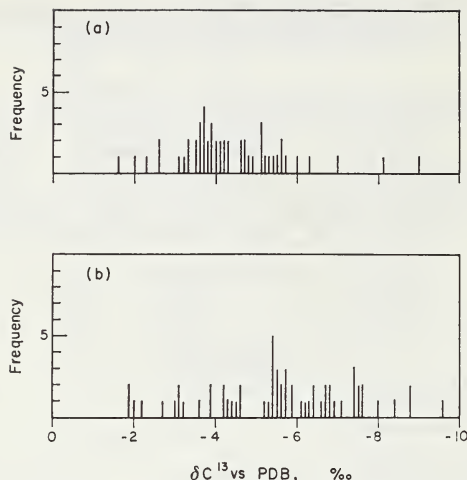


Fig. 2 The carbon isotopic composition of carbonates from kimberlites (A), and of diamonds (B).

shift of the diamond carbon isotopic compositions towards lower C^{13} concentrations is not apparent (see Fig. 2) from the present data, although the number of available analyses may be too small to show this effect. Analyses of both carbon-bearing phases from the Mir Pipe shows essentially the same isotopic composition for carbonate and diamond.

If carbonatite or kimberlite carbonates as well as diamonds represent samples of carbon, the isotopic composition of this carbon can be bracketed only within the limits of -2 to -8 ‰. The overall average C^{13} content of such carbon might be close to the average of the three sample types studied here, which is -5.2 ‰. However, the selection of this or any other value within the above given range as a criterion for deep-seated carbon sources cannot be justified, because the source of kimberlite, carbonatite and diamond carbon may not be uniform isotopically.

Acknowledgement: This article has been abstracted mainly from the following paper, in which many other references are cited - too many to be recorded here.

Deines, P., and D.P. Gold, (1973). The Isotopic Composition of Carbonatite and Kimberlite Carbonates and their Bearing on the Isotopic Composition of Deep-Seated Carbon. *Geochimica et Cosmochimica Acta*, v. 37, p. 1709-1733.

XENOLITH-BEARING GRAPHITIC DIKES IN THE RONDA
HIGH-TEMPERATURE PERIDOTITE INTRUSION

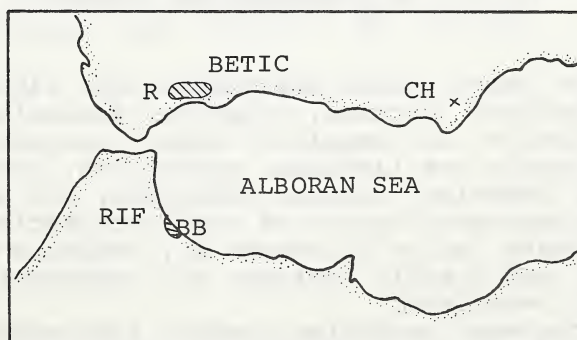
John S. Dickey, Jr. and Masaaki Obata

Department of Earth and Planetary Sciences
Massachusetts Institute of Technology
Cambridge, MA, U.S.A., 02139

Introduction

The Serrania de la Ronda peridotite intrusion is located on the south coast of Spain within the deformed, internal zone of the Betic-Rif orocline (Fig. 1). The intrusion is on the crest of one of two narrow ridges of high density material, which lie along the margins of the Alboran Sea (Bonini *et al.*, 1973). The southern ridge surfaces as the Beni Bouchera high-temperature peridotite intrusion in Morocco. Unlike peridotite massifs of the ophiolite association, the Ronda and Beni Bouchera peridotites are not overlain by pillow lavas and gabbros. Both ridges intruded thick sections of sialic rocks between late Triassic and Miocene times. The Ronda massif, which is surrounded by marbles, hornfelses, and gneisses, is thought to have intruded the crust at more than 1000°C (Loomis, 1972).

Fig. 1. Localities mentioned in the text.



Key: R = Ronda Massif
CH = Cerro del Hoyazo
BB = Beni Bouchera Massif

The Ronda intrusion is 85 to 90% peridotite, and also contains a variety of mafic sheets and felsic dikes. Field relations and chemistry suggest that the mafic sheets, which vary from garnet pyroxenites to olivine gabbros, formed by partial fusion of mantle rock (Dickey, 1970). The origins of the felsic rocks are obscure: some may be indigenous to the intrusion, others may be related to exotic magma systems, and still others may have been formed by assimilation and fusion of crustal rocks.

This paper describes a particularly interesting group of garnet-bearing quartz diorite dikes in the western part of the peridotite body, which contain extraordinary quantities of graphite, a large assortment of accessory minerals, and a variety of xenoliths.

Field Relations

The graphite-bearing dikes (5 to 150 cm thick) cross-cut all layering and foliations in the peridotite. They have not yet been observed in the adjacent country rocks; however, volcanic rocks of similar mineralogy (but containing little graphite) have been described among Neogene limestones of Cerro del Hoyazo (Zeck, 1968) (Fig. 1). The Ronda dikes are dark gray, fine grained, and in places, vesicular. Typically the dike margins are not chilled, but the contacts are sharp and in some dikes the concentration of graphite increases markedly (to 100%) at the contacts. Textures vary from homogeneous to heterogeneous. Some dikes contain no inclusions; others are laden with a mixture of rounded serpentine, peridotite, gabbro, and gneiss xenoliths and angular fragments of white quartz. The latter are probably derived from shattered quartz veins which issue from some dikes. Most of the xenoliths are represented in the peridotite massif or among the country rocks.

Petrography

The major constituents are plagioclase (40-90% An), quartz, hypersthene, biotite, graphite, almandine-rich garnet, cordierite, and amphibole after hypersthene. Accessory minerals are ilmenite, pyrrhotite, pentlandite, chalcopyrite, cubanite, zircon, hercynite, and apatite.

The heterogeneous varieties are characterized by high graphite contents (up to 16 weight %), graphite-enriched dike margins, and chaotic textures with abundant crystal fragments and xenoliths.

The homogeneous varieties contain less graphite (about 5 weight %) and few or no xenoliths and crystal fragments. The textures are uniform with intergrown, xenomorphic crystals. Some specimens show weak preferred orientation of quartz, plagioclase and biotite. Blades of graphite are disseminated throughout.

Carbon Isotopes

Stable carbon isotope ratios of graphites from these dikes range from -20.8 to -24.1 ‰ (expressed as δC^{13} relative to PDB). Similar values are reported for reduced carbon from chondritic meteorites and terrestrial igneous, metamorphic and sedimentary rocks. These data are, however, quite different from δC^{13} values reported for diamonds (-3 to -8 ‰) (Schwarz, 1969).

Discussion

Mineralogical, chemical and geological evidence indicate that the garnet-bearing, quartz diorite dikes in the Ronda high-temperature peridotite intrusion originated by fusion of sialic crust or by contamination of magma with sialic crust. This process may have occurred during the intrusion of the mantle-derived peridotite. Crystallization of the gas-charged magmas at depth resulted in unusual graphite concentrations which are not observed in volcanic rocks of otherwise similar mineralogy at Cerro del Hoyazo.

References

Bonini, Loomis, and Robertson, 1973, J. Geophys. Res., 78, 1372-1382
Dickey, 1970, Min. Soc. America Spec. Paper 3, 33-49
Loomis, 1972, Geol. Soc. America Bull., 83, 2449-2474
Schwarz, 1969, Handbook of Geochemistry, 6-B-I
Zeck, 1968, Contrib. Min. Petrol., 26, 225-246

THE IGWISI HILLS EXTRUSIVE "KIMBERLITES"

C. Donaldson, Lunar Science Institute, Houston, TX 77058; A. M. Reid, NASA Johnson Space Center, Houston, TX 77058; W. I. Ridley, Lunar Science Institute, Houston, TX 77058; R. W. Brown, Lockheed Electronics Corporation, Houston, TX 77058; and J. B. Dawson, University of St. Andrews, Scotland.

The Igwisi Hills are a group of volcanic hills in Tanzania where a unique series of eruptions has produced volcanic rocks that have many of the features of kimberlites. The rocks are "igneous conglomerates" that are characterized by the presence of abundant oblate spheres of olivine in a fine grained crystalline matrix. The matrix contains major amounts of carbonate and complexly-zoned Mg-Al-Cr spinels, minor perovskite, apatite and limonite. The larger grains are magnesian olivines that are highly rounded and show strain effects. Some of the original olivine spheres have partially recrystallized to more Fe-rich and Ni-poor anhedral to euhedral grains. Several olivine ellipsoids are partly or wholly rimmed by a black coating consisting of perovskite, ilmenite, and Mg-Al spinel. Special attention has been given to the study of mineral inclusions within the olivine. These include chrome pyrope, similar in composition to garnets in kimberlites, low Al enstatite, low Al magnesian chrome diopside, Mg-Al chromite, and a highly magnesian phlogopite ($Mg/Mg+Fe \sim .93$). All of these are apparently primary phases in equilibrium with olivine. The total assemblage is similar in many respects to that found in peridotite xenoliths from the Lashaine volcano in northern Tanzania.

The Igwisi irruptives thus apparently contain material derived from phlogopite-bearing, garnet and/or spinel peridotites with a primary mineral assemblage (assuming that these phases coexist) indicative of equilibrium at upper mantle temperatures and pressures. This primary assemblage was disrupted and brought rapidly to the surface in a gas-charged, carbonate-rich fluid. Abrasion of the ultramafic xenoliths to produce smoothly rounded pebbles suggests energetic transport in a fluidized system. Transport and cooling were sufficiently rapid (possibly due to continuous endothermic expansion of the gas-rich medium) to prevent both re-equilibration of the high pressure phases and major reaction between xenoliths and the fluid. Rapid upward transport, extrusion, and rapid cooling have preserved inclusions of upper mantle peridotite in a carbonate-rich matrix and have tended to prevent the reaction between inclusions and matrix that would otherwise have yielded a more typical kimberlite.

CO₂ AS A VOLATILE COMPONENT OF THE MANTLE

David H. Eggler, Geophysical Laboratory, 2801 Upton St., N.W.,
Washington, D.C. 20008

There appears to be wide agreement among petrologists that the volatiles CO₂ and H₂O are important components of kimberlite. There is less agreement on the relative proportions of H₂O and CO₂ and on the role of the volatiles -- whether they occurred primarily in a low-density vapor phase, or in immiscible carbonatite melt (Koster van Groos and Wyllie, 1973), or dissolved in silicate melt, either a melt of kimberlite affinity (Dawson, 1971) or a melt encountered by the kimberlite on its eruptive path (Boyd and Nixon, 1973). This study is a determination of phase equilibria in the system Mg₂SiO₄-SiO₂-H₂O-CO₂ at 20 kbar. The system is considered to be a simple model of a peridotitic mantle, as it contains two of the four principal peridotite phases, forsterite (Fo, Mg₂SiO₄) and enstatite (En, MgSiO₃), plus two volatile components. The study provides information on three questions, the solubility of CO₂ in silicate melt, the role of CO₂ in solution of silicates in vapor, and the role of CO₂ in determining the composition of magmas produced by melting of peridotite.

Solubility of CO₂ in silicate melt. Experiments have been previously conducted on the solubility of CO₂ in silicate melts, at 20 kbar, with the compositions CaMgSi₂O₆, MgSiO₃, and NaAlSi₃O₈ (Eggler, 1973). Solubilities ranged from 9.5 wt % (34 mole %) in relatively basic CaMgSi₂O₆ melt to only 0.9 wt % (5 mole %) in relatively acidic NaAlSi₃O₈ melt. Melts containing H₂O in addition to CO₂ dissolve slightly more CO₂. At pressures at least to 30 kbar, a large miscibility gap exists between silicate melts and H₂O-CO₂ vapor (see Fig. 1). For all compositions, CO₂ is much less soluble than H₂O; the vapor-absent region is much smaller for compositions containing more CO₂ (see, for example, relations involving the four-phase tetrahedron Fo-En-L-V at 1450° C (Fig. 1)). Melt of MgSiO₃ composition dissolves a maximum of about 3.7 wt % CO₂ at 20 kbar. In Fig. 1 the melt region is outlined by a "caterpillar" shape and is drawn on the assumption of negligible CO₂ solution in SiO₂ melt.

Vapor composition. The kimberlite vapor phase is often assumed to dissolve excess alkalis (Boyd and Nixon, 1973; Koster van Groos and Wyllie, 1973). Experiments on this effect are uncompleted; however, the considerable effect of CO₂ in reducing solution of silica is shown schematically in Fig. 1 and in more detail in the subsolidus region of the system En-H₂O-CO₂ in Fig. 2. When subsolidus vapor contains more H₂O than 0.65 mole %, vapor dissolves sufficient silica in excess of stoichiometric MgSiO₃ that the assemblage is Fo+En+V. However, in more CO₂-rich vapor, very little excess silica dissolves, producing En+V.

Melting relations. In the system Mg₂SiO₄-SiO₂-H₂O, compositions of liquids in equilibrium with Fo and En can be either silica-oversaturated or silica-undersaturated, depending on whether or not enstatite melts to a liquid in equilibrium with forsterite. Kushiro, Yoder, and Nishikawa (1968) have demonstrated these relations at a pressure of 10 kbar. Eggler (1973) confirmed this behavior at 20 kbar. At 20 kbar the assemblage Fo+En+V melts to H₂O-saturated liquid at 1305° C. At temperatures below 1400° C, liquids in equilibrium with Fo+En are silica-oversaturated while at temperatures above 1400° C, they are silica-undersaturated. The effect of CO₂ on this relation was studied in the join 5MgSiO₃:

$4\text{CO}_2\text{-H}_2\text{O}$ (Fig. 2). Two points are of interest: first, that the solidus temperature is higher in the presence of CO_2 , and second, that the temperature at which Fo+En are no longer in equilibrium with silica-oversaturated liquid (that is, where Fo+En+L+V is no longer a stable assemblage on the join $\text{En-H}_2\text{O-CO}_2$) is still 1400°C .

Phase relations are clarified in the semi-schematic Figure 1. In the system $\text{Mg}_2\text{SiO}_4\text{-SiO}_2\text{-H}_2\text{O}$ the assemblage Fo+En is in equilibrium with

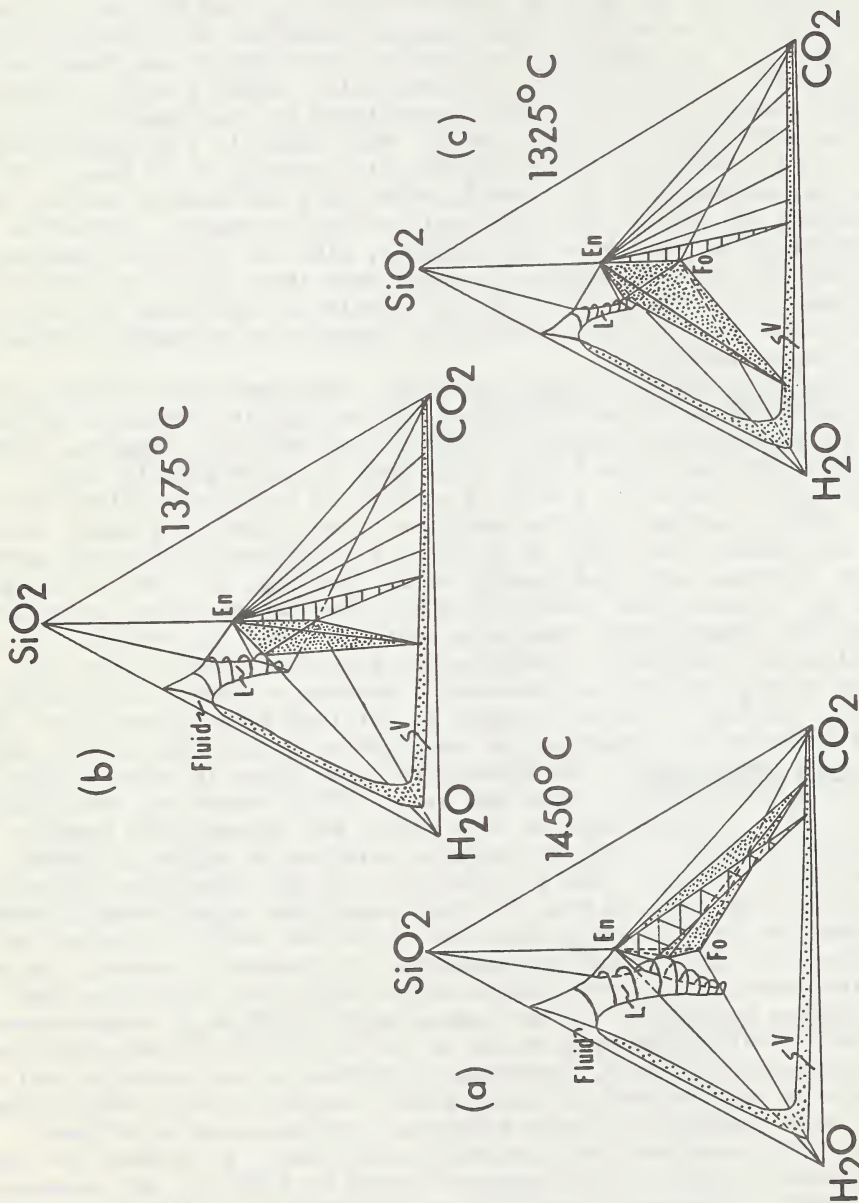


Figure 1. Phase relations (semi-schematic) in the system $\text{Fo-En-H}_2\text{O-CO}_2$ at 20 kbar pressure (wt %). Stippled areas outline the vapor field and the four-phase tetrahedron Fo-En-L-V .

silica-oversaturated, H_2O -rich melt at temperatures below $1400^\circ C$, whereas above $1400^\circ C$ those phases are in equilibrium with silica-undersaturated, less H_2O -rich melt. Figure 1 shows that in the presence of CO_2 the same situation holds (the difference is that, in the presence of CO_2 , the solidus of a peridotite is considerably higher in temperature than $1305^\circ C$). At $1375^\circ C$, the stippled tetrahedron is the four-phase volume $Fo+En+L+V$; the vapor contains about 45 wt % CO_2 and excess SiO_2 . The liquid, which is silica-oversaturated, contains about 3.5% CO_2 and 10% H_2O . Back of that tetrahedron is the three-phase volume $Fo+En+L$; these vapor-absent liquids are also silica-oversaturated. Compositions on the plane $En-H_2O-CO_2$ or in the volume $Fo-En-H_2O-CO_2$, lying to the right of the stippled tetrahedron do not melt at $1375^\circ C$.

At $1400^\circ C$, En and Fo are in equilibrium with a slightly more CO_2 -rich vapor and with a liquid that now lies exactly on the plane $En-H_2O-CO_2$ and is exactly silica-saturated. It is clear that the presence of CO_2 , even in amounts sufficient to saturate the liquid and produce a free vapor phase, does not alter the silica-saturated or undersaturated nature of the melt. At $1450^\circ C$, $En+Fo$, both in equilibrium with a CO_2 -rich vapor and in the vapor-absent region, are in equilibrium with silica-undersaturated liquids. At $1325^\circ C$, all liquids, even those in equilibrium with Fo or $Fo+V$, are silica-oversaturated.

The assemblage $Fo+En$ is a model peridotite. Figure 1 shows that the temperature at which that assemblage melts is a function of the H_2O-CO_2 content of the source region. The composition of the first-formed melt is a function of temperature (and indirectly, therefore, of H_2O-CO_2 ratio). Compositions containing more than 55 mole % CO_2 will melt above $1400^\circ C$, and liquids are silica-undersaturated. These relationships hold whether or not the liquids are vapor-saturated.

The dominance of the melting behavior of enstatite in controlling composition of melts produced from peridotite is seen from experiments of Mysen (1973). He has found a change in composition of liquids produced by melting natural peridotite from silica-oversaturated to undersaturated at nearly the same CO_2-H_2O ratio (0.55) as in the simple system discussed here.

Conclusions. Petrologic studies of kimberlite and related rocks have indicated that a CO_2-H_2O vapor phase was involved in their origin. This phase equilibria study indicates at least three reasons why such vapor associated with kimberlite and alkaline rocks should be CO_2 -rich: (1) The model system $Fo-En-H_2O-CO_2$ indicates that in the presence of CO_2 or CO_2-H_2O mixtures peridotite comprising the upper mantle melts at higher temperature. Although the presence of CO_2 has little effect on the silica-saturated or undersaturated nature of liquid produced by partial melting at any particular temperature, liquids produced at higher temperatures are less silica-saturated because of the "enstatite effect". Higher melting temperatures also produce a smaller degree of melting, at any point along the geotherm, yielding more alkalic melts. The effect of CO_2 is therefore the production of less silica-saturated, more alkalic, melts. There may be primordial areas of the mantle rich in CO_2 , or CO_2 -rich vapor may rise to certain localities. Mantle regions with vapor richer in H_2O would melt more completely to yield silicic magmas. (2) Silicate melts dissolve rather large amounts of H_2O at high pressures. The presence of a free vapor is unlikely. Melts dissolve much less CO_2 , so that the miscibility gap between melt and CO_2 -rich vapor is wider, and the presence of a free vapor is more likely.

(3) Vapor rich in CO_2 does not dissolve excess silica, unlike H_2O -rich vapor and may well dissolve excess alkalies. Such vapors would produce many alteration effects observed in kimberlite.

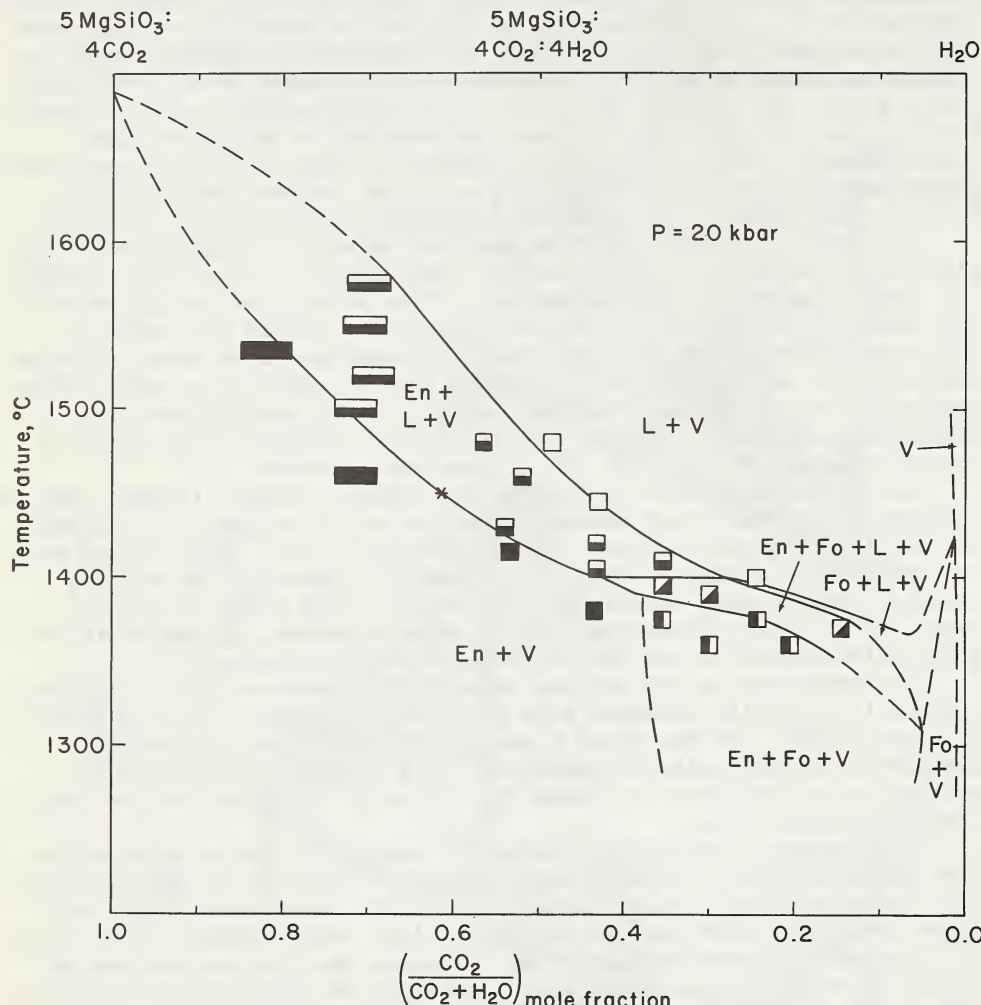


Figure 2. Phase relations on the join $5\text{MgSiO}_3:4\text{CO}_2-\text{H}_2\text{O}$ at 20 kbar.

REFERENCES CITED

Boyd, F.R., and P.H. Nixon, 1973, Carn. Inst. Wash. Y.B., in press.
 Dawson, J.B., 1971, Earth-Science Reviews, 7, 187-214.
 Eggler, D.H., 1973, Carn. Inst. Wash. Y.B., in press.
 Koster van Groos, A.F., and P.J. Wyllie, 1973, Amer. Jour. Sci., 273, 465-487.
 Kushiro, I., H.S. Yoder, Jr., and M. Nishikawa, 1968, Geol. Soc. Amer. Bull., 79, 1685-1692.
 Mysen, B.O., 1973, Carn. Inst. Wash. Y.B., in press.

MINERALOGY AND PETROLOGY OF KIMBERLITE DYKE AND
SHEET INTRUSIONS IN SOUTH-WEST GREENLAND

by
C.H. Emeleus¹ and James R. Andrews²

1. Dept. of Geological Sciences, University of Durham, Durham, England.
2. Dept. of Geology, University College, Belfield, Dublin 4, Ireland.

Dykes and thin sheets of kimberlite intrude Precambrian rocks between Holsteinsborg and Ivigtut. At three localities, Nigerdlikasik (62°02'N, 48°51'W), Midternaes (61°33'N, 48°10'W) and Pyramidefjeld (61°25'N, 48°15'W) a dyke and sheet complexes, dated at about 220 my., consists of fresh kimberlite with frequent peridotite nodules and sparser inclusions of crustal rocks. Modal analyses of the kimberlites show considerable variations (Andrews & Emeleus 1971, Table 1) particularly in diopside, phlogopite and carbonate. The nodules are generally very olivine rich with lesser amounts of orthopyroxene, clinopyroxene and other minerals (*ibid.*, Table 2). Whole rock analyses (8) from two of the localities show little variation, these analyses and trace element determinations on kimberlite from Nigerdlikasik give compositions closely comparable to a composite sample from the Benfontein kimberlite (Dawson & Hawthorne 1973, Tables 2 & 3; Hawthorne 1968).

The kimberlites contain olivine, chromite, titanomagnetite, perovskite, clinopyroxene, phlogopite, calcite, ferroan dolomite, and serpentine, which crystallised in approximately that order, together with minor apatite and amphibole. An earlier tentative identification of mellilite was not confirmed. Peridotite nodules consist of dominant olivine together with variable amounts of orthopyroxene, chrome diopside, garnet, chrome spinel and phlogopite. Textures are generally xenomorphic granular though idiomorphic and poikilitic crystals may also be present. Several dunite mylonite nodules and olivine-rich nodules with incipient granulation and crushing were found at Pyramidefjeld. The nodules are rounded, up to 200 mm in diameter and sharply defined against the kimberlite. There is little sign of reaction between nodules and kimberlite although penetration by kimberlite veins occurs and there may be serpentinisation of olivines in the nodules. Compositional data for selected minerals are given in the table (see page 4).

Olivines in the kimberlites are of variable compositions, examples with normal and with reversed zoning are present. The olivine habits also vary, several of the types distinguished at Benfontein may be recognised (Groups i, iii and iv, Dawson & Hawthorne 1973, pp.66, 67). Peridotite olivines are remarkably constant in composition, the only major departure from ca. Fo90 was in the more iron rich olivines forming the larger, strained crystals in some dunite mylonites and crushed peridotites. The diopside in the kimberlite shows slight normal zoning. Nodule clinopyroxenes differ from those in the kimberlite, they are appreciably more magnesian, show a range of enstatite-diopside solid solution (largely within field 'A' of Boyd & Nixon, 1973) and contain higher Cr and Na. Chrome diopsides from phlogopite-, spinel- and garnet-peridotites are characterised by different amounts of Al, Ti and Cr. The chrome diopside usually occurs as discrete crystals but in the phlogopite peridotites it is

also found intergrown with low-Al chromite and phlogopite. Orthopyroxene is restricted to peridotites. It is fairly constant in composition although variation in Al parallels that found in peridotite clinopyroxenes. Inclusions are uncommon in orthopyroxene, exsolution lamellae analysed in one sample are of chrome spinel, accompanied by (unanalysed) clinopyroxene lamellae. Garnet, chrome spinel and phlogopite are the principal aluminous phases in the peridotites and have been used to classify them. The garnet is a chrome pyrope. The crystals almost invariably show signs of instability, a prominent reaction rim is developed consisting of chrome spinel, orthopyroxene and minor chrome diopside. Phlogopite is frequently intimately associated with the reaction rims. Spinel of the spinel peridotites is a dark brown variety rich in Mg, Al and Cr, the nodules containing spinel are remarkably fresh and there is a complete absence of mica. Other spinels found in the peridotites include well-formed chromites in garnet and in chrome diopside. Opaque minerals in the kimberlites include chromite and titanomagnetite as composite grains, chromite may form the core to a crystal or both may be complexly intergrown. Phlogopite in the peridotites occurs as large well-formed crystals and intergrown with clinopyroxene and chromite. It is present in most nodules except the spinel peridotites and dunite mylonites. The kimberlite micas are zoned to colourless margins or to margins showing intense reversed pleochroism in deep red-brown to pale brown colours. (Al-poor tetraferriphlogopite, cf. Rimskaya-Korsakova & Sokolova 1964). The peridotite and kimberlite phlogopites differ in the relatively high Si and Mg of the former, and the higher Al and Fe of the latter. The latest minerals to crystallise from the kimberlite magma were phlogopite, carbonate (sometimes with clear calcite rims to ferroan-dolomite) and fine-grain serpentine of unusually iron-rich composition (up to 11.6% FeO). Late-stage veins, cross-cutting nodules and kimberlite, show the same crystallisation sequence, early marginal phlogopite is oriented approximately perpendicular to the vein edges, later carbonate develops good crystal faces towards the vein centre which is filled with fine-grain, pale green serpentine.

The kimberlite intruded as a low temperature magma with little effect on its surroundings apart from marginal shattering and extensive carbonation of siltstones on Midternaes. The zoned olivines and pyroxenes indicate differentiation prior to emplacement and/or crystallisation over a temperature range. The normal and reversed zoning of the olivines converges on a compositional band around Fo₈₈₋₈₄, the derivation of Fe-rich reversed zoned olivines from a crustal source is suggested by their association with fragments of crustal rock containing Fe-rich orthopyroxene. Forsteritic olivines may have originated as phenocrysts and/or through fragmentation of peridotite nodules. The absence of other xenocrysts (enstatite, chrome diopside, garnet) may be attributed to their low concentrations in the peridotites. The virtual absence of clinopyroxene in the Nigerdlikasik kimberlite and its presence elsewhere (up to 25 vol.%) may be a reflection of silica variation. The general mineralogy of the kimberlites is similar to kimberlites from other areas, although the Greenland example appears remarkably fresh; however, the absence of picroilmenite is notable. The mineral analyses show the latest liquid in the kimberlite was depleted in Al almost to the extent of its elimination (cf. the tetraferriphlogopite rims and the absence of any Al phase with the

last-crystallised serpentine) and somewhat Fe enriched (cf. the presence of tetraferriphlogopite and the serpentine compositions).

The garnet and spinel peridotites are considered to represent mantle material derived respectively from relatively deep and shallow levels. There is no sign of instability in minerals of the spinel peridotites but in the garnet peridotites the garnet is almost always altered. Phlogopite is often found closely associated with the reaction rims surrounding garnet; in some examples garnet has a thick reaction rim near phlogopite but little or no rim next to olivine or pyroxenes. In this situation the large phlogopites are also found to be corroded and replaced. The petrographic relations thus suggest a reaction involving primary garnet and phlogopite resulting in the formation of chrome spinel, orthopyroxene and chrome diopside, and the apparent elimination of K and (OH) from the system. In this situation the phlogopite appears to be of primary, deep-seated origin. The majority of the phlogopite peridotites, found mainly in Pyramide-fjeld, contain no garnet. However, some of the phlogopite occurs intergrown with other minerals, as described earlier. These intergrowths may represent the end product of alteration of an earlier aluminous phase (spinel, garnet) in the presence of potash and water-rich kimberlite magma; thus, some of the phlogopite kimberlites may have originated through reaction between mantle wall rock and active kimberlite magma, while other phlogopite-bearing peridotites appear to pre-date the kimberlite.

The distribution of minor elements between pyroxenes, the absence of reaction rims around nodules and where late veins cut kimberlites and peridotites, indicate that the peridotite assemblages equilibrated with their Al-rich phase (garnet, spinel or phlogopite) prior to emplacement at their present crustal levels.

Andrews, J.R. and Emeleus, C.H. 1971 Gronlands geol.Unders., Rapp 31.pp. 26.

Boyd, F.R. and Nixon, P.H. 1972 Carnegie Inst.Yr.Bk, 71, 362-373.

Dawson, J.B. and Hawthorne, J.B. 1973 Jl.geol.Soc.Lond., 129, 61-86.

Hawthorne, J.B. 1968 Trans.geol.Soc. S. Afr, 71, 291-311.

Rickwood, P.C. 1968 Contr. Mineral. and Petrol., 18, 175-198.

Rimskaya-Korsokova O.M. & Sokolova, E.P. 1964 Zap. Vses. Min.Obshch. 93, 411-423. (also Mineral.Abs. 17, 504, 1966)

For table see overleaf

Summary of mineral compositional ranges

	<u>Peridotites</u>			<u>Kimberlites</u>		
<u>Olivine</u> (atom %)	Mg 92.4 - 88.5 Mg 86.0 - 76.6 (1)			Mg 92.4 - 75.7		
<u>Orthopyroxene</u> (atom %)	Mg 92.4 89.5	Fe 6.6 9.8	Ca 1.0 0.7	Mg 80.2	Fe 18.1	Ca 1.7 (2)
<u>Clinopyroxene</u> (atom %)	Mg 53.2 47.0	Fe 3.4 4.3	Ca 43.4 48.7	Mg 47.4 44.3	Fe 4.0 5.8	Ca 48.6 49.9
<u>Phlogopite</u> (wt.%)	SiO ₂ Al ₂ O ₃ FeO MgO	42.1 11.9 3.8 25.9	37.4 15.6 5.4 20.3	37.6 11.1 7.8 25.7	35.3 18.2 8.0 19.0	42.6 1.1 14.8 25.0 (3)
<u>Garnet</u> (Mol. end- members; Rickwood, 1968) NB. In peridotites only.	Uvarovite Pyrope Spessartite Grossular Almandine Haneite			11.7 71.3 0.0 1.9 15.1 0.0	15.9 65.3 0.7 0.0 14.0 4.2	

Notes: (1) Range in dunite mylonite inclusions
 (2) OPX from crustal rock inclusion
 (3) Tetraferriphlogopite rim

(All microprobe determinations)

KIMBERLITE POTASSIC RICHTERITE AND THE DISTRIBUTION
OF POTASSIUM IN THE UPPER MANTLE

A. J. ERLANK

Department of Geochemistry, University of Cape Town

The occurrence of the rare amphibole potassic richterite (magnophorite), which has the generalised formula $\text{KNaCaMg}_5\text{Si}_8\text{O}_{22}(\text{OH},\text{F})_2$, in kimberlite materials was first noted by Erlank and Finger (1970), who identified potassic richterite in a phlogopite nodule from the Wesselton kimberlite. Subsequent work has revealed the existence of potassic richterite in an ultrabasic hypabyssal rock with kimberlite affinities and in four lherzolite nodules; for convenience this report will refer to Types A, B, and C potassic richterite respectively to denote the separate modes of occurrence involved. Representative electron microprobe analyses of each type are given in Table 1; as shown, they may be well expressed in the amphibole formula. The varieties studied are generally colourless, with slight and variable pale pink to pale green pleochroism, and it is likely that potassic richterite has been overlooked or mis-identified as orthopyroxene in previous studies. The analyses in Table 1 are reasonably similar and agree in a general way with analyses of potassic richterite from potassium-rich lavas in the West Kimberley area, Australia (Prider, 1939) and in the Leucite Hills, Wyoming (Carmichael, 1967). However, the latter types have markedly higher TiO_2 contents (3.5-6.2% TiO_2) than the kimberlitic varieties indicated in Table 1. Kushiro and Erlank (1970) showed that although potassic richterite, in the presence of water, is stable to 30 kb at 1100°C , the recrystallized products had much lower TiO_2 contents than the starting material, which was from the type locality in Australia (Prider, 1939). It is to be noted that all potassic richterites analysed to date are characterized by an Al deficiency, i.e. there is insufficient Al to make up the tetrahedral sites to 8 with Si, and thus it is assumed that some Ti is present in fourfold co-ordination. Specific comments related to the three types follow:

TYPE A potassic richterite is present in several phlogopite nodules or aggregates, which are usually mainly composed of phlogopite. Varying amounts of chrome-diopside are present; one nodule which has roughly equal proportions of phlogopite and diopside has a layered appearance. The first occurrence of potassic richterite noted by Erlank and Finger (1970) was in the form of 100 μm inclusions contained within diopside from a nodule from the Wesselton mine; larger (500 μm in diameter) and discrete grains have since been observed in a nodule from the Du Toitspan mine. The origin of these unusual nodules is enigmatic, possibly they are high pressure cumulates from a fractionated magma or the products of limited degrees of partial melting.

TYPE B potassic richterite has been found in a medium grained ultramafic hypabyssal rock from Bester's mine, Pniel Estate, Barkly West. Large partly rounded and corroded olivine crystals (Fo_{90}) are set in a matrix of euhedral phlogopite, potassic richterite and clinopyroxene, and accessory olivine, calcite and opaque mineral. The major element composition of this rock overlaps that shown by published analyses of kimberlite (e.g. 43% SiO_2 , 31% MgO , 3.8% K_2O) and it is also characterized by relatively high concentrations of both ferromagnesian and incompatible elements (1980 ppm Cr, 1460 ppm Ni, 1010 ppm Ba, 160 ppm Rb).

TABLE 1 CHEMICAL COMPOSITION OF POTASSIC RICHTERITES (wt.%)

	Type A (WESS 156)	Type B (Pn 1)	Type C (JJG 360)
SiO ₂	54.29	55.60	54.92
TiO ₂	0.59	0.88	0.57
Al ₂ O ₃	1.24	0.44	1.70
FeO	4.31	4.52	2.31
MnO	0.07	0.03	0.01
MgO	21.16	21.43	22.52
CaO	7.12	5.81	6.70
Na ₂ O	3.24	4.04	3.84
K ₂ O	4.72	4.88	4.61
Cr ₂ O ₃	0.06	0.15	0.89
Total	96.80	97.78	98.07

NUMBER OF CATIONS FOR 23 OXYGENS

Si	7.770)	7.870)	7.697)
Al	0.209)8.000	0.074)8.000	0.281)8.000
Ti	0.021)	0.056)	0.022)
Ti	0.043)	0.038)	0.038)
Mg	4.514)5.000	4.522)5.000	4.705)5.000
Cr	0.006)5.000	0.016)5.000	0.098)5.000
Fe	0.437)	0.424)	0.159)
Fe	0.078)	0.111)	0.112)
Mn	0.008)2.000	0.003)2.000	0.002)2.000
Ca	1.091)2.000	0.881)2.000	1.006)2.000
Na	0.823)	1.005)	0.880)
Na	0.077)0.939	0.103)0.984	0.163)0.987
K	0.862)	0.881)	0.824)

It differs in composition from other potassic richterite bearing lavas (jumillites, wolgidites, orendites etc) notably by its lower K₂O and higher MgO content and lack of feldspar and felspathoid. Small degrees of partial melting are presumably involved in the production of all these K-rich lavas.

TYPE C potassic richterite has thus far been identified in four lherzolite nodules (2 from the Bultfontein, and 1 each from the DuToitspan and Monastery mines). Olivine is the dominant constituent in each type, with variable amounts of enstatite, chrome-diopside, potassic richterite and phlogopite comprising the other essential minerals. These rocks are coarse grained and locally contain patches of diopside, potassic richterite and phlogopite. Their altered nature does not readily allow textural evaluation, but the potassic richterite, although a late

crystallizing phase, clearly shows equilibrium relationships with olivine, diopside and phlogopite. Trace element analyses (XRF) of three of the lherzolites show, as expected from their mineralogy, high abundance of the incompatible elements when compared to granular and sheared nodules which do not contain potassic richterite, with the latter types exhibiting the greatest depletion. This may be especially illustrated by the refractory elements Zr and Nb, viz:

	<u>Zr, ppm</u>	<u>Nb, ppm</u>
Potassic Richterite bearing lherzolites	42,169,82	17,17,36
Granular nodules	6-21	2-6
Sheared nodules	2-10	1-3

High pressure work by Kushiro and Erlank (1970) showed that although potassic richterite is by itself and in the presence of diopside stable under upper mantle conditions, it is not stable in the presence of garnet with which it reacts to form phlogopite. The bulk rock chemistry, and the alumina deficiency in the calculated mineral formulae show that potassic richterite crystallizes in an environment in which the chemical potential of K is high relative to that of Al. Only one of the rocks studied here (Monastery mine) contains garnet, present in trace amounts in the form of small rounded grains enclosed by enstatite. Whatever the origin of the potassic richterite bearing rocks discussed here, it appears that they are derived from a locale in which garnet or aluminous spinel are not present or do not participate in their development, or from liquids which have high K/Al ratios. Thus the potassic richterite bearing lherzolites, while mantle derived and equilibrated as shown by pyroxene compositions, are not considered to be representative of upper mantle materials and special conditions are required for their formation.

As shown above, potassic richterite is not likely to be an important mantle phase. Electron microprobe studies have shown that much of the K present in kimberlite nodules is secondary in origin, being located in cracks, along grain boundaries, reaction rims and alteration products (Erlank, 1970). Olivine, orthopyroxene and garnet contain <30 ppm K as measured by microprobe analysis; higher concentrations reported in the literature measured on separated fractions indicate the separates to be impure. The K concentration of clinopyroxenes is variable; up to 500 ppm K is found in chrome-diopside and up to 1500 ppm K in eclogitic omphacite. These concentrations, taken in conjunction with average modal mineralogy for four phase garnet lherzolite and predicted upper mantle concentrations using independant approaches indicate that phlogopite (0.5 - 1%) is the most likely upper mantle potassic phase. This conclusion may have been expected from simple thin section examination of kimberlite nodules, but textural relationships do not indicate what proportion of the phlogopite now observed in kimberlite nodules is an original pre-melt constituent of the upper mantle. It is considered that much of the phlogopite in kimberlite nodules is equilibrated under upper mantle conditions, but has formed by either metasomatic processes or represents trapped partial melt.

Available evidence suggests that in shield regions phlogopite should be stable to depths of about 175 km (Modreski, 1972). Below this depth

the distribution of K in the mantle is not well known, but it is likely that clinopyroxene is an important phase, partly because of the lack of a potassium mineral but also because there is some evidence to show that the K content of clinopyroxene is temperature and pressure dependant. Thus electron microprobe measurements show that:

- (a) clinopyroxene from intrusive and extrusive igneous rocks (Bushveld gabbros and Karroo dolerites) and from xenoliths in basaltic lavas (Hawaii) and volcanic breccias (Kakanui, Delegate) contain < 50 ppm K.
- (b) calcic diopsides from kimberlite nodules contain < 250 ppm K while sub-calcic diopsides, equilibrated at higher temperatures (Boyd, 1973), contain up to 500 ppm K.
- (c) eclogitic omphacites contain up to 1500 ppm K; the distribution of K in these minerals may be bimodal (Erlank, 1970). Omphacite from diamond apparently contains up to 2200 ppm K (Sobolev, 1972).
- (d) synthetic clinopyroxenes produced at high temperatures and pressures show that < 150 ppm K enters the clinopyroxene structure at pressures of up to 30 kb (Erlank and Kushiro, 1970). However, at higher pressure more K is apparently able to substitute in clinopyroxenes, 2200 ppm K being measured in a synthetic clinopyroxene produced at 100 kb and 1400°C (Shimizu, 1971).

Thus, at depths below which phlogopite is stable, and unless K is contained in interstitial melts or other potassium minerals, clinopyroxene is likely to be an important phase for controlling the distribution of K in rocks and basaltic melts at these depths.

References:

- Boyd, F.R. (1973) *Geochim. Cosmochim. Acta*. (in press).
- Carmichael, I.S.E. (1967) *Cont. Mineral. Petr.* 15, 24-66.
- Erlank, A.J. (1970) *Carnegie Inst. Wash. Yr. Book* 68, 433-439.
- Erlank, A.J. and Finger, L.W. (1970) *Carnegie Inst. Wash. Yr. Book* 68, 442-443.
- Erlank, A.J. and Kushiro, I. (1970) *Carnegie Inst. Wash. Yr. Book* 68, 439-442.
- Kushiro, I., and Erlank, A.J. (1970) *Carnegie Inst. Wash. Yr. Book* 68, 231-233
- Modreski, P.J. (1972) *Carnegie Inst. Wash. Yr. Book* 71, 392-396.
- Prider, R.T. (1939) *Mineral. Mag.* 25, 373-387.
- Shimizu, N. (1971) *Earth Planet. Sci. Lett.* 11, 374-380.
- Sobolev, N.V. (1972) *24th Int. Geol. Congress, Section 2*, 297-302.

GROSS BRUKKAROS: A KIMBERLITE-CARBONATITE VOLCANO

John Ferguson*, H. Martin⁺, L.O. Nicolaysen* and R.V. Danchin^f

* University of the Witwatersrand

+ Georg-August-Universität, Göttingen

^f Anglo-American Research Laboratories

The Gross Brukkaros massif lies at the southern extremity of the Gibeon kimberlite province in South West Africa; it is a well-formed shallow volcanic vent with a central depression whose diameter exceeds two kilometres and rises approximately 700 metres above the great Namaqualand plain. The country rocks surrounding the main crater at Gross Brukkaros form a well-defined up-domed collar whose structure has been described in some detail by Janse (1969). The vent is lined by a 130 metre succession of stratified non-pyroclastic microbreccias, blown out by repeated explosions of the central volcano. This activity cuts through the late Precambrian strata of the Nama Super-group which underlies the microbreccias, and is dominated by vents and radial fissures having kimberlitic and carbonatitic affinity. A sheet-like monticellite peridotite intrusive is also present on the southern slopes of Gross Brukkaros.

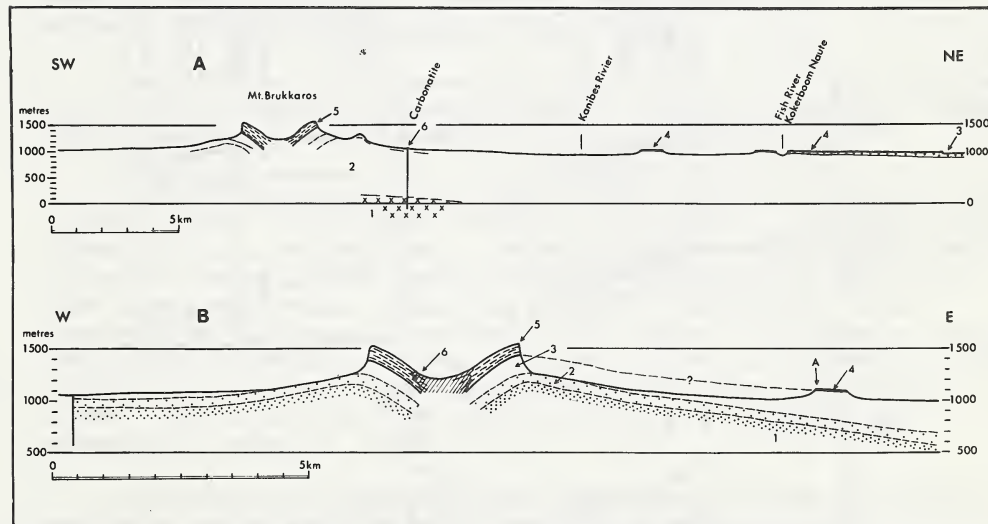


Figure 1 A. Section from Gross Brukkaros to Kokeboom Naute. 1 = Pre-Nama basement, 2 = Nama Super-group, 3 = Dwyka Group, 4 = Eolian quartzitic sandstone overstepping Dwyka and Nama beds with an angular unconformity, 5 = layered microbreccias, 6 = carbonatite vent with Basement inclusions.

B. East-West section. 1 to 3 = Quartzites, flagstones and shales of the Nama Super-group, 4 = Eolian quartzitic sand-

stone, 5 = layered microbreccia, 6 = contact of microbreccia of volcanic neck and layered microbreccia.

There is striking petrographic evidence of fenitisation, affecting both basement fragments and sedimentary fragments in the microbreccias. Pre-explosion fenitisation is demonstrated by metasomatism of some angular inclusions along one margin only, and by the restriction of some calcite veins to single inclusions. Post-depositional fenitisation is displayed by thick, steeply-inclined alteration zones spectacularly exposed in the high walls of a gorge cutting through the microbreccias. The layered microbreccias were originally of a pale-brown variety displaying angular fragments with the basement inclusions showing intact quartz grains. Post-depositional passage of carbonate and K-rich hematite solutions have been responsible for production of buff and red varieties of microbreccia respectively.

Pre-explosion fenitising solutions have produced a strong desilication of argillite fragments, and have introduced Na, Ca, Mg, Ti, Fe^{3+} , total Fe and C (Fig. 2). Post-depositional late-stage fenitising solutions have also produced a local enrichment in K, P and C. Enrichment in the characteristic elements of the ultramafic suites is shown by data for Cr, Ni, V and Sc. The elements particularly characteristic of residual associations, Li, Nb, Be, Zr, Y and Sr, have also been introduced.

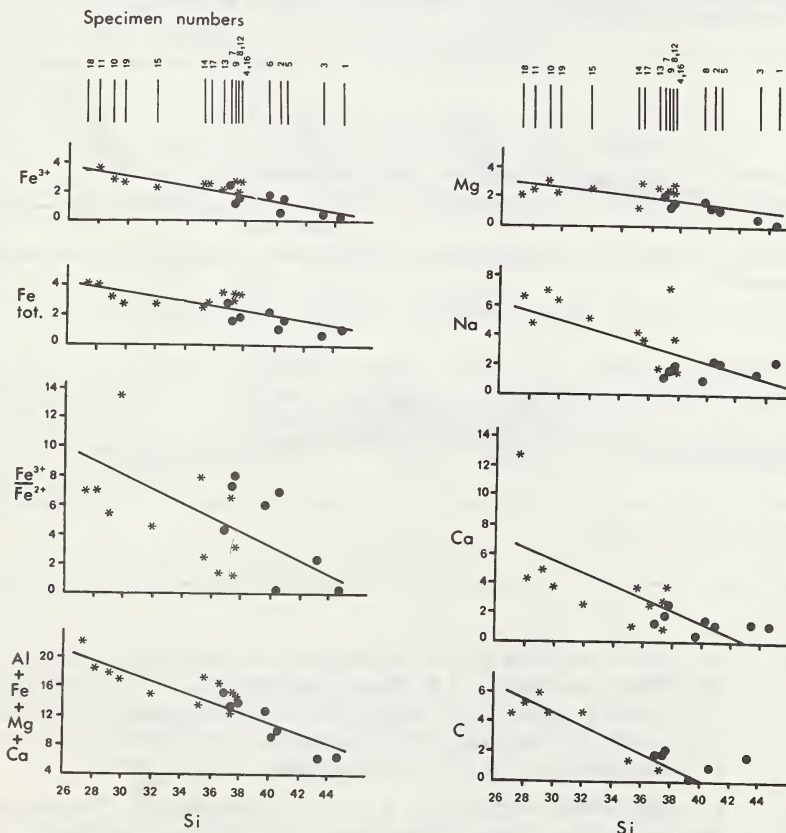


Figure 2. Variation of cation content of standard cell with Si for argillites and their fenitised equivalents. Solid circle = Nama argillites, star = microbreccias.

Rocks exposed on the northern slopes of the Gross Brukkaros structure, in the subsidiary vents termed J1 and L1 by Janse (1969), have a matrix of carbonated kimberlitic rocks with ~ 70 per cent of olivine pseudomorphs; phlogopite and perovskite also occur here. In vent J1, rounded fenitised granitoid inclusions are concentrically mantled by this kimberlitic rock. Similar autoliths have been recorded from a number of kimberlite pipes and are a feature restricted to diatreme facies (Ferguson *et al.*, in press, ref. a, and Danchin *et al.*, this volume). Autoliths are interpreted as nucleation of kimberlitic magma around solid fragments (Ferguson *et al.* *op. cit.*). Between Gross Brukkaros and the kimberlite diatremes at Mukarob, some 70 km to the northeast, there are abundant calcitised dikes of kimberlite and olivine melilitite (Frankel, 1956). Janse (1971) noted the significant presence of a monticellite peridotite on the southern slopes of Gross Brukkaros. Two new chemical analyses of this rock reveal a composition almost identical to a specific group of kimberlites and, furthermore, to a group of melilite- and monticellite-bearing rocks (Ferguson *et al.* in press, ref. b). Rb-Sr isotopic data for mica and carbonate fractions taken from the monticellite peridotite body at Gross Brukkaros yield an age of 84 m.y. and an initial $\text{Sr}^{87}/\text{Sr}^{86}$ ratio of 0.7041 (D. Barrett personal communication). This Sr-isotope ratio is markedly similar to those obtained for fresh kimberlites (Berg and Allsopp, 1972 and Danchin *et al.*, this volume)

Heavy mineral concentrates from soil samples within the crater and its immediate surroundings contain pyrope and chrome diopside. Kimberlitic ilmenite has been identified in the microbreccias.

In the CMAS tetrahedron of O'Hara (1968) kimberlites lie on a well-defined olivine control line trending sub-parallel to the CAM plane (Danchin *et al.*, this volume). The melilite- and monticellite-bearing ultramafic rocks plot at the extremity of the kimberlite trend with some degree of overlap, indicating possible consanguinity (also supported by the isotope chemistry). The control line of these ultramafic rocks associated in space and time produces an inflection in the olivine control line of the kimberlites trending away from the MAS plane. This inflection represents an equilibrium condition at a pressure in excess of 30 Kb.

No evidence was found of shock metamorphism at Gross Brukkaros. A meteorite impact origin for the structure is rejected on several grounds. The suggested alternative model is that kimberlitic magma was generated at a depth in excess of 100 km and rapidly ascended the mantle and lower crust reaching a depth of 2-3 km below surface. At this level a carbonatitic fraction unmixed and also reacted with the olivine and ilmenite, to form monticellite and perovskite respectively, with the dense mineral phases and xenoliths settling out of the residual silicate magma. It is also possible that the rise of the kimberlite magma was arrested at a depth in excess of 100 km where equilibrium conditions included the reaction of olivine and ilmenite to produce melilite and perovskite respectively. This latter magma

would then rapidly rise to the hypothetical depth of 2 - 3 km below surface where the melilite would react to produce monticellite. At this high level in the crust an immiscible carbonatitic top developed. The carbonatitic and alkaline ultramafic magmas were in equilibrium, together with their alkali volatile phase which impregnated and fenitised the wall rocks in joint zones. The volatile pressure built up until it was just greater than the lithostatic pressure, and bulging of the roof began. With a breach of the containment of the volatile phase, there was violent disruption of the roof. Much of the brecciation and fine disruptive veining is interpreted as episodic failure in containment of fluid pressure. At lower pressure, melilite reacted to produce monticellite and this degassed magma intruded the outer flank of the volcano in the initial stages of eruption.

Berg, G.W. and Allsopp, H.L. 1972. Earth and Planetary Sci. Letters 16, 27-30.

Danchin, R.V., Ferguson John, McIver, J.R. and Nixon P.H. This volume.

Ferguson, John, Danchin, R.V. and Nixon, P.H. in press (a) In:
Lesotho Kimberlites (P.H. Nixon, Ed.)

Ferguson, John, Nicolaysen, L.O., Martin, H. and Danchin R.V. in
press (b) Nature, London.

Frankel, J.J. 1956 Trans. Roy. Soc. S. Afr., 35, 115-123.

Janse, A.J.A. 1969. Geol. Soc. Amer. Bull. 80, (4), 573-586.

1971 Trans. geol. Soc. S.Afr., LXXIV, 45-56.

O'Hara, M.J. 1968. Earth Sci. Rev., 4, 69-133.

A COMPARATIVE TRACE ELEMENT STUDY OF DIAMONDS FROM PREMIER,
FINSCH AND JAGERSFONTEIN MINES, SOUTH AFRICA

H.W. Fesq, D.M. Bibby, C.S. Erasmus, E.J.D. Kable and J.P.F. Sellschop
NIM-WITS A.A.R.G., N.P.R.U., Univ. of the Witwatersrand, Johannesburg

Natural diamonds, the high pressure polymorph of primary carbon, are generally believed to have formed under stable, equilibrium conditions at depths of 100 km or greater in the upper mantle (1). They are found as phenocrysts in some kimberlites and less commonly in related upper mantle derived rocks e.g. eclogites.

The present hypotheses of diamond genesis favour their crystallisation from igneous melts (1). Inclusions found in diamonds are either minerals which formed in equilibrium with diamonds or the liquid from which these phases crystallised. The impermeable and inert nature of diamonds prevents any mineral, or fluid inclusions from re-equilibrating with the magma transporting the diamonds to the earth's surface. Important information on the geochemistry of the upper mantle and the genesis of igneous rocks can therefore be gained from a study of diamonds and their syngenetic inclusions.

The predominant mineral inclusions reported in diamonds are forsterite and pyropic garnet; less common are enstatite, diopside, chromite, rutile, the sulphides and coesite (1, 2). The chemistries of these inclusions resemble those of minerals found in cognate peridotite, eclogite, and xenocrysts/phenocrysts present in the host kimberlites (3).

In order to study the trace element geochemistry of natural diamond, and by inference their syngenetic inclusions, a total of 520 carats of diamonds from South African sources were analysed by instrumental neutron activation analysis (INAA). Details of the analytical technique and the standardisation procedure followed are reported elsewhere (4).

Diamonds were obtained from three regionally well-separated kimberlites: Premier, Finsch and Jagersfontein. The former is of Precambrian age (5) whilst the latter two are probably Cretaceous.

Representative 1 gram samples consisting on the average of 15 individual stones were selected from one month's production of each mine. Samples were sorted on the basis of four main colour categories (colourless, yellow, green and brown); and the presence of visible inclusions, or their absence at 50x magnification under a polarizing microscope. No distinction was made between coated (6) or clean inclusions but diamonds with fractures were avoided with the exception of the boart samples. Prior to analysis great care was taken in the cleaning of the diamonds. Quantitative results for 16 elements in "inclusion free" diamonds (Table 1), and 26 elements in diamonds with inclusions (Table 2) are presented. Differences greater than two orders of magnitude in the abundance of some elements can be observed. This is a function of the dominant mineral inclusions. An indication of the predominant minerals present in diamonds can be obtained by comparing the chemistry of inclusions contained in diamonds with both the major element chemistry of individual mineral inclusions found in diamonds (1), and the trace element content of kimberlite minerals (7).

Correlation matrices based on the 26 elements analysed were computed for each of the three sources investigated. Significant correlations for the following elements indicate the type of mineral inclusion present:

FIG. 1

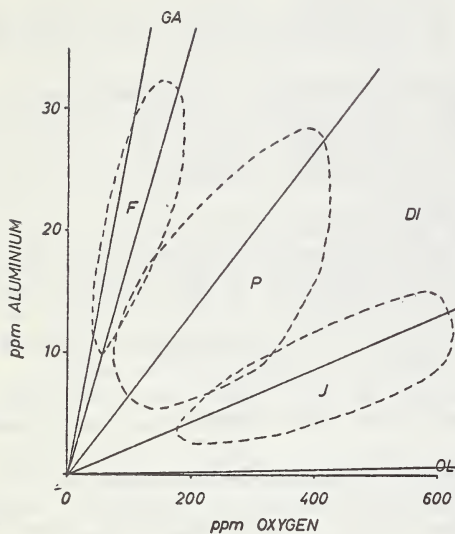


FIG. 2

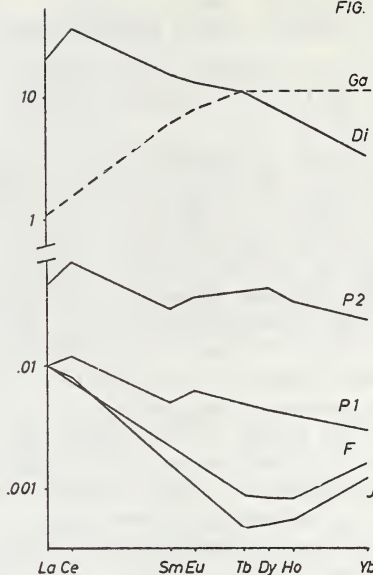


TABLE 2
ELEMENT CONCENTRATIONS IN DIAMONDS WITH VISIBLE INCLUSIONS FROM THREE SOUTH AFRICAN SOURCES

Element	Source:	Premier (19)	Finsch (18)	Jagersfontein (17)	
	Ave.	Ave.	Ave.	Ave.	
Oxygen	ppm	179	35 - 420	65 23 - 103	302 79 - 1620
Mg	ppm	52	14 - 128	23 1 - 83	52 5.5 - 372
Fe	ppm	24	2.6 - 71	16 5.4 - 34.5	42 3.6 - 141
Ca	ppm	16.8	2.2 - 57	2.7 0.3 - 10.5	45 1.5 - 231
Al	ppm	11.8	1.3 - 39	6.2 0.44 - 28	9.7 0.22 - 69
Na	ppm	2.42	0.68 - 9.9	3.14 0.75 - 19.1	1.97 0.12 - 9.91
Ti	ppm	1.15	0.14 - 2.95	0.26 LD - 1.88	4.1 0.05 - 28.7
Mg/(Mg+Fe)	ppb	82.9	67.6 - 92.9	66.3 26.6 - 94.6	68.5 27.3 - 89.2
V	ppb	39.4	5.4 - 152	16.2 1.5 - 51	61.3 1.5 - 262
Sc	ppb	3.84	1.71 - 14.9	2.2 0.17 - 12.2	4.4 0.07 - 17.2
Cr	ppb	166	LD - 518	1450 LD - 5960	374 12 - 1650
Mn	ppb	422	82 - 1280	305 11 - 2270	784 26 - 5440
Co	ppb	142	14 - 1540	92 21 - 245	196 21 - 1080
Ni	ppb	10000	LD - 34000	5460 LD - 14600	8070 LD - 24600
Cu	ppb	1190	LD - 9320	672 LD - 2060	2679 LD - 14600
Sr	ppb	180	LD - 360	240 LD - 2240	630 LD - 2430
Ba	ppb	550	LD - 2160	11300 60 - 23600	2690 60 - 18600
La	ppb	4.86	0.5 - 17.5	16.8 0.07 - 96.4	32.2 0.98 - 161.2
Ce	ppb	14.2	2.8 - 52.0	57.8 LD - 136.0	62.6 LD - 234.0
Sm	ppb	3.32	LD - 4.76	2.15 LD - 11.9	4.53 LD - 25.0
Eu	ppb	0.34	LD - 0.84	0.37 LD - 1.87	1.08 LD - 3.8
Dy	ppb	0.58	LD - 2.19	1.57 LD - 4.93	2.22 LD - 3.9
Ho	ppb	0.16	LD - 0.83	0.25 LD - 0.78	0.49 LD - 1.02
Yb	ppb	0.36	LD - 0.63	1.49 LD - 1.98	1.07 LD - 3.00
Lu	ppb	0.08	LD - 0.10	0.38 LD - 0.56	0.28 LD - 0.65

INCLUSIONS: Di>Ga>Ol, S, Sp?

Di>S>Di

Di>S>Ga+(En, Ol, Sp?)

Numbers in brackets refer to the number of 1 gram samples in the average

LD = Limit of Detection

Ga - Cr-rich Pyrope Garnet, Di - Diopside, En - Enstatite, Ol - Olivine, Sp - Cr-rich Spinel, S - Fe, Cu, Ni, Co Sulphides (Pyrrhotite, Pentlandite)

Diopside	-	O, Ca, Na, Mg, Ti, Al, (Sr), light REE
Garnet	-	O, Al, Sc, Mn, Cr, Mg, heavy REE
Olivine)	-	O, Mg, Ni, Co, low Al
Enstatite)	-	O, Mg, Ni, Co, low Al
Chromite	-	O, Cr, Mg, Co, low Sc, Al, Na
Sulphides	-	Fe, Cu, Ni, Co, low O, Mg

The inferred mineral assemblages in diamonds from the sources we investigated were generally dominated by either garnets (Finsch) or diopside (Premier and Jagersfontein) (Table 2). This statistical analysis was confirmed by plotting the measured Al against oxygen content in all the diamonds analysed (Fig. 1). Superimposed on this diagram are the extreme limits for garnets, diopsides and olivines reported by Meyer and Boyd (1). Generally, the inclusion chemistry is dominated by a diopside-garnet assemblage, for which further evidence is provided by the REE contents in these diamonds relative to that of the average REE in chondrites (8) (Fig. 2). Patterns for average South African kimberlite garnets (GA) and Cr-diopside (DI) are included for comparison. The primitive REE pattern of Premier Cr-diopside (P_1) inclusions is in accordance with the relatively primitive pattern of the Premier kimberlites and minerals (9). This may be a function of the Pre-cambrian age of kimberlite (5) and/or derivation from a relatively undepleted mantle.

In the absence of sulphides the Mg/(Mg+Fe) approaches the ratio for olivines, enstatites and pyropic garnets: 92-96 (1). The deviation of this ratio from ~ 90 could be interpreted as function of the amount of sulphides present (Table 2). Pyrrhotite and/or pentlandite were inferred to be present in nearly all the inclusion containing samples, confirming the observations of Harris (6).

The data obtained for 'inclusion free' samples (all stones; the light coloured ones of gem quality) were analysed statistically for a possible correlation of colour with chemistry. This analysis gave significant correlations between elements found in garnet (Mg, Fe, Al, Sc, Cr, Mn and O) and Cr-diopside (Ca, Al, Na and O) (Table 1).

It is concluded that these elements are present as micro-aggregates - generally amorphous, (10, 11) and represent droplets of trapped liquid which may be expected to be found in diamonds that crystallised from a liquid (1). This conclusion finds further support from the observed excess of oxygen relative to Al, which could indicate the presence of volatiles, e.g. CO_2 , H_2O . The presence of CO_2 on the crystal boundaries of syngenetic mineral inclusions would provide the mechanism for graphitisation on the inclusion - diamond interfaces described by Harris (6).

In this context it is interesting to note that not only do diamonds from Premier contain a fair number of graphite coated inclusions, but they also have an average of ten times higher trace element content when compared to the other two sources investigated. Premier diamonds should therefore contain more 'liquid' inclusions, which may result from a faster crystallisation rate for diamonds from this pipe when compared to diamonds from Finsch and Jagersfontein.

The very primitive but enriched REE pattern P_2 (Fig. 2) may reflect that of the liquid from which Premier diamonds crystallised. From data obtained so far (Table 1) these 'liquid' inclusions appear to have a $\text{Ga} > \text{Di} \pm \text{Ol}$ chemistry relatively rich in sulphur.

TABLE 1
AVERAGE TRACE ELEMENT IMPURITIES IN SOME "INCLUSION FREE"
SOUTH AFRICAN DIAMONDS

Description	O	Fe	Ca	Al	Na	Ti	V	Sc	Cr	Mn	Co	Ni	Cu	Sr	Ba
	ppm	ppm	ppm	ppm	ppm	ppm	ppb	ppb	ppb	ppb	ppb	ppm	ppm	ppm	ppm
Colourless: P (3)*	6.10	2.70	0.66	0.380	0.173	0.060	2.90	0.731	35.03	46.0	8.0	—	2.1	—	0.060
	(3)	5.2	0.27	0.28	<0.20	0.033	0.022	0.050	0.10	0.007	3.58	0.8	0.5	0.25	8
	F (3)	3.9	0.23	0.58	0.16	0.068	0.038	0.021	0.19	0.014	1.08	1.7	6.0	0.27	64
Yellow:	P (4)	0.80	1.39	0.29	0.310	0.090	0.040	1.90	0.063	11.98	6.8	5.0	1.0	1.5	—
	F (3)	4.5	<0.10	0.64	<0.20	0.050	0.023	0.030	2.00	0.004	0.90	0.4	10.0	0.30	9
	J (4)	37	0.15	0.47	0.14	0.127	0.013	0.016	0.49	0.090	1.41	2.4	2.0	0.14	—
Brown:	P (6)	7.1	8.16	4.20	10.0	0.610	0.090	8.00	2.865	67.78	122.0	17.0	—	5.7	—
	F (3)	3.9	3.7	2.15	0.23	0.270	0.057	0.050	1.00	0.118	95.50	18.0	5.0	<0.20	<10
	J (3)	4.2	1.4	1.01	0.35	0.280	0.032	0.032	1.18	0.163	93.07	8.7	5.1	0.28	60
Green:	P (2)	18.1	25.0	16.47	15.2	15.0	3.00	1.00	25.0	4.515	133.25	305.0	50.0	0.60	—
	F (5)	31	0.5	1.57	0.25	0.369	0.047	0.20	0.80	0.211	6.95	11.0	4.0	1.0	30
F-test value (35 degrees of freedom)	2.1	4.36	3.71	2.38	3.57	1.46	1.14	3.92	4.57	4.44	3.73	2.57	0.68	0.11	1.30
Significance (1)*		95	95	95	95	95	95	95	95	95	95	95	95	95	95

* 95% significance $2.88 < F < 4.40$

* The figures quoted in parentheses indicate the number of 1 gram samples analysed. P = Premier, F = Finsch, J = Jaggerstein

REFERENCES:

- (1) H.O.A. Meyer, F.R. Boyd, Geochim. Cosmochim Acta, 36, 1255, (1972)
- (2) J.W. Harris, Contr. Mineral. Petrol., 35, 22 (1972)
- (3) J.J. Gurney, G.S. Switser, Contr. Mineral. Petrol., 39, 103, (1973)
- (4) H.W. Fesq et al, J. Radioanal. Chem. (to be published)
- (5) H.L. Allsopp, et al, Earth Planet. Sci. Lett. 3, 161, (1967)
- (6) J.W. Harris, E.R. Vance, Contr. Mineral. Petrol., 35, 227 (1972)
- (7) J.J. Gurney, et al, in "Lesotho Kimberlites" Ed. P.H. Nixon (1973)
- (8) L.A. Haskin, et al, in "Origin and Distribution of the Elements" Ed. L.H. Ahrens, 889 (1968)
- (9) H.W. Fesq, et al, Int. Kimberlite Conf. (1973)
- (10) M. Seal, Nature, 212, 1528 (1966)
- (11) M. Seal, Diamond Conf. (1970)

SOME ASPECTS OF THE GEOCHEMISTRY OF KIMBERLITES FROM THE PREMIER MINE,
TRANSVAAL, SOUTH AFRICA

H.W. FESQ¹, E.J.D. KABLE¹, and J.J. GURNEY²

¹NIM-WITS A.A.R.G., N.P.R.U., University of the Witwatersrand.

²Department of Geochemistry, University of Cape Town.

The Premier kimberlite pipe is unique in relation to other kimberlite occurrences in Southern Africa in that it is the only known Pre-cambrian kimberlite, $>1150 \pm 15$ m.y. (1), whereas all other occurrences are believed to be of Cretaceous age. It is intrusive into a plug of igneous rocks which is related to the well known Bushveld Igneous Complex (1950 ± 150 m.y.)

The Premier diatreme is a complex, multiple intrusion in which at least eight different types of kimberlite are macroscopically distinguishable, all containing diamonds in economic quantities. These different types are thought to be derivatives of three major brecciated basaltic kimberlites which are associated with separate intrusive events. In order of intrusion they are: Type 2 Brown \rightarrow Type 1 Grey \rightarrow Type 3 Black. Some of these kimberlites contain large numbers of lithic and basic rock fragments generally of Bushveld parentage as well as fragments and rafts of Waterberg quartzite (2).

Representative samples (~ 50 kg) of each type were collected at different levels within the mine and where possible, away from mixed contact zones.

Samples were analysed for major and trace elements by X-ray fluorescence, X.R.F. (3), instrumental neutron activation analysis, I.N.A.A. (4) and conventional chemical techniques. The average chemistry for each of the main Premier kimberlite types is presented in Tables 1,2. Data for other kimberlites are included for comparison (Table 1), particularly with respect to the varying degree and type of crustal contamination.

Kimberlites generally contain large numbers of crustal fragments, normally of the country rock into which they intrude (5). Their major element chemistry in particular will therefore reflect such contamination (Table 1), N.B. samples KN275/75 and 1982 with high Mg/(Mg+Fe) are relatively uncontaminated 'kimberlites'. Unless an attempt is made to remove the contribution of the major crustal contaminant (mixing model analysis), interpretation particularly with respect to the genetic relationship of kimberlite from major element chemistry can be misleading.

For example, from the Mg/(Mg+Fe) for Premier kimberlites a genetic differentiation relationship in the order: Black Type 3 \rightarrow Brown Type 2 may be inferred. However this is in disagreement with evidence available for the refractory elements (6) and the REE (Table 2, Fig. 1). Erroneous Fe values are a function of the overall composition and the amount of crustal contamination. This observation is even better illustrated by the kimberlites from the Bellbank fissure system where contamination is due to high limestone assimilation in the Water Fissure which is definitely the least 'differentiated' of the Bellbank kimberlites (6). The primitive REE pattern highlights both these observations (Fig. 1). The high amount of crustal contamination in Premier kimberlites is well illustrated by their high SiO₂ content particularly in Type 1 (Table 1). Of all the Premier kimberlites Type 2 Brown has the least variable chemistry indicating that it has not been affected by

kimberlite mixing e.g. Type 1 and 2 (2).

Crustal contamination is reflected by:

- (a) the inclusion of crustal fragments in the kimberlite magma; such contamination may be estimated by modal analysis (e.g. Type 1 Grey 43%, Type 3 Black 20%) and
- (b) the assimilation of crustal material, the amount of which is a function of the temperature of the kimberlite magma, its mode of emplacement and the composition of the crustal contaminant, e.g. it would be more difficult to assimilate basic than acid rocks or sediments.

Experiments on the induced graphitisation around mineral inclusions in Premier diamonds indicate emplacement temperatures from 850°C to 1050°C for Premier kimberlites (7). The higher temperature can probably be associated with the Type 2 Brown which on evidence of its chemistry assimilated some basic rocks of Bushveld parentage.

REE GEOCHEMISTRY (Table 2, 3, Fig. 1).

A comparison of the REE geochemistry of Premier kimberlites with other South African kimberlites indicates that Premier kimberlites:

- (a) are basaltic (low REE) and
- (b) are derived from relatively undepleted mantle, probably from the same source region. Cr-diopsides, garnets and ilmenites as well as diamonds (9) studied from this source confirm the above observation. Compared with more differentiated micaceous kimberlites (e.g. OG383, Fig. 1) no Eu anomalies are present in Premier kimberlites. Eu depletion appears to be related to the differentiation of kimberlitic liquids and the crystallisation of phlogopite. The analysis of a 'primitive' phlogopite from a Bultfontein garnet peridotite nodule exhibits a negative Eu anomaly. Such an anomaly may be enhanced by phlogopites crystallising from a differentiating kimberlite magma. It is suggested that phlogopite superimposes its REE chemistry on the more differentiated micaceous kimberlites, which would explain the observed high Eu negative anomaly in Bellsbank Main Fissure kimberlites. These contain from 25-60% phlogopite and up to 6% apatite in the matrix (10).

Ilmenite is at present the only upper mantle mineral which we are aware of, which exhibits a positive Eu pattern. Large amounts of ilmenite fractionation would therefore be necessary to explain the Eu depletion in the more differentiated kimberlites. This is considered to be unlikely, although it has been established that ilmenites of changing composition crystallised from the Premier kimberlite magmas (11).

From the involatile and even volatile geochemistry of Premier kimberlites it appears that Type 2 Grey and Type 3 Black are closely related, the latter being the more differentiated product. However, all Premier kimberlites appear to have originated from the same source of the upper mantle, and since the Type 2 Brown was emplaced first (2), a possible age difference is implied between Type 2 Brown and the other types. This is confirmed by recent Rb/Sr age measurements (Allsopp, pers. comm.).

REFERENCES:

- (1) H.L. Allsopp et al, *Earth Planet. Sci. Lett.* 3, 161 (1967).
- (2) Anglo American Corp. of S.A., Ltd. Cons. Geol. Dep. Rep. (1969).
- (3) J.P. Willis et al, in *Proc. 2nd Lunar Sci. Conf.* 2, 1123 (1971).
- (4) H.W. Fesq et al, *J. Radio-anal. Chem.* (in press).
- (5) P.A. Wagner, *The Diamond Fields of Southern Africa* (1971).
- (6) E.J.D. Kable et al, *Int. Kimberlite Conf.* (1973).

TABLE 1 PREMIER AND SELECTED KIMBERLITES FROM SOUTHERN AFRICA - A COMPARISON

	P/2	P/1	P/3	KOFFY. (10)	EBEN/W (5)	LESOTHO S4B	LESOTHO B/WF (10)	MON. (7)	LESOTHO KN275/75	LESOTHO 1942
SiO ₂	44.67	48.46	39.59	40.67	34.92	40.20	25.27	28.80	27.38	32.23
TiO ₂	1.70	1.76	2.10	0.90	0.78	1.70	0.50	0.79	1.22	1.48
Al ₂ O ₃	4.46	4.12	2.88	5.56	6.61	7.50	1.64	2.47	2.64	1.58
Cr ₂ O ₃	0.17	0.19	0.21	0.12	0.11	0.67	0.25	0.25	0.14	0.23
TFe ₂ O ₃	8.64	8.52	9.31	7.60	5.21	10.68	4.77	7.92	12.87	9.20
MnO	0.14	0.15	0.15	0.13	0.08	0.16	0.13	0.13	0.18	0.37
MsO	22.42	23.04	27.60	23.73	10.13	19.86	10.50	24.95	26.17	26.17
CaO	4.46	4.46	6.84	3.69	15.85	9.75	26.34	11.94	6.14	31.86
Na ₂ O	0.85	0.57	0.33	0.29	0.41	0.67	0.03	0.03	0.21	0.46
K ₂ O	1.31	0.74	1.69	2.00	0.53	1.00	0.97	0.97	0.97	0.97
P ₂ O ₅	0.28	0.18	0.33	0.34	0.10	0.40	0.41	1.33	0.94	0.11
LOI ^a	4.89	4.52	5.21	7.81	7.92	5.10	6.75	10.99	7.42	9.00
H ₂ O	3.01	2.21	0.52	0.81	5.15	2.91	5.93	0.95	0.40	0.83
CO ₂	0.33	0.83	0.16	0.90	11.79	0.37	20.50	7.04	5.83	5.11
Mg/(Mg+Fe) ^b	91.1	91.5	92.1	92.5	89.2	88.0	89.8	92.6	88.4	93.2
PPM										
Cr	890	1060	120	6.90	520	1100	1320			
Ni	870	950	110	10.90	475	1110	1110			
Co	72	73	86	71	40	53	640			
K	10880	6140	13610	5690	17350	390	4			
Rb	104	51	154	44	80	53	53			
Cs	3.2	2.7	4.5	1.8	3.3	4	3.4			
Th	7.1	5.5	5.3	8.6	13.4	13.9	45.8			
U	1.5	0.8	0.8	2.0	1.6	2.5	5.3			
K/Rb	105	120	88	129	217	98	122			
K/Cs	340	2274	304	312	528	97	159			
Th/U	4.7	6.9	6.6	14.3	8.4	5.6	8.6			

^a NUMBER OF SAMPLES ANALYSED^b MOLAR RATIO OF Mg/(Mg+Fe)

LESOTHO KIMBERLITES FROM GURNEY AND EBRAHIM (1973)

P/2 - PREMIER TYPE 2 BROWN

P/1 - PREMIER TYPE 1 GREY

P/3 - PREMIER TYPE 3 BLACK

KOFFY, ROFFEY-FOETEIN PIPE

EBENHAEER WEST PIPE

BELLSBANK WATER FISSURE

BELLSBANK MAIN FISSURE

(7) J.W. Harris and E.R. Vance, Contr. Mineral. and Petrol. 35, 227 (1972)

(8) I.D. MacGregor, Mineral. Soc. Amer. Spec. Pap. 3, 51 (1970)

(9) H.W. Fesq, D.M. Bibby et al, Int. Kimberlite Conf. (1973)

(10) J.L. Bosch, Trans. Geol. Soc. S.A. 74(2), 75 (1971)

(11) J.J. Gurney et al, Lesotho Kimberlite Vol., ed. P.H. Nixon (1973)

(12) J.J. Gurney and S. Ebrahim, Lesotho Kimberlite Vol., ed. P.H. Nixon (1973)

(13) L.A. Haskin et al, in Origin and Distribution of the Elements, ed. L.H. Ahrens, 889 (1968)

L.A. Haskin et al (1966), in Physics and Chemistry of the Earth, 7, 169

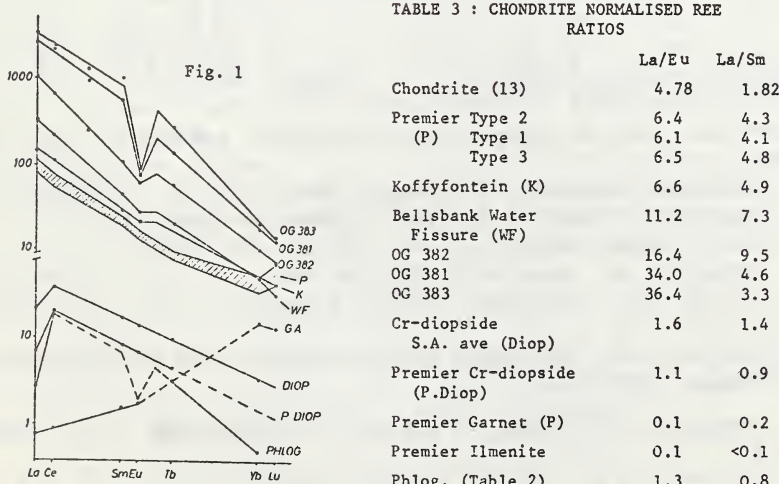
R.H. Mitchell et al (1973), Lesotho Kimberlite Vol., ed. P.H. Nixon

TABLE 2
Sr, Ba AND THE REE IN PREMIER AND SELECTED SOUTH AFRICAN
KIMBERLITES AND SOME KIMBERLITE MINERALS

KIMBERLITES	Sr	Ba	La	Ce	Nd	Sm	Eu	Tb	Yb	Lu	
PREMIER											
Type 2 Brown	(7)*	401	507	38.0	59	< 25	4.8	1.25	0.41	1.1	0.24
Type 1 Grey	(4)	183	211	27.6	49	< 25	3.7	0.95	0.39	0.9	0.14
Type 3 Black	(4)	492	1018	32.2	55	< 25	3.7	1.03	0.49	0.7	0.15
KOFFYFONTEIN GROUP											
KOFFYFONTEIN	(10)	394	229	48.9	102	~ 35	5.5	1.54	0.83	0.9	0.14
EBENHAEZER West	(5)	350	379	54.9	91	~ 40	5.7	1.45	0.93	1.0	0.14
East	(5)	603	256	83.0	157	80	9.5	2.17	1.09	0.9	0.14
BELLSBANK GROUP											
WATER FISSURE	(10)	430	128	108	198	70	8.1	2.02	1.00	1.0	0.11
BOEBEJAAN FISSURE	(6)	1230	4720	315	523	152	17.3	4.13	2.02	2.1	0.20
OG 382 HOLIDAY & DE BRUYN	1120	4900	553	585	150	20.3	4.50	2.33	2.2	0.18	
MAIN FISSURE	(3)	1520	2540	293	500	146	16.2	3.79	1.79	1.7	0.16
OG 381 DE BRUYN MINE (BLOW)	715	1890	870	1910	560	104	5.35	9.23	3.7	0.47	
OG 383 DE BRUYN MINE	972	1830	1120	2080	780	155	5.44	18.8	4.4	0.52	
MULLERSVLEI	1220	3340	174	254	150	15.4	3.49	0.72	1.8	0.22	
DU TOITSVLA*			200	510	134	11.6	0.28		1.20	0.16	
MONASTERY*			97	243		12.6	3.70	1.30	0.99		
KIMBERLITE MINERALS											
SOUTH AFRICAN CHROME DIOPSID*	(16)			7.5	34.0		3.02	0.96	0.52		
PREMIER CHROME DIOPSID* (AVE)				2.4	18.4		1.44	0.47	0.21		
PREMIER CARNET (AVE)				0.25	0.8		0.91	0.58		3.1	
PREMIER ILMENITE (100)				(<0.1)			<0.4	0.23		0.44	
PHLOGOPITE FROM KOFFY- FONTEIN GARNET PERL- DOTTITE	310		0.5	15.8			~0.6	0.15	0.15	< 0.10	

* DATA FROM HASKIN ET AL (1965)

* DATA FROM MITCHELL ET AL (1973)

* NUMBER OF SAMPLES ANALYSED
ALL ANALYSES EXPRESSED IN FPMTABLE 3 : CHONDRITE NORMALISED REE
RATIOS

THE GEOLOGY, MINERALOGY AND PETROLOGY OF THE
PREMIER MINE KIMBERLITE PIPE

By

C. Frick
Geological Survey, South Africa.

The geology of Premier Mine is discussed and it is shown that the Premier Mine kimberlite formed as a consequence of four intrusions. The first intrusion, a heterolitic kimberlite breccia is heavily contaminated by wall rock xenoliths (Fig. 1) as it had to drill a vent through the overlying rocks. The succeeding two intrusions of autolitic kimberlite breccias caused the eastern and western bulges to form, and brought ultramafic xenoliths to the surface. The igneous activity terminated with the emplacement of the dykes of massive kimberlite (Fig. 2).

According to the textural and mineralogical data, the constituents of the kimberlite breccias can be classified into primary phenocrystal phases, a carbonate matrix, and wall rock inclusions. The massive kimberlites only consist of secondary phenocrystal phases and matrix, and are thus considered as the 'carbonate' (Wyllie, 1966) kimberlite magma. The primary phenocrystal phases are mostly resorbed and altered, and were not in equilibrium with the kimberlite magma in which they are enclosed. They also show mineralogical, petrographical and petrochemical characteristics similar to those mineral phases in the ultramafic xenoliths, and are considered to represent crystallates from the 'silicate' (Wyllie, 1966) kimberlite magma.

The secondary phenocrystal phases are mostly euhedral in shape, only slightly altered, and appear to be in equilibrium with the kimberlite magma in which they were enclosed. The textural and mineralogical data thus suggest that the secondary phenocrystal phases crystallized intratellurically from the 'carbonate' kimberlite magma below the thermal devide in the $\text{CaO}-\text{CO}_2-\text{H}_2\text{O}-\text{SiO}_2-\text{MgO}$ system (Wyllie, 1966 and 1963).

The effects of the autometamorphism (formation of minerals such as serpentine, bastite, sphene, and phlogopite) of the Premier Mine kimberlites could be distinguished from those of the pyrometamorphism (formation of minerals such as brucite, hydrogrossular, biotite, diopside, tremolite, enstatite and olivine) caused by the intrusive tholeiite sill. It appears that the autometamorphism was accompanied by a very water-rich volatile phase which was absent during the pyrometamorphism. Except for the immediate upper contact of the tholeiite sill with the kimberlite, the contact metamorphism occurred in the hornblende hornfels facies.

According to the petrochemistry of the kimberlites and ultramafic rocks from Premier Mine, it appears that fractional crystallization of the constituents of the ultramafic xenoliths within their solid solution series, and ilmenite would be able to explain the derivation of the carbonate kimberlite magma from an alkali peridotite (King, 1965) or picrite (O'Hara, 1970) primary silicate kimberlite magma. The evidence suggests that extreme fractionation, the formation of a volatile phase, and liquid immiscibility caused the formation of the carbonate kimberlite magma from the silicate kimberlite magma.

It is proposed that the sudden release in pressure which coincides with the explosive eruption of the volcano enhanced the exsolution of the carbonate magma from the residual silicate magma, and that this carbonate magma, by virtue of its lower density, and higher vapour content, is largely instrumental in bringing the ultramafic constituents to the surface. Slow cooling of the kimberlite magma after the last kimberlite breccia has been emplaced, could result in an accumulation of some of the exsolved carbonate magma, which would emplace as dykes if the vapour pressure becomes sufficiently high.

References

King, B.C. (1965). - *Jour . Pet.*, 6, p. 67-101.

O'Hara, M.J. (1970). - *Phys. Earth Planet Int* , 3, p.236-245.

Wyllie, P.J. (1963). - Carbonatites edited by O.F. Tuttle and J. Gittins, --. 591.

Wyllie, P.J. (1966). - *Int. Mineral. Association, I.M.A.* volume, p. 67-82.

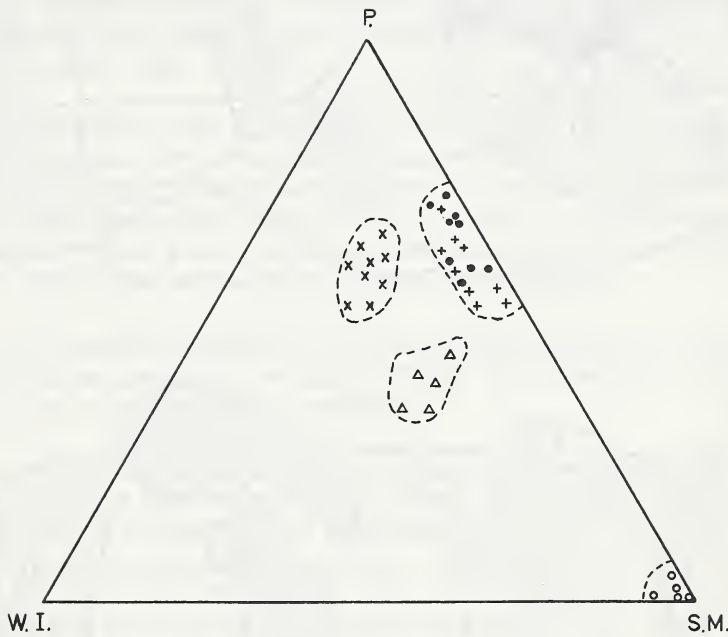


Figure 1. The distribution of primary phenocrystal phase inclusions (P), secondary phenocrystal phases and matrix (S.M.), and country rock inclusions (W.I.) in the heterolithic (x), eastern autolitic and western autolitic (• and + respectively) kimberlite breccias. The symbols Δ and \circ represent the carbonated western kimberlite and the massive kimberlite respectively.

Scale
0 100 200 metres

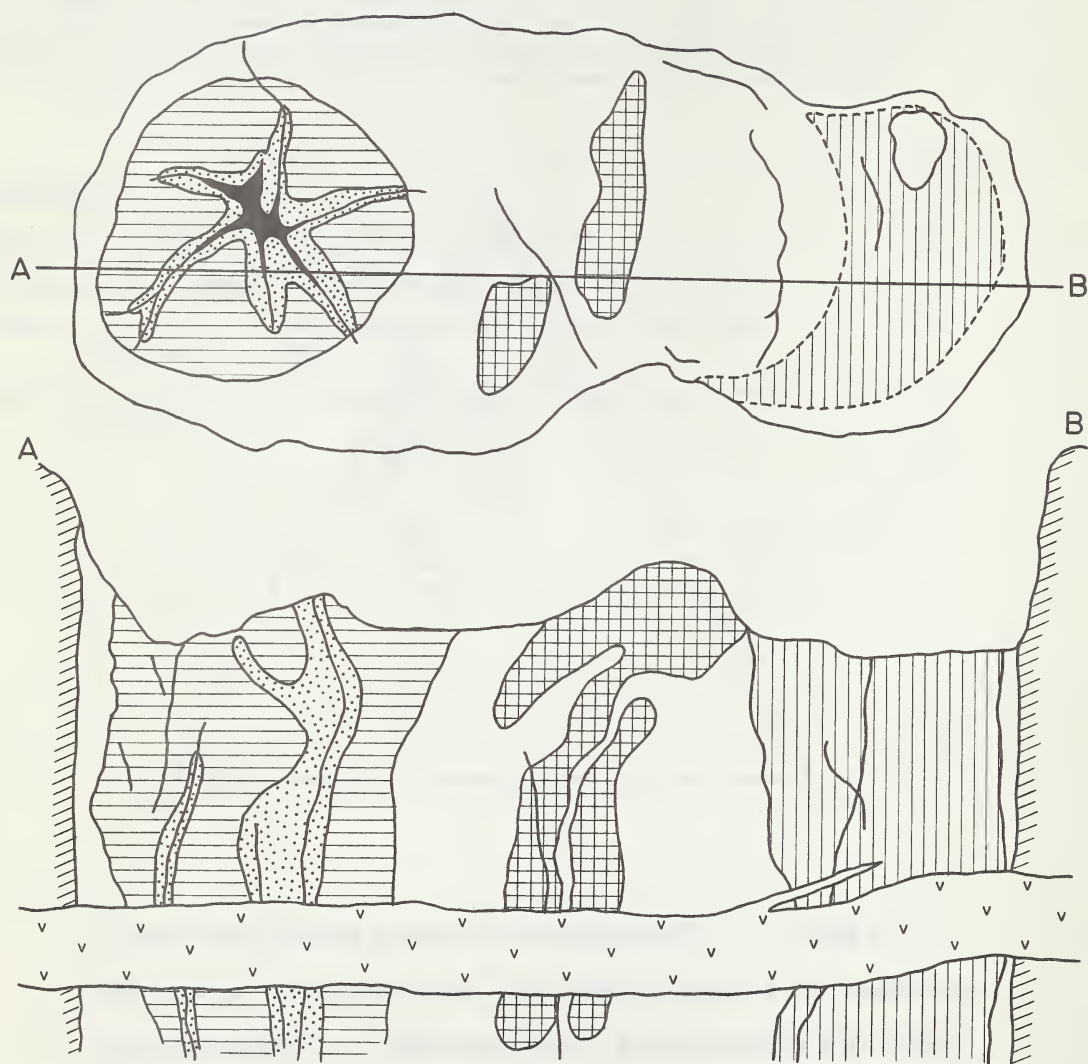


Figure 2. The distribution of the heterolithic kimberlite breccia , the western kimberlite , the eastern kimberlite , the massive kimberlite , and the carbonated western kimberlite in Premier Mine.

DIFFERENTIATION IN THE UPPER MANTLE DEDUCED FROM
MINERALS FOUND IN THE KIMBERLITE OF THE ROBERTS
VICTOR MINE IN THE BOSHOE-DEALESVILLE AREA

G.J. Geringer, Department of Geology, U.O.F.S.

The kimberlite body of the Roberts Victor Mine is situated some 40 km from Boshof in the western Orange Free State. It consists of two parallel fissures, No. 1 and No. 2.

The kimberlite has a porphyritic texture and contains xenocrysts of olivine, garnet, pyroxene and phlogopite in a fine grained ground-mass of phlogopite, calcite and magnetite. Inclusion-rich and inclusion-poor kimberlite occur in this locality. A great variety of inclusions of which some ultramafic xenoliths are probably derived from the upper parts of the upper mantle, are present.

The ultramafic xenoliths in the kimberlite of the Rovic Mine can be classified as garnetite, eclogite (Group A), phlogopite-eclogite, garnet-pyroxenite and garnet-peridotite.

A comparative study, carried out on 67 garnet xenocrysts and on garnets recovered from ultramafic xenoliths indicates that the xenocrysts represent monomineralic fragments of crushed xenoliths. Investigation of phlogopite xenocrysts, phlogopite from ultramafic xenoliths and phlogopite from the groundmass indicates that phlogopite xenocrysts are also derived from ultramafic xenoliths. Pyroxene is a major constituent of the ultramafic xenoliths, some of which contain chrome diopside. Chrome diopside is also found in the tailings of the concentration plant. The pyroxene xenocrysts are therefore also remnants of crushed xenoliths.

According to the composition of the garnet, phlogopite and pyroxene as well as the presence of diamond in ultramafic xenoliths it is postulated that they are derived from a deep-seated source probably from the upper mantle.

The position of the various layers in the upper mantle can be deduced from the optical properties of garnet, phlogopite and pyroxene. At the top almandine-pyrope, with a refractive index of 1,7670 - 1,7730 occurs. This zone is followed by a zone containing pyrope with refractive index of 1,7560 - 1,7620. Below this zone, chrome-pyrope

with refractive index of 1,7410 - 1,7560 is present.

The pyroxene present consists of chrome-diopside, diopside and omphacite. In the upper parts of the upper mantle omphacite with refractive index $\beta = 1,6896$ is present. This omphacite is rich in the diopside component (64% diopside, .36% jadeite). In the deeper parts of the upper mantle omphacite with refractive index $\beta = 1,6790$ occurs. This pyroxene consists of 28% diopside, 68% jadeite and 4% acmite.

The refractive indices of phlogopite decreases with increasing depth in the upper mantle. This can be due to an increasing titanium and decreasing iron content in the phlogopite.

Detailed work also showed that the specific gravity of the ultramafic xenoliths increases with increasing depth.

A differentiated upper mantle is proposed consisting of garnet-peridotite at the top, followed by garnet-pyroxenite and then by eclogite of Group A. Below this zone phlogopite-eclogite and diamondiferous eclogite might occur (Table I).

TABLE I

Rock Type	Garnet		Pyroxene		Phlogopite		Sp. gr. of xenoliths	Depth in km
	Refr. Index	Composition	β Refr. index	2V	Composition	β Refr. index		
Garnet-peridotite	1,7700	Almandine-pyrope	1,6896	64°	64% diopside 36% jadeite	1,6032	Titanium and iron rich	not available Above 175 km
Garnet-pyroxenite	1,7670	Almandine-pyrope	1,6896	62°	64% diopside 36% jadeite	-	-	About 175 km
Garnet-pyroxenite	1,7620	Almandine-pyrope	1,6896	64°	64% diopside 36% jadeite	1,5970	Titanium rich	2,78 Between 175 and 500 km
Garnetite	1,7601	Almandine-pyrope	1,6853	73°	64% diopside 35% jadeite 1% acmite	1,6273	Titanium rich	3,40 Between 175 and 500 km
Garnet-pyroxenite	1,7600	Almandine-pyrope	1,6880	63°	64% diopside 35% jadeite 1% acmite	-	-	3,48 Between 175 and 500 km
Eclogite (Group A)	1,7560	Pyrope	1,6720	61°	40% diopside 60% jadeite	1,6084	Titanium rich	3,55 Below 500 km
Hypersthene-eclogite (Group A)	1,7500	Pyrope	1,6790	73°	28% diopside 68% jadeite 4% acmite	1,5980	Titanium rich	2,94 Below 500 km
Phlogopite-eclogite	1,7460 1,7410	Chrome-pyrope	-	-	-	-	-	Below 500 km

KIMBERLITIC-CARBONATITIC DIKES OF THE SAGUENAY RIVER VALLEY, QUEBEC,
CANADA

by

John Gittins, Department of Geology, University of Toronto, Toronto,
Canada, M5S 1A1

Roger H. Hewins, Department of Metallurgy and Materials Science,
Lehigh University, Bethlehem, Pennsylvania, U.S.A. 18015

André F. Laurin, Ministère des Richesses Naturelles, Québec, Canada.

Dikes of carbonatitic and kimberlitic affinity cut the Precambrian granulite and anorthosite terrane of the Saguenay River Valley in the Arvida Region of Quebec. They are not kimberlites, *sensu stricto*, but have features of carbonatitic kimberlites and appear to indicate the separation of a carbonatitic fluid from a kimberlitic magma, albeit in small amount.

The Saguenay River is a one-hundred mile long tributary of the St. Lawrence river and is now recognized as a rift valley that forms part of the St. Lawrence rift system which includes the Ottawa rift and the Mattawa rift with which many carbonatite and alkalic rock complexes are associated.

The dikes are of Cambrian age (546 my by K/Ar on biotite) and range from a few centimetres to about a metre in width. They have igneous textures such as seriate texture in phlogopite and magnetite, fluidal texture in groundmass phlogopite flakes, quench dendrites of calcite at chilled margins and what appear to be phenocrysts of calcite.

The dikes are composed of former olivine (now pseudomorphed by talc in some cases and by antigorite in others), phlogopite, apatite, titaniferous magnetite, calcite and minor amounts of aluminous diopsidic titan-augite and aluminous titaniferous pargasite.

Three broad groups are recognized: a) those which are primarily kimberlitic and composed of large talc-pseudomorphed olivines, small antigorite-pseudomorphed olivines, strongly zoned phlogopites, apatite and titaniferous magnetite all set in a fine-grained groundmass of phlogopite, calcite, apatite and titaniferous magnetite; b) those which are primarily carbonatitic and composed of calcite, often in phenocrysts, with lesser amounts of phlogopite (largely unzoned), apatite and magnetite all set in a calcite matrix; c) those which are of intermediate character and might be termed carbonatitic-kimberlitic dikes. These have micro-phenocrysts of antigorite-pseudomorphed olivines, phlogopite that is principally unzoned, although some zoned phlogopite is present, apatite, magnetite, calcite and minor pyroxene and amphibole.

Rarely a fourth type of dike is found. These are pure calcite dikes in some of which a prominent comb structure is developed and in which xenoliths of anorthosite are found.

The three principal types of dike display chilled margins and it is in these that the quench dendrites of calcite are found. There seems to be a distinct similarity between these dikes and Benfontein sills

(Dawson and Hawthorne, 1973).

The evolution of the magma is to some extent reflected in the variation of mineral composition with grain size and in mineral zonation.

Phlogopite (Fig. 1)

Phlogopite phenocrysts are zoned from deep brown cores through pale brown mantles to pale green rims, and groundmass phlogopite is pale green. Average compositions for these colour variants are Phlog₇₄ Annite₁₇ Ti-biotite₉ (cores), Phlog₈₀ Annite₁₅ Ti-biotite₅ (mantles), Phlog₉₀ Annite₉ Ti-biotite₁ (rims and groundmass). In short there is a progressive increase in Mg and decrease in both Ti and Fe as crystallization proceeds which is the reverse of what might normally be expected in a magmatic sequence.

Magnetite (Fig. 2)

The range of magnetite composition is from Ulvöspinel₁₆ Magnetite₈₄ to Ulvöspinel₆₁ Magnetite₃₉. Again this is manifested both in zonation of grains and in grain size, the smaller (latest?) grains being the most titaniferous. All the magnetites are single-phase grains and the compositional trend toward iron-poor margins corresponds to crystallization down temperature along the magnetite-ulvöspinel join. Magnetites are somewhat aluminous (up to 6% Al₂O₃), magnesian (up to 8% MgO), and manganese (up to 5% MnO) all by weight.

The most likely interpretation of the mineral chemistry is that early crystallization of magnetite progressively raised the Mg/Fe ratio of the magma so that phlogopite which crystallized throughout the cooling history becomes progressively more magnesian. This also appears to have been the case in the Upper Canada Mine kimberlite (Rimsaite, 1971).

In the more carbonatitic dikes phlogopite is both unzoned and varies widely in composition. It seems likely that much of this phlogopite has been scavenged from the more kimberlitic dikes and has not crystallized in equilibrium with the carbonatitic melt.

No fresh olivine is present and it is now represented by pseudomorphs. These are of two distinct sizes and appear to represent two generations. Large phenocrysts are 0.5 to 5 mm across generally ovoid but occasionally six-sided. These consist of fine scaly talc having Fe/Fe+Mg of 0.20. Small (late?) phenocrysts are less than 0.5 mm across and consist of fibrous antigorite aggregates having Fe/Fe+Mg of 0.14. Antigorite also occurs in the groundmass and as a rim on some talc pseudomorphs.

Apparently the kimberlitic magma has undergone extensive differentiation and its crystallization history began prior to its emplacement in dikes. Clearly the carbonatitic fluid had begun to separate before this emplacement since the chilled margins of some of the dikes

contain quenched calcite and apatite. The calcite is in the form of long dendrites and the apatite forms elongate prismatic grains; both are in marked contrast to the rounded phenocrysts.

Analyses of eight rocks are set down in Table I; they lie within the general range of kimberlites *sensu stricto* and the kimberlite-related rocks.

In general they have a much higher Ca/Mg ratio than true kimberlites and this reflects their intermediate character between kimberlites and carbonatites. They appear to lack the pyrope and picro-ilmenite which is generally considered essential to a true kimberlite and in this respect they further resemble the Benfontein rocks.

The development of a carbonatitic liquid during the crystallization of the kimberlitic magma in the Arvida dikes is indisputable and strengthens the view that kimberlitic magmas can generate carbonatitic residual fluids. It should be emphasized, however that the amount is rather small and it would seem to be a great mistake to assume that carbonatite bodies in general are so derived.

References

Dawson, J.B., and J.B. Hawthorne, 1973, *Jour. Geol. Soc.*, v. 129, p. 61-85.

Rimsaite, J., 1969, *Contr. Mineral. and Petrol.*, v. 33, p. 259-272.

Table I

	1	2	3	4	5	6	7	8
SiO ₂	24.1	13.6	14.4	13.8	8.8	9.0	5.8	7.4
Al ₂ O ₃	4.1	2.6	2.3	3.4	2.9	1.1	1.2	1.8
Fe ₂ O ₃	8.9	7.2	8.0	6.9	4.4	0.6	0.6	3.3
FeO	7.2	5.2	5.4	5.0	4.2	6.5	6.8	3.6
CaO	13.5	31.6	26.6	32.4	34.8	29.6	37.4	43.5
MgO	16.3	8.5	12.9	7.1	8.5	10.5	9.6	6.0
TiO ₂	3.7	2.4	2.5	2.6	1.8	1.0	1.1	1.5
P ₂ O ₅	1.3	4.7	4.8	6.1	4.0	5.3	6.1	4.8
MnO	0.4	0.4	0.4	0.5	0.3	0.6	0.6	0.5
Na ₂ O	1.6	0.2	0.1	0.3	0.1	0.3	0.3	0.2
K ₂ O	1.3	0.9	0.9	1.0	0.6	0.8	0.7	0.1
CO ₂	7.6	19.2	17.2	17.5	25.5	33.6	28.9	25.3
H ₂ O+	4.7	2.4	2.9	2.1	2.7	0.3	0.3	1.3
BaO	0.07	0.01	0.55	0.02	0.51	tr	0.09	tr
SrO	0.01	0.03	0.09	0.01	0.19	0.01	0.03	0.03
	99.8	98.9	99.0	99.2	99.3	99.2	99.5	99.3

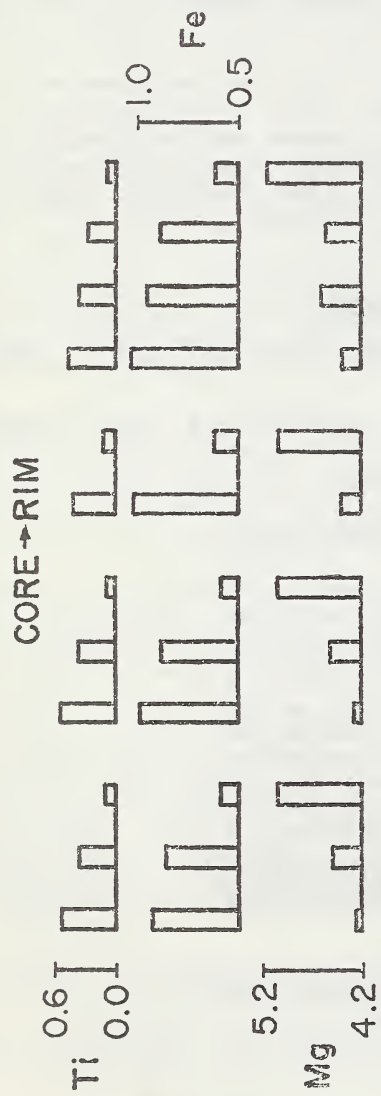
1 kimberlitic dike
 2-4 kimberlitic-carbonatitic dikes
 5-8 carbonatitic dikes

Analyst: A.G. Loomis

MANTLED PHLOGOPITES IN ROCK P5-508

Fig.1.

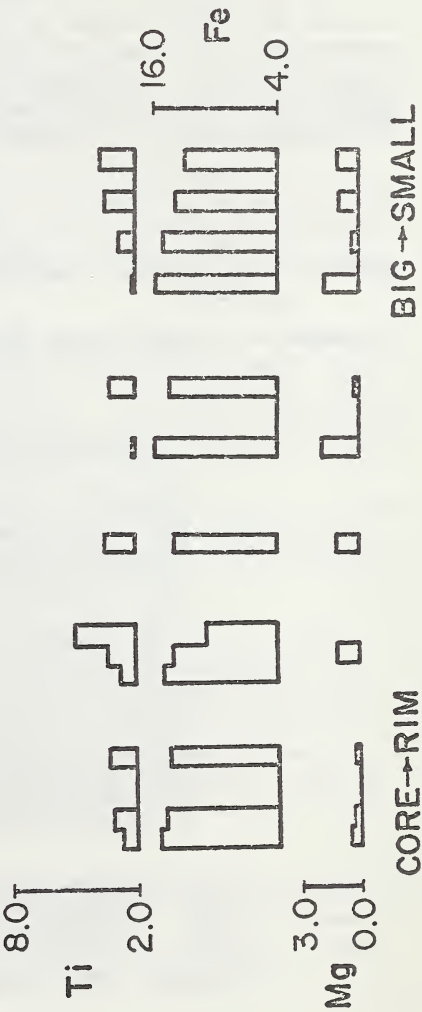
Variation in composition of four phlogopite grains from a single thin section.



MAGNETITE IN ROCK P5-508

Fig.2.

Variation in composition from core to rim of four magnetite grains and of four grains of different size, in a single thin section.



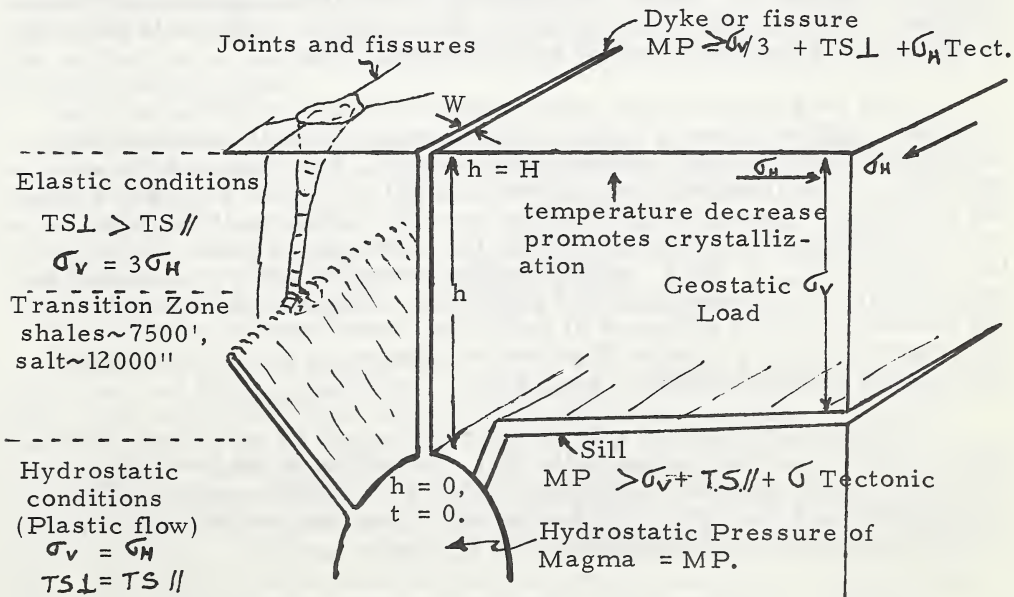
CRUSTAL CONTROL ON THE EMPLACEMENT OF KIMBERLITES

David P. Gold, Department of Geosciences, The Pennsylvania State University, University Park, Pa. 16802

Although much is known about the composition and distribution of intrusive rocks, relatively little is known about their mechanism of intrusion. The latter has been hampered by (a) a purely descriptive terminology that does not relate to intrusion conditions e. g., for dykes (discordant) and sills (concordant) with respect to the layering in the country rocks, (b) the paucity of data on stress distribution and magnitude of the near surface rocks and (c) only speculative inferences on stress states under the deep-crustal or subcrustal conditions. Likewise hypothetical emplacement mechanism include passive injection into openings and intrusion according to laws of hydrostatics (Gilbert, 1887), injection from "telluric pressure" (Spurr, 1923), magmatic stoping (Daly, 1903), a salt-dome type mechanism by differential geostatic loading (Gussow, 1962) and a gas-solid erosion and entrainment process (fluidization) (Cloos, 1941; Reynolds, 1954). All the postulated mechanism require an unbalanced hydrostatic condition regardless of the method of achieving it (tension, compression, differential loading, heat, crystallization, outgassing).

The emplacement of kimberlites as funnel shaped pipes, irregular fissures and dykes, and as sills indicates a structural control in the near surface environment of the ascending kimberlite magma and the volatile phases that might be outgassed during crystallization. The

Figure 1. Schematic view of dykes, fissures, pipe and sill and their controlling parameters



emplacement mechanisms are linked to magma pressure, saturated vapour pressure, elastic limit and yield strength of the host rock perpendicular and parallel to bedding, and the horizontal and vertical stresses prevailing in these rocks. Also emplacement time should be equal to or less than crystallization time, especially in thin dykes. In addition the laminar flow transport distance of magma in a conduit is dependent on the geometry, specifically the width W and depth H , and has been expressed mathematically by Szekely and Reitan (1971) as

$$\frac{dh}{dt} = \frac{W^2 (\sigma_v - \rho gh)}{12 \mu(h) h} \quad \text{where } h = 0 \text{ at time } t = 0 \text{ (see Fig. 1) and}$$

$\mu(h)$ is the position dependent viscosity defined by the Hagen-Poiseuille equation

$$\mu(h) = \mu_0 e^{kh}, \text{ where } \mu_0 = \text{ viscosity at } h = 0.$$

For latent heats of fusion of the order of 150 cals/gm, they show that dykes from magma sources greater than 30 km deep would have conduit widths greater than 12 m, which decreases asymptotically to about 1.5 m wide at 15 km focal depth. Only by fissure propagation from the magma interface to the free surface, with the entrainment of solid particles in a gaseous medium, could thinner conduits be emplaced from such depths. Also the mass transport would be directly proportional to differential pressure and indirectly proportional to friction between particles and with the walls.

Assuming ideal conditions of near surface rocks below their elastic limit and free of any tectonic stress, then the horizontal stress (σ_h) should be equal to approximately 1/3 of the vertical load (σ_v). Hydrostatic condition should prevail ($\sigma_v = \sigma_h$) at greater depths, corresponding to stress states above the elastic limit or yield strength of crustal rocks (about 90 K/cm²). The threshold between elastic and ductile behaviour for shales corresponds generally to depths of 3000 to 7500 feet (Mudge, 1968), and requires depths of the order of 12000 feet to overcome the elastic limit of salt (Gussow, 1962).

The lack of extrusive, and volumetric rarity of intrusive kimberlites, implies either a rarity of these events or that relatively little magma reaches the near surface environment. For dyke and fissure (see Fig. 1) development magma pressure (M. P.) must be greater than the horizontal stress plus the tensile strength of the overlying layered rocks perpendicular to bedding (T. S. 1). For near surface conditions M. P. $\geq 1/3 \sigma_v + TS_1$, which implies intrusion pressures less than the overburden or lithostatic load pressure. These conditions favoring tension, must be enhanced at depths by superimposed crustal and subcrustal tension (tectonic) if dykes and fissures are to form under hydrostatic stress conditions i.e. $MP_v + (-\sigma_{Tectonic})$.

The development of sills would be favoured by conditions (see Fig. 1) where magma pressure (M. P.) + superincumbent load (σ_v) + tensile strength parallel to bedding (T. S. II); condition unlikely to prevail at depth greater than 7500 feet unless there are anomalously high superimposed horizontal compressive stresses.

Assuming the kimberlite source is deep (60 - 340 km) then a rapid gas streaming process is mandatory to explain (a) the disequilibrium mineral assemblages in kimberlite breccias, (b) the extreme stratigraphic mixing of inclusions and (c) the paucity of metamorphism of these inclusions, and (d) anomalous width to depth ratio of kimberlite dykes and fissures. The high diffusivity of gas, (e.g., underground nuclear explosions suggest that the precursor gas has little drilling power), and the excessive demand on a low heat carrying capacity gas to fracture, brecciate, erode, and heat the host rock requires that it move upward in essentially open fractures, otherwise frictional factors on particles and the walls would be sufficiently large to shut off the system. Notwithstanding an open fracture, which could not exist for long at these depths of high plastic flow, the entrained xenolith require a large volume of gas for mass transport, a steep pressure gradient at the base of the fissures, and particle acceleration to near sonic velocities. Szekely and Reitan (1971) calculated that 40 cm³ of H₂O would be evolved per cm³ of magma of density 2.8 gm/cc containing 1% H₂O and a temperature drop from 1200 to 400°C due to adiabatic expansion over a pressure gradient of 8 kb (8 cm³ vapor would be evolved from a 0.2% H₂O magma.

Moreover the travel time for water vapor at 1000° and 500°C respectively from a 30-km deep fissure would be 34 and 41 seconds, compatible with the requirement of a short duration for the fissure opening stage. This does not imply a unique event in time or space; intrusions would take place as long as the source material was not depleted and conditions of tectonic tension prevailed. In fact for a regime of regional tension, multiple fissuring would be expected.

Although most pipes are irregular fissures and may extend to great depth, the cylindrical and funnel shaped pipes are essentially near surface features controlled by intersecting fissures and joint systems, and in place may originate from a sill (Francis, 1967). Moreover, kimberlite intrusions must originate in deep-seated tension fractures, which are unlikely to occur in a uniaxial stress field, a necessary condition for pipe development.

Alternatively a rising volatile-rich magma with no gas phase would become saturated at lesser depth and exsolve a gaseous phase with a marked pressure increase, (Morey 1922) perhaps sufficient to cause upward migrating fractures. Any release of pressure would enhance crystallization and promote additional outgassing with entrainment of both magma and wall rocks in the gas stream. This process would enable sills to form whose assemblages were essentially in equilibrium.

Monticellite-mica peridotites, sills, and diatreme breccia pipes, fissures, and dykes of alnoitic, carbonatitic, and kimberlitic materials occur in a restricted area west of Montreal area, Canada. The sills contain megacrysts of augite and olivine, and xenoliths of websterite, harzburgite, dunite, peridotite and rare lherzolites in a coarse grained poikilitic textured matrix. The matrix consists of phlogopite, monticellite, forsterite, titansalite, melilite with accessory apatite, magnetite, perovskite, calcite, scapolite and secondary carbonates and zeolite. Phlogopite and/or monticellite oikocrysts are up to 1 cm across, commonly contain inclusions of forsterite and magnetite. Locally,

monticellite and melilite are intergrown. The regional association with diatreme pipes and the high temperature moderate to low pressure mineral assemblage suggest the sill is an "equilibrated kimberlite".

References

Anderson, E. M., 1942, Dynamics of Faulting, Oliver and Boyd.

Daly, R. A., 1903; Amer. Jour. Sci., V. 15, pp. 269-298.

Francis, E. H., 1967; Geol. Rdsch. V. 57, pp. 219-240.

Gilbert, C. R., 1877, Geology of the Henry Mountains (Utah): U. S. Geog. Geol. Survey, Washington.

Gussow, W. C., 1962; Trans. Royal Soc. Canada, V. 56, pp. 1-19.

Imbo, G., 1965; Am. dell Observatorio Vesuviano V. Settimo, pp. 1-24.

Morey, G. W., 1922; Jour. Wash. Acad. Sci., V. 12, pp. 219-230.

Mudge, M. R., 1968; Bull. Geol. Soc. Amer., V. 79, pp. 315-332.

Reynolds, D. L., 1954; Amer. Jour. Sci., V. 252, pp. 577-614.

Szekely, J., & P. H. Reitan, 1971; J. Geophys. Res., V. 76, pp. 2602-2609.

Voight, B., 1966; Proc. 1st Cong. Int. Soc. of Rock Mechanics, V. III, pp. 332-348.

THE FEN DAMKJERNITE: PETROLOGY OF A "CENTRAL-COMPLEX KIMBERLITE"

W.L. Griffin and P.N. Taylor

Mineralogisk-Geologisk Museum, Oslo, Norway
Dept. of Geology, Oxford, England

The circular complex of carbonatites and alkalic rocks at Fen (Telemark, S. Norway) is cut by numerous diatremes and dikes of damkjernite, a porphyritic alkalic ultrabasic rock that megascopically resembles kimberlite. The diatremes contain numerous rounded fragments of spinel lherzolite, granitic gneiss and carbonatite. The damkjernite makes up only 7% of the surface area (versus 63% for the carbonatites), but gravity studies show that the carbonatites are only a thin (300-500 meter) cap on a pipe of very dense rock extending at least to the lower crust. Unbrecciated hypabyssal-facies damkjernite, which is common in dikes outside the circular complex, has the density (3.17 g/cc) needed to explain the gravity anomalies; we suggest that this is the dominant rock of the complex.

Analyses of inclusion-free damkjernite dike rocks show that, when its high content of primary calcite is disregarded, the damkjernite is similar in composition to other strongly undersaturated rocks of the monchiquite-ouachitaite-alnøite type (Table). The major differences are in the higher TiO_2 , $Fe/Fe+Mg$, and Fe^3/Fe of the damkjernite dikes. The diatreme facies has lower $Fe/Fe+Mg$ and TiO_2 ; this is partly due to mechanical contamination with lherzolite and crustal rocks. The damkjernite is higher in Al_2O_3 , $Fe/Fe+Mg$, TiO_2 and Na_2O than most kimberlites.

Phenocrysts include biotite, clinopyroxene, nepheline (altered to albite, sericite and calcite), ilmenite_{ss}, magnetite_{ss}, and possibly perovskite. The groundmass consists of laths of pyroxene, biotite, chlorite and apatite, with interstitial sericite, albite, K-feldspar, nepheline, and locally melanite. Magnetite, ilmenite, rutile, pyrite and sphene are scattered abundantly through the groundmass. Some pyroxene phenocrysts have resorbed cores of high-P phases (augerine-augite, acmitic titanaugite, kaersutitic hornblende). Overgrowths on these cores are zoned toward increasing Fe/Mg , but the trend is reversed at the outermost rims and the groundmass pyroxenes are more magnesian than the phenocrysts (Table). A similar trend, and a drop in Ti , are seen in the biotites. Large Il_{ss} grains contain up to 10% $MnTiO_3$ and 12% Hm ; bulk compositions of large unmixed Mg_{ss} grains imply Usp contents > 42%. Intergrowths of rutile with sphene and/or calcite are common; they appear to be pseudomorphs after perovskite phenocrysts. Calcite occurs as a late-magmatic interstitial phase, and as coarsely crystalline rounded globules, suggesting the presence of an immiscible carbonate melt.

The pyroxene cores are quite different from the clinopyroxenes of the lherzolite nodules, and no olivine, opx or

spinel have been observed in the hypabyssal facies. The rounded megacrysts of these phases in the diatreme facies were derived by breakup of the lherzolite inclusions, which are probably accidental in origin.

Compositions of Fe-Ti oxides imply $T > 900^{\circ}\text{C}$ and $\log f_{\text{O}_2} > -12$ atm. during crystallization ($P \sim 1$ Kb). The composition of biotites crystallizing with magnetite and K-feldspar indicates that $f_{\text{H}_2\text{O}}$ under these conditions was about 1-400 bar. The occurrence of albite and nepheline in the groundmass, and the alteration of perovskite to sphene (+rutile+calcite) require that $\log a_{\text{SiO}_2} \approx -0.6$ for $T = 1000-1200^{\circ}\text{C}$. The lack of albite or sphene phenocrysts indicates that the magma was not buffered with respect to silica activity until emplacement; this magma would have been in equilibrium with the mantle represented by the lherzolite nodules at $P = 13-18$ Kb for $T = 1000-1200^{\circ}$. These pressures are somewhat higher than those obtained for equilibration of the lherzolite nodules (9-11 Kb: Griffin, 1973).

Analyses of six dike rocks show no correlation between $\text{Sr } 87/86$ and $87\text{Rb}/86\text{Sr}$. Initial ratios (assumed age, 550 m.y.) range from 0.70399 ± 8 to 0.70465 ± 6 . The higher I.R. of one diatreme sample (0.7069 ± 6 : Mitchell & Crockett, 1972) may be due to admixture of gneiss fragments. One sample of sôvite analyzed by M & C has $\text{I.R.} = 0.7028 \pm 6$. The I.R. of the dikes is proportional to both $\% \text{CO}_2$ and ppm Sr, suggesting mixing of the silicate magma ($\text{I.R.} \sim 0.7035 ?$) with a carbonatite magma contaminated by crustal Sr. This is also consistent with the higher Na content and Na/K of the more carbonate-rich rocks, since modern carbonatite magmas are rich in sodium.

Field evidence shows that the damkjernite was intruded after the sôvite, but was accompanied or followed by ankeritic carbonatite. We suggest that the damkjernite magma was mixed with a previously-generated ankeritic carbonatite magma that had exchanged Sr isotopes with crustal rocks. This mixing may have taken place in a magma chamber at or near the base of the crust during the ascent of the damkjernite from its site of generation. Explosive eruption from this chamber entrained lherzolite nodules in the damkjernite dikes and diatremes emplaced around the complex. Subsequent or nearly simultaneous emplacement of ankeritic carbonatite magma caused metasomatism of damkjernite within the complex. The model suggests that the carbonatites and damkjernite may have had a common site of generation at $P = 13-18$ Kb, but that they were largely separated from one another at an early stage because of the immiscibility of the magmas at these low pressures and their differing physical properties.

The various associations of undersaturated rocks with carbonatite suggest that carbonatite magmas represent accumulations of the free or easily liberated volatile components of the upper mantle. The associated silicate rocks may be derived by reaction of these volatiles with mantle perido-

tite, accompanied by varying small degrees of partial melting at pressures ranging from < 15 to > 60 Kb. At Fen these processes appear to have taken place at relatively shallow depth and to have been the precursor of large-scale magmatic activity along a developing intracratonic rift system.

References:

Griffin, 1973: Contr. Min. Petrol. 38, 135-146.
 Mitchell and Crocket, 1972: Jour. Pet. 13, 83-98.

	<u>Analyses</u>								
	SiO ₂	TiO ₂	Al ₂ O ₃	Fe ₂ O ₃	FeO	MgO	CaO	Na ₂ O	K ₂ O
1)	30.71	5.02	8.59	8.26	6.83	9.14	16.53	1.46	2.03
2)	37.2	6.0	15.4	---	7.2	18.8	0.0	0.6	9.4
3)	37.3	4.3	15.1	---	8.4	20.6	0.1	0.4	9.6
4)	38.1	3.0	14.6	---	8.0	21.1	0.0	0.5	9.3
5)	48.0	1.9	6.3	---	10.0	10.7	20.6	1.8	---
6)	47.6	2.9	6.0	---	6.4	13.4	23.4	0.6	---
7)	48.0	2.6	4.5	---	6.1	14.2	23.7	0.5	---

1, average of 6 analyses of damkjernite dikes (includes P₂O₅=1.60, H₂O=2.80, CO₂=6.14, F=0.40)
 2, core of biotite phenocryst
 3, rim of biotite phenocryst
 4, groundmass biotite
 5, resorbed core in clinopyroxene phenocrysts (aver. 2)
 6, overgrowths on (5)
 7, groundmass pyroxenes (aver. 4)

THE COMPOSITION OF MANTLE XENOLITHS IN THE MATSOKU KIMBERLITE PIPE

J. J. Gurney, B. Harte and K. G. Cox

The ultramafic xenoliths of mantle origin (Group 1 of Cox, Gurney and Harte 1973) from the Matsoku Pipe consist essentially of olivine, opx, cpx and garnet. The megascopic and microscopic features of the rocks have been described in detail (Cox, Gurney and Harte 1973, Harte, Cox and Gurney 1973).

The bulk chemistry of selected samples and the major element chemistry of the constituent minerals have been determined and show a wide spread but a largely continuous series of compositions (See Fig.1). End members show the following range in Mg/Mg+Fe ratio (at%): bulk 80.8-92.8, gt 69.8-85.2, cpx 84.2-94.7, opx 85.6-93.8, ol. 83.4-94.8. Equilibrium between co-existing minerals is indicated by the regular sympathetic variation in Mg/Mg+Fe (Fig.2) and the consistent partitioning of elements such as Cr, Ti & Na. The clinopyroxene compositions show a restricted Ca/Ca+Mg in the range of 0.440-0.453 for 14 xenoliths indicating a temperature of equilibrium of approximately 1050°C on the 30kb solvus (Boyd 1970). The orthopyroxene Al_2O_3 content lies in the restricted range 0.71-0.87 which is identical to the range in Al_2O_3 as shown by 6 xenoliths of garnet lherzolite from Kimberley. Taken as a whole the above shows the rocks to have come from a restricted mantle location and to have equilibrated under sub-solidus conditions, and is further shown by their petrography (Harte, Cox, and Gurney 1973). In the following discussion in which selected groups of rocks are discussed and compared, it is assumed that relative compositions of minerals (in particular Fe/Mg ratios) in different rocks have not been changed from their values at above solidus temperatures.

1. The Common Peridotites (e.g. LBM9, LBM11 and BD1355) are coarse granular rocks similar in the modal proportions of minerals present and in chemistry to the common garnet lherzolite found in other Kimberlite Pipes in South Africa. The Mg/Mg+Fe (at%) is: bulk (5) 92.0-93.0, gt (3) 83.4-85.2, cpx (3) 92.3-94.7, opx (3) 93.1-93.8, ol. (3) 92.3-92.5. Even if only the garnet of these rocks is the major contributor to a partial melt it is not possible to generate a magma with as high an iron content or as low a bulk Mg/Mg+Fe ratio as those reported for LBM12, 18 or 11102. The Common Peridotites are therefore thought to be residua.

2. The Coarse Granular Banded Rocks (e.g. LBM33, LBM36, LBM37) show a range in Mg/Mg+Fe within the range for coarse granular unbanded rocks (See Section 3). The banded rocks are enriched in clinopyroxene and this is reflected in a high CaO content (CaO/Al_2O_3 generally > 1). No differences in chemical composition have been noted between the minerals of separate bands but the bulk composition of the bands varies widely because of the differences in mineral proportions. The occurrence of constant mineral compositions in bands of widely different mineral proportions and bulk composition, and the presence of a continuous spectrum of modal and chemical compositions unaligned to normal differentiation trends suggests the banding to be cumulitic in origin. The presence of cumulates is also confirmed by dunite LBM20 (See Section 4).

3. The Coarse Granular Unbanded Rocks (e.g. LBM6, LBM12, LBM18 and 11102), have lower whole rock and mineral Mg/Mg+Fe ratios than the Common Peridotites (bulk (3) 80.8-89.0, gt (4) 69.8-79.2, cpx (4) 84.2-90.7, opx (4) 85.6-90.8, ol. (4) 83.4-89.5 (at %)). These rocks, like the banded rocks do not show marked enrichment of titanium or potassium, have very high chromium and nickel contents relative to basalts and do not contain any

primary hydrous mineral phases. The unbanded rocks could possibly represent liquids formed during an igneous event in the mantle, but on the basis of their chemistry are more likely to be cumulates closely related to the banded rocks discussed above. It is noticeable that these rocks and the banded rocks do not plot on a single line of liquid evolution in Fig.1.

4. The Dunites (e.g. LBM20, LBM39) are not all the same composition. LBM39, a coarse grained olivine rock has an olivine of composition Fo 94.8, LBM20, a recrystallised and finer grained dunite with < 2% opx, and minor cpx, has an olivine of Fo 90. This is less magnesian than the olivines in the Common Peridotites whilst LBM39 is more magnesian than these.

In addition the opx and olivine of LBM20 is more magnesian than the olivines in all the coarse granular rocks other than C.P. LBM39 is thought to represent residual material and LBM20 is interpreted as a cumulate.

5. The Recrystallised Rocks have been subdivided into two types, those with flaser structure (e.g. LBM16 and LBM32), and those with more uniform grain size (e.g. LBM20, LBM38B). The recrystallisation which has taken place has not obviously affected the composition of the constituent mineral assemblages except where the rock has also been metasomatised. The minerals in the recrystallised rock remain in equilibrium with each other and have compositions within the series mentioned earlier and represented in Fig.2.

6. The Metasomatised Rocks (e.g. LBM32 and LBM38B) have been affected by a metasomatic event which has altered the bulk and mineral compositions and led to the development of ore minerals and phlogopite in the rock. Only recrystallised rocks have been extensively metasomatised. The bulk composition of LBM32 and LBM38B shows enrichment of TiO_2 , K_2O , S^2 and some trace elements (e.g. Cu). Nevertheless the gt, cpx, opx and olivine compositions also conform to the series outlined earlier and reflected in Fig.2.

7. LBM38 is a unique rock in the suite studied because it consists of two parts separated by a sharp, at least partly metasomatic contact. LBM38A is a common peridotite, close in mineral compositions to LBM11. In comparison LBM38B is a recrystallised metasomatised rock with minerals of lower Mg/Mg+Fe ratio, and lower chrome content, though remaining similar to the general span of mineral compositions described above.

8. General The coarse granular rocks contain no primary hydrous phase. Phlogopite, where present, appears secondary and is a minor phase. Potassium was not detected in the major phases of the coarse granular rocks (detection limit 100 ppm) and the bulk analyses show low potassium contents.

These rocks also contain little titanium although small concentrations were detected in all the major minerals. The iron-rich rocks (e.g. LBM12, LBM18) appear to be slightly enriched in titanium and this is reflected in the bulk and mineral analyses.

The P_2O_5 content of all the xenoliths except LBM41 is on the detection limit of the method used and extremely low in concentration.

The Nickel content of the Group 1 xenoliths studied ranges from 0.45% NiO in LBM20 (approximately 98% olivine) to 0.11% NiO in LBM18 (no olivine). The NiO contents of other xenoliths lie between these two extremes and appear to be closely related to the olivine content of the particular rock.

The Cr_2O_3 content of the bulk samples ranges from 0.05% Cr_2O_3 in LBM20 to 0.93% in LBM32. The range for four phase xenoliths is from 0.34% in LBM10 and LBM16 to 0.93%. Chrome is consistently distributed amongst the major mineral phases of the four phase xenoliths being concentrated in the

garnet followed by clinopyroxene, orthopyroxene and finally olivine in which the Cr_2O_3 content is never greater than 0.05%. With the exception of LBM12 and 11102 there is a tendency for the chrome content of the minerals to increase with increasing $\frac{\text{Mg}}{\text{Mg+Fe}}$.

The garnet analyses indicate on inspection that the trivalent lattice site in the garnet is predominantly occupied by chromium and aluminium, the combined total of chromium plus aluminium in atomic proportions indicating a 99.3 average occupancy of the trivalent site. It is possible that there is no ferric iron present in these garnets. In addition the only significant variations noted in the divalent lattice site involve the elements calcium, magnesium and iron.

A good correlation has been noted between the sodium content of the clinopyroxene and its $\text{Al} + \text{Cr}$ content.

Conclusions: The Group 1 xenoliths are considered to be a closely related suite of rocks derived from a restricted mantle location, and to have formed during a single partial melting event which predates kimberlite emplacement. They have subsequently re-equilibrated under sub-solidus conditions but it is considered that their relative compositions have not changed.

LBM39 is a sample of residual mantle as are the Common Peridotites, though these latter rocks have not contributed as fully to the partial melt as the coarse grained dunite.

The coarse grained granular banded rocks are interpreted as cumulates from the melt from which the above rocks are residua. LBM12, LBM18 and 11102 which are coarse grained unband rocks are also considered to be cumulates, as is LBM20.

Some of the Group 1 rocks have subsequently been recrystallised and metasomatised by fluids enriched in K, Ti, Si and other elements, and where this latter has occurred the bulk chemistry, mineralogy and mineral compositions have been affected.

The xenoliths have finally been rapidly transported to the surface in the kimberlite magma, to which they are unrelated in origin.

References

Cox, K.G., Gurney, J.J., and Harte, B., 1973. Lesotho Kimberlite. Ed. P.H. Nixon.
 Harte, B., Cox, K.G., and Gurney, J.J., 1973. This volume.
 Boyd, F.R., 1970. Min. Soc. Am. Sp. Pub. No.3, 63-75.
 O'Hara, M.J., 1968. Earth Science Reviews. 4, 69-133.

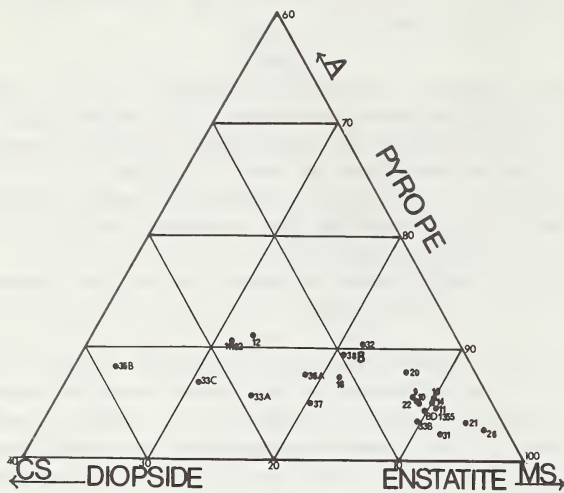


FIG. 1 Bulk compositions of Matsoku xenoliths (Group 1) projected from olivine into the plane CS-MS-A, within the CMAS tetrahedron (see O'Hara, 1968, Fig.4).

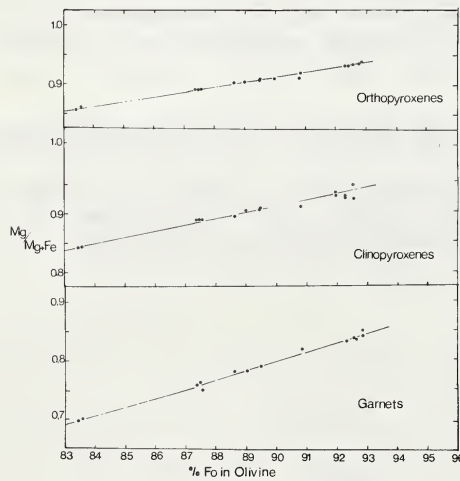


FIG. 2 Mineral atomic Mg/Mg+Fe plotted against % Forsterite in co-existing olivine. Matsoku xenoliths.

POTASSIUM, THORIUM AND URANIUM IN SOME KIMBERLITES FROM SOUTH AFRICA

J.J. Gurney, Dept. of Geochemistry, and J.B.M. Hobbs, Dept. of Physics,
University of Cape Town, Rondebosch, Cape, South Africa.

Samples Analysed: The samples of kimberlite analysed were, for the most part, collected *in situ* in the present day underground workings of the mines. The samples from Newlands Mine, Koffiefontein Mine and samples KRV 12 and KRV 13 from Roberts Victor Mine were collected from mine dumps where they may have lain for a considerable time. The majority of the samples were collected by G.W.Berg who is conducting a detailed petrological and mineralogical and geochemical study of the same suite of rocks (Ph.D. Thesis). Data already published can be found in Gurney and Berg (1970) and Berg and Allsopp (1972).

Analytical Method: Potassium, thorium and uranium were determined by gamma spectroscopy as described by Cherry et al. (1970).

Results: The individual determinations together with the statistical precision (calculated from counting statistics) and the Th/U, Th/K and U/K ratios of each sample are presented in Gurney (1968). Average Th, U and K values for the kimberlites from each locality, average Th/U ratios and the ranges of these are presented in Table I.

Discussion: Thorium and uranium increase in concentration during normal magmatic differentiation, but cannot substitute for the highly charged abundant cations such as Si^{4+} , Al^{3+} , Fe^{3+} and Ti^{4+} because of the larger size of the thorium and uranium ions. Thorium and uranium only occur in very small amounts in the abundant silicate minerals therefore, and both elements are substantially concentrated in accessory minerals, and, in the case of extrusive rocks, in glass. In addition, it has been shown (Hurley and Fairbairn, 1957) that a phase containing thorium and uranium may develop along grain boundaries. This was demonstrated to be the case for an eclogite from the Delegate Pipe, New South Wales, by Kleeman and Lovering (1967). Lambert and Heier (1968) postulate that Th and U are absorbed on to biotite surfaces during progressive regional metamorphism of granulite facies rocks, offering yet another possible site for the accommodation of these elements into many rocks.

The thorium/uranium ratios of most rock types cluster around the value of 3.7 used by some authors as a crustal average. A close coherence of thorium and uranium can be said to exist (Adams et al., 1959) and this would be expected on the basis of the similar properties of the thorium and uranium ions. For a given suite of rocks there are sometimes trends within the general coherence, but the significance of these is difficult to assess. It is not clear from existing data whether the Th/U ratio tends to change with differentiation or not. The position is complicated because uranium is easily oxidised to the U^{6+} uranyl ion which is stable and soluble and concentrates in residual solutions. It is further complicated by evidence that thorium and uranium are redistributed by hydro-thermal fluids and by leaching of uranium during weathering.

Heier and Rogers (1963) noted that potassium tended to increase with differentiation in a similar way to uranium and thorium and that the ratios Th/U, U/K and Th/K also tended to increase. They noted that basaltic and granitic rocks have, on the average, distinctly different U/K and Th/K ratios.

Turekian and Wedepohl (1961) give a value of 0.001 ppm uranium as typical for an ultrabasic rock, but this is derived from an analysis of one dunite. Their value of 0.004 ppm thorium was obtained by assuming a Th/U ratio of 4. The potassium content of ultrabasic rocks is low,

usually less than 500 ppm.

The average values obtained in this work on kimberlites are very high by comparison. Potassium values in South African kimberlite are well established, but the values for uranium (up to 7.1 ppm) and thorium (up to 58 ppm) are new data. These high values for all three elements confirm the extremely differentiated nature of the kimberlite magma.

The absolute abundance level of the three elements studied is higher in the micaceous kimberlites than for the basaltic varieties. This may simply be related to the fact that the basaltic varieties, found chiefly in the pipe occurrences, have lost volatiles to the atmosphere during emplacement, or alternatively the micaceous kimberlites have undergone a greater degree of differentiation. In practical terms, the high concentrations of radioactive elements in the micaceous kimberlite may be detectable instrumentally in areas where the country rock has contrastingly low natural radioactivity, such as the Drakensberg lavas. Natural radioactivity is known to turn diamonds green, for instance in the gold-bearing conglomerates of the Wits system. Especially high values for the radioactive elements are reported here for the Roberts Victor and Bellsbank kimberlite occurrences. Diamonds from these two localities are characterised by having a greenish tinge. It is suggested that this may have been created by the natural radioactivity of the kimberlite in which they are found.

The average Th/U ratios of the basaltic kimberlites (8) cluster closely around 5 (see Table I). The average Th/U ratios of the micaceous kimberlites (4) are all distinctly higher (6.9 - 9.3), a feature which may again be related to differentiation. The U/K and Th/K ratios are high, generally higher than those given by Heier and Rogers for granitic rocks ($U/K \times 10^4 = 1.3$; $Th/K \times 10^4 = 5.0$).

Eclogite and peridotite xenoliths are found in kimberlite and are studied extensively. It has already been conclusively shown that these inclusions have been contaminated by the introduction of potassium, rubidium and cesium from the host kimberlite (Gurney et al., 1966; Berg, 1968; Gurney and Berg, 1970; Erlank, 1970). The high concentrations of thorium and uranium in kimberlite and the close geochemical association of these elements with potassium are very strong reasons for expecting a similar introduction of thorium and uranium to have occurred into the inclusions.

Acknowledgements: J.J. Gurney gratefully acknowledges the financial assistance of the C.S.I.R., Pretoria, throughout the period of this investigation.

References:

Adams, J.A.S., Osmond, J.K., and Rogers, J.J.W. (1959) The geochemistry of thorium and uranium. *Phys. Chem. Earth*, Vol. 3, Chap. 6, pp. 298-348. Pergamon Press.

Berg, G.W. (1968) Secondary alteration in eclogites from kimberlite pipes. *Amer. Mineral.* Vol. 53. pp. 1336-1346.

Berg, G.W. and Allsopp, H.L. (1972) New $Sr^{87}/86$ ratios in fresh South African Kimberlites. *Earth Plan. Sci. Lett.* Vol. 16. pp. 27-30.

Cherry, R.D., Hobbs, J.B.M., Erlank, A.J. and Willis, J.P. (1970) Thorium, Uranium, Potassium Lead, Strontium and Rubidium in Silicate Rocks by Gamma Spectrometry and/or X-ray Fluorescence. *Canadian Spectroscopy*. Vol. 15. pp. 1-8.

Erlank, A.J. (1970) Distribution of potassium in mafic and ultramafic nodules. Carnegie Inst., Washington, Yearbook 68, pp. 433-439.

Gurney, J.J. (1968) The geochemical distribution of some elements in ultrabasic rocks. Ph.D. Thesis. University of Cape Town.

Gurney, J.J., Berg, G.W. and Ahrens, L.H. (1966) Observations on caesium enrichment and the potassium/rubidium/caesium relationship in eclogites from the Roberts Victor Mine, South Africa. Nature, Vol. 210, pp. 1025-1027.

Gurney, J.J. and Berg, G.W. (1970) Potassium, Rubidium and Caesium in South African kimberlites and their peridotite xenoliths. Upper Mantle Project. Geol. Soc. S. Afr. Special Publication No. 2, Chap. 19, pp. 417-427.

Heier, K.S. and Rogers, J.J.W. (1963) Radiometric determination of thorium, uranium and potassium in basalts and in two magmatic differentiation series. Geochim. Cosmochim. Acta, Vol. 27, pp. 137-154.

Hurley, P.M. and Fairbairn, H.W. (1957) Abundance and distribution of uranium and thorium in zircon, sphene, apatite, epidote and monazite in granitic rocks. Trans. Amer. Geophys. Union, Vol. 38, pp. 939-944.

Kleeman, J.D. and Lovering, J.F. (1967) Uranium distribution in rocks by fission track registration in lexan plastic. Science, Vol. 156, pp. 512-513.

Kushiro, K. and Aoki, K. (1968) Origin of some eclogite inclusions in kimberlite. Amer. Mineral, Vol. 53, pp. 1347-1367.

Lambert, I.B. and Heier, K.S. (1968) Estimates of the crustal abundances of thorium, uranium and potassium. Chem. Geol., Vol. 3, pp. 233-238.

Turekian, K.K. and Wedepohl, K.H. (1961) Distribution of the elements in some major units of the earth's crust. Bull. Geol. Soc. Amer., Vol. 72, pp. 175-192.

Wagner, P.A. (1914) "The Diamond Fields of Southern Africa", The Transvaal Leader.

TABLE I

AVERAGE VALUES OF THE THORIUM, URANIUM AND POTASSIUM DETERMINATIONS FOR EACH OCCURRENCE

Name of Mine	Locality	*Kimberlite Type	No. of Samples	Thorium ppm	Uranium ppm	Range of Potassium %	Range of Th/U	Range of Th/U
Bultfontein	Kimberley, Cape	Basaltic	13	12.5	7-18	2.7	1.6-4.4	1.62
Du Toits Pan	Kimberley, Cape	Basaltic	3	10.8	10-11	2.2	2.1-2.2	0.95
De Beers	Kimberley, Cape	Basaltic	4	14.2	8-22	3.1	1.8-5.0	0.98
Wesselton	Kimberley, Cape	Basaltic	5	9.0	7-11	1.7	1.4-2.0	1.77
Jagersfontein	Jagersfontein, 0.F.S.	Basaltic	10	13.2	9-21	2.7	1.1-4.0	1.61
Koffiefontein	Koffiefontein, 0.F.S.	Basaltic	4	18.1	16-20	3.3	2.7-4.0	1.01
Monastery	Marquard, 0.F.S.	Basaltic	1	13.5	-	2.6	-	1.01
Wessels Sill	Lochard, Rhodesia	Basaltic	3	22.1	20-24	4.6	3.9-5.2	0.84
Roberts Victor	Boshof, 0.F.S.	Micaceous	8	43.7	30-54	5.1	4.0-7.1	3.34
Southern Fissures	Boshof, 0.F.S.	Micaceous	2	24.2	23-25	3.5	2.8-4.2	2.34
Newlands	Barkly West, Cape	Micaceous	6	33.8	23-38	3.8	2.5-4.4	1.15
Bellsbank	Barkly West, Cape	Micaceous	1	57.9	-	6.2	-	1.37

* Classification after Wagner (1914).

THE CHEMISTRY AND GENESIS OF OPAQUE MINERALS IN KIMBERLITES.

Stephen E. Haggerty, Department of Geology, University of Massachusetts, Amherst, Mass. 01002 U.S.A.

A detailed reflection microscopy study and over 500 electron microprobe analyses of an extensive suite of kimberlites from some 30 southern and west African localities has been undertaken in an attempt to characterize the opaque mineralogy of kimberlites. The results of this study indicate that in addition to the ubiquitous occurrence of geikielite-rich ilmenite that an exotic and chemically variable suite of other opaque minerals are also commonly present. The oxides include members of the spinel mineral group, armalcolite ($FeMg)Ti_2O_5$, the polymorphs of TiO_2 , perovskite, and two new minerals, a primary Ba-Fe-Ti-Cr-vanadate, and a phase that is essentially intermediate between $CaTiO_3$ and Fe_2O_3 , and of secondary origin. The sulfides identified are restricted to pyrite, pyrrhotite, chalcopyrite and pentlandite; and the native metals, aside from graphite, are Cu and Ni-Fe alloys. Subsolidus reactions that include oxidation, reduction and solid state decomposition of the primary assemblages are widespread. The effects of solid-liquid, solid-solid, solid-gas and hydrothermal alteration are also recognised. The variable intensity of these reactions coupled with non-systematic chemical trends within the reaction assemblages and superimposed or indeterminate paragenesis of minerals of identical or related composition in different samples from the same pipe preclude a uniform interpretation of the conditions that prevailed during crystallization or during subsequent crystallization events. However, these effects contrast strongly with the primary mineralogy which in most cases are clearly defined as liquidus phases.

Spinels. Five distinct petrogenetic types of spinels are recognised and these are classified as follows: 1) xenocrystic spinels; 2) primary groundmass spinels; 3) secondary spinels associated with (1) and (2), and in association with perovskite in ilmenite reaction mantles; 4) secondary spinels in garnet kelyphitic rims and in partially serpentinized olivine; and 5) exsolved spinels in ilmenite. Compositionally, the xenocrystic and primary spinels are in the system $MgCr_2O_4$ - $FeCr_2O_4$ - $MgAl_2O_4$ - $FeAl_2O_4$, whereas the secondary spinels are more typically in the system Fe_2TiO_4 - Mg_2TiO_4 - $FeAl_2O_4$ - Fe_3O_4 . There is however considerable overlap of these subsystems and a further characteristic feature of both types is that the spinels are strongly zoned. Zonal trends are either of a clearly defined nature from Mg-Al to Fe-Cr, and from Fe-Cr to Fe-Ti, in which the role of Fe^{+3} is limited, or alternatively one in which Fe_2TiO_4 - Fe_3O_4 is dominant. Apart from the complexity of zonal patterns the single outstanding chemical characteristic of kimberlitic spinels is the presence of extensive Mg_2TiO_4 solid-solubility; the outstanding textural characteristics are skeletal spinels in garnet reaction rims and a variety of exsolved spinels in ilmenite. Typical analyses are listed in Table 1.

Ilmenite. The compositions of the ilmenites determined range from 10-70 mole % $MgTiO_3$ and from <1-40 mole % Fe_2O_3 . Cr_2O_3 ranges from <0.5 wt% to a maximum of 5.6 wt%; and Al_2O_3 varies between <0.1 wt% to 1.3 wt%. The paragenetic types of ilmenite are classified as follows: 1) xenocrystic ilmenite; 2) groundmass primary ilmenite; 3) subsolidus oxidation ilmenite in titanomagnetite; 4) ilmenite-spinel-perovskite mantles on xenocrystic ilmenite; and 5) ilmenite-rutile and ilmenite-rutile-armalcolite intergrowths. The xenocrystic ilmenites fall within two groups: those that are non-magnetic are typically high in MgO (e.g. 15 wt%), contain <10 mole % Fe_2O_3 , and Cr_2O_3 contents close to 1.5 wt%; those that are magnetic contain 25-40 mole % Fe_2O_3 , variable Cr_2O_3 contents and <5

wt% MgO. Groundmass ilmenites and oxidation ilmenites are characterized by low MgO and Cr_2O_3 contents (1 wt% and <0.5 wt% respectively), whereas ilmenites associated with rutile or with armalcolite may contain up to 4 wt% Cr_2O_3 and 9-12 wt% MgO. Exsolution-like and crystallographically oriented spinel lamellae in ilmenite are chromite, titanian-chromite, or aluminian-titanomagnetite; these phase intergrowths are considered to be the result of subsolidus reduction. The ilmenite-rutile assemblages, although bearing some relationship to exsolved FeTiO_3 from TiO_2 are more likely the result of armalcolite decomposition ($\text{FeMgTi}_2\text{O}_5 \rightarrow \text{FeMgTiO}_3 + \text{TiO}_2$).

Armalcolite. The first terrestrial occurrence of armalcolite ($\text{FeMgTi}_2\text{O}_5$) is reported from DuToitspan, in discrete crystals 25-50 μm in dimension, and in association with rutile + MgO-rich ilmenite. This mineral is comparable in optical properties and major element chemistry to the type armalcolites present in the Lunar samples, although within the precision of the analyses the presence of Fe^{+3} cannot be unambiguously excluded (Table 1).

TiO_2 polymorphs. Rutile is the most commonly occurring polymorph, it is present typically as a groundmass phase and is generally associated with lamellar or mantled overgrowths of picro-ilmenite. The purity of these rutiles is variable, particularly with respect to Fe, Cr and Al. The limited solid-solubility of Fe in TiO_2 , the widespread ilmenite association, the identification of armalcolite, and broad-beam analyses of $(\text{FeMg})\text{TiO}_3\text{-TiO}_2$ intergrowths that approximate armalcolite in composition, suggests that the majority of rutile-ilmenite intergrowths may be derived by armalcolite thermal decomposition. Anatase (+ hematite) is restricted to ilmenite decomposition in deeply weathered pipes, and brookite is positively identified only in concentrates - both tend to be compositionally stoichiometric.

Rare minerals. In addition to armalcolite the following minerals have been identified, a complex vanadate (Table 1) from De Beers; intermediate members of a proposed series between perovskite and hematite (Table 1) from Ka0, the Ti-rich garnet schorlomite (Table 1) from both of above localities, and Ni-Fe alloys from Ramatseliso. The vanadate is a primary mineral included in phlogopite, the $\text{CaTiO}_3\text{-Fe}_2\text{O}_3$ phase forms a secondary mantle on microxenocrystic picroilmenite, schorlomite (+ sphene) replaces titanomagnetite-ilmenite intergrowths, and Ni-Fe is included in olivine.

Distinctive assemblages such as graphite + pyrrhotite, rutile + ilmenite, titanomagnetite + ilmenite, picroilmenite + chromite, and rhythmically mantled zones of alternating ilmenite and spinel on xenocrystic picroilmenite, suggest that prevailing redox conditions, rates of cooling, and the physiochemical kinetics of solid-solid, solid-liquid and solid-gas reactions during kimberlite emplacement and specifically during groundmass crystallization are widely variable. The outstanding examples that underscore the extremes of these variabilities are: (1) Redox conditions. The presence of native metals and armalcolite, in contrast to the occurrence of subsolidus oxidation of titaniferous magnetite; (2) fO_2 -Cooling rate. Homogeneous chromian-rich picroilmenite and low- Cr_2O_3 picroilmenite but with exsolved chromite; and (3) Reactions. Alteration rims on picroilmenite of variable thickness and widely varying chemistry in contrast to pristine picroilmenite. Groundmass enrichment trends as exhibited by spinel core-mantle relationships (i.e. from Mg-Al to Fe-Cr, and from Fe-Cr to Fe-Ti, and culminating in Ca-Ti, perovskite, in the outermost border zones) are compatible with crystal fraction models and

provide unambiguous evidence for the existence of late stage Ti-rich liquids in the majority of the kimberlites examined.

Table 1

Spinels (KaO: 1947, 2229)

	Core	Int.	Mantle	Core	Int.	Mantle	Core	Mantle
TiO ₂	4.07	5.42	10.96	0.60	1.89	4.37	0.18	0.23
MgO	16.11	13.19	11.75	11.66	13.37	16.13	16.40	9.26
MnO	0.44	0.52	0.54	0.27	0.32	0.04	0.20	0.37
CaO	0.08	0.06	0.15	0.07	0.04	0.02	0.02	0.11
FeO	13.88	17.82	23.53	15.57	14.84	14.28	10.88	19.79
Fe ₂ O ₃	9.26	29.33	43.62	5.35	6.73	9.37	0.95	1.06
Al ₂ O ₃	17.69	7.40	6.36	5.59	9.50	17.63	25.11	10.93
Cr ₂ O ₃	39.18	25.30	2.50	60.05	53.48	37.89	46.02	59.04
SiO ₂	0.28	0.27	0.29	0.38	0.27	0.29	0.06	0.13
Total	100.99	99.31	99.70	99.54	100.44	100.02	99.82	100.92

Spinels (Lipelaneng: 1363)

	Core	Mantle	Core	Mantle	Core	Mantle	Core	Mantle
TiO ₂	0.06	0.27	0.01	16.08	8.19	12.21	0.13	0.70
MgO	15.98	12.82	16.67	13.75	14.30	13.04	14.05	9.08
MnO	0.08	0.30	0.04	0.39	0.28	0.78	0.23	0.30
CaO	0.14	0.01	0.01	0.02	0.05	0.08	0.01	0.02
FeO	15.57	16.63	15.71	26.36	21.07	24.15	15.61	23.20
Fe ₂ O ₃	2.65	2.66	7.38	27.37	15.84	32.30	3.81	7.66
Al ₂ O ₃	50.36	32.20	52.70	12.52	23.13	6.38	30.91	29.47
Cr ₂ O ₃	15.69	35.63	7.51	2.95	17.41	11.01	35.64	29.45
SiO ₂	0.05	0.15	0.01	0.23	0.22	0.68	0.13	0.13
Total	100.58	100.67	100.04	99.67	100.49	100.63	100.52	100.01

	Armal-colite	Phase 1	Phase 2	Schorlomite	Sphene	Rutile	Perovskite
TiO ₂	76.92	53.16	36.31	20.35	40.64	96.49	57.39
MgO	7.08	3.66	3.96	2.35	0.02	0.63	0.19
MnO	0.54	0.14	0.33	0.05	0.02	0.01	0.02
CaO	0.06	0.39	23.78	31.96	28.90	0.31	38.93
BaO		4.07					
FeO	13.47*	11.28*		16.79*	0.25*	1.04*	1.21*
Fe ₂ O ₃			33.22**				
Al ₂ O ₃	0.02	0.27	1.09	0.13	0.89	0.00	0.24
Cr ₂ O ₃	1.64	17.98	0.36	0.00	0.00	1.87	0.16
V ₂ O ₃		8.46					
SiO ₂	0.28	0.20	0.18	27.94	29.55	0.20	0.21
Total	100.01	99.61	99.23	99.57	100.27	100.55	98.35

* Fe as FeO

** Fe as Fe₂O₃

REGULARITIES IN THE CHARACTERISTICS OF SOUTH AFRICAN DIAMONDS.

J.W. Harris, De Beers Industrial Diamond Division Limited, P.O. Box 916, Johannesburg. S.A.
 J.B. Hawthorne, Geology Department, De Beers Consolidated Mines Ltd., P.O. Box 616, Kimberley. S.A.
 M.M. Oosterveld, Computer Services Department, De Beers Consolidated Mines Ltd., P.O. Box 616, Kimberley. S.A.
 E. Wehmeyer, De Beers Diamond Sorting Office, Kimberley. South Africa.

In 1970 a study of the physical characteristics of diamonds was initiated. The project was undertaken to establish whether or not the diamonds from individual sources could be separated by observations of physical parameters.

Approximately 80 000 diamonds from various southern African localities were examined initially to formulate the classification scheme. A further 68 000 stones from the Premier, Finsch, Koffyfontein and Dreyers Pan mines were then classified.

The classification scheme is based primarily on the morphology of the diamond. Additional parameters such as colour, angularity and regularity allow further sub-division to be made. The classification scheme is outlined in Table 1.

TABLE 1.

<u>DIAMOND CHARACTERISTICS CLASSIFICATION.</u>			
<u>PRIMARY DIVISION:</u>			
<u>CRYSTAL FORMS:</u>		<u>OTHERS:</u>	
Octahedra*: Dodecahedra*		Macles	
Flattened Dodecahedra* : Cubes		Spheres	
Tetrahedra : Cubo-Octahedra		Irregular Forms*	
Octa-Dodecahedra : Cubo-Dodecahedra		Crystal Aggregates	
Cubo-Octa-Dodecahedra			
<u>SECONDARY DIVISIONS:</u>			
(i) <u>Transparency</u>	Transparent Opaque	(v) <u>Colour</u>	Colourless Yellow
(ii) <u>Crystal Angularity</u>	Planar Rounded		Brown Green
(iii) <u>Crystal Regularity</u>	Regular Distorted		Orange and Amber Pink and Mauve Blue
(iv) <u>Inclusion Content</u>	None Few (1 - 3) Many (> 3)		Black Multiple Colours Grey

SECONDARY DIVISIONS: (Continued)(v) Colour Smokey(vi) Surface Feature

Transparent Coats

Opaque Coats

Graphite Coats

Frosting

* Macle shape divisions. In addition, "triangular macle" accounts for commonly depicted form.

Prior to examining the diamonds from each source they had been screened into various size ranges. From pilot studies it became apparent that diamond characteristics for a particular source varied with the size of the diamonds.

Hence sizes of diamonds must be taken into account when comparison from different sources is made. The size ranges used are shown in Table II.

TABLE II.

<u>SIEVE CLASS*</u>		<u>APPROXIMATE AVERAGE SIZE</u> (Carat Weight)
- 23	+ 21	5,00
- 21	+ 19	2,72
- 19	+ 17	1,70
- 17	+ 15	1,30
- 15	+ 13	0,88
- 13	+ 12	0,57
- 12	+ 11	0,39
- 11	+ 9	0,23
- 9	+ 7	0,14

* Diamond sieves with round aperture openings.

Tabulations of the more general and significant relationships which emerged from the study are shown below. Extremes of diamond sieve classes are chosen to illustrate difference between the various diamond sizes; no linear relationships necessarily exist between these extremes.

1. CRYSTAL FORMS:

The following table shows the percentage of the major crystal forms per mine for diamonds in the +9 -11 diamond sieve class and the +17 -19 sieve class.

TABLE III.

	FINSCH		PREMIER		KOFFY		DR. PAN.	
	+ 9	+17	+ 9	+17	+ 9	+17	+ 9	+17
	-11	-19	-11	-19	-11	-19	-11	-19
Octahedra	11	18	6	5	6	16	16	38
Dodecahedra	27	25	20	17	26	19	61	23
Flat Dodecahedra	3	3	2	2	2	2	15	13
Macles	18	17	11	22	8	13	4	18
Irregular Forms	41	37	61	54	58	50	4	8

The table shows the predominance of irregular forms at Premier and Koffyfontein and the low percentage of irregular forms at Dreyers Pan. Differences exist for the percentages of Octahedra, Dodecahedra and Macles from the different mines. In general there is an increase in octahedra and macles with increasing stone size and a decrease in dodecahedra.

2. COLOUR.

The predominant colours of the percentage of diamonds from each mine is shown in Table IV.

TABLE IV.

	FINSCH		PREMIER		KOFFY.		DR. PAN.	
	+ 9	+17	+ 9	+17	+ 9	+17	+ 9	+17
	-11	-19	-11	-19	-11	-19	-11	-19
Colourless	43	28	41	40	66	78	55	52
Yellow	7	18	4	10	9	8	17	10
Brown	40	26	48	28	13	4	6	3
Green	8	16	1	6	0	0	22	35
Grey and Black	2	12	6	16	12	10	0	0

The table shows significant colour differences between the mines. Typical for Koffyfontein is the high percentage of colourless stones and the virtual absence of green diamonds. Typical for Dreyers Pan is the high percentage of colourless and green diamonds and the low percentage of brown and black. At Finsch there is a higher percentage of yellow and green diamonds than at Premier. A further characteristic of the Premier Mine is the occurrence of blue diamonds.

3. COLOUR AS FUNCTION OF MINE AND FORM:

In Table V the percentages of diamonds are shown.

TABLE V.

	FINSCH					PREMIER					KOFFYFONTEIN					DREYERSPAN.				
	O	D	FD	M	I	O	D	F	E	M	I	O	D	FD	M	I	O	D	FD	M
Colourless	32	34	36	38	30	34	32	46	53	41	90	79	69	77	67	64	51	56	66	74
Yellow	14	20	25	15	12	5	7	11	7	8	6	11	20	14	6	9	17	16	8	10
Brown	30	29	25	25	34	52	49	34	29	35	1	3	9	3	13	4	6	8	4	12
Green	22	13	13	16	8	3	4	6	4	3	-	-	-	-	-	23	26	20	22	3
Grey/Black	2	4	1	6	16	6	8	3	7	13	3	7	2	6	14	-	-	-	-	1

O = octahedra
 D = dodecahedra
 FD = flattened dodecahedra
 M = macles
 I = irregular forms.

Overall the macles class contain the largest proportion of colourless diamonds, although at Koffyfontein the percentage of colourless octahedra is very high. Flat dodecahedra show the highest proportion of yellow diamonds. In general the colour of diamonds appears to be predominantly related to the source, and relationships between form and colour are less evident.

4. There are small but significant differences between the sources and between different sizes in respect of transparency, angularity, regularity, number of inclusions, frosting, and coats.

As a result of these investigations an attempt is to be made to identify the source of diamonds from secondary deposits where the primary source is not known. Also it is likely that a structure will be provided which will enable other relationships to be quantitatively framed. For example relationships between morphology and physical properties such as crystal perfection, optical anisotropy and luminescence.

PETROGRAPHY AND GEOLOGICAL HISTORY OF UPPER MANTLE XENOLITHS
 FROM THE MATSOKU KIMBERLITE
 By
 B. Harte, K. G. Cox and J. J. Gurney

Xenoliths of garnet peridotite facies origin (Group 1 of Cox, Gurney and Harte, 1973) usually consist only of varying proportions of the minerals: olivine, orthopyroxene, clinopyroxene (chrome-diopside), and garnet (ignoring late-stage alteration products). The majority of the xenoliths (common peridotites - CP) consist predominantly of olivine and orthopyroxene (ol. > opx.) with <5% of chrome-diopside and <11% of garnet. Dunites, garnet orthopyroxenites (with subordinate olivine + chrome-diopside), and garnet websterite also occur in small amount, as well as rare unbanded garnet lherzolites enriched in chrome-diopside and/or garnet.

BANDING

A banded distribution of minerals is seen in 10 specimens, with bands corresponding to modal varieties listed above, but also including types considerably enriched in chrome-diopside (and garnet). The transitional nature of most band contacts and absence of sharp distinctions in modal proportions (excepting LBM 40; Cox, Gurney & Harte 1973), together with a lack of intrusive relationships or metasomatic features (excepting LBM 38; op. cit.), suggests a cumulate origin for much of the banding. Such an origin is supported by the constant mineral chemistry of adjacent bands (Gurney, Harte & Cox 1973), and the presence in LBM 31 of a dunite band between harzburgite bands.

TEXTURAL TYPES

Texturally the following principal types of xenolith (both banded and unbanded) may be recognised:

(a) Coarse-granular (Fig. 1a) This is the commonest type and shows a predominantly coarse grain size of anhedral crystals. Grain boundaries are usually quite wavy and irregular, but vary towards smoothly curving. Slight undulose extinctions and some broad deformation bands are not uncommon within large olivine and orthopyroxene grains, but crystals are not strongly deformed. Preferred dimensional elongation of minerals is not usually visible, but weak crystallographic fabrics may be present.

(b) Coarse-granular with slight recrystallisation Similar to (a) but with more pronounced deformation of minerals, accompanied by polygonisation within large olivine and orthopyroxene crystals, and thin zones of recrystallisation along grain boundaries.

(c) Flaser (Fig. 1b) Showing prophyroclasts and lenticles of coarse grain size (especially of orthopyroxene), with large garnets frequently drawn out into schlieren. Between the relics or original minerals the rock shows recrystallisation to a fine grained aggregate. (Although flaser, the structure and fabric of these rocks is not nearly so pronounced as that figured in Williams (1932, plate 145), or described by Boyd (1973, and personal communication).

(d) Fully recrystallised (even textured) (Figs. 1c & 1d). These rocks show varying grain size depending on the amount of grain growth following recrystallisation. Within individual specimens the grain size is usually quite uniform, and grain boundaries are characteristically regular and smoothly curving. The latter features with regular triple junctions

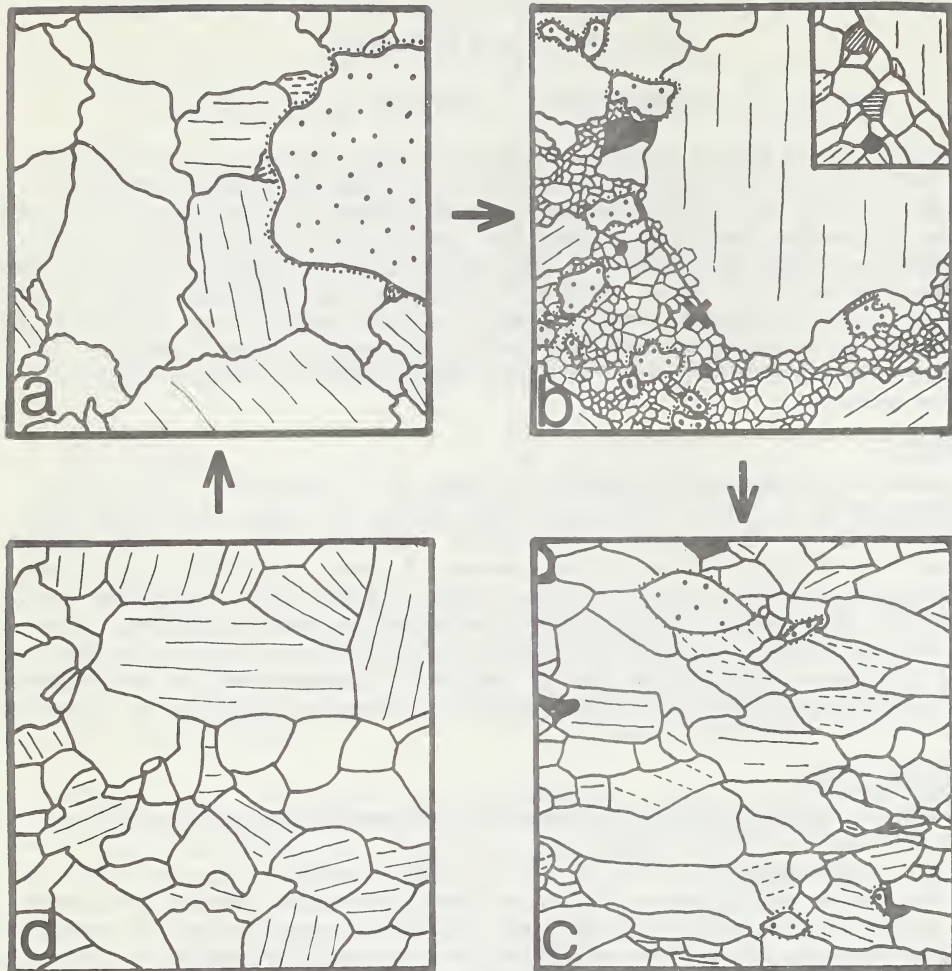


FIG. 1 Diagrams illustrating different textures in Matsoku rocks - see text. All traced from photographs and with constant magnification ($\times 12.5$) except inset in 1b ($\times 25$).

- (a) Coarse-granular
- (b) Flaser - showing very fine grained recrystallised areas and large prophyro-clasts.
- (c) & (d) Fully recrystallised.

ORNAMENTATION (not shown in recrystallised areas of main part of b):

	olivine		garnet
	orthopyroxene		phlogopite
	clinopyroxene		ore mineral

distinguish medium to coarse grained rocks of this category from those of category (a) - compare Figs. 1a & 1d. In some fully recrystallised rocks there is a distinct dimensional elongation of mineral grains (Fig.1c) producing schistosity, and strong fabrics may be present.

All gradations are seen between each of the above types and those listed immediately above and below it. Subsequent deformation leading to undulose extinction and broad deformation bands may be seen to have affected occasional grains in some type (d) rocks, and more irregular grain boundaries are often associated with such grains (contrast the centre left with the right hand side of Fig. 1d). Thus one may envisage type (d) rocks (Fig.1d) passing into type (a) rocks (Fig. 1a) with continued grain growth and slight deformation. A continuous 'cycle' of deformation, recovery, recrystallisation and grain growth is thus generated as shown on P.4; although there is no specific evidence in the case of the Matsoku nodules for any rock having undergone more than one complete cycle. The textural changes seen, and the gradual and progressive nature of the reconstitution coupled with its occurrence under constant conditions of high T. and P. (Gurney, Harte & Cox 1973) suggests an origin by mantle creep (Ave'lallement & Carter 1970; Raleigh & Kirby, 1970).

METASOMATISM AND THE FORMATION OF PHLOGOPITE AND ORE MINERALS

In the recrystallised areas of some flaser rocks, and in some fully recrystallised rocks small amounts of phlogopite and ore minerals (ilmenite, rutile, chalcopyrite, pyrrhotite, and pentlandite) are seen. These additional minerals show smooth grain boundary contacts with recrystallised olivine, orthopyroxene, and clinopyroxene, and thus appear texturally primary (Fig. 1b inset). Such relations contrast with those of phlogopite and ore mineral seen in all xenoliths, where these minerals are associated with kelyphite and serpentine and are clearly related to very late-stage alteration (within the kimberlite?). The general absence of other than the latter phlogopite and ore mineral in coarse-granular xenoliths, suggests that the texturally primary material has been introduced metasomatically during the coarse of recrystallisation. The introduction of metasomatic fluid may have promoted the recrystallisation in some instances.

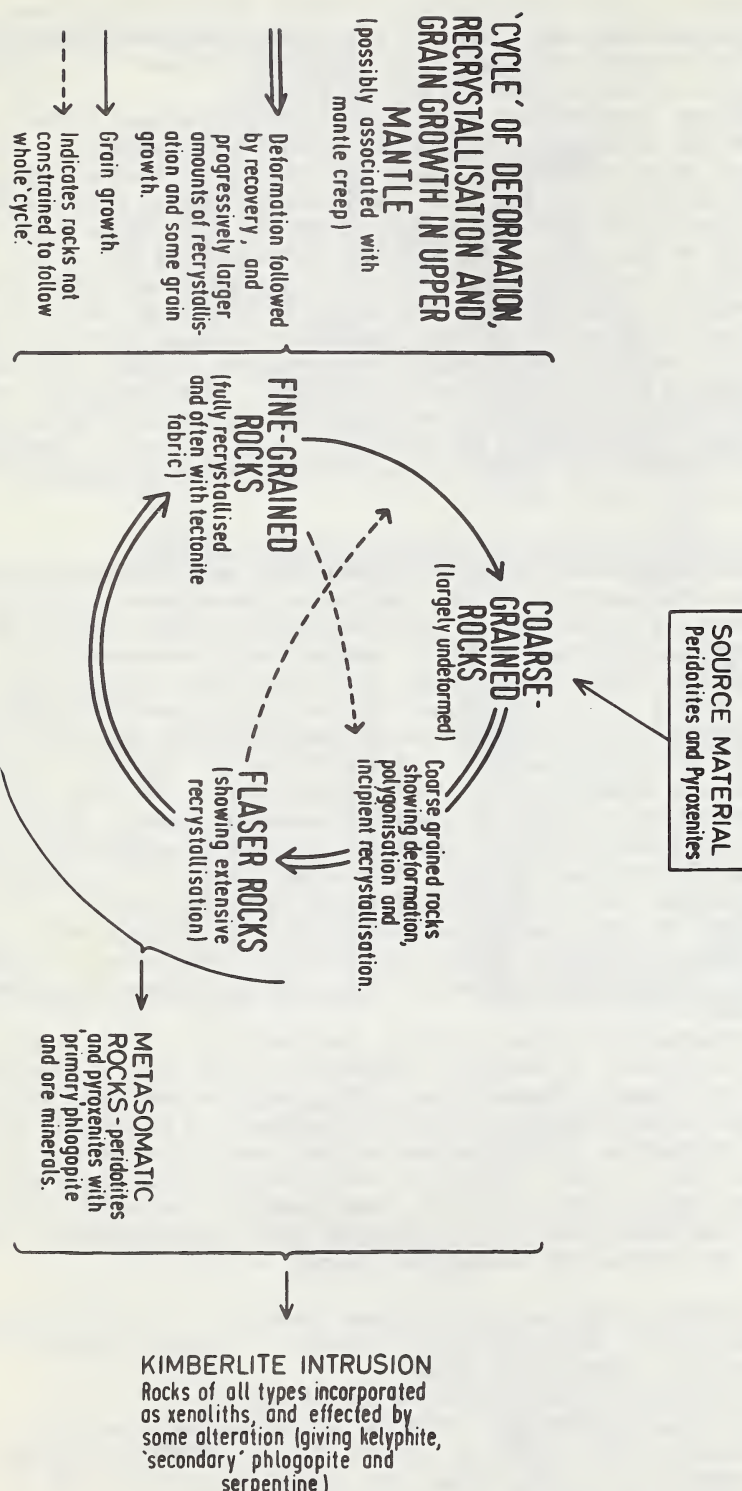
Specific evidence of infiltration metasomatism is shown by a vein enriched in phlogopite and ore mineral in LBM 22. The vein truncates a flaser structure present in this rock, and within the vein all minerals appear fully recrystallised.

Minerals in metasomatised areas of rocks (including the LBM 22 vein) show only slight departures in chemical composition from minerals outside metasomatised areas (Gurney, Harte & Cox, 1973), and the metasomatism is therefore believed to have occurred under the common T. & P. conditions indicated by all xenoliths. The metasomatic fluid may be derived from the low velocity zone (Boyd, 1973). Since the metasomatism (and associated recrystallisation) are the last definite events seen in the nodules prior to their eruption in kimberlite, it is possible that the metasomatic fluid was derived from the developing kimberlite 'magma'.

References:

Ave'lallement, & Carter, 1970 Bull. Geol. Soc. Amer.
 Boyd, F.R. & Nixon, P.H., 1973. Origin of Ilmenites-Silicate Nodules in Lesotho Kimberlites, edited P.H. Nixon.
 Boyd, F.R., 1973. Geochem et Cosmoschem. Acta (in press).
 Cox, K.G., Gurney J.J., & Harte, B., 1973. in Lesotho Kimberlites edited P.H. Nixon. / Gurney, J.J., Harte B., & Cox, K.G., 1973. This Volume.
 Raleigh C.B., & Kirby, S.H., 1970. Miner Soc. Amer. Spec. Pap. 3, 113-121.
 Williams, A.F., 1932. The Genesis of the Diamond.

SUMMARY OF GEOLOGICAL HISTORY OF UPPER MANTLE XENOLITHS FROM MATSOKU PIPE



EVOLUTION OF CLINOPYROXENE AND GARNET IN AN ECLOGITE NODULE FROM THE
ROBERTS VICTOR KIMBERLITE PIPE

B. Harte and J. J. Gurney

The eclogite nodule studied is bimimetic and shows a variable texture, which may be crudely banded. One half of the nodule is dominated by very large clinopyroxene crystals (up to 6.0 cms) which are separated by narrow zones of granular garnets (2.0 to 5.0 mms). Internally these clinopyroxenes show numerous, prominent exsolution lamellae of garnet (up to 1.25 mm thick), and occasional more granular garnet inclusions. In the other half the texture is dominantly of granular type with roundish garnets (2-5 mm) and anhedral clinopyroxenes (4 to 20 mm): the large clinopyroxenes showing scattered exsolution lamellae. In the fine-granular part, the garnets again tend to surround individual clinopyroxenes. The bulk composition of the whole nodule shows wt.-%: SiO_2 44.03, TiO_2 0.17, Al_2O_3 15.30, Cr_2O_3 0.05, Fe_2O_3 4.74, FeO 4.76, MnO 0.18, MgO 12.21, CaO 17.65, Na_2O 0.65, K_2O 0.23, P_2O_5 0.03.

There is a very wide spread of both garnet and clinopyroxene compositions. Individual garnet lamellae and granules show fairly constant compositions, except at the margins and in occasional apophyses of large granules. Individual clinopyroxene crystals show marked changes in composition with most particularly: Al_2O_3 gradually decreasing, and SiO_2 and MgO gradually increasing, as garnet (either lamellar or granular) is approached. These changes accord with the high Al_2O_3 and lower SiO_2 and MgO of garnet compared with clinopyroxene, and indicate the occurrence of granular as well as lamellar exsolution. It appears that the latter exsolution has been dominant in the coarse-lamellar part of the nodule, and the former in the fine-granular part. These differences may reflect initial variation in grain size within the rock, and it is probable that different initial proportions of garnet and clinopyroxene occurred in the two parts of the nodule. That some garnet must have been present in the rock initially is shown by the failure to homogenise the bulk rock composition (Fig.3), and accords with its high R_2O_3 content (cf. O'Hara, 1969).

Within the large clinopyroxene crystals, garnet lamellae of widely varying size are seen. Coarse lamellae may run continuously for several cms. and clusters of parallel fine lamellae tend to terminate adjacent to these coarse lamellae; suggesting the earlier development of coarse lamellae.

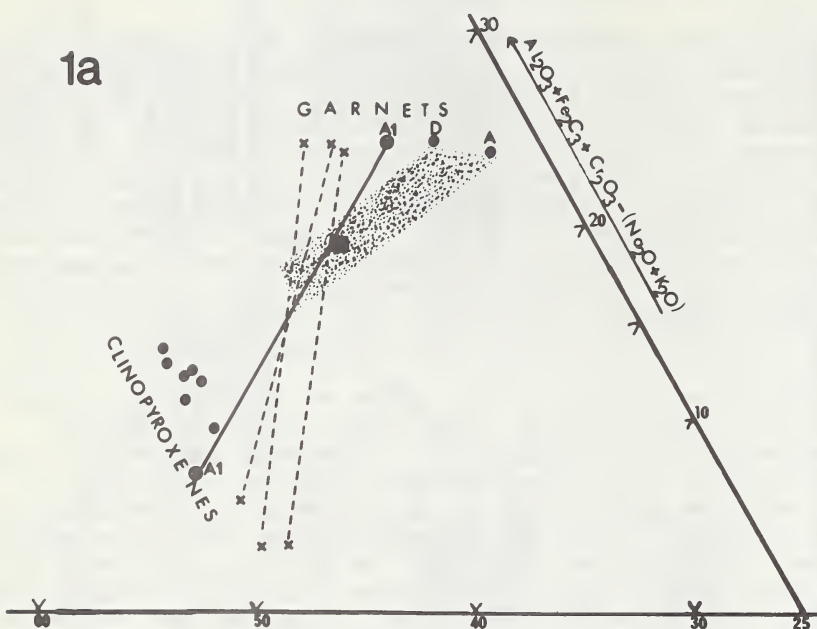
Despite the lack of chemical equilibrium within the rock on a large scale, it may be expected that the garnet exsolved at any one time would be in equilibrium with the clinopyroxene from which it was forming, and thus garnet and clinopyroxene in immediate contact would approximate to local chemical equilibrium. Fig.1 shows the composition (all Fe as FeO) of garnets and clinopyroxenes, with tie-lines joining garnet lamellae (classified according to size) and immediately adjacent clinopyroxene compositions in the coarse-lamellar part of the nodule.

Fig.1 also shows the garnet and clinopyroxene compositions of points as far removed from the other phase as possible; and the calculated average bulk composition (A2) of a region of clustered fine parallel garnet lamellae within a large clinopyroxene crystal. Composition A₂ has 14.1 wt.% Al_2O_3 , and the maximum Al_2O_3 content of actual clinopyroxene found in the rock is 13.82%; suggesting an initial content approaching 14.5%.

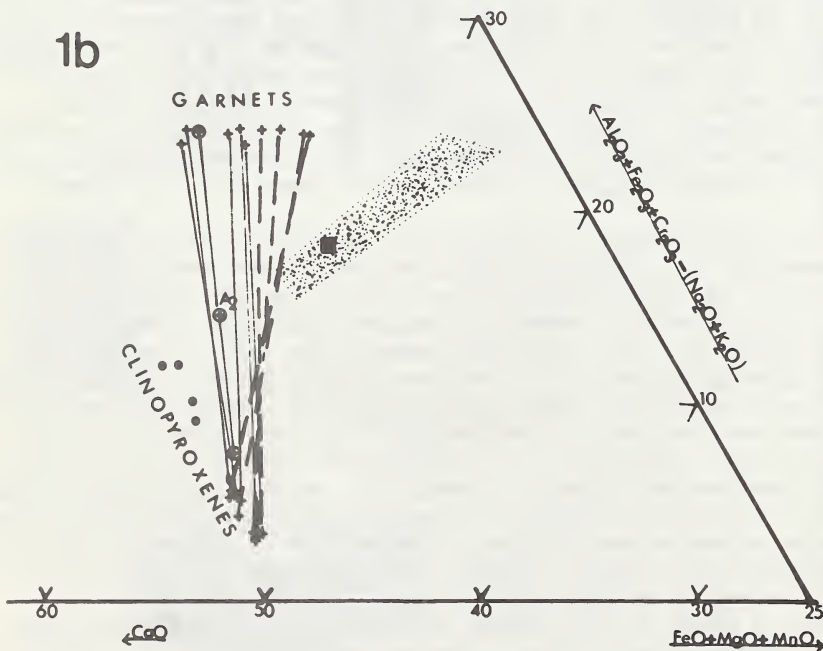
Fig.1 shows a swing in orientation of garnet-clinopyroxene tie-lines during the progressive exsolution of garnet, associated with an overall

FIG 1

1a



1b



variation of garnet C (atoms Ca/Ca+Mg+Fe+Mn) from 36.2 to 55.0. The change in tie-line orientation may be expected to occur with decreasing T. &/or increasing P. (O'Hara & Mercy, 1966; Lovering & White, 1969). The data indicate that a sufficiently CaO- and $Al_{2-3}O_3$ -rich clinopyroxene (initially capable of co-existing with pyrope-rich garnet) may exsolve to yield clinopyroxene and garnet compositions related to those of gospodites (Sobolev et al., 1968).

Fig.2 shows Fe/Mg ratios of garnet lamellae and adjacent clinopyroxene (from Fig.1), together with approximations (A&D) towards the Fe/Mg ratios of co-existing garnet and clinopyroxene prior to exsolution. Point A is calculated using garnet A and clinopyroxene A2 of Fig.1, while point D is calculated from garnet D and the most aluminous clinopyroxene found in the region around garnet D. The distribution coefficient, $K = Fe/Mg_{Garnet}/Fe/Mg_{Clinopyroxene}$, shows a progressive increase during the course of exsolution, corresponding to decreasing T &/or increasing P (Banno, 1970) and is consistent with the change in tie-line orientation in Fig.1. Temperature rather than pressure is expected to have the major effect on K (op.cit).

Fig.3. summarises experimental data on a crushed large clinopyroxene complete with its exsolution lamellae. Data points are also shown for two runs on a starting material formed by the bulk rock composition (P.1). The large clinopyroxene with exsolution lamellae homogenises to clinopyroxene alone in a wedge shaped field adjacent to the solidus. Assuming that the initial eclogite (consisting of unexsolved clinopyroxene and initial garnet) formed by crystallisation from magma and was therefore in equilibrium with liquid, an initial T. and P. of formation of the nodule at approximately $1400^{\circ}C$ and 34-38 kb. are indicated by Fig.3 (subject to variation in the composition of the liquid). The exsolution of garnet from clinopyroxene and the relations of Figs. 1 & 2 could then develop as a result of cooling to the geotherm at roughly constant depth.

References

Banno, S., 1970. *Phys. Earth Planet Interiors* 3, 405-421
 Lovering, J.F., & White, A.J.R., 1969. *Contr. Mineral. Petrology* 21, 9-52.
 O'Hara, M.J., 1969. *Geol. Mag.* 106, 322-330.
 O'Hara, M.J., & Mercy, E.L.P. 1966. *Nature* 212, 68-9
 Sobolev, N.V., Kuznetsova, I.K., & Zyuzin, N.I., 1968. *J. Petrology* 9, 253-80.

FIG.1. Molecular plot of bulk rock composition (■), and clinopyroxene and garnet compositions. Tie-lines join garnet lamellae and immediately adjacent clinopyroxene compositions: ✕ indicates coarse garnet lamellae, + indicates intermediate and fine garnet lamellae (solid tie-lines join points occurring in clusters on fine garnet lamellae. Al ⊗ represent an exceptionally coarse garnet lamella and adjacent clinopyroxene.

⊕ represent the average compositions of garnet and clinopyroxene (including all clinopyroxene occurring in between lamellae) in a scan across a cluster of fine garnet lamellae, with A2 being the overall bulk composition. ● (unlabelled) in 1a are clinopyroxenes as far removed from garnet as possible; and in 1b are clinopyroxenes midway between clusters of fine garnet lamellae. ● (A&D) are the centres of large granular garnets in the coarse-lamellar and fine-granular parts of the nodule respectively. The dotted area indicates the probable location of garnet-clinopyroxene tie-line(s) before exsolution.

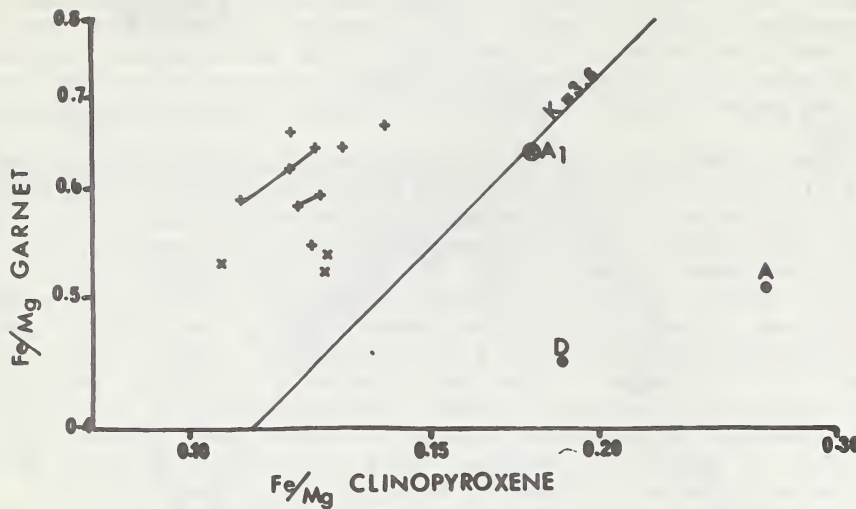


FIG. 2. Fe/Mg distribution in garnet and associated clinopyroxene. Symbolism as in FIG.1. The short lines join points occurring in the same cluster of fine garnet lamellae. The line $K=3.6$ is from Banno (1970, p.409) for Roberts Victor eclogites .

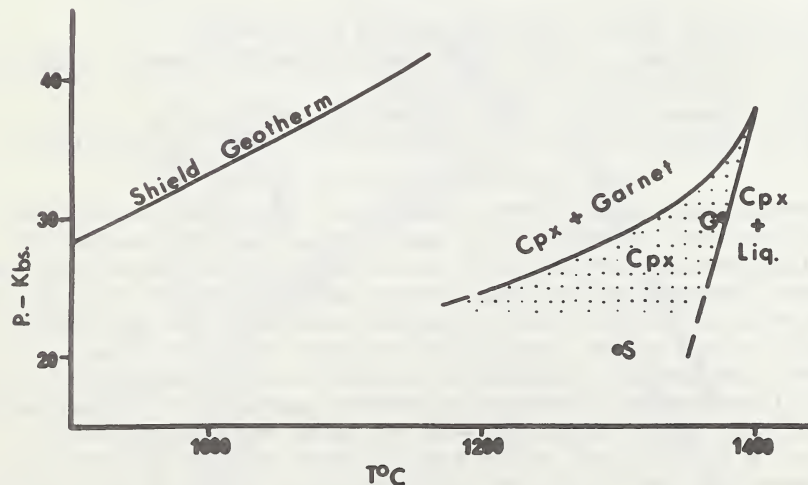


FIG. 3. Summary of experimental data on the composition of a large clinopyroxene crystal (with included garnet lamellae), showing an extensive field (dotted) of homogenisation to clinopyroxene only. The points G and S represent runs on the whole rock bulk composition showing cpx + garnet + glass, and cpx + spinel + ? garnet + ? glass respectively.

MODEL OF A KIMBERLITE PIPE

J.B. Hawthorne
Geology Department,
De Beers Consolidated Mines Limited
P.O. Box 616,
KIMBERLEY
South Africa.

Recent discoveries of kimberlites in Tanzania, Zambia and Botswana together with new evidence from pipes which are being mined in Angola and Zaire show that in central Africa there is widespread development of pipes which differ in several respects from those which are mined in South Africa. The occurrences in central Africa of which the Orapa pipe in Botswana is typical are often found to be overlain by large basins containing re-worked kimberlite. The inward dip of the pipe walls below these basins tends to be much shallower than that of the South African pipes, ranging from 30° to 70° . The basins are interpreted as being the remnants of ancient crater lakes of maar type kimberlite volcanoes, filled with reworked kimberlitic ejectamenta which formed epiclastic kimberlite deposits. The presence of crater sediments and the shallow inward dips of the pipe walls suggest that these pipes have undergone relatively little erosion since they were formed.

In South Africa crater sediments are found only in some of the kimberlite diatremes of the Bushmanland. Elsewhere, in the Karroo Kimberlite Province, in Lesotho and the Transvaal crater sediments in kimberlite pipes are not found.

Detailed studies of the shapes of eleven South African pipes have been undertaken.

It was found that at depths of 300m to 500m, pipes in the Kimberley area have smooth regular walls and near vertical axes. Below these depths the pipe walls become irregular, breccia zones and domes are developed and the pipe axes are no longer vertical. Further to the southeast as the thickness of present day Karroo rocks increases this transition is found to take place at greater depths.

A method of average slope measurement based on variations in the pipe area was devised and applied to the upper parts of the pipes. This enabled a comparison of the slope of various pipes to be made. It was found that the slopes of the regular upper parts of the pipes investigated were highly consistent, ranging between 79° and 85° and averaging 82° .

AVERAGE INWARD DIPS OF PIPE WALLS

Pipe	Wallrock	Levels between which measurements were made	No. of levels used.	Av. Dip
Premier	Bushveld Felsite	170m-538m	5	84,5°
Finsch	Transvaal System Ironstone and Dolomite	9m-95m	2	82,0°
Dutoitspan	Karoo Dolerite & Shale, Ventersdorp Lava & Quartzites Archaen Granite Gneiss	0m-411m	4	79,0°
Koffyfontein	Karoo Dolerite, Shale	46m-244m	3	85,0°
Wesselton	Ventersdorp Lava, Quartzite	250m-470m	3	81,0°
Jagersfontein	Karoo Dolerite, Shale	238m-570m	5	81,0°
Bultfontein	Ventersdorp Lava, Quartzite Archaen Granite & Schists	296m-670m	3	83,5°
De Beers	Ventersdorp Lava, Quartzites	105m-300m	3	84,0°
Kimberley	Karoo Shale, Ventersdorp Lava, Quartzite	91m-294m	4	80,5°
West End	Transvaal System Dolomite	0m-165m	2	81,0°
Kao (Lesotho)	Stormberg Lava	0m-90m	2	85,0°
			Av.	82,4°

The differences in pipe profile described are thought to be due primarily to differences in the depth to which erosion has proceeded since the emplacement of the pipes.

In central Africa the depth of erosion has been considerably less than at most South African pipes suggesting a substantially different age or geomorphological history. In the Kimberley area this depth of erosion is estimated to be between 900 and 1900m. The estimate is based on the nature of the wall rock inclusions found in the pipes and on evidence obtained from studies of the depth of formation of kimberlite sills supplemented by geochemical and diagenetic studies of the wall rocks around the pipes.

Williams (1932) described many of the inclusions found within the pipes. In addition to deep seated inclusions he identified inclusions derived from the upper part of the Karroo System which is no longer preserved in the area. It is concluded from the character of the Karroo inclusions that the full sequence of the Karroo System including at least some of the Stormberg Lava was present when the pipes were intruded.

A number of kimberlite sills in the Kimberley area have been described (Hawthorne 1968). These sills are confined to the flat lying sedimentary rocks between the base of the Karroo System and the lowest dolerite sill which intrudes the Karroo rocks. Many are close to the present land surface. Mudge (1968) examined a large number of concordant masses of igneous rocks in flat lying sedimentary environments and concluded that the limiting depths of emplacement for these bodies was between 900m and 2300m below the surface. If the kimberlite sills were emplaced under similar controls then the surface around Kimberley has been lowered by a similar amount since then. If the pipes and sills were more or less contemporaneous this depth range also indicates the depth to which the pipes have been eroded.

In an attempt to reduce these fairly wide limits for the depth of erosion, the results of geochemical and diagenetic studies undertaken by the Southern Oil Exploration Corporation were investigated. Regional studies on the Karroo System have been carried out and samples of near surface lower Karroo sediments obtained from borehole cores in the vicinity of Kimberley and Koffiefontein have been examined. (De Swardt and Rowsell in prep). The degree of crystallinity of illite, the residual to total carbon ("CR/CT") ratios and the bulk grain densities were measured. These measurements suggest a total depth of burial of 1900m for the lower Karroo in the vicinity of Kimberley. This figure represents the total thickness of Karroo rocks removed by erosion. The Karroo thickness at the time of pipe emplacement must have been less than this because of post-Stormberg pre-kimberlite erosion during a period of some 80 to 100 million years. This reduction of the Karroo thickness cannot be determined at present but for a graphic representation of the kimberlite pipe model an arbitrary reduction to 1400m is made. This figure is the average of the upper limit of sill formation (900m) and the total thickness of the Karroo System (1900m) in the Kimberley area.

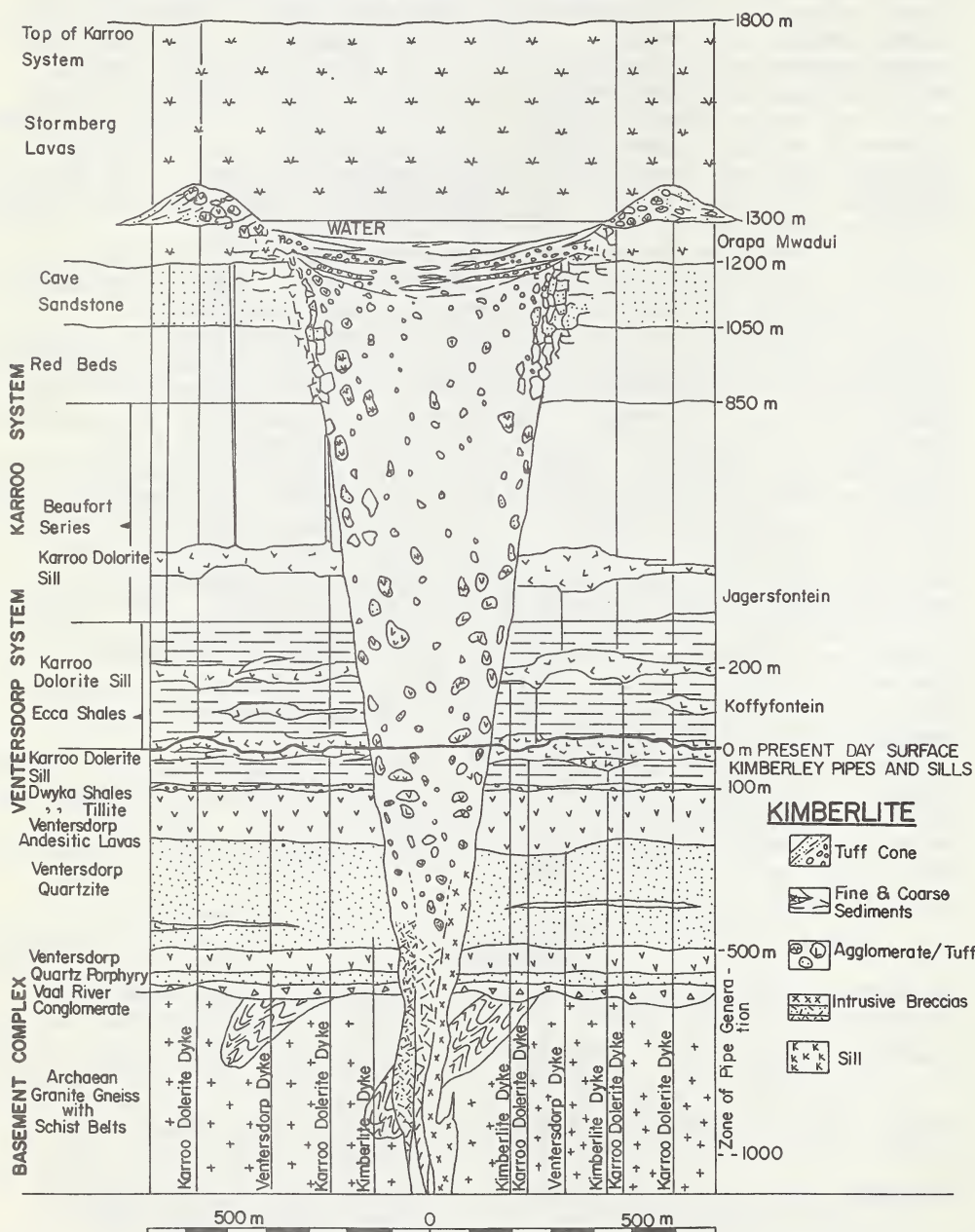
The information on shape obtained by studying kimberlite pipes which appear to have been eroded to different depths has been incorporated into the accompanying diagram of a hypothetical pipe. This model serves as a means of identifying the relative depth to which a pipe has been eroded and of predicting changes in its character which may be found in depth.

REFERENCES

De Swardt, A.M.J. and Rowsell, D.	(In prep.)	Diagenesis in the Cape and Karoo Supergroups.
Hawthorne, J.B.	(1968)	Trans. Geol. Soc. S. Afr. 71: 291-311.
Mudge, M.R.	(1968)	Bull. geol. Soc. Amer. 79: 315-332.
Williams, A.F.	(1932)	The genesis of the diamond. 2 vols. Ernest Benn, Ltd., London, 636p.

MODEL OF A KIMBERLITE PIPE

PLATE V



Garnet peridotite xenoliths in a Montana, USA, kimberlite

B. Carter Hearn Jr., U. S. Geological Survey,
Washington, D. C. 20244, USA

and

F. R. Boyd, Geophysical Laboratory, Carnegie Institution
of Washington, Washington, D. C. 20008, USA

In Montana, USA, one diatreme within a swarm of subsilicic-alkalic diatremes (Hearn, 1968) contains common xenoliths of granulite, and rare xenoliths of spinel peridotite and garnet peridotite. The main diatreme is 270 by 370 meters, with a rounded irregular shape partially controlled by pre-existing faults. The border of the diatreme contains a short ring dike of igneous monticellite peridotite and slices of higher wall rocks of early Eocene age, similar to the occurrences of descended slices in other Montana diatremes which do not contain deep-seated xenoliths. A nearby xenolith-bearing subsidiary dike is in part massive with apparent igneous texture and in part fragmental with pelletal texture. Micas give K/Ar ages which are too old, as a result of excess argon or xenocrystic origin; fission-track dating will probably show a late-middle Eocene age similar to the other diatremes. Such an age is toward the end of widespread subsilicic- to silicic-alkalic igneous activity in north-central Montana.

Although many North American kimberlites contain characteristic xenocrysts probably derived from garnet peridotite, xenoliths of garnet peridotite are extremely rare and have been reported from only two diatremes in Utah and one in Colorado. Six relatively unaltered garnet peridotite xenoliths from Montana range from 2.5 cm diameter to 23x18x12 cm. All six contain garnet lherzolite mineral assemblages, although diopside is less than 0.5 percent in two. The garnet peridotites show distinctive textures: four are granular (either unsheared, or showing necklace texture of thin zones of fine-grained olivine surrounding large strained olivines) and two are highly sheared (large rounded to augen-shaped crystals of garnet, strained olivine, orthopyroxene and clinopyroxene in a fine-grained groundmass of granulated olivine and orthopyroxene, giving a banded appearance). Phlogopite, which is probably primary in part, occurs as rims around garnet, as veins, and as isolated grains in granular xenoliths, but is absent from sheared xenoliths, similar to phlogopite distribution reported by Boyd and Nixon (1973) for Lesotho garnet peridotite nodules.

Olivine and orthopyroxene show a restricted compositional range, $Fo_{90.5}$ to Fo_{94} , $En_{90.5}$ to En_{94} . Clinopyroxenes range from $Wo_{47}En_{50.5}Fs_{5.5}$ (granular xenolith) to $Wo_{32.5}En_{59.5}Fs_8$ (sheared xenolith). CaMgFe compositions of garnets from five xenoliths plot within the same fields as Lesotho garnets from sheared and granular lherzolites respectively. Garnet in one Montana lherzolite is strongly pyropic, $Ca_3Mg_8Fe_7$. Cr_2O_3 of xenolith garnets ranges from 0.7 to 7.8 percent. Five of six analysed garnet megacrysts, up to 4 cm diameter, have Mg/Fe similar to xenolith garnets, but with more restricted range of Ca; their Cr_2O_3 ranges from 0.7 to 2.1. An ilmenite megacryst is typically magnesian with composition $Il_{48}Gk_{41}He_{11}$.

Equilibration temperatures and depths of the six garnet lherzolite assemblages, estimated from pyroxene compositions as discussed by Boyd (1973) and corrected for FeO by the method of Wood and Banno (1973), range from $920^{\circ}C$, 106 km to $1315^{\circ}C$, 148 km (fig. 1). The xenoliths show increasing amount of shearing with greater depth. Temperature-depth points for the Montana xenoliths suggest a geotherm which is similar in slope to the steep portion of the Lesotho geotherm, and is considerably steeper than the normal shield geotherm. The steepened geotherm defined by the xenoliths, coupled with deformation textures, could indicate their origin from the low-velocity zone in Eocene time, with increased temperature due to the inter-related processes of continental drift and magma generation. Preservation of textures of intense shearing requires active deformation of dry rock and rapid transport of xenoliths to the surface.

Xenolith data show that this diatreme was derived from a depth of at least 148 km, and the associated igneous rock (monticellite peridotite) indicates that the diatreme is related to ascent of a potassic gas-rich magma from upper mantle depths. Such magmas are involved in the genesis of many, but not all, kimberlites elsewhere in the world. The close relationship of kimberlite, carbonatite, and the monticellite peridotite-alnösite suite may define the spectrum of fluids responsible for transport of heterogeneous materials from upper mantle depths to near-surface levels where the resultant mixtures were emplaced as kimberlite.

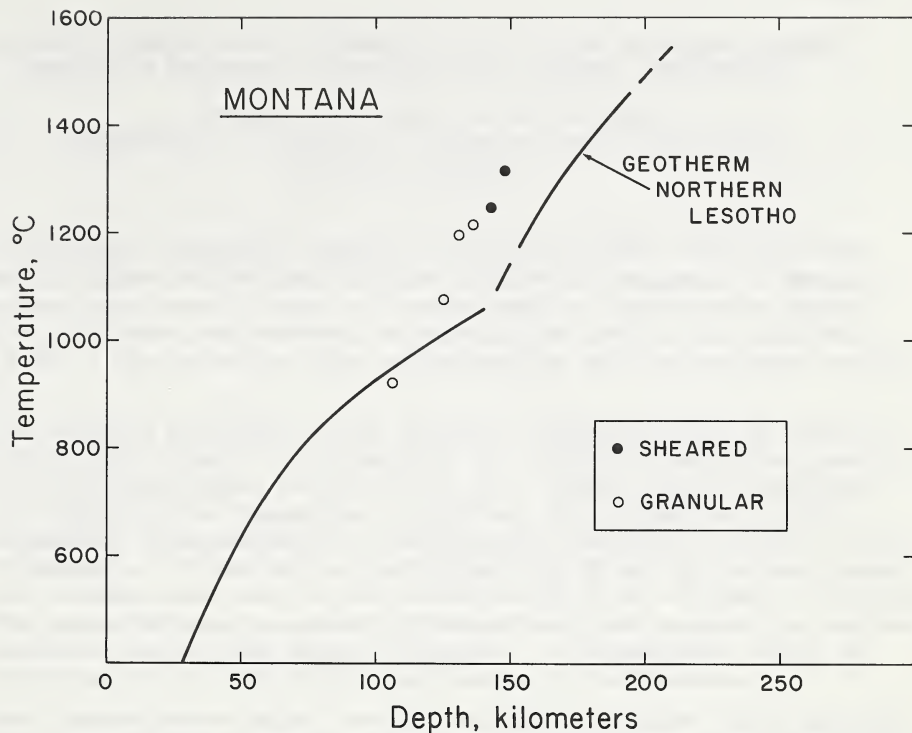


Fig. 1 Estimated temperatures and depths of equilibration of six garnet peridotite xenoliths from Montana, with the pyroxene-determined geotherm for northern Lesotho (Boyd and Nixon, 1973) for comparison.

References

Boyd, F. R., 1973, *Geochim. Cosmochim. Acta*, in press.

Boyd, F. R., and Nixon, P. H., 1973, this volume.

Hearn, B. C., Jr., 1968, *Science*, 159, 622-625.

Wood, B. J., and Banno, S., 1973, *Contr. Mineral. Petrol.*, in press.

ECLOGITE NODULES FROM KIMBERLITE PIPES OF THE COLORADO PLATEAU -
SAMPLES OF SUBDUCTED FRANCISCAN-TYPE OCEANIC LITHOSPHERE.

Herwart Helmstaedt and Ronald Doig
Department of Geological Sciences, McGill University
Montreal, Canada.

This paper interprets lawsonite-bearing eclogite xenoliths from kimberlite pipes on the East Colorado plateau as fragments of Mesozoic Franciscan-type oceanic crust which was subducted beneath the North American continent and returned to the earth's surface via the kimberlite pipes. The basis for this interpretation will be presented in four parts:

- 1) The eclogite xenoliths do not resemble eclogites normally found in kimberlites (Group A of Coleman et al., 1965) but eclogites associated with glaucophane schists (Group C). Their mineral assemblage is typical of low-temperature eclogites and consists of pyropic almandine, chloromelanitic clinopyroxene, phengite, rutile, \pm pyrite, \pm lawsonite. Distribution coefficients of Fe and Mg between garnet and clinopyroxene are low and overlap with those of Group C eclogites. The xenoliths have a notably differentiated bulk composition and are nepheline and in part acmite normative. A metamorphic origin is indicated by the rock fabric and igneous relict textures.
- 2) Most investigators agree that the eclogite xenoliths were derived from beneath the Precambrian gneisses of the Colorado plateau which consists of high-temperature mineral assemblages and yield absolute ages of about 1800 m.y. This implies that rocks with high-temperature mineral assemblages were overlying lawsonite-bearing eclogites at the time of the kimberlite intrusion, 30 m.y. ago. Such incompatibility in mineral assemblages coupled with the evidence for a metamorphic origin of the eclogites can only be explained by a tectonic emplacement of the eclogites beneath the Precambrian of the plateau. Our conclusion that this tectonic emplacement was unrelated to the Precambrian orogenic events in the Colorado Plateau basement but is a Phanerozoic event is based on the fact that lawsonite is unknown from rocks older than 1000 m.y. old and on Rb-Sr isotopic analyses of the xenoliths.
- 3) There are remarkable similarities between the eclogite xenoliths and Franciscan eclogites including mineral assemblages, physical and chemical properties of constituent minerals, textures, and bulk compositions. Initial $\text{Sr}^{87}/\text{Sr}^{86}$ ratios of the xenoliths are remarkably high and resemble those of Franciscan basalts.
- Franciscan eclogites have recently been interpreted as remnants of subducted oceanic crust. If lithologic correlation cannot prove a common source for the xenoliths and the Franciscan eclogites, the great similarity nevertheless permits the conclusion that the two rock groups had a similar mode of origin.
- 4) Plate tectonic models of the Western United States require the underflow of several thousand kilometers of oceanic crust beneath the North American continent during the Mesozoic and Cenozoic. Considering the most recent literature we show that an emplacement of

Franciscan eclogites beneath the Colorado Plateau is feasible and compatible with the presently available data. This process requires a horizontal translation of approximately 800-900 km between 80-75 m.y. (the approximate end of Franciscan metamorphism and the magmatism in the batholith belt) and 30 m.y. ago (the time of the kimberlite emplacement). The survival of lawsonite in some of the xenoliths places the limit of downward movement at about 50 km.

Our model invokes a combination of subduction and underplating resulting from the consumption of oceanic lithosphere in trenches along the western margin of North America and the active westward movement of North America following the opening of the Atlantic.

This interpretation of the origin of the eclogite xenoliths differs radically from one proposed recently by McGetchin and Silver (1972) in a crustal-upper mantle model for the Colorado plateau based on a suite of inclusions identical to that used in this study. If correct, the model presented here has important implications for the tectonic evolution of the southwestern United States. It would constitute direct proof that large scale underflow of oceanic crust and mantle beneath the North American continent has indeed taken place.

References

Coleman, R.G., D.E. Lee, L.B. Beatty, and W.W. Brannock, Eclogites and eclogites: Their differences and similarities, *Geol. Soc. Amer. Bull.*, 76, 483-508, 1965.

McGetchin, T.R. and L.T. Silver, A crustal-upper mantle model for the Colorado plateau based on observations of crystalline rock fragments in the Moses Rock Dike, *J. Geophys. Res.*, 77, 7022-7037, 1972.

CRYSTALLIZATION OF SOME NATURAL ECLOGITES AND GARNETIFEROUS ULTRABASIC ROCKS AT HIGH PRESSURE AND TEMPERATURE

S. Howells, C. Begg and M.J. O'Hara, Grant Institute of Geology,
University of Edinburgh.

Results of short (1-15 mins in presence of liquid; 15 mins - 1 hr in subsolidus) solid media equipment experiments in platinum capsules on dry charges of natural eclogite, garnet-olivine-pyroxenite and garnet-herzolite from kimberlite are presented and results for eclogite summarised in fig 1. Chemical analyses of the four samples investigated appear in O'Hara *et al* (1973 a,b).

O'Hara and Yoder (1967) reported solidus temperatures at 30 kb in two natural eclogites and several reconstituted mineral assemblages from kimberlite. Their samples 37079 and TAN 503 resemble sample 1044 (fig 1) in being soda-poor and relatively low M($=\text{Mg}/(\text{Mg}+\text{Fe})$). They yielded a solidus temperature of c. 1515°C at 30 kb, similar to that observed in the new experiments. Garnet was present to the solidus, and clinopyroxene was liquidus phase as for 1044, but the new sample displays a higher liquidus temperature.

In the new study, garnet does not appear as a liquidus phase below 40 kb but there is an immediately subsolidus field at 20 kb within which all garnet of the sample has dissolved in the pyroxene. O'Hara and Yoder (1967) also reported a high solidus temperature of c. 1535°C in a kyanite

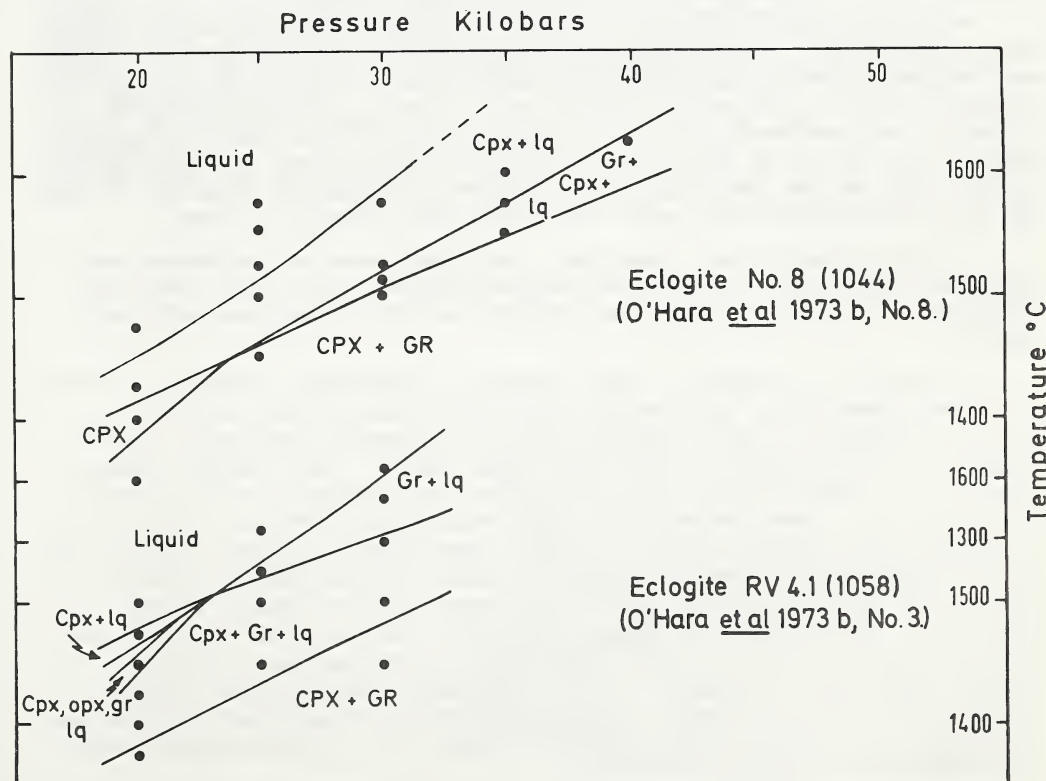


Fig 1

eclogite, TAN 501, at 30 kb, confirming solution of oriented kyanite intergrowth in the clinopyroxene prior to the onset of melting.

Eclogite 1058 from the Roberts Victor mine has high M, combined with high Na/Ca in the pyroxene; the solidus temperatures are lower than for 1044 (fig 1) despite the higher M value. The garnet does not dissolve entirely in the pyroxene under any investigated conditions, and garnet appears as the liquidus phase at pressures below 25 kb. Orthopyroxene appears near the liquidus at 20 kb but reacts out after garnet appears.

Olivine-garnet websterite 1031, suggested (O'Hara 1973; O'Hara *et al* 1973a) as a possible cumulate from the fractionation of two pyroxenes plus olivine from a liquid proceeding down the trend D-B (O'Hara 1970) apparently develops the predicted mineral assemblage in the solidus only at pressures less than 30 kb. The large liquidus-solidus interval of early orthopyroxene crystallization is consistent with the proposed cumulus origin

The very fertile looking garnet lherzolite 1032 (O'Hara *et al* 1973a, No. 1) which might represent a very high pressure primary magma, has been run at 45 kb. At this pressure olivine is still the liquidus phase, persisting to temperatures greater than 1750°C. Orthopyroxene is present from c. 1715°C and the solidus lies below 1650°C. If this rock is to represent a primary liquid in equilibrium with garnet harzburgite or garnet lherzolite, the pressure of its derivation must be greater than 45 kb.

No significance can yet be attached to the pressure at which garnet and clinopyroxene are cotectic at the liquidus of these eclogites; we can not be sure that the hand specimen samples fairly represent the garnet-pyroxene ratio of the source region, nor is there a secure basis for assuming that the pressure at which garnet and pyroxene appear simultaneously at the liquidus in this bulk composition bears any predictable relationship to the pressure or temperature at which the original eclogite may have accumulated from some more complicated magmatic system.

If the eclogites are cumulates, the temperature of the magmas must have been lower than the observed solidus temperatures, i.e. less than 1385±35°C at 20 kb, or less than 1480±30°C at 30 kb (perhaps very much lower).

Bimimetic eclogite is most unlikely to represent the total crystallization product of a high pressure liquid because of the special restricted nature of bulk compositions which develop bimimetic assemblages on solidification (O'Hara and Yoder 1967). The liquidus temperatures are c. 100°C higher than the solidus temperatures for these two eclogites, and these compositions would only have existed as dry liquids at temperatures higher than the solidus temperature of garnet-lherzolite. It is impossible for them to represent total crystallization products of dry primary magmas (olivine and orthopyroxene do not appear on the liquidus). The dry primary magmas would have formed by partial melting of garnet-lherzolite at lower temperatures than required to convert these eclogites to liquids. It is, therefore, unlikely that higher temperature eclogite liquid has been produced by fractional crystallization of a lower temperature parental liquid, (even taking into account the effects of pressure decrease).

Olivine does not appear in the liquidus/solidus interval of these or other investigated bimimetic eclogites. The partial melting of dry eclogite cannot, therefore, yield peridotite or garniferous peridotite

residua in the pressure range investigated (20-40 kb) and is even less likely to do so at higher pressures due to the contraction of the primary liquidus phase volume of olivine (O'Hara 1968). At lower pressures the eclogite mineralogy is not stable to the solidus, olivine may appear in the melting interval joined perhaps by orthopyroxene but spinel-lherzolites rather than garnet-lherzolites would be the residual peridotite assemblage developed (O'Hara *et al* 1971). While such peridotites might recrystallize to garnet-lherzolite on cooling in the sub-solidus, the simplest interpretation of the experimental data suggests that this could not have happened at less than 15 kb (O'Hara *et al* 1971). Models which call for bimimetic eclogite upper mantle to yield garnet-lherzolite residua in partial melting presuppose initial restriction of the process to c. 45-60 km depth, or selective sampling by diatremes of wall rocks from those depths (because peridotites greatly exceed eclogites in abundance).

These restrictions would not necessarily apply if eclogite were to undergo partial melting in a water-bearing or water-saturated system (e.g. Bravo and O'Hara 1973) but the liquids produced would then necessarily be much richer in silica than, for example, kimberlite fluids.

References

Bravo, M.S. and O'Hara, M.J. 1973, this volume.
O'Hara, M.J. 1970. Phys. Earth Planet. Int. 3, 236-245.
O'Hara, M.J. 1973, this volume. Subsolidus mineral assemblages etc.
O'Hara, M.J. *et al* 1971. Contrib. Min. Pet. 32, 48-68.
O'Hara, M.J. *et al* 1973a, this volume. Chemistry of ultramafic nodules from kimberlite etc.
O'Hara, M.J. *et al* 1973b, this volume. Chemistry of some eclogite nodules etc.
O'Hara, M.J. and Yoder, H.S.Jr. 1967. Scott. J. Geol. 3, 67-117.

KIMBERLITES AND RELATED ROCKS FROM THE NAMA PLATEAU OF SOUTH
WEST AFRICA

by A.J.A. JANSE formerly Research Institute for African Geology
The University of Leeds, England

presently Australian Selection Pty. Ltd.
Box R.1274, G.P.O. PERTH, W.A. 6001

The Gibeon kimberlite province contains at least 46 pipes and 16 dykes which show a variety of rock types transitional from basaltic massive kimberlites and kimberlitic breccias to carbonatitic dykes. It is located between 25° and 26° S.Lat. and 17°30' and 18°30' E. Long. Besides kimberlites, it also comprises the Gross Brukkaros carbonatite complex (Janse 1969), the Blue hills monticellite-bearing porphyritic peridotite (Janse 1971), the Hatzium dome (Heath & Toerien 1965) and several carbonatitic dykes. The writer believes that all these rocks are related and form part of the Gibeon kimberlite province.

Rocks of the Nama System (Precambrian to Lower Paleozoic) cover most of the country side. They are unconformably overlain to the east by the Dwyka Series (Carboniferous). The upper part of the Fish River Series (upper Nama), represented by maroon shales, and the lower part of the Dwyka - tillites and mudstones - underlie the Great Namal and Plain, which has an average altitude of 1000 metres. West of the plain lies the higher Schwarzrand Plateau (1500 to 1800 metres a.s.l.) formed by sandstones of the Fish River Series. The eastern border of the plain is outlined by the Urinanib escarpment (45 metres in height) where the Dwyka rocks disappear beneath the Kalahari Beds (middle Tertiary?)

Outcrops of fine-grained bluish-black amygdaloidal basalt and coarser ophitic dolerite which can be correlated with the Stormberg lavas in Lesotho (DuToit 1954) occur between the Dwyka rocks and the Kalahari Beds in areas north and east of Mariental, i.e. north of the Gibeon kimberlite province. Accidental inclusions of similar amygdaloidal basalt in the Gibeon kimberlites suggest the existence of a far more extensive basalt cover at the time of intrusion of the kimberlites.

The kimberlites are intruded into the Nama and Dwyka rocks, but are overlain by the Kalahari Beds. Eleven of the pipes are located in the Schwarzrand Plateau in Nama sandstones, one pipe outcrops from underneath the Kalahari Beds on the slopes of a small hill outlier in front of the Urinanib escarpment, while the rest of the pipes lie in the Great Namaland Plain in Nama shales and Dwyka tillites. It is probable that more kimberlites are hidden under the Kalahari Beds.

The kimberlites were found by aerial photo interpretation and stream sediment panning for the typical kimberlitic heavy minerals. The streams are dry for most of the year and the lack of soil formation and strong deflation in the prevailing hot dry climate favours the formation of eluvial heavy mineral concentrates on the kimberlite outcrops which consist generally of hardebank and less often of softer blue ground. Yellow ground is absent in this climate.

The typical outcrop in this area is flush with the surrounding surface or forms slight depressions bordered by steeply upturned host rocks which flatten out in a distance of less than 15 metres. Contact metamorphism is very slight. In some places the red colour of the Nama rocks has been changed into green for less than 10 metres, while angular fragments of country rock included in the kimberlite are bleached and bordered by baked edges which indicates a slight thermal reaction. The basalt inclusions in some kimberlites possess angular cavities filled with dark green earthy chlorite, translucent calcite and much

fibrous, nodular or massive matrolite, unlike the basalt at Mariental which contains only chlorite. This change in mineralogy suggests also a slight metasomatic reaction.

In some occurrences most of the outcrop is covered by a continuous mass of dolerite which suggest that these vents represent the feeding ducts to lavas of the Mariental type which have been eroded from this area. Blue ground or hardebank forms only a minor part of the outcrop at the side of the vent or occurs only in fractures in the dolerite. It appears that the kimberlite used the older feeding ducts as intrusion channels.

The size of the Gibeon kimberlites is rather small compared to kimberlites from other areas; it varies from a mere 10 metres to 900 metres for the Hanaus No. 1 pipe which is formed by the coalescence of two intrusion chimneys. Many of the occurrences are distinct fissure-pipes; i.e. 2 or 3 pipes elongated in outcrop on the same fissure or in a straight line not visibly connected on the surface. The strike of the fissures and the elongation of the pipes follows the directions of the fracture pattern in the Nama sandstones (N 55°E and N 125°E) or in the Nama shales (N 65°E to N 75°E and N 145°E to N 160°E.)

Most of the vents and fissures (dykes) contain basaltic hardebank; only 8 out of the 46 pipes show much phlogopite on the surface and these outcrops are mainly composed of blue ground. In hand specimen the basaltic hardebank consist mainly of numerous macroscopic crystals of forsterite, more or less replaced by serpentine, few crystals of phlogopite and occasional crystals of pyrope, ilmenite and chrome-diopside set in a fine-grained dark grey matrix. Aggregate crystals of pyrope, chrome-diopside, forsterite and ilmenite and intergrowths of pyrope/chrome-diopside and forsterite/ilmenite also occur. Diamonds have not been found. The replacement of forsterite by serpentine occurs in every stage of transition but appears to have progressed least in basaltic fissure hardebank. The forsterite of the more micaeous blue ground is completely replaced. Thin sections show the usual mineral assemblage, i.e. olivine, phlogopite, serpentine, calcite, ilmenite, perovskite, apatite and magnetite.

The Gibeon kimberlites contain numerous angular and rounded inclusions. The angular inclusions consist mainly of sedimentary country rock or basalt - dolerite fragments, while the rounded ones are derived from rocks from a deep seated origin as indicated by their mineralogy which comprises variable proportions of olivine, pyroxene, garnet, plagioclase and amphibole. Included amongst the various modular rock fragments are: garnet peridotite, garnet pyroxenite, hyperstene or pyroxene granulite, anorthosite and nodules containing garnet (almandine-pyrope), pyroxene, plagioclase, amphibole, quartz and kyanite which are believed to represent retrograde eclogites.

Several kinds of rocks with more carbonatitic affinities are found in the periphery of the Gibeon province. The Gross Brukkaros carbonatite complex with its central explosion vent filled with fine-grained, layered, comminuted country rocks, its satellite vents with coarse breccias set in a carbonate matrix and its radial beforsite dykes (Janse 1969) is located at the southern end. At the northern end, 110 km north of Brukkaros, lies the Hatzium dome, which is a Brukkaros type complex in an incipient stage (Janse 1969) while at the eastern side occurs an olivine melilitite (Mukorob dyke, Frankel 1956) and the carbonatitic Amalia dyke; similar dykes occur at the western side in the Ovas area. The Mukorob dyke contains peculiar black shiny ellipsoidal inclusions of olivine with concentric shells of ilmenite forming the outside of the inclusions which have also been found in the carbonate-rich Hatzium pipe. This pipe (at the northern end of the province) contains also an apatite-rich rock in its centre.

The major element analysis (see table) show the usual kimberlitic characteristics i.e. low SiO_2 and Al_2O_3 , high TiO_2 , Fe_2O_3 and MgO , but CaO is higher than the usual Nockold's average and corresponds better to Lebedev's average. The left hand side of the table presents the more "normal" kimberlite with $\text{K}_2\text{O} = \text{NaO}$, while towards the right hand side increasingly carbonatitic rocks are shown with $\text{Na}_2\text{O} > \text{K}_2\text{O}$ and high CO_2 and H_2O .

Trace element analyses show a pronounced decrease in heavy metals (Co, Cr, Ni, Ti and V) and a less distinct increase in light elements (La, Y and Zr) moving from the kimberlites to the carbonatitic rocks.

Garson (1962) and Dawson (1966) plotted rocks from different world-wide localities in a variation diagram to show the chemical gradation between kimberlites and carbonatites. Mitchell (1970) remarked that the deduced trends are artificial because the plotted rocks were not likely to be related in time and space. When the consanguineous rocks of the Gibeon province are plotted in such a diagram, there is a better suggestion of such a trend.

Milashev and Tabunov (1973) presented evidence from world-wide distribution patterns of kimberlites that the ideal kimberlite province is formed by concentric zones of a) most ultrabasic diamond-bearing kimberlites in the centre, b) pyrope-bearing ones next and c) increasingly alkaline rocks towards the periphery where pyrope disappears. The Gibeon kimberlite province corresponds to the pyrope zone of Milashev while the central diamond zone is lacking. It further corresponds to the non diamondiferous zone pattern in that the individual bodies are rather small while the largest one (Hanaus) is located in the centre.

References

Dawson, G.B., 1966, Mineralog. Soc. India, Int. Mineralog. Assoc. papers, pp 1-4.

Dutoit, A.L., 1954, Geology of South Africa.

Frankel, J.J., 1956, Royal Soc. Sth. Afr. Trans, v35, pp 115-123

Garson, M.S., 1962. Memoir Geol. Surv. Nyassaland, No. 2.

Heath, D.C. & Toerien, D.K., 1965, Sth. Afr. Survey Annals Z1, vi for 1962 pp 81-85

Janse, A.J.A., 1969, Geol. Soc. Am., Bull. V.83 pp 573-586.

Janse, A.J.A. 1971, Geol. Soc. Sth. Afr., Trans v 74, pp 45-55.

Lebedev, A.P., 1964, Geol. Journ. 4, pt.1, pp 87-105.

Milashev & Tabunov, 1973, Sovetsk. Geol., No.1, pp 48-65 (in Russian)

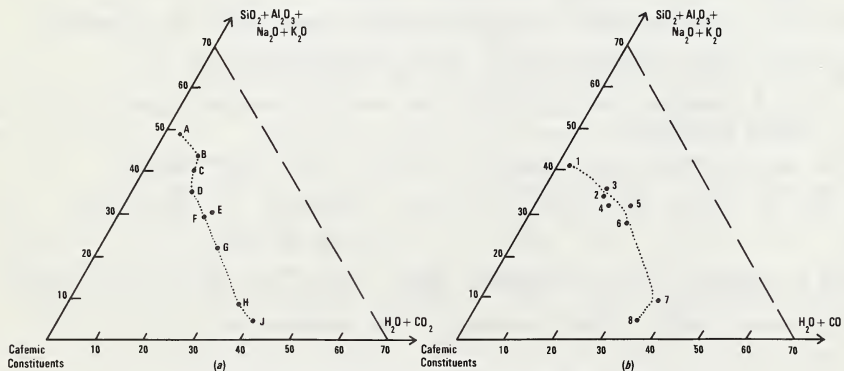
Mitchell, R.H., 1970, Journ. Geol., v 78, pp 686-704.

TABLE 1. Major element analyses of Gibeon kimberlites and related rocks

	1	2	3	4	5	6	7	8	9	10
SiO ₂	31.16	28.0	33.0	30.0	30.67	25.0	4.6	2.93	35.02	29.57
TiO ₂	3.44	2.28	1.15	1.77	0.82	1.17	0.49	0.69	1.22	1.31
Al ₂ O ₃	5.63	3.8	2.2	2.7	2.34	2.4	3.5	0.68	3.90	3.48
Fe ₂ O ₃	7.32	8.18	6.27	9.69	6.28	7.69	1.08	9.69	5.15	5.04
FeO	9.04	2.37	4.19	1.89	2.47	0.99	2.41	0.00	4.14	2.63
MnO	0.27	0.22	0.19	0.19	0.15	0.15	0.25	0.33	0.06	0.11
MgO	20.18	19.0	27.0	27.0	20.4	26.0	9.4	0.79	31.29	26.26
CaO	17.09	20.3	12.49	11.1	16.94	15.9	39.35	45.63	6.80	11.92
Na ₂ O	2.12	0.44	0.30	0.33	0.21	0.20	0.23	0.22	0.34	0.25
K ₂ O	1.52	2.71	0.70	0.30	0.18	0.41	0.07	0.03	1.05	0.54
H ₂ O+	1.45	5.53	7.61	13.79	9.51	9.60	1.57	1.49	7.43	--
P ₂ O ₅	0.28	n.d.	0.90	0.40	1.10	1.40	1.0	2.53	0.87	0.45
CO ₂	0.62	8.12	5.52	1.17	10.76	11.63	36.87	34.29	2.73	18.06*
Total	100.65		101.52		101.83		100.82		100.00	
		100.95		100.30		102.54		99.30		100.30
										18.06* = total loss on ignition

Specimen references for table 1 and the diagrams below:

- 1- Monticellite peridotite, Brukkaros complex
- 2- Calcite-phlogopite rock, Brukkaros complex
- 3- Surface hardebank, Gibeon Reserve no 2 pipe
- 4- Surface blueground, Hanaus no 1 pipe
- 5- Surface hardebank, Amalia no 1 pipe
- 6- Surface hardebank, Hatzium pipe
- 7- Carbonatitic dyke, Amalia
- 8- Beforsite dyke, Brukkaros complex
- 9- Average composition of basaltic kimberlite, 10 analyses Nockolds
- 10- Average vein kimberlite, 210 analyses- Lebedev 1964.



Diagrams illustrating the petrogenetic relationship of kimberlitic and carbonatitic rocks. (a) After Garson; (b) This Paper.

PETROLOGY AND GEOCHEMISTRY OF ULTRAMAFIC XENOLITHS FROM THE JAGERSFONTEIN MINE, O.F.S., SOUTH AFRICA. Judith L. Johnston, Dept. of Geology, University of California, Davis, California, U.S.A.

A suite of seventy-seven ultramafic xenoliths from the Jagersfontein Mine has been studied and divided into two distinct groups, the granular harzburgites and the sheared xenoliths, on the basis of mineralogy, textural differences and mineral chemistry.

1) The harzburgite group consists of rocks in which olivine and enstatite are the principal minerals; sixty-six rocks fall into this category. These rocks have a granular texture and contain large subhedral grains of olivine and enstatite. Small grains of anhedral diopside, garnet and chrome-spinel occur between the olivine and enstatite grains. These minor phases, plus amphibole, which may be either a major or a minor constituent, serve to further subdivide this group into spinel, garnet and amphibole harzburgites.

Diopside in the harzburgites often occurs in only trace amounts and usually comprises < 5.0% of the rock. In many cases it appears to have exsolved from enstatite. Garnet has also exsolved from enstatite although in some samples-garnet harzburgites containing 6.0% garnet-it may represent a primary phase. Spinel occurs in two different forms; as small (< 2mm.) euhedral crystals or as the oxide phase in oxide-silicate symplektites. The euhedral spinels are thought to be primary and the symplektites the result of subsolidus reactions. All of the symplektites contain chrome-spinel as the oxide phase; the silicate phase is usually diopside, although enstatite-spinel, amphibole-spinel and garnet-spinel symplektites are also present.

Amphibole occurs as a minor phase (< 2.0%) in seven harzburgite samples; in three other harzburgites it is a major component (15.0 to 27.3%). It occurs as large single crystals poikilitically enclosing olivine and enstatite. In these amphibole harzburgites garnet is present as small round grains embedded in the amphibole.

2) The sheared xenoliths contain olivine, enstatite, diopside and garnet except for one sample which is a pure dunite. Spinel and amphibole are absent, as are symplektites. These samples are not granular as were the harzburgites, but have been sheared. The degree of shearing varies from sample to sample: some are definitely foliated while others show granulation with no obvious foliation. Olivine has been most completely granulated and have been fractured into a mosaic of small grains. Enstatite has been elongated parallel to the foliation (if the rock is obviously foliated) and is partially granulated. Diopside is anhedral or subrounded, with very little granulation. It does not appear to be oriented with respect to foliation. Garnet occurs as large round grains with kelyphitic rims; although the round shapes may be due to shearing stress, no pressure shadows or granulation was observed.

Electron microprobe analyses were made of the constituent phases from all samples except when adequate separates of minor minerals could not be obtained. Olivines were analyzed for Mg, Al, Si, Ca, Ti, Cr, Mn, Fe and Ni. Enstatites, diopside, garnets and amphiboles were analyzed for Na, Mg, Al, Si, K, Ca, Ti, Cr, Mn and Fe. Spinel were analyzed for Mg, Al, Ti, Cr, Mn and Fe.

The forsterite content of olivines was found to be an accurate means of distinguishing between the two groups. Olivines from harzburgites had Fo-Fa ratios of Fo95.3 to Fo91.8 while the olivines from sheared xenoliths ranged from Fo91.6 to Fo86.4. In addition the

olivines from sheared xenoliths have higher Al_2O_3 contents than do those from harzburgites.

Enstatites from sheared xenoliths have higher En-Fs ratios than enstatites from harzburgites. When enstatite data, in terms of mole per cent, are plotted onto the pyroxene quadrilateral the harzburgite enstatites fall on the enstatite-ferrosilite join, except for eight samples which contain a high proportion of euhedral spinels. Enstatites from these spinel harzburgites are more calcium-rich, and may be interpreted as having equilibrated at higher temperatures than other harzburgite enstatites. Enstatites from sheared xenoliths are richer in both calcium and iron than enstatites from harzburgites, and are also assumed to represent higher equilibration temperatures.

Diopside chemistry, when displayed on the pyroxene quadrilateral also shows the same separation of harzburgites and sheared xenoliths: the diopsides from sheared xenoliths are more magnesian and therefore represent a higher temperature of equilibration than the diopsides from harzburgites. Diopsides from symplektites are the most calcic, falling on the diopside-hedenbergite join, and show the lowest equilibration temperatures of the entire suite. This is to be expected, as these symplektites represent subsolidus reactions.

Garnets, when considered in terms of pyrope, almandine and grossular end members, are very pyrope-rich. Pyrope variation is greater in the harzburgite group, from $Py_{87.5}$ to $Py_{64.5}$ although most are $< Py_{75.0}$. Garnets from sheared xenoliths tend to show little pyrope variation-all are between Py_{75} and Py_{78} . In general, Cr_2O_3 , TiO_2 , K_2O and Na_2O are higher in garnets from sheared xenoliths than in garnets from harzburgites.

Both symplektite and euhedral spinels are closest to magnesio-chromite ($MgCrO_4$) in composition, with some substitution of Fe^{+2} for Mg and of Al for Cr. The symplektite spinels are more aluminous, and the euhedral spinels are more chrome-rich.

The amphiboles are all varieties of hornblende. If the calcic amphibole classification scheme of Leake (1969) is applied to these amphiboles, two types are recognized: 1) amphiboles which occur as minor constituents are magnesiohornblendes 2) those which are found in amphibole harzburgites are edenites.

An attempt was made to determine pressures and temperatures of equilibration for this suite of xenoliths. Temperatures were estimated for rocks with coexisting enstatite and diopside using the 30 kilobar diopside solvus from the join $Mg_2Si_2O_6$ - $CaMgSi_2O_6$ (Davis and Boyd, 1966). These temperatures, together with Al_2O_3 contents of enstatites, were used to determine pressures of equilibration using MacGregor's isopleths in the system MgO - Al_2O_3 - SiO_2 (1973). The resulting plot (Fig.1) shows that the granular harzburgites and the sheared xenoliths were equilibrated under very different conditions of temperature and pressure: the harzburgites at $\approx 900^{\circ}C$ and 36 to 52 kilobars, and the sheared xenoliths at 1150 to 1280°C and ≈ 60 kilobars. These differences, together with the mineralogical and textural differences already noted, would suggest different processes to account for the evolution, and perhaps genesis of these two groups.

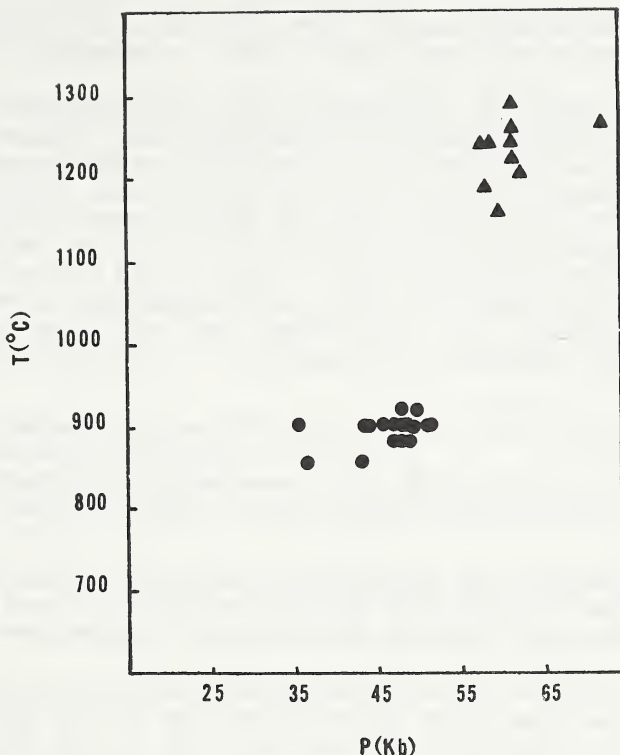


Figure 1. Pressure-temperature plot of Jagersfontein xenoliths. Triangles are sheared xenoliths, circles are granular harzburgites.

REFERENCES

- 1) Davis, B.T.C, and F.R. Boyd, 1966. *Jour. Geophy. Res.* 71, 3567-3576.
- 2) Leake, Bernard E., 1969. *Geol. Soc. America Spec. Paper* 98, 210p.
- 3) MacGregor, I.D., 1973. *Am. Min.* (in press)

THE SIGNIFICANCE OF THE INTER-ELEMENT RELATIONSHIP OF SOME REFRACtORY ELEMENTS IN SOUTH AFRICAN KIMBERLITES

E.J.D. KABLE¹, H.W. FESQ¹ and J.J. GURNEY²

¹ NIM-WITS A.A.R.G., N.P.R.U., Univ. of the Witwatersrand, Johannesburg.

² Dept. of Geochemistry, Univ. of Cape Town, Rondebosch.

The interpretation of the geochemistry of kimberlites is complicated by country rock contamination, as exemplified by the variation of major element chemistry (1), the loss of volatiles on emplacement and the mobility of some elements during secondary processes (2). For these reasons those elements which are least likely to be affected, viz. the refractories: Ti, Sc, Y, Zr, Hf, Nb and Ta, were analyzed in 59 basaltic and micaceous kimberlites. These kimberlites represent different ages, modes of emplacement (pipe, blow, fissure), various degrees of weathering and country rock contamination (e.g. quartzite, gabbro, shale sedimentary carbonate). The kimberlite occurrences investigated include:

- (a) the Premier pipe near Pretoria which is the only known kimberlite of Precambrian age (3),
- (b) Koffyfontein and Ebenhaezer (near Koffyfontein, O.F.S.) and
- (c) the kimberlite dykes on the farm Bellsbank (N.N.W. of Barkly West, C.P.)

The kimberlites from Premier, Koffyfontein and Ebenhaezer have been described as basaltic (4); on Bellsbank both basaltic and micaceous kimberlites were emplaced along existing parallel fissures (5).

X-ray fluorescence spectrography (X.R.F.) was used for the determination of Ti, Zr, Nb and Y while Sc, Hf and Ta were determined by instrumental neutron activation analysis (I.N.A.A.). Full details of the methods and standards used have been described elsewhere (6, 7, 8). Analytical precision for Ti, Sc, Y, Zr, Nb and Ta is better than 3%; Hf has an upper limit of 10%.

Average values for element concentrations and some inter-element relationships are presented in Table 1, together with data for Mullersvlei, (near Theunissen, O.F.S.) and Du Toitspan, Kimberley, C.P.

In general, the basaltic kimberlites have lower concentrations of Sc, Y, Zr, Hf and Nb than the micaceous kimberlites. In the particular case of Bellsbank, all elements, including Ti and Ta have lower concentrations in the basaltic kimberlite (Water Fissure). The Premier kimberlites are characterized by high Ti contents which are at least a factor of two greater than the kimberlites of the Koffyfontein group and Bellsbank. These differences are also reflected by the Ti/Zr, Ti/Nb, Nb/Ta and Hf/Ta ratios.

The Bellsbank fissures provide an ideal opportunity for studying the relationship between the basaltic and micaceous kimberlites. From the inter-element relationships (Fig. 1a) it appears that the basaltic Water Fissure is genetically related to the micaceous Bobbejaan and Main Fissures which represent more "differentiated" kimberlites. Further evidence supporting this interpretation is provided by the

TABLE 1: ELEMENT CONCENTRATIONS* AND INTER-ELEMENT RELATIONSHIPS
IN SELECTED SOUTH AFRICAN KIMBERLITES

	Ti	Sc	Y	Zr	Hf	Nb	Ta	Ti/Zr	Ti/Np	Zr/Nb	Hf/Ta	Zr/Hf	Nb/Ta
PREMIER													
Brown Kimberlite	(7) ⁺	10210	11.4	10	105	2.6	74	12.1	97	137	1.4	0.25	4.1
Grey Kimberlite	(4)	10540	8.8	8	118	2.9	54	6.5	90	194	2.2	0.44	41
Black Kimberlite	(4)	12610	9.5	5	96	2.0	71	8.0	133	178	1.4	0.25	49
KOFFYFONTEIN GROUP													
KOFFYFONTEIN	(10)	5420	10.6	13	118	2.7	50	3.1	46	111	2.4	0.88	43
EBENHAEZER East	(5)	4980	9.9	15	141	3.1	82	4.2	35	61	1.7	0.73	46
West	(5)	4880	9.4	16	130	3.1	43	2.6	39	114	3.0	1.2	42
BELLSBANK													
WATER FISSURE	(10)	2980	8.8	9	140	3.0	41	1.9	22	72	3.4	1.6	48
BOBBEJAAN FISSURE													
Bobbejaan Mine	(2)	4020	19.4	18	267	6.1	173	9.3	15	23	1.5	0.66	44
Dancarl Mine	(3)	3540	16.6	20	263	6.1	158	7.8	14	22	1.7	0.78	43
Holiday & de Bruyn Mine	(1)	4680	23.4	19	344	7.7	201	11.3	14	23	1.7	0.68	45
MAIN FISSURE													
De Bruyn Mine	(3)	5380	23.4	17	343	7.7	188	9.6	16	29	1.8	0.80	45
Martin & de Bruyn Mine	(1)	3780	15.6	257	272	6.7	136	8.4	14	28	2.0	0.80	41
Blows along Main Fissure	(3)	4440	17.7	18	284	6.0	132	7.3	16	35	2.2	0.83	47
MULLERSVLEI	(1)	7010	23.4	18	304	6.8	105	6.6	23	67	2.9	1.0	45
DU TOTSPAN	(1)	10	218		101						2.2		

* Element concentrations expressed as ppm

+ Number of samples analyzed

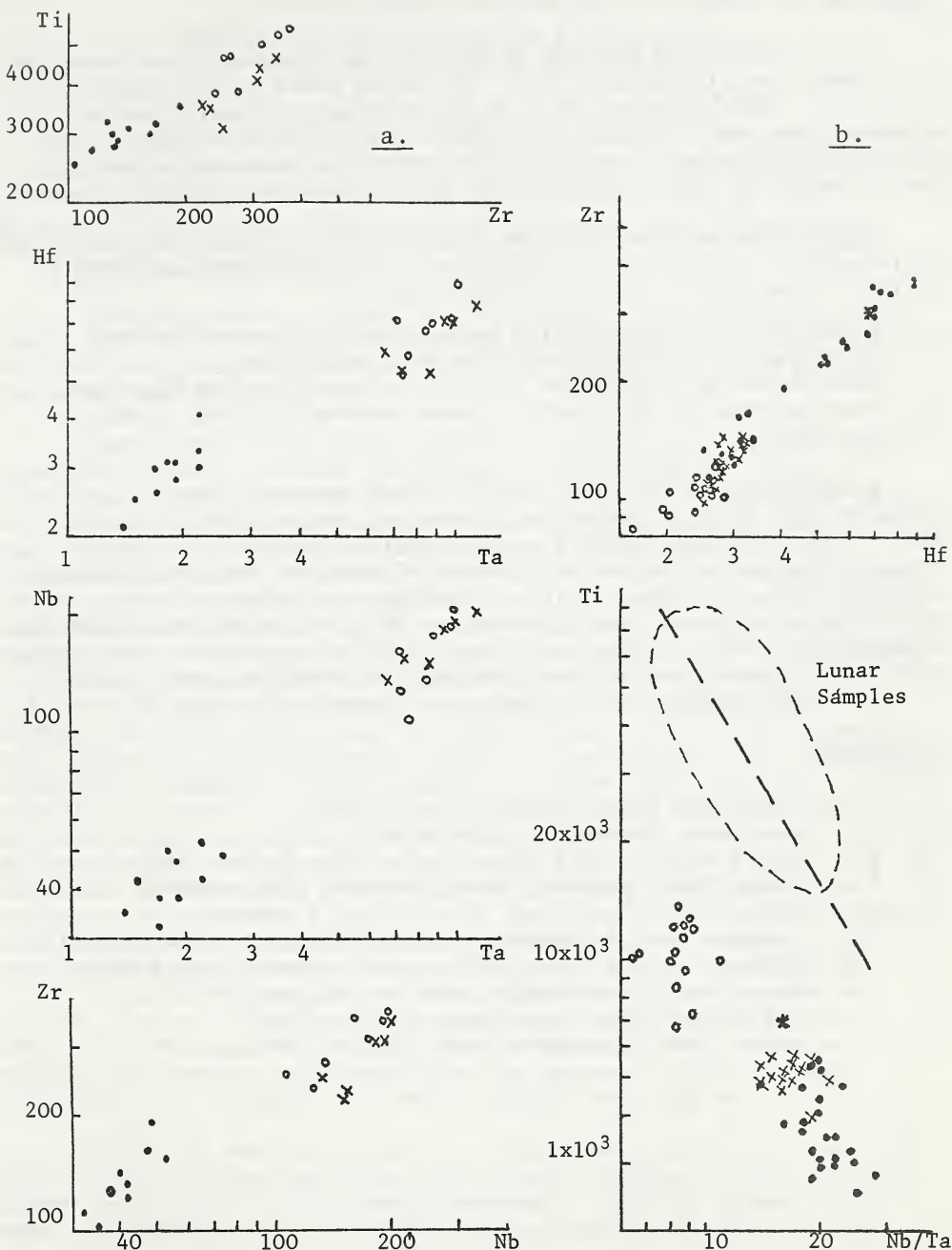


FIGURE 1: Some inter-element relationships in S.A. Kimberlites

(a) Bellsbank : . Water
 Fissures x Bobbejaan
 o Main

Concentrations expressed as ppm

(b) Bellsbank .
 Koffyfontein x
 Mullersvlei *
 Premier o

light REE enrichments in the micaceous kimberlites (1).

It is significant that the Zr/Hf ratio is reasonably consistent for all kimberlites studied here (N.B. Hf values based on 14.0 ppm GSP-1) (Fig. 1b). This suggests that, as Zr and Hf are strongly coherent elements, the source regions from which these kimberlites were originally derived have been constant (with respect to these two elements) over a period of time extending from the Pre-cambrian to the Cretaceous.

High Ti contents in the Premier kimberlites are associated with low Nb/Ta ratios. In the case of Koffyfontein and Bellsbank the inverse applies. From this it may be inferred that

- (a) kimberlites are derived from upper mantle regions which have undergone different degrees of partial melting or
- (b) kimberlites have undergone different crystallization histories.

Attention is drawn to the similar trends observed in lunar samples (Fig. 1b) (9).

Although the Zr/Nb ratio exhibits fractionation, there is a remarkable similarity in the ratio between the various kimberlites (1.3 - 3.4). Lesotho kimberlites have similar ratios (10). This suggests that Zr and Nb are not grossly affected by early fractional crystallization processes. The crystallization/accumulation of perovskite in differentiated kimberlites (e.g. Bellsbank, Main/Bobbejaan Fissures) may result in the enrichment of Nb relative to Zr. The range of Zr/Nb in kimberlites is less than that recorded for garnet lherzolites from Bultfontein (2 - 6) and oceanic basalts (4 - 40) (6).

REFERENCES:

- (1) H.W. Fesq et al, Int. Kimberlite Conf. (1973)
- (2) G.W. Berg, Amer. Mineral 53, 1336 (1968)
- (3) H.L. Allsopp et al, Earth Planet. Sci. Lett. 3, 161 (1967)
- (4) P.A. Wagner, The Diamond Fields of Southern Africa (1971)
- (5) J.L. Bosch, Trans. Geol. Soc. S.A. 74(2), 75 (1971)
- (6) E.J.D. Kable et al, in Marion and Prince Edward Islands, 78(1971)
- (7) J.P. Willis et al, in Proc. 2nd Lunar Sci. Conf. 2, 1123 (1971)
- (8) H.W. Fesq et al, J. Radioanal. Chem. (to be publ.)
- (9) Proc. 2nd and 3rd Lunar Sci. Conf. (1971, 1972)
- (10) J.B. Dawson, Bull. Geol. Soc. Amer. 73, 545 (1962).

URANIUM PARTITIONING IN KIMBERLITES
AND THEIR DEEP-SEATED INCLUSIONS.

J. D. KLEEMAN* AND J. F. LOVERING**

* Department of Geology, University of New England, Armidale, N.S.W., Australia.

** School of Geology, University of Melbourne, Parkville, Victoria, Australia.

Fission track "Lexan" print studies of kimberlites and their associated suites of deep-seated inclusions are reported from localities in South Africa, Tanzania, Sierre Leone, Kentucky and Siberia.

Kimberlites have been shown previously by Morgan and Lovering (1971) to have relatively high uranium (1.05 - 3.97 ppm U) and thorium (4.3 - 25.3 ppm Th) abundances with Th/U ratios averaging 4.8 and ranging from 4.1 to 7.1. The "primary" kimberlite phases are highly depleted in uranium (garnet < 3 ppbU, olivine < 0.2 ppbU, orthopyroxene < 0.5 ppbU, ilmenite < 1 ppbU). On the basis of a Ucpx/Uopx partition coefficient of ~ 7 , and Ucpx/ULiquid partition coefficient of ~ 0.0012 , then the U content of orthopyroxene in kimberlites is characteristic of equilibrium with a silicate liquid containing < 3 ppmU. This is a value well within the observed range of U abundances in kimberlites. The typically fine-grained matrix of kimberlite, usually consisting largely of hydrated silicates and calcite, is relatively enriched in uranium (0.2 to 1 ppm) although the specifically "secondary" kimberlite phases, such as phlogopite (< 10 ppb U) and calcite (< 10 ppb U), are not enriched in uranium. The highest uranium abundances are observed in secondary perovskite (> 23 ppm U) which commonly partly replaces ilmenite in most kimberlites studied. The only kimberlite studied which did not contain perovskite (i.e. from Siberia) also showed similarly U-enrichments around altered ilmenite grains. Apparently uranium is mobilised during late-stage "hydrothermal" activity in the kimberlite matrix and deposited in phases formed at the interface of "primary" ilmenite grains during this activity.

Granulite and amphibolite inclusions, possibly derived from lower crustal sources, have been studied from kimberlites from South Africa and Kentucky. In the granulites, some uranium is located along grain boundaries and probably represents addition of U-rich hydrothermal fluids from the kimberlite matrix. However the major contributions are found in minor "primary" phases such as zircon (< 20 ppm and > 200 ppm U), rutile (18 ppm, 50 ppm U) and apatite (1.8 - 2.5 ppm U) while the major primary phases are relatively depleted in uranium. The amphibolites show some uranium along grain boundaries but the major contribution of uranium is located in the amphibole ($\sim 0.32 - 0.43$ ppm) and in accessory

apatites (15 - 52 ppm and 37 - 100 ppm).

The other inclusions (e.g. eclogites, garnet peridotites etc.) are of possible upper mantle origin. The primary phase in the eclogites are depleted in uranium with garnet ranging from 1 - 3 ppb U and clinopyroxene from 0.8 - 82. ppb U and most of the uranium reported in the rock (see Morgan and Lovering 1971) is found along grain boundary alteration zones and has apparently been added from the kimberlite matrix. The primary clinopyroxenes have U contents consistent with crystallization from magmas ranging in U content from 0.6 to 6.8 ppm U. This range is broad and could be consistent with equilibration with basic magmas or with kimberlites.

In the garnet peridotite inclusion the garnet contains moderate U abundances (2 - 140 ppb), clinopyroxene from 7 to 30 ppb, orthopyroxenes from <1 to 7.2 ppb and olivine < 0.3 ppb. There are no uranium-enriched phases in these rocks and most of the uranium is located along grain boundaries as in the eclogite inclusions. The clinopyroxenes have U contents consistent with equilibration with magmas containing 5.8 ppm to 25 ppm U and generally well outside the range of either basaltic or kimberlitic types. A similar (though even more extreme) anomaly was reported by Kleeman et al. (1968) for some primary clinopyroxenes in lherzolite nodules from Victorian alkali basalt. If current estimates of Ucpx/ULiquid distribution coefficients are correct, then many of these ultramafic inclusions must have formed in association with a special vapour or fluid phase relatively enriched in uranium and have not subsequently been subject to removal of basaltic liquids by partial melting processes.

KIMBERLITIC ZIRCONS

Peter Kresten

Department of Mineralogy, University of Stockholm, Sweden

Kimberlitic zircons usually are rounded or subrounded. Euhedral forms are rare. They vary in colour from colourless to yellow and brown. Cleavage is often perfectly developed (basal and/or prismatic), in contrast to zircons from other sources.

Generally, the zircons are covered with a whitish coating, which may be chalky, crystalline (with or without spots or lines of opaque material) or vitreous in appearance. Chemical analyses confirms the material to be zirconium with minor amounts of hafnium (fig. 1). X-ray diffraction reveals the presence of both monoclinic (γ) and tetragonal (β) zirconia, in variable proportions. Therefore, the coating does not consist of baddeleyite only (Nixon et al., 1963), but is similar to the zirconia obtained artificially by decomposition of zirconium compounds (nitrate, oxychloride) at temperatures between 500 and 800°C (Gmelin, 1958). The coating most likely formed by reaction of zircon with magnesia (brucite) or carbonate (calcite) at moderate temperatures. Reactions at temperatures above 1150°C would result in the formation of baddeleyite (via β -ZrO₂) only. No major fractionation between Zr and Hf was connected with the process of formation (fig. 1).

The various types of coating show similar mineralogical compositions, and may merely reflect variable pressures of formation. The chalky coating must have been formed by late reactions within the kimberlite *in situ*, due to its extremely low resistance against abrasive action. The vitreous variety shows evidence of being pre-intrusively formed, and is either partially abraded or covered by a crystalline coating. Therefore it seems likely that the rounded forms of kimberlite zircons cannot always be explained as being secondary, i.e., due to abrasion. Instead, they might represent the primary high-pressure morphology of zircon.

Twenty-seven zircons from ten different kimberlites (mainly Lesotho) have been analyzed for Zr, Hf and, in part, Si. X-ray spectrometry and electron microprobe techniques were used. The zircons are rather pure, the sum of oxides being about 98 weight-%. The Zr/Hf-ratio varies between 17 and 81 (fig. 1, Hf-poorest sample not shown), with an average of 36. This value is lower than the one obtained by Nekrasova et al. (1970) for Yakutian kimberlitic zircons (46). Their value is greatly influenced by one locality (Mir pipe: 10 of total 13 samples) and cannot be considered to be representative. The average of all data available (Nekrasova et al., 1970; Schutte, 1966, and this paper) is Zr/Hf = 41 for all analyzed samples (N=42), or Zr/Hf = 40, for all individual kimberlites (N=15).

The average Zr/Hf-ratio of kimberlitic zircons is therefore similar to the Zr/Hf-ratio of zircons from granitic rocks (42; Kresten, 1970), as well as ultrabasic alkaline intrusions (43; Kukharenko et al., 1960). Present data suggest that each kimberlite pipe possesses a specific Zr/Hf-ratio for its zircons, see table 1. Main and satellite intrusions also show differences in this respect. For

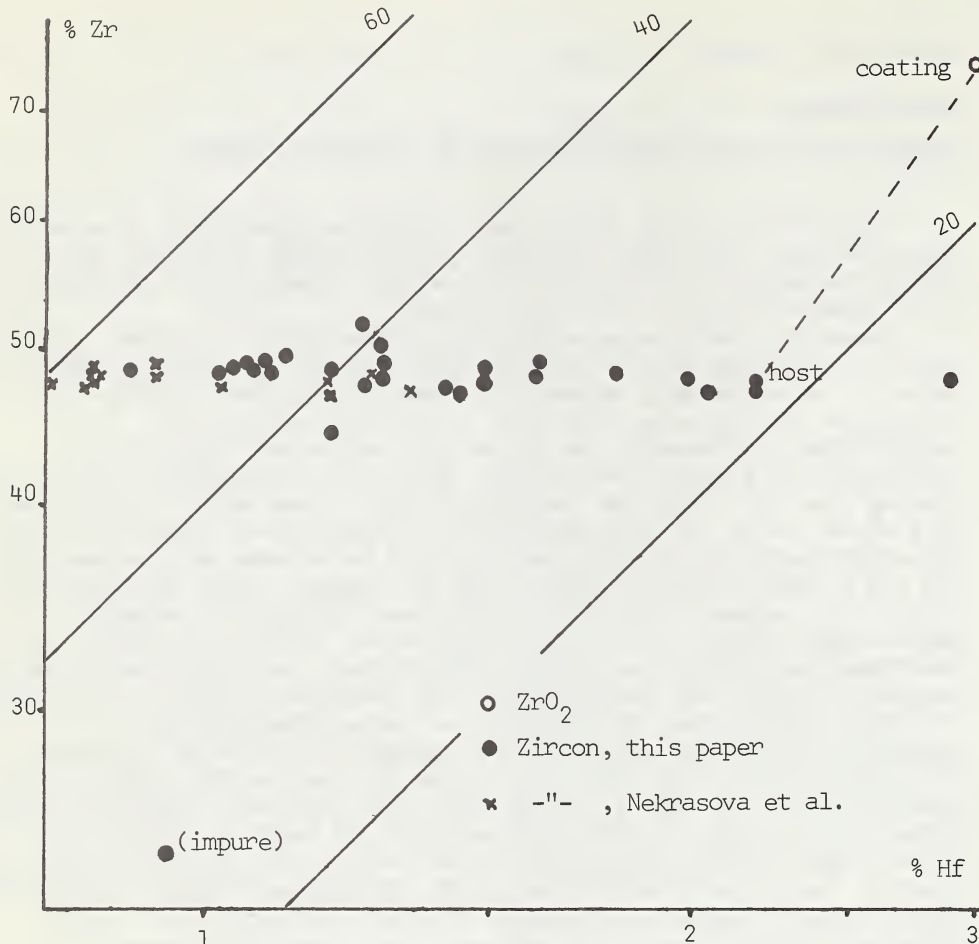


Figure 1

Table 1. Zr/Hf-ratios of zircons from various kimberlites

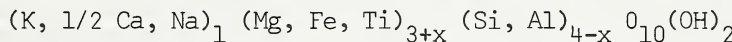
Kimberlite	Aver.	Range	N=
Mir, Yakutia	50	32-59	10 (Nekrasova et al.)
Letseng-la-terai, Lesotho	48	42-54	2
Nzega, Tanzania	46	45-57	5
Dyke no 170, Lesotho	39	22-81	5
Mothae, Lesotho	35	31-40	5
Kao main pipe, Lesotho	21	17-24	4

example, zircons from the Kao main pipe have an average Zr/Hf-ratio of 21 (table 1), while one zircon from the satellite pipe showed Zr/Hf = 44. Among the zircons from one pipe, only limited variation in the Zr/Hf-ratio is observed. Five zircons from Nzega gave Zr/Hf = 45, 46, 46, 47, 47; five samples from Mothae 31, 33, 34, 38, 40.

Zircons from a kimberlite dyke (No 170, Butha Buthe, Lesotho) showed much larger variation in the Zr/Hf-ratio: 22, 30, 32, 33, 81. Even if the majority fall within the range 30-33, the probability of finding extremely high or low values seems greater for dykes than for pipes. This may be ascribed to the incorporation of wall-rock material in comparatively larger amounts in the dykes.

Five zircons have been analyzed for uranium, using the delayed neutron technique. The average uranium content is 10,9 ppm U, range 8,0 - 16,8 ppm, well in agreement with the values obtained by Ahrens et al. (1967).

Inclusions are rare. Of some 150 zircons investigated, two showed phlogopitic inclusions, one an inclusion of ilmenite, and one a colourless diamond. The phlogopitic inclusions are green, fine-grained spherical particles, measuring 1-2 mm in diameter. They consist of phlogopite with a little opaque material (ilmenite ?), and an outside shell of zirconia. The chemical analyses of the phlogopites (table 2, nos 1-4) show a deficiency of cations in the tetrahedral sheets, and a surplus of cations in the octahedral sheets. The low contents of larger cations (K, Ca) suggest the presence of small amounts of sodium. The formula of the phlogopite found as inclusions in zircons is:



The proportion Si:Al is about 3,5. This is somewhat higher than the theoretical value (3) for phlogopite. It seems unlikely that the deficiency of cations in the tetrahedral sheets is balanced by the substitution of Fe³⁺ and Ti⁴⁺ for Al³⁺ and Si⁴⁺.

It is suggested that vacant positions in the tetrahedral sheets are balanced by the surplus of cations in the octahedral sheets (probably accompanied by a decrease in the molar volume). In the case of the Kao sample, the phlogopite inclusion was completely surrounded by zircon, which might indicate a possible upper mantle origin of the phlogopite.

The ilmenite included in zircon from Kao mine (table 2, no 5) shows 70,2 mole-% ilmenite and 29,8 mole-% geikielite. This is comparable to kimberlitic ilmenites in general (Frantsesson, 1969; Frick, 1970), except for the apparently low content of trivalent iron. The analysis favours the assumption that essentially all iron is in the divalent state.

Table 2. Inclusions in kimberlitic zircons

	1	2	3	4	5
SiO ₂	40,21	39,38	39,72	36,97	-
TiO ₂	0,94	2,32	2,62	0,03	53,55
Al ₂ O ₃	8,80	9,85	10,13	10,98	1,58
Cr ₂ O ₃	0,02	0,02	0,05	-	0,57
FeO	8,36	8,68	7,42	6,61	36,63
MnO	0,05	0,04	0,05	-	0,20
NiO	0,05	0,06	0,08	0,00	0,12
MgO	26,85	26,72	25,68	26,16	8,77
CaO	0,14	0,14	0,13	0,66	-
K ₂ O	10,48	9,85	9,97	-	-
Total	95,90	97,06	95,85	81,41	101,42

Dash indicates: not determined. Total iron expressed as FeO.

Number of ions (24 (0,OH) for 1-4, 6 (0) for 5):

Si	5,83	5,56	5,70	-
Al	1,50	1,63	1,71	0,09
Ti	0,10	0,24	0,28	1,89
Cr				0,02
Fe	1,02	6,91	6,89	6,67
Mg	5,79	5,62	5,50	1,44
Ca	0,02	0,02	0,02	0,61
K	1,94	1,80	1,83	2,05

1-3: Phlogopite, granular inclusions in zircon from Monastery mine.

4: Phlogopite, fine-grained greenish inclusion in zircon, Kao mine.

5: Ilmenite inclusion in zircon, Kao mine.

References

Ahrens, L.H., Cherry, R.D., and Erlank, A.J., 1967. *Geochim. Cosmochim. Acta* 31, 2379-2387.

Frantsesson, E.V., 1969. The petrology of kimberlites. "Nedra", Moscow.

Frick, G., 1970. D. Sc. Thesis, University of Pretoria.

Gmelins Handb. d. anorg. Chemie, 1958. "Zirkonium". Verlag Chemie, Weinheim/Bergstr., W. Germany.

Kresten, P., 1970. *Geol. Fören. Förh.* 92, 414-418.

Kukharenko, A.A., Vainshtein, E.E., and Shevaleevskii, I. D., 1960. *Geokhimiya (Geochemistry)* 1960/7.

Nekrasova, R.A., and Rozhdestvenskaya, I.V., 1970. *Geochem. Intern.* 7, 1970.

Schutte, C.E.G., 1966. *South Afr. Geol. Surv., Bull.* No 46.

THE CHEMISTRY AND MINERALOGY OF TWO ECLOGITES
FROM THE ROBERTS VICTOR PIPE, ORANGE FREE STATE, SOUTH AFRICA

By

M.A. Lappin, Department of Geology and Mineralogy,
Marischal College, University of Aberdeen,
Aberdeen, Scotland.

J.B. Dawson, Department of Geology,
University of St. Andrews,
St. Andrews, Scotland.

Microprobe and bulk chemical analyses are presented for two eclogites. Both contain relatively Ca-rich garnets (25-45% grossular) and Na-rich (approximately 50% jadeite), tschermakite poor (less than 1% Al⁴⁺) clinopyroxenes which have however about 30% excess Al⁶⁺.

The first eclogite (6913) is foliated and layered. Garnet-clinopyroxene pairs, identified by numbers in Figs. 1 and 2, were analysed across the layering. The layers consist of garnet-clinopyroxene (analyses 1-5), a 10 mm thick layer of garnet-clinopyroxene-(kyanite) (analyses 6-7) in which almost all garnet forms overgrowths on kyanite in a fashion similar to the diablastic intergrowths of Sobolev et al. (1968), and garnet-clinopyroxene-kyanite. In the latter layer, only one thin overgrowth rim was seen (analysis 9A). Otherwise the three phases seem to be in mutual equilibrium (analyses 8, 9B, 10-12).

The second eclogite (6914) contains garnet, clinopyroxene and apparently primary graphite. The minerals of 6914 have lower Fe/Mg ratios than those of 6913 (Fig. 1). The garnet is unusually Ca-rich for a kyanite-free assemblage. The occurrence of graphite in Siberian alumina-rich assemblages has been noted by Sobolev (1971). Switzer and Melson (1969) however note the occurrence of diamond in a Roberts Victor kyanite eclogite. The general similarities of fabric and mineralogy of 6913 and 6914 suggest that they represent similar conditions of equilibration in the vicinity of the graphite/diamond equilibrium curve. Both specimens show extensive alteration which resembles the interstitial quenched melts described by Switzer and Melson (1969).

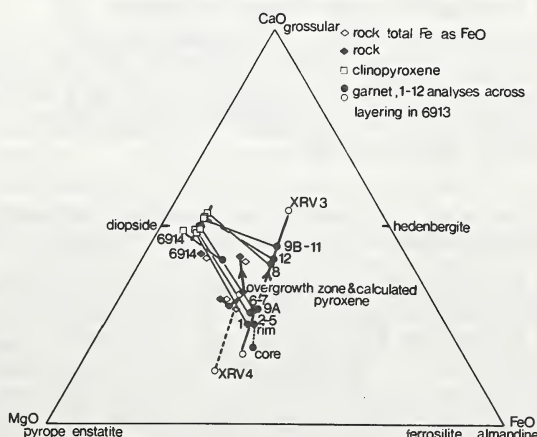


Fig. 1 Mo1% CaO, MgO, FeO diagram. The trends of bulk compositions, garnet and clinopyroxene compositions for 6913 are shown as solid arrowed lines.

Cryptic variations in mineral compositions occur in 6913, seen largely through variations in Ca and Mg in garnets (Fig. 1). The garnets from the overgrowth layer (6, 7), and also 9A, are slightly but distinctly, different from the gt-cpx layer (1-5) and markedly different from those of the gt-cpx-ky layer (9B-11). Within the latter layer garnets with lower Ca occur near the layer interface (8) and at the edge of the specimen (12). The compositional trends for these garnets are similar to those found in another Roberts Victor layered eclogite (XRV3, Rickwood et al., 1968) whilst XRV4 shows a similar trend in garnets of lower Fe/Mg ratios (Fig. 1). Some of the garnets of the gt-cpx layer are zoned with small (100-400 microns wide) cores somewhat enriched in Mg and depleted in Ca. (Figs. 1 and 2).

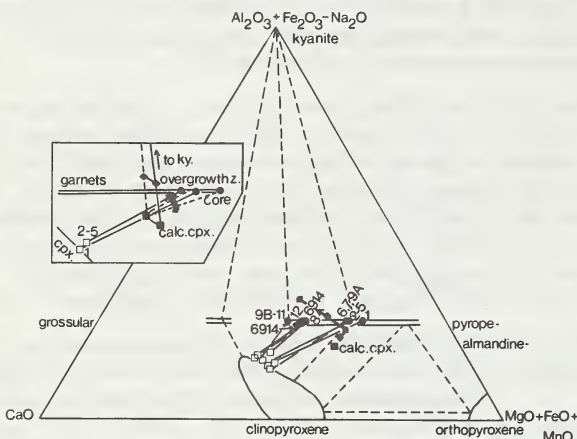


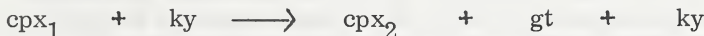
Fig 2 Mol% A, C, F diagram showing the synoptic relationships amongst Roberts Victor eclogites (MacGregor and Carter, 1970). The inset shows probable bulk compositional trends within the gt-cpx layer of 6913. The modified compositions of cpx₁ and the overgrowth layer are shown together with possible high T-P tie lines (dashed lines).

The clinopyroxenes of 6913 show a less marked, but sympathetic variation, when compared with the garnets. (Figs. 1 and 2).

Conditions of equilibration are estimated from the distribution function $K' = (\text{Fe}/\text{Mg})_{\text{gt}} / (\text{Fe}/\text{Mg})_{\text{cpx}}$ modified so that all iron is given as Fe^{2+} . Average K' values are 6913 gt-cpx and overgrowth layer 3.8, gt-cpx-ky 4.7, and 6914 3.5. Equilibration temperatures derived from these K' values using curves of Banno (1970) and Mysen and Heier (1970) give temperatures in the range 750-900°C with a mean value about 850°C. Pressures at these temperatures are defined by the graphite/diamond curve (Bundy et al., 1961) and by appropriate eclogite equilibrium curves (Green,

1967). A reasonable range would be 22-32 kilobars with a maximum pressure of 30 kilobars at highest temperatures for the graphite bearing sample 6914.

The garnet overgrowths on kyanite and the zonation in garnet (?) provide information about processes prior to this subsolidus equilibration. The overgrowth garnets (6, 7, 9A) cannot form by reaction between the analysed clinopyroxenes and kyanite (Fig. 2). This reaction can thus be interpreted as an open system one where clinopyroxene and kyanite have reacted with a fluid of defined chemical potential. Alternatively a closed system reaction of the type



must be invoked. The cryptic variations suggest the presence of local bulk systems and limited diffusional volumes (as do the overgrowth textures) more in keeping with a closed system reaction. The composition of cpx_1 for the overgrowth layer was calculated on the basis of the above equation from analysed minerals (6, 7) and a modal analysis (and assuming pyroxene stoichiometry). The structural formula of this pyroxene is Si 1.698, Al^[4] 0.302, Al^[6] 0.477, Ti 0.004, Fe²⁺ 0.352, Mn 0.004, Mg. 0.530, Ca 0.444, Na 0.189.

This calculated pyroxene is plotted in Figs. 1 and 2 where its position relative to the bulk compositional trends in 6913 might indicate whether a similar clinopyroxene was stable within adjacent layers. Four bulk analyses are available for 6913, two from the gt-cpx layer, one calculated bulk composition of the overgrowth layer, and one from the gt-cpx-ky layer. These bulk compositions do not lie on appropriate gt-cpx tie lines in Figs. 1 and 2. This is not due to analytical error but is the result of the extensive alteration of the primary minerals when the rocks have become depleted in Fe and Ca and enriched in Mg (and also K, H₂O and CO₂). An attempt has been made to make some allowance for this alteration and for the presence in Fe³⁺ in cpx_1 (see inset of Fig. 2). The bulk compositions of the gt-cpx layer can be represented by mixtures of cpx_1 and garnets whose compositions range from those found in the Ca-depleted cores to the typical compositions of this layer. In a similar way the composition of the gt-cpx-ky layer can be represented by mixtures of cpx_1 , kyanite and a garnet of Ca content similar to that found (Fig. 2) but somewhat enriched in Mg relative to Fe (Fig. 1). Mg-rich cores were not found in microprobe traverses of garnets in this layer.

The general reaction for this layered eclogite is thus



This reaction involves a marked decrease in the amount of clinopyroxene and an increase in the amount of garnet together with a small decrease in the amount of kyanite, if present. The early clinopyroxene is tschermakite and orthopyroxene rich and jadeite poor relative to the analysed pyroxenes and thus has high P liquidus characteristics. Early garnets may be somewhat enriched in Mg. The distribution coefficient K' for cpx_1 /core gt is small (1.2) and supports the high T origins of the possible early assemblage. The conditions under which early assemblages might form can be assessed relative to the later subsolidus equilibration. Increasing proportions of garnet relative to clinopyroxene will be favoured by decreasing temperature and increasing pressure (Green 1967). The increasing amount of jadeite in clinopyroxenes and the possible increase in Fe/Mg ratio of the garnets could result from isobaric cooling but both reactions would be favoured by an increment of pressure. T-P conditions of 1400-1500°C and 26-28 kilobars seem appropriate since eclogites of similar composition are stable at the solidus (Green, 1967) and, provided higher pressure estimates are favoured for the subsolidus equilibration (say 28-32 kilobars), an increase of pressure is involved.

The fabric of the layered eclogite suggests that this incremental pressure is of tectonic origin. The kyanites have abundant strain bands. Deep embayments of garnet into kyanite occur in the vicinity of these strain bands within the overgrowth layer. The strain bands are considered to be regions of preferential garnet nucleation and reaction. Thus the tectonic processes causing strain must precede the development of overgrowths. It seems likely that the foliated fabric of the eclogite, defined by elongate aggregates of garnet and clinopyroxene and by elongate kyanites, formed at this stage of tectonic development. MacGregor and Carter (1970) have classified Roberts Victor eclogites into two types, 1 and 2, on a basis of fabric, mineralogy and chemistry. Specimen 6913 has the layering and mineralogy said to be characteristic of Type 1 eclogites but is also foliated, a feature restricted to Type 2 eclogites. These authors suggest that the Type 1 eclogites, because of their layering and textures (sunhedral to anhedral garnets and poikilitic clinopyroxenes) are formed by igneous cumulate processes. In specimen 6913, however, the best formed garnets occur in the overgrowth layer and are formed by subsolidus processes.

The cryptic mineral variations in 6913 are considered to reflect gradual compositional variations within the layering. Such variations, together with the gross layering, provide stronger evidence for cumulate processes at the temperatures and pressures outlined above. The sequence of primary cumulate minerals would be clinopyroxene and minor garnet, clinopyroxene and minor kyanite and then clinopyroxene, kyanite and minor garnet. Little can be said about the magma from which these phases crystallised except that the relatively high Fe/Mg ratio of the early pyroxene and the variable but high Ca contents of possible early garnets suggest an evolved magma relative to possible high pressure primitive partial melts (O'Hara 1968).

References

Banno, S., 1970. - *Phys. Earth Planet. Interiors* 3, pp. 405-21.

Bundy, F.P., Bovenkerk, H.P., and Wentorf, R.H., 1961. - *J. Chem. Phys.* 35, pp. 383-91.

Green, T.H., 1967. - *Contr. Mineral. and Petrol.* 16, pp. 84-114.

MacGregor, I.D., and Carter, J.L., 1970. - *Phys. Earth Planet. Interiors* 3, pp. 391-97.

Mysen, B.O., and Heier, K.S., 1972. - *Contr. Mineral. and Petrol.* 36, pp. 73-94.

O'Hara, M.J., 1968. - *Earth Sci. Revs.* 4, pp. 69-133.

Rickwood, P.C., Mathias, M., and Siebert, J.C., 1968. - *Contr. Mineral. and Petrol.* 19, 271-301.

Sobolev, N.V., Jr., Kuznetsova, I.K., and Zyuzin, N.I., 1968. - *Jour. Pet.* 9, 253-80.

Sobolev, N.V., Jr., 1971. - *Jour. Geophys. Res.* 76, pp. 1309-14.

Switzer, G., and Melson W.G., 1969. - *Smithsonian Contr. Earth Sci.* 1, pp 1-9.

LIGHT ELEMENT METASOMATISM OF THE CONTINENTAL MANTLE:
THE EVIDENCE AND THE CONSEQUENCES

By

F. E. Lloyd and D. K. Bailey
(Dept. of Geology, University of Reading, England)

The highly potassic volcanics of S.W. Uganda and the sodi-potassic volcanics of the West Eifel, Germany, represent two distinctive aspects of the highly alkaline volcanism characteristic of uplifted and rifted continental cratons. The sparse lavas are feldspathoidal clinopyroxenites and the associated explosive volcanism provides highly typical ultramafic nodules composed of dark mica + clinopyroxene \pm amphibole with titanomagnetite, sphene and apatite. These are, generally, alkali clinopyroxenites. The Eifel suite also includes lherzolites, harzburgites, wehrlites and dunites. Olivine-bearing nodules are scarce in the highly potassic fields of Bunyaraguru and Katwe Kikorongo, but more abundant in the less potassic Bufumbira province. No eclogite, garnet lherzolite or gabbro nodules have been found in West Eifel or S.W. Uganda.

Carbonatitic nodules are found, and carbonates are abundant among the pyroclastics, the soluble extracts showing characteristic carbonatite trace-element enrichment (Rb, Sr, Y, Nb, Ba and La). The volcanic gases are CO_2 -rich.

Evidence of metasomatism. All stages of transition from anhydrous nodules to alkali clinopyroxenite can be found - the olivine, orthopyroxene and chrome diopside being replaced by diopside-salite, dark mica, amphibole and iron ores. The early stages of replacement are localized along cracks and fissures, traversing the crystalline anhydrous assemblages, and cross-cutting phase boundaries. The nature and manner of replacement are analogous to the process of fenitization (alkali metasomatism) in crustal rocks. The final stages of the process are preserved in an alkali clinopyroxenite which contains scattered relicts of spinel lherzolite. Small amounts of glass are found within the veins of hydrous minerals in some cases. There are no signs of reaction with the adjacent minerals. The glass is commonly vesiculated, presumably due to the pressure drop on eruption. Where nodules are in contact with lava the hydrous minerals are dehydrated, so that the formation of hydrous minerals and glass within the nodules must relate to higher vapour (and total) pressures or lower temperatures, or both. (See Tables, page 4).

The transitions between anhydrous and hydrous ultramafic nodules eliminate the possibility that the latter are of crustal origin. There is no evidence to show that the hydrous nodules are xenoliths from a deep igneous intrusion, although some could have such an origin. All the internal evidence suggests that the ultramafic nodule suite is a sample of the local mantle, which has been partly metasomatised (by the addition especially of alkalis, iron, H_2O and CO_2).

Supporting evidence. (a) Recent experimental studies of the stabilities of phlogopite and amphiboles, indicate that these phases would be stable in the upper mantle, and therefore alkali clinopyroxenite is a permissible mantle composition.

(b) Geophysical studies of the Rhine and East African rifts have indicated the existence of low density (3.2) mantle below the crust. Alkali clinopyroxenite with about 25% mica (which is average for the W. Eifel and Uganda) has the appropriate density.

(c) These regions are characterized by geologically long-persistent uplifts. Most explanations relate the uplift to thermal disturbances in the underlying mantle, but these are inadequate in terms of amount of uplift and its geological persistence (Bailey, 1972). Conversion of the top 15 km of anhydrous mantle to alkali clinopyroxenite, however, could produce uplift of the right order (~ 1 km), and this uplift would be geologically persistent.

(d) The associated magmatism is characterized by extreme richness in alkalis and volatile emission. Plutonic equivalents, in other provinces, display widespread crustal fenitization, and the feldspathic magmas in many of these cases appear to be rheomorphic fenites.

(e) The overall chemical compositions of the lavas resemble those of the alkali clinopyroxenite nodules, and their Mg, Cr and Ni contents suggest mantle derivation.

Proposed Model. All the above evidence is consistent with a model in which long-sustained degassing of the underlying mantle leads to progressive metasomatism at the top, where the alkalis (and H_2O) are fixed within the stability range of phlogopite and amphibole. The increased volume causes uplift of the overlying crust. Continued passage of volatiles ultimately induces melting (Bailey, 1970) producing volatile-rich magmas and the characteristic explosive alkaline magmatism. The experimentally-determined stabilities of amphibole and phlogopite are such that in regions of low-geothermal gradient ($30^\circ C/kb$) amphibole could be stable to depths around 80 km, whilst phlogopite would be stable to 120 km: along steep geothermal gradients ($100^\circ C/kb$) these depth limits converge around 30 km and the separate existence of phlogopite-enriched mantle seems out of the question. Time is an essential term in the metasomatic argument, allowing for the long and gradual development of light-element minerals in the top layers of the mantle. We propose that the alkali-rich magmas are rheomorphic mantle fenites. Highly potassic lavas are generated where the initial continental geothermal gradient was low, from phlogopite-rich mantle below the level of amphibole stability: sodi-potassic lavas are formed at higher levels, when amphibole-bearing mantle becomes involved in melting (see Figure). In the oceans highly potassic lavas are not recorded, (Lloyd, in press). This accords with the present hypothesis because under conditions of steep oceanic geotherms phlogopite stability is only slightly greater than that of amphibole: thus there will be very little opportunity for a layer of potassium-enriched mantle to develop, except possibly in the older and cooler parts of the oceanic lithosphere, near the margins.

References.

Bailey, D.K., 1970. - Geol. J. (Special Issue) No. 2, pp. 177-86.
 -----, 1972. - J. Earth Sci. (Leeds), 8, pp. 231-45.

FIG. Schematic cratonic crust-mantle sections, showing the generation of different alkaline magmas by melting of metasomatized upper mantle. Phlogopite-rich mantle underlies the zone of amphibole stability.

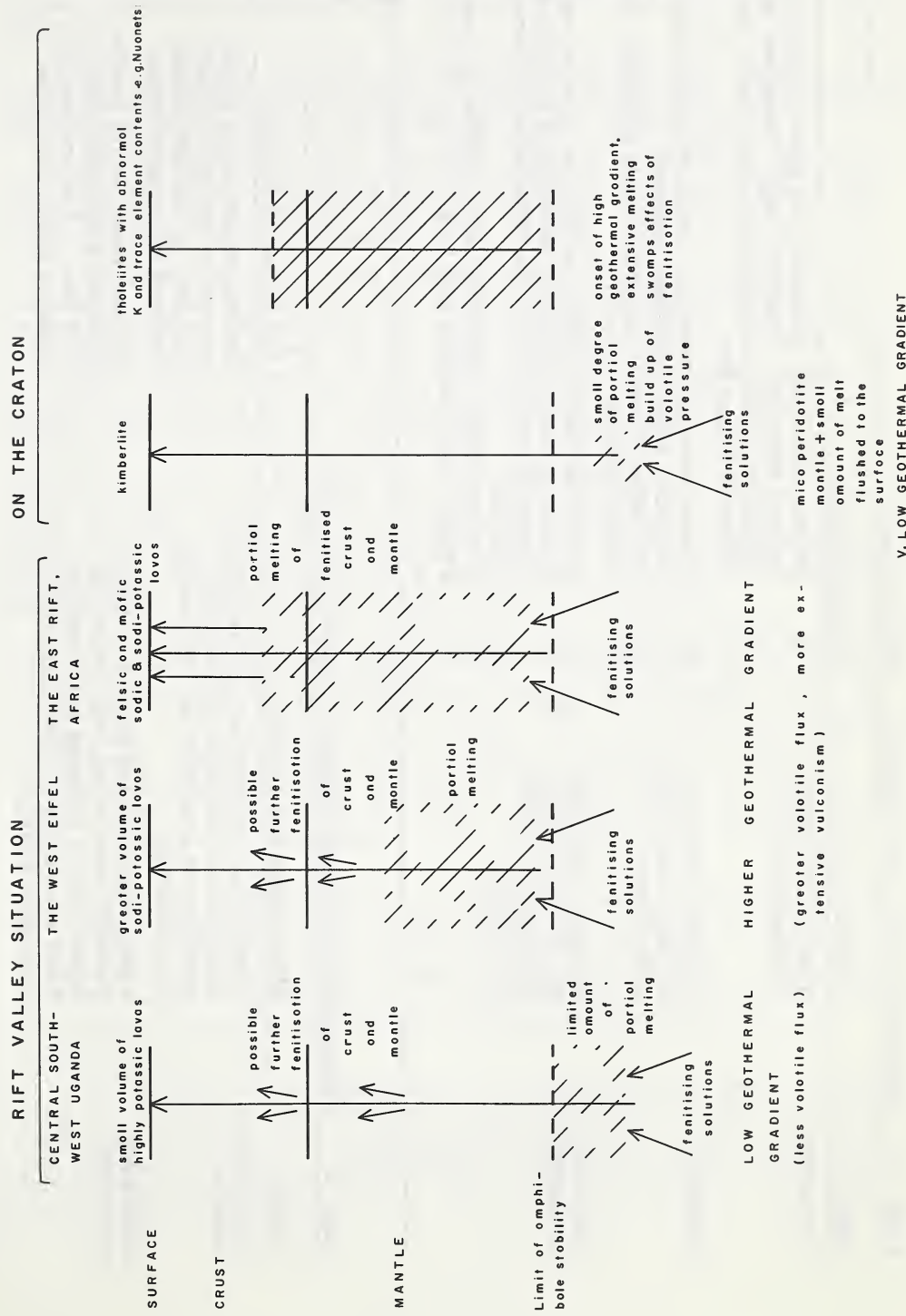


Table 1. Paragenesis of the nodule phases 1 - clinopyroxene

Nodule	Primary cpx.	Secondary cpx.
Lherzolite	Pale green chromiferous diopside	(i) Darker brown cpx. associated with glass, spinel and hydrous minerals. Found in "vugs" throughout nodule. (ii) Alteration of pale green diopside to pale brown cpx. by contact with host lava.
Wehrlite	Diopside with more Fe and Ti than lherzolite diopside	(i) Darker greenish brown cpx. associated with opaque iron minerals, glass and hydrous minerals. (ii) Alteration of primary diopside to pale brown cpx. by contact with host lava.
Alkali clino-pyroxenite	Diopside with more Fe, Ti and Ca than lherzolite or wehrilite diopside	(i) Dark green salite forming patchy edge or centre zones. Zoning often follows lines of weakness in nodule and is frequently associated with the introduction of hydrous minerals. (ii) Purple brown, titaniferous outer oscillation zones. Product of interactions with lava.

Table 2. Paragenesis of the nodule phases 2 - hydrous minerals

Nodule	Mineral type and occurrence	Low pressure alteration
Lherzolite and Wehrlite	Pale yellow amphibole and pale red mica occupy lenses and bands of alteration together with secondary cpx. and opaque iron minerals.	Hydrous minerals are notably corroded where they contact host lava - they are usually replaced by cpx and olivine.
Alkali clino-pyroxenite	Alkali hornblende and dark mica occupy corroded areas of cpx. and olivine and follow lines of weakness in the nodules. Their occurrence is often associated with salite zoning.	Hydrous minerals are notably corroded where they contact host lava - they are usually replaced by cpx and olivine.

FORMATION OF MAAR-DIATREME VOLCANOES AND ITS RELEVANCE TO KIMBERLITE DIATREMES.

Volker Lorenz, Geologisches Institut der Universität, Mainz, Germany.

The author's studies of numerous diatremes, maars, and tuff-rings in Europe (Germany, France, Scotland, Iceland) and USA suggest a specific process in their formation.

Magma rises along a fissure and, at a certain depth below the surface, contacts water that pours into the fissure from either aquifers or from the surface - sea-water, lake-water, river or stream water.

At the interface the magma is chilled; it solidifies into glass and consequently disintegrates into discrete, angular, solid fragments of ash or lapilli size. The water is heated at the base of the water column until it boils and finally flashes into steam giving rise to a phreatomagmatic eruption. During refill of the system with water pressure within the fissure is considerably lower than the lithostatic pressure in the surrounding country-rocks. As a consequence spalling leads to enlargement of the fissure into an eruption channel and introduction of wall-rock material into the eruptive system. This cyclic, geysir-like activity gives rise to bedded air-fall and base surge deposits at the surface characterized by wet and partly muddy deposits and consisting of a mixture of wall-rock and juvenile material.

Above a critical diameter of the enlarged eruption channel instability of the walls leads to formation of a ring-fault which may be considerably larger in diameter than the eruption channel and reach several 100 to 1.5 km. Along the ring-fault the enclosed wall-rocks and overlying subaerially deposited, bedded pyroclastic debris subside and form a saucer-shaped structure at depth. This process results in a large crater at the surface with a diameter at its rim 1.5 to 2.5 times the diameter of the ring-fault at near-surface level.

At a relatively shallow level of contact between magma and water spalling of country-rocks into the fissure is of minor importance. Consequently the ring-fault will be smaller in diameter and the resulting pyroclastic debris relatively poor in wall-rock material. At the surface a tuff-ring forms, the crater floor of which is elevated compared with the regional surface.

At a relatively deep level of magma/water contact spalling is of major importance. A much greater amount of wall-rock material is thus incorporated into the system and ejected during eruptions. Subsidence along the ring-fault therefore leads to a maar crater the floor of which is cut into the regional surface.

Prolonged activity results in continuing subsidence. In addition the faulted and fractured subsided rocks get intruded by pyroclastic debris which in part may replace the subsided rocks.

Owing to subsidence and pyroclastic intrusion as well as shifting of the eruption channel the saucer-shaped subsidence structure is finally destroyed and the whole content inside the ring-fault circulates. An eruption channel with upward movements during eruptions is surrounded by a marginal zone characterized by slow downward movement.

Once the ring-fault has formed very little additional country-rock material is introduced into the system. During eruptions a certain percentage of country-rock and juvenile material is ejected and lost to the surrounding area. Simultaneously, however, juvenile material is introduced from the fissure into the diatreme. With time this leads to a decrease of country-rock debris in the ejecta as well as in the debris inside the diatreme. Prolonged activity in the case of a deep magma/water contact will therefore give rise to a transformation of a maar into a tuff-ring.

At the end of eruption subsidence owing to compaction of the whole diatreme content takes place in addition to slumping and erosion of the rim deposits. Thus redeposited tuffs and other sediments (lake sediments) even subside along the ring-fault as e.g. at the maar at Senèze, France, and at some diatremes in Scotland and Arizona. If the water supply is cut off prior to the end of magma supply magma may intrude the diatreme and even extrude.

Kimberlite diatremes display various features that seem to be consistent with the above model:

At depth they extend into fissures along which hot magmatic kimberlite rose. The diatreme contents, however, indicate emplacement by a cool gas phase, which may have been, at least in part, derived from ground or surface water. An appreciable amount of water in the respective eruption clouds seems to be indicated by large accretionary lapilli occurring in the Murfreesboro kimberlite diatreme, Arkansas (MOORE & PECK 1962). Adiabatic expansion of the juvenile gas phase has been assumed responsible for the cool emplacement of the pyroclastic debris (DAWSON 1971). This ignores the presence of the hot juvenile particles. Their heat capacity takes part in controlling the temperature and expansion of the gas phase. It would be large enough to heat copious amounts of ground or surface water. If juvenile gas was responsible for the eruptions many highly vesicular lapilli should exist especially if they were cooled rapidly by the gases.

If the gases would be of juvenile origin it is also not clear why kimberlite dykes and sills which contained similar amounts of gas were emplaced at even shallower depth than the

diatreme roots (DAWSON & HAWTHORNE 1970) without showing any evidence of disruption of the magma into pyroclastic debris. Phreatomagmatic formation of the diatremes would solve this apparent problem.

Fluidization has been advocated for explaining the large subsided 'floating reefs' and concentrations of xenoliths of specific horizons within certain areas (DAWSON 1971). Both features, however, could be interpreted as remnants of nearly completely destroyed subsidence structures. Vertical striae on diatreme walls and zoning of diatreme contents indicate en masse subsidence of a marginal zone whereas the inner zone represents an eruption channel. Such channeling also contradicts formation of the whole body of large diatremes by fluidization. Once a small channel has been formed only reaction of the wall-rocks - initially by spalling and later also by formation of a ring-fault - seems to provide the space for the later large kimberlite diatreme body.

The kimberlite diatremes in Montana clearly are saucer-shaped subsidence structures that extend into dykes at depth and are surrounded by ring-faults (HEARN 1968).

References:

Dawson, J.B., 1971: Earth-Sci.Rev., 7, 187 - 214.
Dawson, J.B. and Hawthorne, J.B., 1970: Bull. volcanologique, 34, 740 - 757.
Hearn, Jr., B.C., 1968: Sci., 159, 622 - 625.
Lorenz, V., 1973: Bull. volcanologique, 37, in press.
Moore, J.G. and Peck, D.L., 1962: J.Geol., 70, 182 - 193.

PETROLOGICAL STRUCTURE OF THE UPPER MANTLE
BENEATH THE SOUTH AFRICAN SHIELD

Ian D. MacGregor, Department of Geology, University of California,
Davis, California 95616

Suites of ultramafic xenoliths from the Laurenzia, Bultfontein, Wesselton, Roberts Victor, Monastery, Malibo Matsu and Kao kimberlite pipes may be grouped together to characterize the petrology of the upper mantle beneath the South West Africa Kimberley and Lesotho regions.

Ultramafic xenoliths from the Laurenzia pipe in South West Africa are primarily lherzolites with widely varying ratios of pyroxenes and aluminous phases. Spinel, spinel-garnet and garnet lherzolites are all found. A few harzburgites also occur. In the Kimberley area the samples from the Wesselton and Roberts Victor mines are composed primarily of garnet, spinel, and garnet-spinel harzburgites with a few lherzolites showing similar combinations of the aluminous phases. In the Lesotho area xenoliths from the Kao mine are predominantly pure harzburgites with a few spinel, spinel-garnet, and garnet lherzolites. At the Monastery mine spinel-garnet lherzolites have only been found and samples from the Malibo Matsu pipe cluster close to harzburgite. A contrast of the three main regions indicates a significantly wider spread of modal proportions for the samples from South West Africa, and a greater proportion of samples with low clinopyroxene contents for the Kimberley and Lesotho regions. The olivine contents in all localities show no special distributions. All samples are subject to varying degrees of serpentinization with the intensity of serpentinization decreasing in the order South West Africa Kimberley and Lesotho.

Two main textural types occur, a coarse-grained, granular variety and a sheared variety. The coarse-grained granular rocks are composed of large subhedral to rounded olivine crystals interspersed with interstitial to irregular orthopyroxene crystals. Garnet, when present, occurs either as rounded grains or wormy, irregular, intergranular blebs. Similarly spinel is found either as euhedral crystals or as eutectoid-like intergrowths with clinopyroxene or amphibole. Clinopyroxene may occur as rounded grains or more commonly as irregular intergranular crystals. Exsolution textures are common in these rocks. Clinopyroxene, spinel and garnet lamellae exsolve from the orthopyroxene and often form rims or irregular boundaries to large orthopyroxene grains suggesting that much of the intergranular clinopyroxene, garnet and spinel has been exsolved from the orthopyroxene host. Occasionally clinopyroxene grains will also have orthopyroxene exsolution lamellae. Generally the granular textured rocks show little evidence of deformation, although in some cases olivine and orthopyroxene have variable degrees of kink banding. Olivine is always partially serpentinized along a series of veined networks. Phlogopite when present occurs as intergrown flakes, often along with clinopyroxene and spinel in large intergranular areas, or may be associated with the kelyphitic rims characteristically surrounding all the garnets.

The sheared textured xenoliths are composed of sheared and streaked lenses of deformed orthopyroxene and clinopyroxene in a mosaic of finely granulated olivine. Garnet when present occurs as rounded crystals in the mylonitized olivine groundmass, and is usually surrounded by a rim of kelyphite. The rock has a distinct foliation. Exsolution textures are absent. Serpentinitization exploits the rounded boundaries of the olivine grains. Phlogopite is generally absent in these rocks. Garnet is the sole aluminous phase found in the sheared xenoliths, whereas all combinations of aluminous phases occur in the granular textured rocks. Sheared and granular textured samples occur in all the major regions.

The mineral chemistry shows that the South West African xenoliths have olivines, orthopyroxenes and garnets with lower Mg/Mg+Fe ratios than the Kimberley and Lesotho regions. Clinopyroxenes show a similar range of composition, but the Kimberley and South West African samples are slightly more iron rich than the Lesotho samples. All minerals in the sheared textured rocks are characteristically higher in Cr₂O₃, TiO₂ and Na₂O, while garnets and olivine have higher CaO contents, and the Mg/Mg+Fe ratio of the clinopyroxenes is significantly higher and CaO lower than the granular textured samples.

Assignment of temperatures and pressures to the xenoliths indicates that the samples from all localities have come from a wide range of pressures (depths) and temperatures. It is therefore apparent that the xenoliths are not genetically related to the kimberlite, but accidentally related as fragments of the mantle torn off and transported to the surface. The maximum depth of any fragment from a single locality thus gives the minimum depth below which the kimberlites must have originated. At the Lawrenzia pipe the minimum value is at 150 kilometers, but increases to 170 and 200 kilometers at the Kimberley and Lesotho areas, respectively. The location of the xenoliths indicates a suite of samples originating along a linear profile of increasing temperature with increasing depth or pressure, and leads to the interpretation that the trend marks the location of a paleogeotherm, presumably of Cretaceous age, commensurate with the age of kimberlite extrusion. An anomalous feature which is not commensurate with the simple geotherm interpretation is that the samples with sheared textures mark a linear trend which suggests a sudden steepening of the interpreted geothermal gradient. This phenomenon has also been noticed by Boyd for Lesotho xenoliths and by Johnston for the Jagersfontein pipe. Boyd has interpreted the sudden rise of the geothermal gradient to arise from frictional effects in the low velocity zone during the period of Cretaceous drift. The region with the steep gradients is thus interpreted to mark the Low Velocity Zone, and the sheared nature of the xenoliths from this region is compatible with their deformation during a period of drift. Other possibilities for an increased gradient could be variations in the thermal conductivity such as may arise in a layer of highly deformed rocks. On the basis of these interpretations, the xenoliths thus mark the Cretaceous geotherm beneath the South African Shield, and define the top of the Low Velocity Zone.

A comparison of the geothermal gradients beneath the different localities studied shows that each mine or pipe gives a different value. The Laurenzia and Lesotho localities have the highest geothermal gradients, while values from the Kimberley region are significantly lower. The depth to the top of the Low Velocity Region also varies, being at approximately 140 kilometers beneath South West Africa, increasing to 180 kilometers beneath the Lesotho area, and extending to a depth of approximately 200 kilometers beneath the Kimberley area. The general picture suggests that the Cretaceous lithosphere beneath the South African Shield was at a maximum in the Kimberley area and thinned to the east and west.

CHEMICAL COMPOSITION OF THE MAJHGAWAN KIMBERLITE,
CENTRAL INDIA

By

S. M. Mathur
Mineral Exploration Corporation Limited
Nagpur, India

Majhgawan is situated about 19 km south-west of Panna, headquarters of the district of the same name in Madhya Pradesh. The rock occupying the diamond-bearing pipe was called 'agglomeratic tuff' by Sinor (1930) who was the first to recognize its intrusive volcanic nature. In plan the pipe is pear-shaped, its longer axis is about 500 metres and at its widest it is about 350 metres across. It is surrounded by the Dhandraul (Kaimur) Quartzite of the Vindhyan System (Mathur, 1962; Mathur and Singh, 1963).

On the basis of petrological studies Mathur and Singh (1971) considered it a kimberlite. Olivine is the most abundant constituent of the pipe rock, and is serpentinised to an extreme degree. Phlogopite, chlorite, carbonate minerals, magnetite, ilmenite, haematite, leucoxene, iddingsite, rutile, perovskite, and rarely garnet, are the other constituents of the pipe rock, besides diamond. The top section of the pipe rock is traversed by abundant calcite veinlets, which decrease with depth. In an underground drive at 100 metres depth, the rock is free of calcite veinlets.

The chemical analyses of the Majhgawan samples resemble those of kimberlites from South Africa (Wagner, 1914; Washington, 1917; and Williams, 1932) and Siberia (Burov and Sobolev, 1957). Samples of kimberlite obtained from the Majhgawan mine from the pit on the surface and from the drive give somewhat variable chemical analyses, depending mainly upon the amount of calcite veinlets present and on the degree of weathering.

Silica in the samples of the Majhgawan kimberlite obtained from the deeper levels of the pipe is roughly 37 to 40 percent, which is more akin to the South African kimberlites where the silica percentage ranges from 38 to almost 47 percent, but is higher than the Siberian kimberlites where it varies between 25 and 30 percent. Magnesia in the Majhgawan rock is generally between 14 and 16 percent in the upper parts of the pipe, but in the sample from the drive 24 percent has been recorded. On the whole this is lower than in the typical kimberlites from South Africa and Siberia where magnesia is 22 to 32 percent; it is more like melilite basalt. Titania, on the other hand, is significantly higher in the Majhgawan samples, as it ranges between 4 and 7 percent; in the kimberlite samples from other parts of the world it rarely exceeds 3 percent. Both ferric and ferrous iron, alumina and other oxides of the samples from the Majhgawan pipe are similar in percentage to the typical kimberlites from many parts of the world. Due to the profusion of calcite veins in the upper part of the Majhgawan pipe rock, the lime percentage recorded is 15 to 18, and with the increase in depth it becomes lower as the incidence of the calcite veinlets decreases; ultimately in the drive at the 100-metre depth, where there is hardly any visible calcite, the amount of lime drops to less than 2 percent. Lime is also highly variable in the South African and Siberian kimberlites.

References

Burov, A.P. and Sobolev, V.S. (Ed.), 1957. - "Almazi Sibiri" (Russian). Moscow: Scientific and Technical Publishing House, pp. 1-158.

Mathur, S.M., 1957. - Geology of the Panna diamond deposits. Rec. Geol. Surv. India, Vol. 87, pp. 787-816.

Mathur, S.M. and Singh, H.N., 1963. - Geology and sampling of the Majhgawan diamond deposit, Panna district, Madhya Pradesh. Bull. Geol. Surv. India, Sr A, No 21, pp. 1-59.

-----, 1971. - Petrology of the Majhgawan pipe rock. "Diamond", Misc. Pub. Geol. Surv. India, No. 19, pp. 78-85.

Sinor, K.P., 1930. - "The Diamond Mines of Panna State in Central India". Bombay: Times of India Press, pp. 1-189.

Wagner, P.A., 1914. - "The Diamond Fields of Southern Africa". Johannesburg: Transvaal Leader, pp. 1-347.

Washington, H.S. 1917. - Chemical Analyses of Igneous Rocks Published from 1884 to 1913. U.S.G.S. Prof. Paper 99, pp. 1-1201.

Williams, A.F., 1932. - "The Genesis of the Diamond", Vol. 1, London: Everest Benn Ltd., pp. 1-352.

"PYROXENE" - ILMENITE XENOLITHS FROM THE STOCKDALE PIPE;
KANSAS: CHEMISTRY, CHRYSTALLOGRAPHY, AND ORIGIN

Robert H. McCallister: Department of Geosciences

Henry O. A. Meyer : Purdue University, West Lafayette,
Indiana, 47907, U.S.A.

Douglas G. Brookins : Department of Geology,

University of New Mexico, Albuquerque
New Mexico, 87106, U.S.A.

Originally Harger (1906), Williams (1932) and MacGregor, Ferguson and Amm (1937) described the occurrence of xenoliths of enstatite-ilmenite and diopside-ilmenite intergrowths in kimberlite. In recent years a number of pyroxene-ilmenite intergrowths have been studied and reported on by several authors including: MacGregor and Wittkopp (1970); Ringwood and Lovering (1970); Dawson and Reid (1970); Brookins (1971); Boyd (1971); Boyd and Dawson (1972); Boyd and Nixon (1973) and Mitchell et al. (1973). In this paper we present and discuss results of a study on the chemistry of an ilmenite- "serpentinized" pyroxene xenolith from the Stockdale kimberlite pipe of Riley County, Kansas. Also, we will discuss the crystallographic relationships between intergrowth phases of the types previously mentioned as well as possible mechanisms of formation.

Texturally the Stockdale and other pyroxene-ilmenite xenoliths, mentioned above, are alike in that both are composed of alternating lamellae of two phases. In the Stockdale intergrowth the lamellae consist of ilmenite and serpentine with an average interlamellar width of 0.8 mm, and a serpentine lamellae thickness of approximately 0.6 mm. The ilmenite-serpentine ratio was determined to be 27%: 73% \pm 2%. In thin-section calcite stringers were observed cutting across serpentine lamellae. This was confirmed by electron-microprobe analysis. We did not observe the varying habits of ilmenite or the 120° intersection of lamellae which were described by Dawson and Reid (1970).

Representative analyses of the ilmenite and serpentine are presented in Table 1. The ilmenite has been recast to give the relative proportions of FeTiO_3 (ilmenite) to MgTiO_3 (geikielite). The high geikielite content of the ilmenite is consistent with compositions of ilmenites from other kimberlites. The excess Fe after Mg, Fe, and Mn atomic proportions were subtracted from Ti corresponds to approximately 6.0 wt % Fe_2O_3 although we only give iron as FeO . The serpentine is relatively homogeneous throughout the section and corresponds chemically to antigorite. The results of x-ray diffraction and scanning electron microscope studies confirmed antigorite as the polymorph.

Table 1.
Representative analyses of Stockdale intergrowth

	Ilmenite	Antigorite
SiO ₂	0.20	43.1
TiO ₂	54.9	0.45
Al ₂ O ₃	0.90	1.97
FeO	30.8	3.87
MgO	12.8	39.5
CaO	0.04	0.06
MnO	<u>0.25</u>	<u>0.03</u>
	99.9	89.0 less H ₂ O 11.0

Ilmenite 55
Geikielite 45

In an attempt to understand the structural relations between intergrowth phases of ilmenite and silicates precession photographs were taken of an ilmenite plate from Stockdale, a clinopyroxene-ilmenite couple from Monastery Mine (supplied by Dr. Ian MacGregor) and an orthopyroxene-ilmenite couple from Monastery Mine (supplied by Dr. F.R. Boyd). Unfiltered MoK radiation was used in all diffraction experiments.

The ilmenite in each sample was found to be oriented such that the plane of the lamella was equivalent to the basal plane of ilmenite (i.e. $[0001]$ was perpendicular to the plane of the ilmenite plate).

For the case of the clinopyroxene-ilmenite couple however, it was found that b^* of the clinopyroxene is parallel to $h\bar{h}o^*$ of the ilmenite. Also, the plane of the clinopyroxene which is parallel to basal plane of the ilmenite is (201).

In the orthopyroxene-ilmenite intergrowth b^* of orthopyroxene is also parallel to $h\bar{h}o^*$ of the ilmenite; however, the common plane between the two structures is parallel to (100) of the orthopyroxene and (001) of the ilmenite.

On the assumption that the configuration of oxygen atoms in the two phases is nearly coincident for some layer parallel to (100) in the orthopyroxene and (0001) in the ilmenite, successive plots of oxygen positions were made for both members in planes at varying distances along their respective $[100]$ and $[0001]$. Allowing for certain approximations a rather good fit was obtained between the two structures at 3.51 \AA along c of ilmenite and the composite oxygen positions at 17.05, 17.12 and 17.30 \AA along a of the orthopyroxene. The common layers closely correspond to a close-packed layer of oxygens, and the nearness of fit

suggests a low strain energy configuration.

A number of suggestions with regard to the mechanism of formation of these intergrowths have been made by several authors and reviewed by Boyd (1971). These include:

- a. Eutectic crystallization which was originally proposed by Williams (1932) on the basis of the graphic texture, and later confirmed as a possibility by MacGregor and Wittkopp (1970) through their experimental work on the diopside-geikielite system.
- b. Discontinuous precipitation suggested by Dawson and Reid (1970). In this instance ilmenite is exsolved from a supersaturated Ti-rich clinopyroxene phase.
- c. Eutectoid transformation proposed by Ringwood and Lovering (1970). This is also a solid state reaction however, all three phases taking part in the reaction are structurally distinct. The reaction, proven experimentally, is a single garnet phase transforming at pressures less than 105 kb at 1000°C to ilmenite + clinopyroxene.

In terms of theoretical considerations, the equations for predicting interlammellar spacing as a function of undercooling are virtually identical for all three processes. Textures produced by the three mechanisms all look similar. Thus, a textural study alone will not aid in definitively answering the question of mechanism. Furthermore, the crystallographic relations observed between the pyroxene and ilmenite lamellae could be produced by any of the three processes mentioned above.

REFERENCES

Boyd, F.R., (1971), Carneg. Inst. Wash. Year Bk., 70, 134-138.

Boyd, F.R. and J.B. Dawson, (1972), Carneg. Inst. Wash. Year Bk., 71, 373-378.

Boyd, F.R. and P.H. Nixon, (1973) In press.

Brookins, D.G., (1971), Abstr. with Programs for 1971 (Geol. Soc. Amer.), 3, 233.

Dawson, J.B. and A.M. Reid, (1970), Contrib. Mineral. Petrol., 26, 296-301.

Harger, H.S., (1906), Trans. Geol. Soc. S. Africa, 8, 110-134.

MacGregor, A.M., J.C. Ferguson and F.L. Amm (1937), Bull. Geol. Surv. S. Rhodesia, 30, 1-175.

MacGregor, I.D. and R.W. Wittkopp (1970) Abstr. with Programs for 1970 (Geol. Soc. Amer.), 2, 113.

Mitchell, R.H., D.A. Carswell, A.O. Brunfelt and P.H. Nixon, (1973), In press.

Ringwood, A.E. and J.F. Lovering, (1970), Earth Planet. Sci. Lett., 7, 371-375.

Williams, A.F., (1932), The Genesis of the Diamond. 2 vol., E. Benn Ltd., London.

KIMBERLITIC DIATREMES IN NORTHERN COLORADO AND SOUTHERN WYOMING

M. E. McCallum, Dept. of Earth Resources, Colorado State University, Fort Collins, Colorado 80521

David H. Eggler, Geophysical Laboratory, 2801 Upton St., N.W., Washington, D.C. 20008

L. K. Burns, Dept. of Earth Resources, Colorado State University, Fort Collins, Colorado 80521

Since 1960, 36 kimberlitic diatremes and dikes have been discovered in the northern Front Range of Colorado and southern Laramie Range of Wyoming. The diatremes occur in three groups: a single pipe near Boulder, Colorado (Kridelbaugh and others, 1972); a cluster of 19 pipes approximately 120 km north of Boulder near the Colorado-Wyoming state line (McCallum and Eggler, 1968, and this report); and a group of 16 pipes and dikes 190 km north of Boulder at Iron Mountain (Farthing), Wyoming (W. A. Braddock, pers. comm., 1973). The diatremes penetrate Precambrian granitic rocks which comprise much of the cores of the Ranges. Local geologic setting and ages of sedimentary rock inclusions in many of the pipes indicate Middle Paleozoic (Late Silurian to Early Devonian) intrusion.

The pipes range from 3 to 550 m in longest dimension. Most are roughly circular to elliptical in surface outline. Larger pipes exhibit a greater degree of ellipticity, which is generally a reflection of joint control. The largest known diatreme (Sloan diatreme) is situated at the intersection of two prominent faults. Joint-controlled, kimberlitic dikes up to about 2 m in width are abundant at several of the Iron Mountain localities. On a regional scale, the north-south trend of pipe locations roughly parallels the eastern mountain front, and kimberlite emplacement may have been controlled by a deep-seated fracture system that also dominated the structural evolution of the Laramie and Front Ranges.

The cluster of 19 diatremes near the Colorado-Wyoming state line has been studied in considerable detail, including petrographic, X-ray, and electron microprobe techniques. Kimberlite is predominantly an intrusive breccia of subrounded to angular clasts in a finely-crystalline matrix of serpentine, calcite, dolomite, phlogopite, chlorite, talc, hematite, and perovskite. Clasts include individual grains of magnesium ilmenite, olivine, enstatite (rare), garnet, diopside, phlogopite, chromite, picotite, perovskite, magnetite, and serpentine pseudomorphs after olivine and enstatite; nodules of cognate kimberlite, spinel and garnet lherzolite, eclogite (rare), and carbonatite (sövite); and xenoliths of country rocks, including Precambrian crystalline rocks and blocks of fossiliferous Lower Paleozoic carbonates.

Cognate kimberlite and carbonatite (sövite) nodules are present in several pipes but are abundant only at the Sloan diatreme. Well-rounded kimberlite nodules are compositionally similar to host kimberlite, and commonly contain angular cores of sedimentary or granitic xenoliths. Carbonatite nodules range up to 25 cm in diameter and include biotite, phlogopite (?), and barite-rich varieties. Oxygen and carbon isotope data indicate an igneous origin for the carbonatite and for most of the matrix calcite in kimberlite (McCallum and Eggler, 1971).

Eight eclogite nodules have been found. Most are bimimetic, containing pyropic garnet (40-60 mole % Py) and omphacitic clinopyroxene

(28-43 mole % jadeite). Two eclogites contain accessory kyanite. Finely-crystalline interstitial material present in some samples is locally rich in Na_2O or K_2O and may contain minor secondary (?) kaersutitic amphibole or phlogopite. However, these eclogites lack the hydrous phases that characterize most of the Colorado Plateau eclogite inclusions of probable crustal origin (Essene and Ware, 1970). They are more similar to nodules from the Stockdale kimberlite in western Kansas (Meyer and Brookins, 1971) which, like these nodules, is interpreted to have come from the mantle.

Lherzolite nodules are relatively abundant in the diatremes, but most are altered to serpentine, hematite, and carbonates, and locally to talc and quartz. Both spinel and garnet-bearing varieties are present, and a few contain appreciable phlogopite. Many spinel lherzolites contain fresh olivine (Fo_{91}) and enstatite (En_{91}). However, in garnet lherzolites all olivine and enstatite have been replaced by serpentine, quartz, and hematite. Garnets are very pyropic (65-75 mole %) and have high Cr_2O_3 contents (3-11 weight %). Diopsides are also chromian; spinel lherzolite clinopyroxenes are more calcic than those from garnet lherzolites (Fig. 1).

Monomineralic inclusions have been classed into two groups, nodules and megacrysts, depending on whether the mean diameter is greater than 2 cm. Megacrysts include subcalcic diopside, garnet, and ilmenite. Diopside megacrysts show little compositional variation (Fig. 1) and are distinguished from monomineralic nodules and lherzolite diopsides chiefly by their low Cr_2O_3 content (0.20 wt %). Garnet megacrysts also show little chemical variation, with one exception (Fig. 1). The main group is characterized by higher Fe, much lower Cr, and somewhat higher Ti content than lherzolite garnets. Garnet megacrysts range up to 13 cm in length. Ilmenite megacrysts and ilmenite monomineralic nodules contain 25-50 mole % MgTiO_3 ; Mg-rich ilmenite megacrysts are enriched in Cr_2O_3 (about 3.0 wt %).

Monomineralic diopside nodules are very similar in composition to diopsides from lherzolite, and many are probably derived from disaggregated lherzolite. However, some are much larger than lherzolite phases, notably one megacryst from the Sloan pipe. Monomineralic garnet nodules probably have a variety of sources. Many purple chromian garnets are similar to garnets from lherzolite, while others resemble garnet megacrysts. A group of orange to pink garnets with less than 10 mole % Ca has variable Fe content but uniformly low content of TiO_2 (less than 0.15 wt %) and 2.0 wt % or less Cr_2O_3 .

All polymineralic nodules are considered to be accidental inclusions in kimberlite. Temperature and depth of equilibration of spinel lherzolite, estimated from the diopside-enstatite solvus (Davis and Boyd, 1966) and Al_2O_3 content of enstatite (MacGregor, in preparation), are about $850\text{-}950^\circ\text{C}$ and 50-65 km. From a geotherm passing through those points and temperature estimates from the diopside solvus and Fe-Mg distribution between clinopyroxene and garnet (Hensen, 1973), it is considered that eclogites equilibrated in the deep crust or in pockets in mantle below the crust (about 50 km, 850°C), and that garnet lherzolites have equilibrated at 60-100 km ($950\text{-}1250^\circ\text{C}$).

Certain chemical trends in the nodules and the large size of many megacrysts suggest that melting has occurred in the source region some time before inclusion of the nodules in kimberlite. Compositions of garnets and diopsides of lherzolites and associated monomineralic

nodules are consistent with the model of Boyd and Nixon (1973), whereby lherzolite nodules are subjected to varying degrees of partial melting before inclusion. Such depletion is reflected in Fe/Mg ratios and in Cr content, inasmuch as Cr is strongly partitioned into residual garnet or spinel. The large size of some chromian diopside nodules, noted above, suggests these nodules grew in the presence of melt. Olivine compositions, used with data on Fe-Mg partitioning between melt and crystals (assuming negligible Fe^{3+} content), indicate the melt was very magnesian ($Mg/Mg+Fe_{tot} = 0.75$).

On the other hand, diopside and garnet megacrysts could not have grown in such a melt, because they have low Cr contents and because they are more Fe-rich. The limited compositional variation of these megacrysts suggests they grew together in a batch of magma separated from host peridotite (Eggler and McCallum, 1973). The $Mg/Mg+Fe$ ratios of diopside (0.87) and garnet (0.77) indicate they have equilibrated at $1250^{\circ}C$ and that the melt (if a melt existed at $1250^{\circ}C$) had $Mg/Mg+Fe_{tot} = 0.67$. The melt may well have been alkaline, as diopside contains 1.4 wt % Na_2O ; the Fe/Mg ratio is consistent with an olivine basanite or melilitite composition. A magma temperature of $1250^{\circ}C$ is possible, inasmuch as it falls below the peridotite solidus, only if the mantle contained H_2O or H_2O+CO_2 . Ilmenite megacrysts, unlike diopside and garnet, show wide compositional variation, suggesting they were phenocrysts in a fractionating magma. Data on partitioning of Mg-Fe between ilmenite and silicates indicates the Mg-rich ilmenites could have been in equilibrium with garnet and diopside megacrysts. However, whether they grew from the same melt is problematic.

Summary. A north-south trending belt of kimberlitic diatremes in Colorado and Wyoming penetrated Precambrian crystalline rocks in the Middle Paleozoic. The intrusive breccia is interpreted to have come from a depth of at least 100 km through an upper mantle section consisting of garnet and spinel lherzolite and pockets of eclogite. The lherzolites have been melted before inclusion in kimberlite; a separate melt has precipitated megacrysts of chrome-poor diopside, garnet, and ilmenite. The pipes also contain distinctive nodules of sövite.

REFERENCES CITED

Boyd, F.R., and P.H. Nixon, 1972, Carn. Inst. Wash. Y.B. 71, p. 362-373.
 Davis, B.T.C., and F.R. Boyd, 1966, J. Geophys. Res., 71, p. 3567-3576.
 Eggler, D.H., and M.E. McCallum, 1973, Carn. Inst. Wash. Y.B., in press.
 Essene, E., and N.G. Ware, 1970, Geol. Soc. Amer. Abstr. Prog., 2, no. 7, p. 548.
 Hensen, B.J., 1973, Carn. Inst. Wash. Y.B., in press.
 Kridelbaugh, S.J., R. Hoblitt, K. Kellogg, and E.E. Larson, 1972, Geol. Soc. Amer. Abstr. Prog., 4, no. 6, p. 387.
 McCallum, M.E., and D.H. Eggler, 1968, Geol. Soc. Amer. Spec. Paper 121, p. 192.
 — 1971, Amer. Mineral., 56, p. 1735-1749.
 Meyer, H.O.A., and D.G. Brookins, 1971, Contr. Mineral. Petrol., 34, p. 60-72.

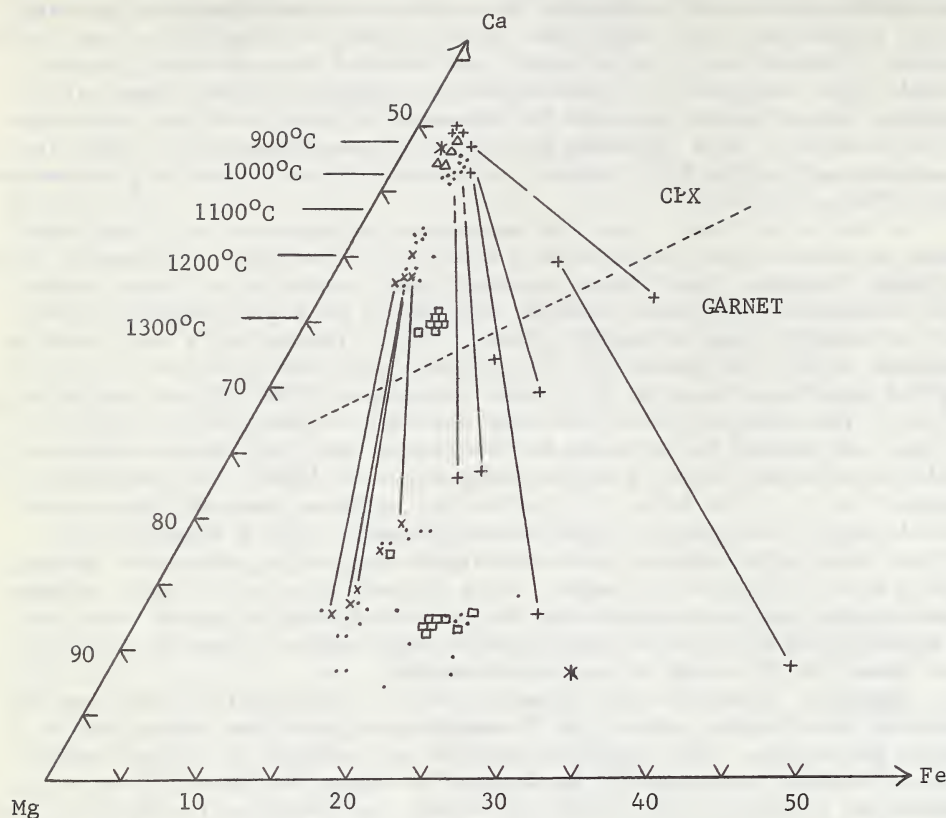


Fig. 1. Compositions of clinopyroxenes and garnets from Colorado-Wyoming kimberlitic diatremes, in mole per cent. Temperatures on diopside solvus are from Davis and Boyd (1966). Solid lines connect compositions of coexisting phases.

- monomineralic nodules
- monomineralic megacrysts
- △ spinel lherzolite
- ×
- ✗ garnet lherzolite
- * other inclusions
- +
- eclogites

A PALAEOMAGNETIC STUDY OF THE DE BEERS DIAMOND MINE
P.L. McFadden

Sampling

A technique has been devised which enables the collection of accurately oriented block samples for palaeomagnetic research from deep underground without recourse to magnetic methods, but utilizing the mine survey pegs. Twenty two such blocks have been collected from the De Beers Mine comprising fourteen samples of kimberlite (three being unusable), five samples of Precambrian Ventersdorp lava from the immediate contact with the kimberlite, two accidental inclusions of Ventersdorp lava and a sample of Ventersdorp lava well away from the contact with the kimberlite pipe. All of these samples were taken from the 585 and 595 m levels.

In addition results from five kimberlite samples collected in an earlier pilot study at higher levels have been included in the analysis. These samples were oriented by means of a Brunton compass

Direction and origin of the magnetisation

The kimberlite samples have been subjected to both alternating field and thermal demagnetisation. The directions of magnetisation after the application of these techniques are as follows.

Alternating field demagnetization in 5 to 20 mT; declination $D = 333,8^\circ$, inclination $I = -70,4^\circ$, $\alpha_{95} = 4,5^\circ$: thermal demagnetisation at 400°C ; $D = 332,2^\circ$, $I = -72,7^\circ$, $\alpha_{95} = 3,6^\circ$.

Here α_{95} is the angular radius of the cone of 95% confidence for the mean direction of magnetisation. Statistically these two directions are identical at the 95% confidence level. All samples showed stability of magnetic properties with respect to both alternating field and thermal demagnetisation. Although the direction obtained is very close to that of the present Earth's field at Kimberley ($D = 340,0^\circ$, $I = -65,3^\circ$) it is significantly different, and this supports the contention that the direction obtained was not acquired in the present Earth's magnetic field.

The directions of magnetisation of inclusions of Ventersdorp lavas and the lavas very close to the kimberlite contact were updated by the heating effects of the kimberlite intrusion. The direction of magnetisation of one inclusion ($D = 343,0^\circ$, $I = -72,1^\circ$) was identical to the kimberlite direction and the directions removed by demagnetisation of the lavas on the contact and the other inclusion were close to the kimberlite direction. This effect diminishes with distance from the contact (1).

It may therefore be concluded that the direction of magnetisation obtained is that of the Earth's field at the time of the kimberlite intrusion approximately 85 m.y. ago (2).

A Virtual Geomagnetic Pole may be calculated from this direction of magnetisation. However, the time during which this magnetisation was acquired was almost certainly less

than the time necessary to average out secular variation. As a result the pole calculated cannot be considered a palaeomagnetic pole (a full study, at present in progress, of several pipes is expected to yield a palaeomagnetic pole). The near pole, so calculated is at 53,8° E and 57,2° S which is close to the poles of the Mesozoic Quasi-Static Interval (3,4) of mean position 80,8° E and 64,5° S, the angle between them being 14,6°. This supports the radiometric age of 85 m.y.

Intrusion Temperature

An attempt has been made to determine a maximum for the temperature of the intruding kimberlitic material by analysis of the magnetic updating of the Ventersdorp lava contact. It was necessary to use a mathematical model of the kimberlite pipe and heat flow therein. On the basis of this model an emplacement temperature was calculated from the results of thermomagnetic experiments on Ventersdorp lava contact samples.

It was assumed that the magnetization of the specimens in question obeyed Neel's equation

$$\delta p = \frac{1}{C} e^{-\frac{E}{kT}} \delta t$$

where δp is the probability that a grain will reverse its magnetic moment in a time δt when at the temperature T K. E is the energy barrier that must be overcome for a reversal to occur, k is Boltzmann's constant and C is a frequency factor. This equation predicts the time required for the relaxation of a magnetic direction, the rock being at a temperature of T K. The frequency factor C is of the order 10^9 to 10^{10} . The value used in calculations has been 10^{10} as this gives a higher value for the emplacement temperature.

The model used for the kimberlite pipe was that of a dyke of rectangular cross-section (220 m x 29 m) and infinite vertical extent. These values were chosen to give the same length and area as the pipe at the 590 m level. The amount of kimberlitic material involved was therefore the same. It was assumed that the latent heat of solidification of the material was negligible, that the thermal properties of the kimberlitic material, solidified kimberlite and country rock were the same and that the effects of transport of heat by volatiles from the kimberlite and of convection in the kimberlite were negligible. It was assumed that the kimberlite was intruded into the rectangular cross-section at a uniform temperature, the country rock being at 20°C. Under these conditions an analytical solution for the differential equation of heat flow exists (5).

Thermomagnetic analysis of lava specimens actually on the contact with kimberlite shows that these specimens contain a considerable number of magnetic grains which are still magnetised in the Ventersdorp direction. Thermal

demagnetisation at a temperature less than or equal to 550°C will therefore remove the kimberlite direction from these specimens. An iterative numerical integration of the solution given in (5) was performed to determine the emplacement temperature which would, according to Neel's equation, have had the same magnetic effect as laboratory thermal demagnetisation at a temperature of 550°C . The result obtained implies an emplacement of temperature of less than 620°C .

The simplifying assumptions made above all affect the calculations in such a manner as to give a result for the emplacement temperature which is too high (6,7). The temperature given above is therefore an upper limit.

Further thermomagnetic analysis in progress in an attempt to determine the temperature which is actually required to remove the kimberlite direction of magnetisation. Results of these experiments may give an upper limit to the emplacement temperature even lower than 620°C .

- (1) D.L. Jones, M.E.R. Walford and A.C. Gifford, *Nature*, 2, 155-158, 1967.
- (2) D. Barrett & H. Allsopp, personal communication.
- (3) J.C. Briden, *Nature*, 215, 1334-1339, 1969.
- (4) M.W. McElhinny, J.C. Briden, D.L. Jones & A. Brock, *Rev. Geophys.*, 6, 201-238, 1968.
- (5) Carslaw H.S. & Jaeger J.C., 1959, Conduction of heat in solids, 2nd ed.: Oxford, Oxford University Press.
- (6) J.C. Jaeger, *Am. J. Sci.*, 255, 306-318, 1957.
- (7) J.C. Jaeger, *Am. J. Sci.*, 257, 44-54, 1959.

MINERAL INCLUSIONS IN BRAZILIAN DIAMONDS

Henry O.A. Meyer: Department of Geosciences
Darcy P. Svisero*: Purdue University, West Lafayette
Indiana 47907, U.S.A.

Natural diamonds are generally considered to be the products of stable growth (e.g. Kennedy and Nordlie, 1968). On this assumption it has been argued (Meyer and Boyd, 1972) that many crystalline inclusions in diamond represent original phases which formed in equilibrium with diamond. Detailed chemical examination of these minerals should provide valuable data pertinent to both the genesis of diamond and kimberlite.

Recent studies of mineral inclusions in diamonds from South Africa, West Africa, Venezuela, and Thailand (Meyer and Boyd, 1972) and from Siberia and the Urals (Sobolev et al., 1973) have shown a remarkable similarity in the compositions of the various minerals. Furthermore, the inclusions (olivine, enstatite, diopside, garnet, chromite) although generally similar to their counterparts in kimberlite, and associated xenoliths, have elemental abundances that are distinct in detail.

In an attempt to extend the present geographic coverage of diamonds and their inclusions we have examined specimens from Brazil. In general, these new results are in agreement with earlier observations. In addition we have analyzed rutile, ilmenite, pyrrhotite, zircon and quartz, all of which occur as inclusions.

Diamonds have been found in Brazil since about 1725 but no kimberlite has been recorded. Mostly the diamonds are found in river placer deposits throughout several areas, mainly in the states of Minas Gerais, Mato Grosso, Goias, Bahia, Parana and Para. In east-central Brazil (Diamantina in Minas Gerais and Chapada Diamantina in Bahia) the diamonds are associated with meta sediments; conglomerates, arenites, phyllites and quarzites, of upper Pre-Cambrian age.

In contrast the other major region of diamond production is associated with the large sedimentary Parana basin in south central Brazil. Devonian and Carboniferous arenaceous sediments form the rim of the basin and are unconformable on Pre-Cambrian basement rocks. The diamond placer deposits are predominantly found in the rivers draining the Devonian and Carboniferous strata.

The specimens examined in this study are from diamonds obtained in both of the above regions. Morphologically the diamonds are complex but most are characterized by the predominance of dodecahedral forms and a large number of contact twins. Infrared studies showed that about 95% of the diamonds examined are of Type I. The specific gravity of the diamonds varied between 3.500 and 3.530 g/cm³, and trace elements detected by spectrographic emission analysis include Al, Ca, Mg, Si, Fe, Cu and Cr. The inclusions were

released by cracking the diamond host in a small enclosed container.

Olivine - Olivine is the most common inclusion observed. Compositionally, the olivines are similar to previously reported analyses (Table 1). They are characterized by a small range in composition (Fo_{92} to Fo_{95}), low contents of the minor elements Al, Ca, Mn and Ni, and the high values (up to 0.10 wt.%) of Cr_2O_3 .

Enstatite - Enstatite appears to be more common in Brazilian diamonds than in others previously examined. The present analyses, however, agree closely with those of enstatite inclusions from other localities. The enstatite molecule ($MgSiO_3$) accounts for 93 to 94% of the total mineral, with very little solid solution towards diopside. Both Cr_2O_3 and Al_2O_3 contents are low (Table 1).

Clinopyroxene - In keeping with earlier observations clinopyroxenes are comparatively rare as inclusions in diamond. In this study two inclusions of diopside (high Ca, Mg, and Si) were identified by means of energy dispersive techniques. Unfortunately, both inclusions were very small, $<30\mu m$, and were lost during polishing.

Garnet - Garnet appears to be the second most common inclusion in Brazilian diamonds. Two distinct suites occur: Cr-rich, Ca-poor pyrope; and Fe-rich, Cr-absent almandine-pyrope (Table 1). In general the garnets from Brazilian diamonds are similar to those previously examined from other world wide localities.

Rutile - Rutile has been observed as an inclusion in diamond by Harris (1968) and Gurney et al. (1969) using x-ray diffraction methods. We have analyzed rutile from Brazilian diamonds (Table 1) and find it to be extremely pure with less than 0.4 wt.% of other oxides.

Ilmenite - Ilmenite was found in two diamonds. The ilmenite appears to be close to stoichiometry (Table 1); manganese being the major impurity (0.7 wt.% MnO). This composition contrasts markedly that of ilmenite occurring as xenocrysts and in xenoliths in kimberlite. This latter ilmenite has an appreciable content of MgO.

Zircon - Zircon is not uncommon as a mineral in kimberlite but this is believed to be the first record of its occurrence as an inclusion in diamond. The zircon appears very pale brown in color and is slightly elongated. The analyses (Table 1) indicate the zircon to consist almost entirely of Zr and Si with very low contents of minor elements.

Quartz - Quartz and coesite have at various times been considered as inclusions in natural diamonds (Milledge 1961; Harris 1968; Orlov 1959). In this study we have also obtained an inclusion of quartz. The specimen was colorless and had well developed faces. The identification was substantiated by both single crystal x-ray diffraction methods and by electron microprobe analysis.

Sulfides - Sharp (1966) has described troilite and pentlandite as being relatively common among opaque inclusions.

Table 1: Representative analyses of inclusions from
Brazilian diamonds

	Olivine	Enstatite	Pyrope	Almandine	Rutile	Zircon	Ilmenite
SiO ₂	41.3	57.6	41.5	40.5	0.06	31.1	0.22
TiO ₂	<0.01	<0.01	<0.01	0.86	99.8	0.03	50.1
Al ₂ O ₃	<0.01	0.78	16.7	19.6	0.30	-	0.15
Cr ₂ O ₃	0.05	0.47	9.42	0.20	0.16	-	0.03
FeO	7.98	4.36	6.07	16.0	0.21	0.01	48.0
MgO	50.1	36.2	23.4	13.1	0.02	-	0.16
CaO	0.03	0.47	2.30	8.39	<0.01	0.01	<0.01
MnO	0.11	0.11	0.33	0.34	<0.01	0.02	0.74
NiO	0.40	-	-	-	-	-	-
ZrO ₂	-	-	-	-	-	69.7	-
	100.0	100.0	99.7	99.0	100.5	100.9	99.4

Harris (1968) mentions the identification of pyrrhotite and pentlandite. In the Brazilian diamonds the inclusions are opaque, small and irregular in shape. Analyses confirmed the sulfide as being pyrrhotite.

The results presented above are in agreement with earlier studies of mineral inclusions in diamond. For example, many of the silicates are remarkably uniform in composition irrespective of provenance and age. Olivine and chrome-pyrope are the most abundant inclusions. Furthermore, several inclusions are grossly similar in compositions to their counterparts in ultramafic rocks whereas others are similar to the constituent minerals of eclogite.

The rarity of clinopyroxene inclusions is surprising in view of the abundance of this mineral in kimberlite and associated xenoliths. In the Brazilian diamonds the assemblage olivine + garnet + enstatite is present. Using the data of MacGregor (1973) and Boyd and Nixon (1973) it can be argued that clinopyroxene did not coexist with enstatite in diamond.

The occurrence of pure ilmenite as an inclusion is puzzling, especially so when one considers all kimberlitic ilmenites have relatively high contents of MgO. Mitchell (1973) comments that perhaps magnesium ilmenites might be phenocrystal in origin and unrelated to kimberlite genesis. One could extend the argument to include diamond genesis.

Similarly the presence of quartz is also enigmatic. Harris (1968) stresses the fact that quartz is an inclusion and states that "...no obvious fractures emanate from the specimen to the diamond surface." However, in spite of this Harris considers quartz to be epigenetic on the basis of his criteria that many included minerals do not have

stability fields at the conditions envisaged for diamond synthesis. Undoubtedly the time has come to critically appraise the criteria by which we decide what are primary or secondary inclusions.

*Permanent Address: Instituto de Geociencias
Universidade de Sao Paulo
Sao Paulo, Brazil

References

Boyd, F.R. and P.H. Nixon (1973), In press.

Gurney, J.J., J.C. Siebert and G.G. Whifield (1969), Trans Geol. Soc. S. Afr., Spec. Publ. No 2, 351-357.

Harris, J.W. (1968), Industrial Diamond Rev., London, pp. 402-410, 458-461.

Kennedy, G.C. and B.E. Nordlie (1968), Econ. Geol. 63, pp. 495-503.

MacGregor, I.D. (1973), Amer. Mineral., In press.

Meyer, H.O.A. and F.R. Boyd (1972), Geochim. Cosmochim. Acta, 36, 1255-1273.

Milledge, H.J. (1961), Nature, 190, 1181.

Mitchell, R.H. (1973), In press.

Orlov, Yu.L. (1959), Mineralog. Mus. Acad. Sci. U.S.S.R., Trans. (In Russian), No. 10, 103-120.

Sharp, W.E. (1966), Nature, 211, 402-403.

Sobolev, N.V., Yu.G. Lavrent'ev, N.P. Pokhilenko and L.V. Usova, (1973), Contr. Mineralog. Petrol., 40, 39-52.

STRUCTURE PROBLEMS OF GENESIS AND PREDICTION OF
KIMBERLITE PROVINCES

V.A. MILASHEV

(Research Institute of the Geology of the Arctic,
Leningrad, USSR)

1. Kimberlite, picrite rocks and carbonatites were formed by specific processes in the upper mantle of platform areas. Results of study of structure and development regularities of these rocks, physico-chemical conditions of their appearance and production of their melts allow to refine our understanding about main substrate characteristics major tendencies and trend of its evolution.

2. The largest genetically single units of platform ultrabasic volcanic areas are provinces exhibiting in all the case concentric-zonal structure. In central parts of provinces as a rule there are oldest kimberlites of diamond subfacies, in mesozone kimberlites of diamond and pyrope subfacies occur together, near the periphery there are youngest kimberlites of "purely" pyrope subfacies and picrites while at margins only rocks of picrite facies, carbonatites and in places complexes of intrusive alkaline and alkaline-ultrabasic rocks. In kimberlite provinces locating on platform margins and near rift areas central zone (diamond subfacies) is absent or poorly developed while peripheral zone usually of large dimensions. Kimberlite provinces of such a type are called semizonal. In number and resources of diamond primary deposits they yield to holozonal provinces.

3. Kimberlite melts were emplaced in mobilized blocks of superheated, low-density matter of the upper mantle embraced by ascending convective currents. In near axial parts of currents where mobilized substrate had highest temperatures melts were generated (produced) at maximum depths while in peripheral zones of currents melting occurred at higher horizons. Radial movement of magma chambers and differentiation of melts followed the mechanism of partial melting.

4. Evolution of kimberlite melts of diamond subfacies occurred at much higher parameters than that of kimberlite melts of pyrope subfacies. During subcrustal period their temperature was on the average 1800 and 1500°C while minimum pressure was 45 and 20 kb respectively. Picrite magmas generated and evolved at pressure below 20 kb.

5. Main differences of energetic balance, contrast and degree of differentiation of melts producing kimberlites of different subfacies and picrite rocks were established. Minimum values of all these characteristics are typical of kimberlite melts of diamond subfacies while maximum for the group of picrite rocks.

6. Rocks of differnet facies differ in average contents not only of rock-forming but volatile components as well as autometamorphism regime and so in kimberlite zone of subfacies are found only serpentine-carbonate metasomatites while around the periphery of provinces fresh monticellite and melilite kimberlites and picrites are common.

7. A model of the upper mantle matter obtained by multidisciplinary study of kimberlites is close to an average composition of nodules of garnet peridotites in kimberlites differing from them in lower Mg content and higher concentrations of other rock-forming elements.

8. The rise to lithosphere base and subsequent tangentianal diffluence of heated matter from the mantle depth were accompanied by the drop of temperature and considerable increase of its viscosity. According to attenuation of "volcanism" rate from central to intermediate and from intermediate to peripheral zones of the Yakut province the value of dynamic viscosity coefficients of mobilized substrate is evaluated as $2.6 \cdot 10^{23}$ and $9.8 \cdot 10^{23}$ poises on each of these parts respectively.

9. The period of building of each kimberlite province determined by the difference in age of kimberlites in central and peripheral zone is about 250 m.y. Evolution of kimberlite volcanism with time and space was not limited to period of formation and area of separate diamond provinces. There is a certain cyclicity of kimberlite volcanism on the territory of separate regions that is a subsequent formation of adjacent with space kimberlite provinces of different age with the interval of about 1 billion years. Volcanism of each of these cycles is characterized by a number of peculiar features.

10. Along with concentrical - zonal distribution of rocks of different facies within each kimberlite provinces (macrozonality) there is megazonal structure of kimberlite areas reflected in the existence of peculiar features in kimberlite provinces located inside and on the margins of supercontinents of Gondwana and Laurasia.

11. The most favourable for kimberlite formation were large platforms located in the inner parts of supercontinents. Gondwana and Laurasia for mantle processes responsible for platform magmatism were there more intensive. In the middle of Gondwana there was a southern half of Africa while in the middle of Laurasia a territory of the Siberian platform. The both regions are characterized by maximum development of kimberlites as compared to other areas of corresponding continents.

12. On the basis of regularities recognised it seems possible to predict location, age, and type and consequently diamond possibilities of new kimberlite. From 10 predicted and not yet discovered kimberlite provinces four are within Africa, three in Siberia and one on the Russian platform, one in South America and one in Australia.

THEORETICAL ASPECTS OF GASEOUS AND ISOTOPIC EQUILIBRIA IN
THE SYSTEM C-H-O-S WITH APPLICATION TO KIMBERLITES

Roger H. Mitchell

Dept. of Geology, Lakehead University, Thunder Bay, Ont., Canada.

Real gas equilibria are evaluated by assuming that continuous equilibrium is established between graphite or diamond and a gas phase whose composition lies within the system C-H-O-S. It is further assumed that CO_2 , CO , CH_4 , H_2O , H_2S , H_2 and SO_2 are the major species formed and that formation of hydrocarbons more complex than CH_4 is limited. Following the methods of French (1966) the partial pressure (P_i) of any species at any T and P can be calculated if f_{O_2} , f_{S_2} , fugacity coefficients and equilibrium constants are known for the following reactions:-

(1) $\text{C} + \text{O}_2 = \text{CO}_2$; (2) $\text{C} + \frac{1}{2}\text{O}_2 = \text{CO}$; (3) $\text{C} + 2\text{H}_2 = \text{CH}_4$
 (4) $\text{H}_2 + \frac{1}{2}\text{O}_2 = \text{H}_2\text{O}$; (5) $\frac{1}{2}\text{S}_2 + \text{O}_2 = \text{SO}_2$; (6) $\frac{1}{2}\text{S}_2 + \text{H}_2 = \text{H}_2\text{S}$
 Thus if f_{O_2} and f_{S_2} for a given magma can be determined from the mineral assemblages present it is possible to calculate the composition of the gas phase in equilibrium with that magma if it contains carbon as graphite or diamond. Gas equilibria are discussed here for the rapid expansion phase of kimberlite emplacement from high pressures (2-10 kbs) to low pressure (1 kb) over the temperature range $800-600^\circ\text{C}$, i.e. essentially during the time of formation of the groundmass.

Oxygen fugacities are calculated for the groundmass assemblage olivine+magnetite+liquid by the quartz-fayalite-magnetite buffer. Silica activities for this buffer are defined by the akermanite-forsterite-diopside buffer (Mitchell 1973). Sulfur fugacities are estimated to be on the order of 10^{-5} bars (coexisting magnetite and pyrite) but calculations are extended to cover a wide range in f_{S_2} .

During the last stages of kimberlite emplacement it is considered that P variation is more important than T variation, overpressures being responsible for the fluidized gas drive. Figure 1 shows the calculated composition of the gas phase up to 10 kbs., over a T range of 200°K . Prefluidized conditions in pools of kimberlite magma in the lower crust are considered to be within the $1000-1100^\circ\text{K}$, 4-10 kb., portion of the diagram. The most important conclusions to be drawn from the calculations are that over much of the PT range H_2O is the dominant gas and that the proportions of CH_4 to CO_2 can vary widely, falling P at constant T promoting an increase in CO_2 content. The dominant phases during fluidized intrusion are H_2O , CO_2 and CH_4 . As P falls to the post fluidized conditions of the groundmass it can be seen that CH_4 still makes up a considerable percentage of the fluid phase, however low pressures favour a fluid phase composed essentially of H_2O and CO_2 , this conclusion being in accord with the extensive serpentinization and hydration of primary

minerals and the formation of late stage carbonates. Under all conditions of fs_2 , P_{H_2S} is very much greater than P_{SO_2} and H_2S becomes the dominant gas in the C-H-O-S system when fs_2 reaches 10° bars. SO_2 is at all times a minor component. The presence of abundant CH_4 in the fluid phase is in agreement with Kogarko's (1972) calculated fluid phase composition of agpaitic syenites (Table 1) at low pressures. Coexistence of high partial pressures of CH_4 and CO_2 would thus seem to be a feature of both sodic and potassic alkaline rocks.

Table 1. Comparison of gas compositions of kimberlite and Lovozero nepheline syenite (Kogarko 1972) at 1 kb.

C-H-O-S Log. partial pressure

Gas	Kimberlite	Syenite
CO_2	2.48	1.91
CO	0.74	-0.21
CH_4	1.89	2.50
H_2O	2.76	2.52
H_2	1.17	1.15
H_2S	1.41	2.78
SO_2	-5.69	-5.76
fo_2	-20.38	-23.79
fs_2	-5.0	-3.75
T C	627	525

Isotopic studies have shown that diamonds are not of uniform isotopic composition i.e. world wide variation in $\delta^{13}C$ is from -1.9 ‰ to -9.7 ‰ with up to 3 ‰ variation being found in a single pipe (Vinogradov and Kropotova 1967). The natural isotopic variations require that diamonds form in an environment where isotopic fractionation can occur. Deep in the mantle at high P and T fractionation should be negligible. Mitchell and Crocket (1971) have proposed that some diamonds can form metastably by gas reduction mechanisms in the lower crust, the diamond growing on diamond seed nuclei prior to fluidized intrusion. Under these conditions carbon isotopic fractionation between carbon bearing gases is appreciable e.g. at 1000°K the isotopic composition of CH_4 and CO_2 differ by 10 ‰. For solid phases i.e. graphite or diamond forming by gas reduction from carbon bearing gaseous species one can write:-

$$\delta^{13}C_{\text{graphite}} = \delta^{13}C_{\text{C}_2\text{C}} - [(\Delta CO_2 \cdot x CO_2) + (\Delta CO \cdot x CO) + (\Delta CH_4 \cdot x CH_4)] \quad (7)$$

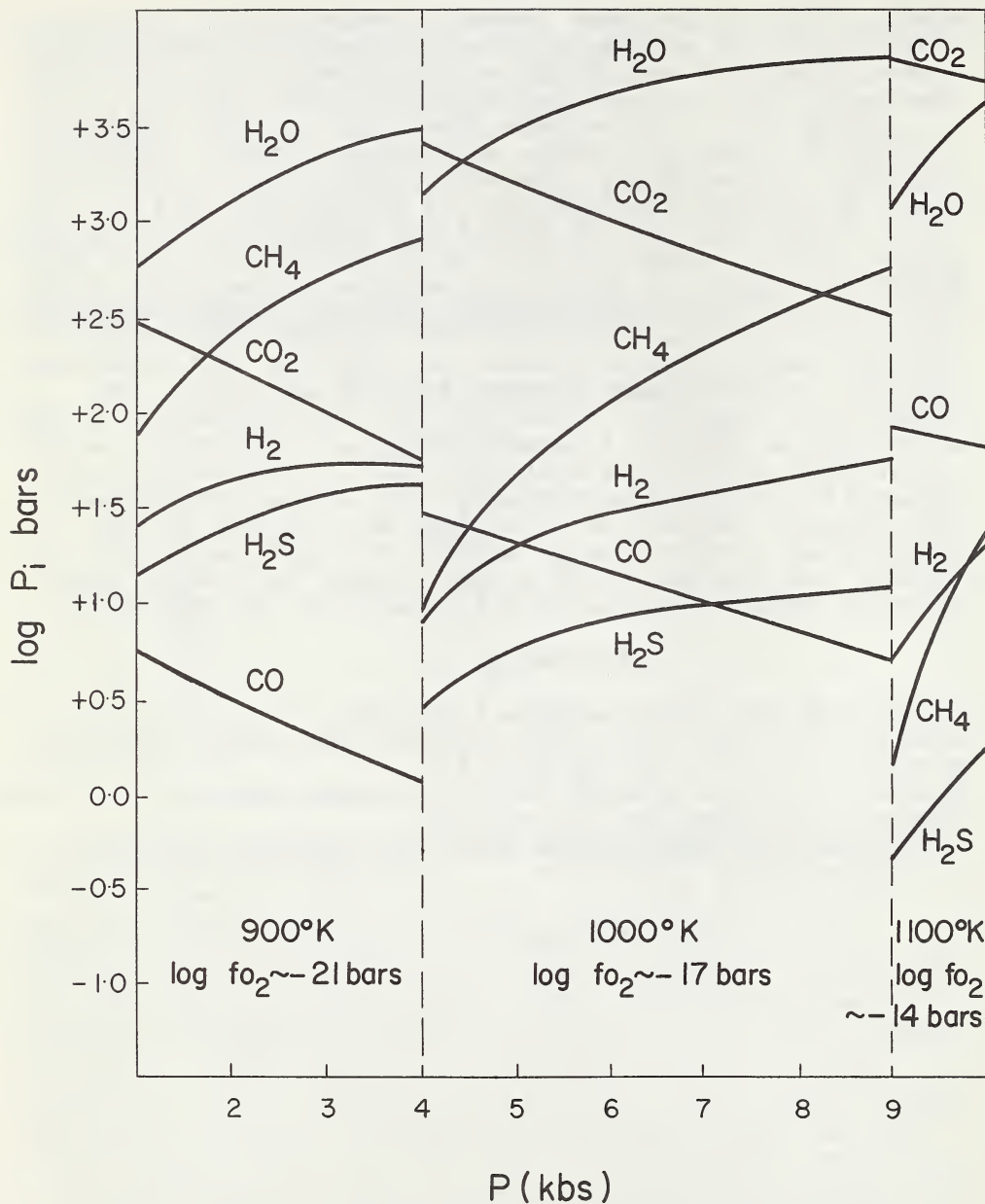
$$\delta^{13}C_{\text{diamond}} = \delta^{13}C_{\text{graphite}} + \Delta_{\text{diamond}} \quad (8)$$

where $\delta^{13}\text{C}_{\text{zC}}$ is the mean isotopic composition of the fluid phase, Δ_i and X_i are the relative isotopic enrichment factors between species i and graphite and the mole fraction of the species in the gas phase respectively (Ohmoto 1972).

Substitution of the data from figure 1 into equations (7) and (8) gives the change in isotopic composition of graphite or diamond with changing composition of the fluid phase in response to variations in $P, T, f_{\text{CO}_2}, f_{\text{S}_2}$. The calculations show that at 1000°K and 5-10 kb a 6 ‰ change in the isotopic composition of the reduced solid phase can occur. This change is largely in response to variation in the CH_4/CO_2 ratio of the parent gases. The calculated isotopic variations can thus account for the observed variation in isotopic composition of diamond and predicts that extensive variation will be found in the isotopic composition of kimberlitic graphites. A problem with the hypothesis is that it is unknown whether a metastable phase (diamond) can exist in isotopic equilibrium with the material from which it formed. If isotopic equilibrium is not allowed the spread in the isotopic composition of diamond must be due to non-equilibrium kinetic isotope effects. The hypothesis also assumes that the amount of carbon present as a solid phase is small compared to the amount present in the gas phase.

References

French, B.W. 1966. *Rev. Geophys.* 4, 223-253.
 Kogarko, L.N., 1972. *Proc. 24th Internat. Geol. Cong.* v. 10, 20-24.
 Mitchell, R.H. 1973. *Lithos*, 6, 65-81.
 Mitchell, R.H., and Crocket, J.H. 1971. *Mineral. Deposita* 6, 392-403.
 Ohmoto, H. 1972. *Econ. Geol.* 67, 551-578.
 Vinogradov, A.P., and Kropotova, O.I. 1967. *Internat. Geol. Rev.*, 10, 497-506.



RARE EARTH ELEMENT GEOCHEMISTRY OF KIMBERLITE

Roger H. Mitchell^{*} and Arild O. Brunfelt

Mineralogisk-Geologisk Museum, Sarsgate 1, Oslo 5, Norway.

*Dept. of Geology, Lakehead University, Thunder Bay, Ont. Canada.

Seven rare earth elements (REE) have been determined in kimberlite (Wesselton) and micaceous kimberlite (Swart-ruggens) by neutron activation analysis (Table 1). Chondrite normalized REE distribution patterns are essentially linear. Micaceous kimberlites have slightly higher REE abundances and are slightly more fractionated than kimberlites, average La/Yb ratios are 139 and 103 respectively. A small negative Eu anomaly is evident in the micaceous kimberlite data (figure 1). REE whole rock abundances and distribution patterns are considered to reflect the proportions of apatite, perovskite and carbonate present, the weak Eu anomaly being due to the presence of perovskite (Eby 1972).

Although the degree of enrichment of light REE in kimberlite is similar to that observed in oceanic and continental nepheline and melilite bearing basalts (Schilling and Winchester 1969, Hermann 1968) the REE distribution patterns are markedly different and do not support any relation between kimberlites and melilitites as proposed by Frey et al. (1971).

The REE data can be considered in terms of two groups of petrogenetic theories, partial melting and eclogite crystallization.

Partial melting of a garnet lherzolite mantle in which only the low melting point fraction, garnet and clinopyroxene is involved is considered as these phases dominate the alkali and alkaline earth geochemistry of such rocks. Following Gast (1969), REE crystal-liquid distribution coefficients are used to calculate the La/Yb ratios of liquids produced by varying amounts of partial melting. La/Yb ratios of kimberlites and micaceous kimberlites can be produced by 0.7 - 0.9% and 0.3 - 0.4% melting of garnet lherzolite respectively. The liquids produced are however poor in La and Yb relative to the actual abundances found and it is postulated that further processes e.g. crystallization of REE free phases acts to increase the REE abundances without further fractionation of the REE.

The effects of high pressure bimimetic eclogite crystallization from a magma of basaltic composition are analysed using the fractional crystallization models of McIntire (1963) to calculate the La/Yb ratios of residual liquids after the separation of eclogites of differing modal compositions. Fractionation of eclogite (Cpx-50, Gnt-50) will only produce kimberlite if greater than 96% of the liquid has crystallized. Removal of eclogite (Cpx-20, Gnt-80)

requires 88-94% crystallization for derivation of kimberlite from tholeiitic parents but only 48-64% crystallization for alkaline olivine basalt parents. La and Yb abundances, as in the partial melting model again do not reach levels found.

The models do not unequivocably point to partial melting or eclogite crystallization as a means of generating the kimberlite REE abundances and distributions. Eclogite crystallization models are however considered to be unlikely on geological grounds, namely, the extensive degree of crystallization required, the known distribution, age and mineralogy of eclogite and garnet lherzolite xenoliths in kimberlite, the lack of the minerals of eclogite as inclusions in diamond and the lack of extensive compositional range in kimberlite olivines. The REE geochemistry of kimberlites is thus considered to be the result of partial melting processes. As a consequence of the small volumes of liquid involved it is likely that most kimberlite remains trapped in the mantle. Partial melting processes thus can explain the rarity and small volume of kimberlite. The relation of kimberlites to basaltic volcanism and continental magmatic cycles can be explained in terms of partial melting and the following thermal cycle. Initially an increase in heat flow results in extensive (15%) partial melting of the undepleted mantle to produce basaltic, (tholeiitic) volcanism. Waning of the heat flow results in a smaller degree of partial melting and generation of undersaturated basaltic magmas together with migration downwards of the zone of melting (Ringwood 1969). Finally at the lowest levels of heat flow and greatest depth a small amount of partial melting, one per cent or less forms kimberlitic liquids over a very broad zone. Only those liquids lying in regions where large scale tectonic features penetrate to depth are able to escape. Micaceous kimberlites represent the very last stages of the cycle and they are consequently rare relative to kimberlite. Kimberlites are not found in oceanic areas as heat flow is too great to allow limited partial melting.

References

Eby, G.N., 1972. Unpub. Ph.D. Thesis, Boston University.
 Frey, F.A., Haskin, L.A., Haskin, M.A., 1971. J. Geophysical Res. 76, 2057-2070.
 Gast, P.W., 1969. Geochim. Cosmochim. Acta, 32, 1057-1086.
 Hermann, A.G., 1968. Contrib. Min. Pet. 17, 275-314.
 McIntire, W.L., 1963. Geochim. Cosmochim. Acta, 27, 1209-1264.
 Ringwood, A.E., 1969. Amer. Geophys. Union Monogr. 13, 1-17.
 Schilling, J.G., and Winchester, J.W., 1969. Contrib. Min. Pet. 23, 27-37.

Table 1. Rare earth content of kimberlites (ppm)

#	La	Ce	Sm	Eu	Tb	Yb	Lu	La/Yb
Wesselton	106	239	13.7	3.28	1.21	1.09	0.13	97
	90	191	12.7	2.98	1.09	1.01	0.11	82
	205	455	28.2	6.57	2.72	2.55	0.28	80
	112	265	14.2	4.05	1.49	1.16	0.14	96
	15	209	550	28.2	7.96	3.35	1.71	0.24
average	196	481	26.9	7.42	2.44	1.53	0.39	137
	153	363	20.6	5.38	2.05	1.48	0.18	128
Swartruggens	254	588	24.0	5.68	2.45	2.65	0.28	96
	259	439	25.1	4.91	1.96	0.95	0.17	132
	238	378	22.9	4.10	1.80	1.24	0.17	192
	230	440	21.6	4.36	1.95	1.68	0.13	137
	245	461	23.4	4.76	2.04	1.63	0.18	139
Monastery	97	243	12.6	3.70	1.30	0.99	—	98
	114	226	10.3	2.69	0.66	0.68	0.08	168
Ison Creek	63	107	5.6	1.28	0.44	0.45	—	140
Somerset I.								

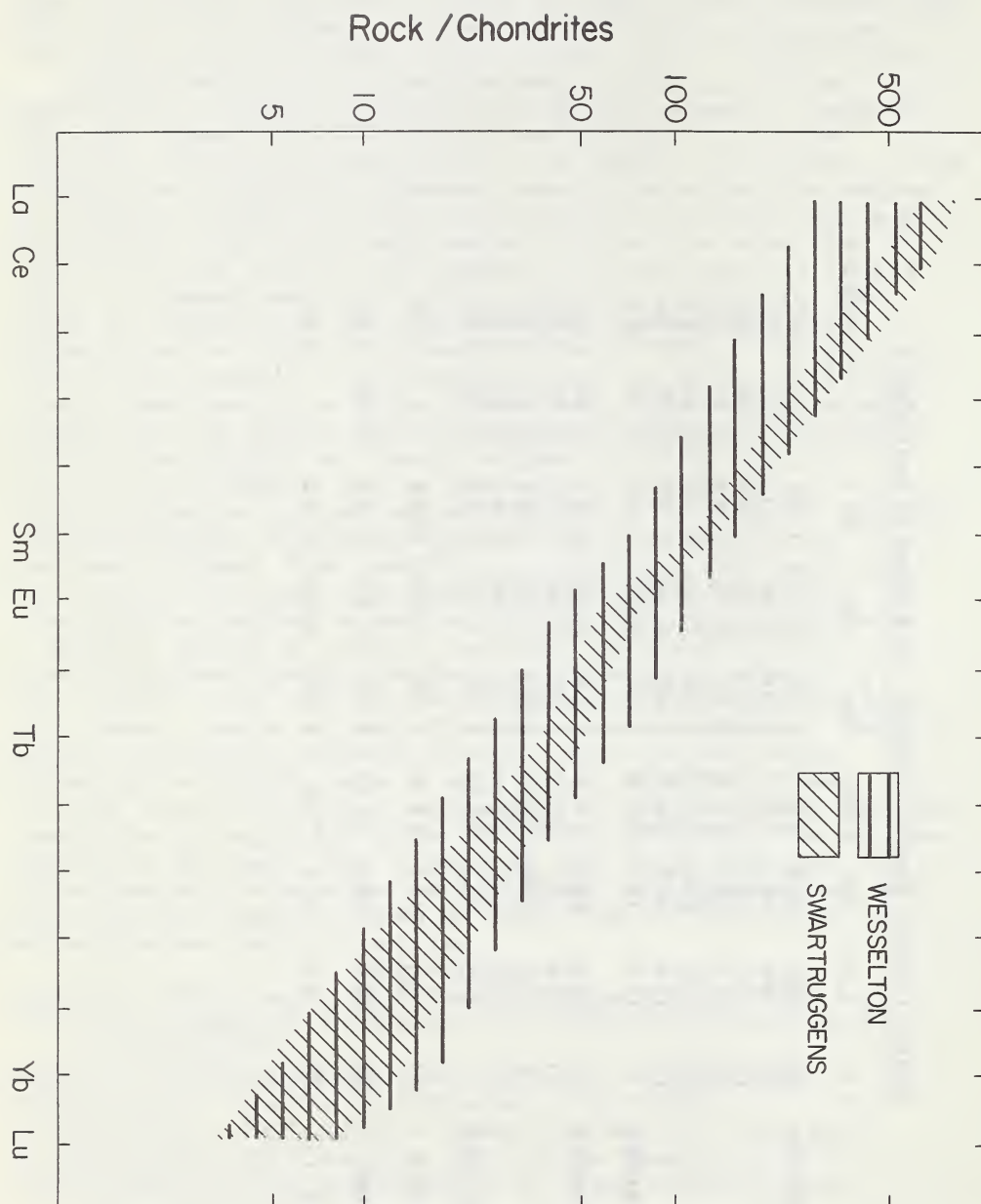


Figure 1. Distribution of REE in kimberlite (Wesselton) and micaceous kimberlite (Swartruggens).

THE OLIVINE MELILITITE - KIMBERLITE ASSOCIATION OF NAMAQUALAND

By

A. E. Moore
Department of Geochemistry, University of Cape Town.

In the Namaqualand-Bushmanland area of South Africa are a large number of diatremes and plugs, representing the youngest phase of volcanism on the sub-continent. They form a dense cluster about the village of Gamoep, in Bushmanland, whilst isolated but apparently related occurrences are found in the vicinity of Bitterfontein in the south ($31^{\circ}10'S$ $18^{\circ}15'E$), and Aggenys to the north ($29^{\circ}10'S$ $18^{\circ}50'E$). These latter are separated by some 70 km. and 40 km. respectively from the main Gamoep cluster. The overall distribution follows a roughly NNE-SSW trend, over a distance of some 200 km.

The diatremes occur on surface as slight depressions, usually accompanied by abundant calcrete. Some are filled with sediment up to depths of 800 ft. Dinosaur fossils from the sediments suggest an Upper Cretaceous age. Recovery of chrome-diopside, pyrope, garnet and ilmenite from borehole concentrates has led to the classification of these diatremes as kimberlites, although, despite extensive prospecting, they have not yielded a single diamond. Such classification is therefore debatable.

Associated with some of the sediment-filled pipes are spectacular breccia necks, composed exclusively of large block of a variety of gneisses. These postdate the sediments, which in places have been forced between the agglomerate blocks.

The volcanic plugs occur as prominent rounded hills in the same general area as the "kimberlites". They include olivine-nephelinites, olivine-nepheline-melilitites and olivine melilitites. A single radiometric date - from a pipe near Bitterfontein - yields an age of 38,5 million years. This is apparently younger than the "kimberlites", but compares closely with a value of 35,7 million years obtained for the phonolites of the Klinghardt mountains of southern South West Africa, (Kröner, 1973).

Major and trace element analyses have been carried out on these Oligocene volcanic of Namaqualand-Bushmanland and have shown significant geochemical variations across the Province.

The most northerly plug studied is markedly enriched in MgO (21%), is highly undersaturated ($35,2\%$ SiO_2), and is best described as a feldspathoid-free phlogopite-perovskite picrite. It contains dunite inclusions, as do a number of other plugs in the north, and has also yielded small xenoliths of chromiferous garnet lherzolite, very similar to those found in kimberlites. Mineral analysis of one of the four phase inclusions (Hox), is given in Table 1. The most important observations are the following:

Olivine composition is Fo_{91} . The garnets are similar in composition

to chromiferous kimberlite varieties, though slightly richer in Ca relative to Cr, and poorer in Mg. (Gurney, pers. comm.). Clinopyroxenes have a Ca/Ca+Mg ratio of 0,47, which is slightly higher than corresponding Matsoku values (0,45), but identical to values from kimberley clinopyroxenes. Using Boyd's solvus at 30 kb (Boyd, 1970), an equilibration temperature of 960°C is indicated. Orthopyroxenes have a low Al_2O_3 content (1,21%), but higher than that found in most kimberlite garnet lherzolites. Gurney, Harte and Cox (this vol.), report values of 0,71-0,87 wt.% Al_2O_3 from 23 orthopyroxene analyses - 16 from Matsoku, 6 from Kimberley and 1 from the Roberts Victor pipe. The Namaqualand inclusion indicates equilibration at 38 kb using McGregors diagram for Al_2O_3 content of orthopyroxenes (McGregor, quoted by Boyd, 1973). As Hox is believed to be an accidental inclusion, the pressure of 38 kb will fix a minimum depth for origin of the lost magma at approximately 130 km.

T A B L E 1
Mineral Analysis of Hox, a Garnet Lherzolite

	<u>Garnet</u>	<u>Opx</u>	<u>Cpx</u>	<u>Olivine</u>
MnO	0,43	0,12	0,09	0,10
Na_2O	0,01	0,10	1,52	0,02
FeO	7,96	5,26	2,18	8,66
SiO_2	41,50	56,50	54,94	40,65
CaO	5,57	0,45	21,06	0,04
Al_2O_3	21,35	1,21	2,14	0,02
TiO_2	0,07	0,03	0,05	0,02
MgO	19,29	34,96	17,04	49,97
Cr_2O_3	2,53	0,45	1,66	0,03
	—	—	—	—
	99,88	99,09	100,68	99,52
	—	—	—	—

(Analysis by Dick Rickard, U.C.T.)

The Bitterfontein pipes in the south are strongly depleted in MgO and Ni, and are even further depleted in SiO_2 compared to those in the north. (MgO: 21% to 10%, Ni: 900 ppm to 73 ppm, SiO_2 : 35,2% to 31,5%). Cr_2O_3 is also significantly depleted to the south. CaO, Al_2O_3 , TiO_2 , and MnO are accordingly enriched relative to the northern pipes.

Further salient geochemical features are the high concentrations of TiO_2 , Na_2O and K_2O throughout the Province, with rather erratic variation of the alkalis. Trace element data available to date show

high concentrations of Zn, Cu and Ba.

Preliminary calculations using available major element data suggest that the rock compositions in different parts of the Province can be related by simple subtraction (or addition) of olivine, together perhaps with minor amounts of clinopyroxene, orthopyroxene, garnet and spinel.

The parent magma is believed to be derived by small amounts of partial melting in the low velocity zone (Green, 1971), possibly involving a Ti-rich phlogopite similar to that described from Lashaine inclusions (Dawson, 1972). Such a mica could supply appreciable amounts of Ba, Rb and Sr to the melt. Melting is thought to yield Ti-andK-rich fluids of olivine-nepheline composition. It is suggested that crystallization of olivine (which is richer in SiO_2 than the parent melt) will result in a denser crystal mush at depth, relatively enriched in SiO_2 and MgO . Strained olivine fragments in some of the rocks are thought to represent disaggregated upper mantle material which has contaminated the crystal mush, enhancing the MgO and SiO_2 enrichment. The remaining, lighter liquid will be depleted in MgO and SiO_2 but enriched in the other oxides. The increase in Al_2O_3 and CaO concentrations results in crystallization of melilite-bearing assemblages on emplacement. Erratic variation of the alkalis may suggest variations in the compositions of separate source areas, but more probably reflects variable loss of volatiles during eruption.

The Middle Tertiary is not represented in South African off-shore sediments, presumably because of marginal uplift and warping of the continent. It is suggested that this caused deep seated fracturing in Namaqualand-Bushmanland, triggering off volcanic activity. Similar parent magmas were formed in different parts of the Province, but in the south, closer to the coast, upper levels of a differentiated magma column were tapped. This resulted in the most undersaturated (melilite-bearing) magmas being extruded. To the north, and further inland, possibly closer to the axis of warping, deeper levels were tapped by these fractures. Extrusion of a Mg-enriched crystal mush resulted.

The Klinghardt phonolites are also of Mid-Tertiary age (Kröner, 1973). It is tentatively suggested that they are related to the Namaqualand-Bushmanland volcanics, but are derived from a more siliceous parent, which was produced by greater degrees of partial melting in the Low Velocity Zone.

The relationship between the "kimberlites" and the melilite-nepheline bearing suite of volcanics remains speculative. It is possible that the sediment filled pipes are derived from the same parent magma as the Oligocene volcanics, but represent an earlier, highly fractionated and volatile enriched fraction. This fraction would then be intruded ahead of the denser and consequently younger portions.

References

Boyd, F.R. (1970). Garnet Peridotites and the System CaSiO_3 - MgSiO_3 - Al_2O_3 . Min. Soc. Am. Spec. Pub. No. 3, pp 63-75.

(1973). Pres. Address to the Geochem Soc.

Dawson J.B. (1972). Kimberlites and their Relation to the Mantle. Phil. Trans. R.S. Lond. A. 271, pp 297-312.

Green, D.H. (1971). Compositions of Basaltic Magmas as Indicators of Conditions of Origin: Application to Oceanic Volcanism. Phil. Trans. R.S. Lond. A. 268, pp 707-721.

Gurney, J.J., Harte, B., and Cox, K.G. (1973). The Composition of Mantle Xenoliths in the Matsoku Kimberlite Pipe (This Vol.).

Kröner, A. (1973). Comments on "Is the African Plate Stationary?" Nature, Vol. 243, pp 29-30.

DISCRETE NODULES (MEGACRYSTS) AND LAMELLAR INTERGROWTHS IN FRANK SMITH KIMBERLITE PIPE

P.H. Nixon, Dept. Of Mines & Geology, Maseru., and F.R. Boyd, Geophysical Laboratory, Carnegie Institution of Washington.

The pipe is characterised by a wide variety of deep seated nodules. There are dunites (some with large opx porphyroclasts or relict gt and cpx) garnet lherzolites (some with 50% cpx), garnet pyroxenites grading with loss of opx, into eclogites, corundum eclogites, phlogopites, and gt pyroxenites with relict dunitic patches. The gt pyroxenite suite includes types with lamellar intergrowths of gt, cpx, opx ± chromite. The discrete nodules and megacrysts, to which this chemical study is mainly confined, include ilmenite, ilmenite-mica, ilmenite-cpx/oxp (both as granular and lamellar intergrowths), garnet with inclusions of corundum or cpx, rare cpx, and opx with garnet inclusions. The mutual crystal intergrowth relationships within this group indicate consanguinity, but electron probe analyses show considerable variation (see table 1).

The discrete garnet nodules are typically, reddish-brown pyropes low in chromium (2381G, table 1; Nixon et al. 1963) with 0.8-1% TiO_2 . However, a deep red nodule 2381F which is 5 cm across contains 3.36% Cr_2O_3 but nonetheless contains sufficient TiO_2 to differentiate it³ from the Cr pyropes of the granular ultrabasic nodules. A pale orange nodule (2381B, table 1) with kyanite inclusions is exceptionally aluminous and contains twice the normal amount of CaO (grossularite and is equated with the grospydite suite.

A diopside inclusion in a discrete pyrope nodule has apparently equilibrated at about 1300°C or higher ($Ca/(Ca+Mg) = 33.7\%$) and this is consistent with the small but perceptible amount of Ca solid solution in associated bronzite nodules (2381D and 2373, table 1). An omphacite nodule (38% jadeite), has a rather higher Cr_2O_3 content (2382, table 1) than most eclogites/griquaites, and may also belong to the discrete nodule suite.

The ilmenite nodules are characterised by high geikielite and haematite contents with <1% Cr_2O_3 . Ilmenites are also intergrown in a granular fashion with both bronzite (a fairly common association) and more rarely, diopside. The pyroxene $Ca/(Ca+Mg)$ ratios show more limited solid solution between enstatite and diopside than those noted above and evidently equilibrated at shallower depth (cf. Boyd and Nixon, 1973).

The lamellar intergrowths comprise the familiar "ilmenite-diopside" "eutectic" graphic intergrowths and also nodules of alternating laminae of garnet, clinopyroxene and orthopyroxene. The ilmenites of the intergrowths and the discrete nodules show an inverse relationship between geikielite and haematite contents. Compared with Monastery Mine and northern Lesotho occurrences the Frank Smith ilmenites appear to be enriched in MgO (figure 1) although zoned reaction mantles can produce wide variations even within a single grain (Haggerty, 1973). In 2353C there are fine exsolution zones similar to magnetite (magnesioferrite) - ulvöspinel phases that we have noted at Monastery Mine.

The clinopyroxenes which coexist with the ilmenites also appear to be enriched in MgO compared with many nodules from elsewhere.

The silicate lamellar intergrowths are commonly associated with garnet pyroxenite and these appear to be mobilised phases since they are often sharply demarcated in the same hard specimen from associated (?residual) dunitic patches. The intergrowths are therefore regarded as quenched products of a garnet pyroxenite melt. An immediate ultrabasic mantle parentage is attested by the high Cr content of the pyrope and diopside, but the latter appears to have equilibrated at similar temperatures to the granular intergrowth of ilmenite and clinopyroxene (table 1).

The existence of differentiated garnet pyroxenites and heterogeneous ilmenite-pyroxene mixtures of intermediate depth (i.e. above the mantle low velocity zone of intense shearing and discrete nodule formation - Boyd and Nixon 1973) is paralleled at Matsoku. Here, the ultrabasic nodules have also suffered sulphide metasomatism and deformation, producing gneissose textures (Cox *et al.* 1973).

These "Matsoku effects" of folding and minor shearing, ilmenite enrichment, metasomatism, melting and recrystallisation, are equated with the upward migration of volatile and mobile constituents, including potassium, through the sheared asthenosphere. The mobile constituents are envisaged as being kneaded out in the manner described by Weertman (1972) and providing lubrication at the base of the African plate (lithosphere) for the dispersal of Gondwanaland.

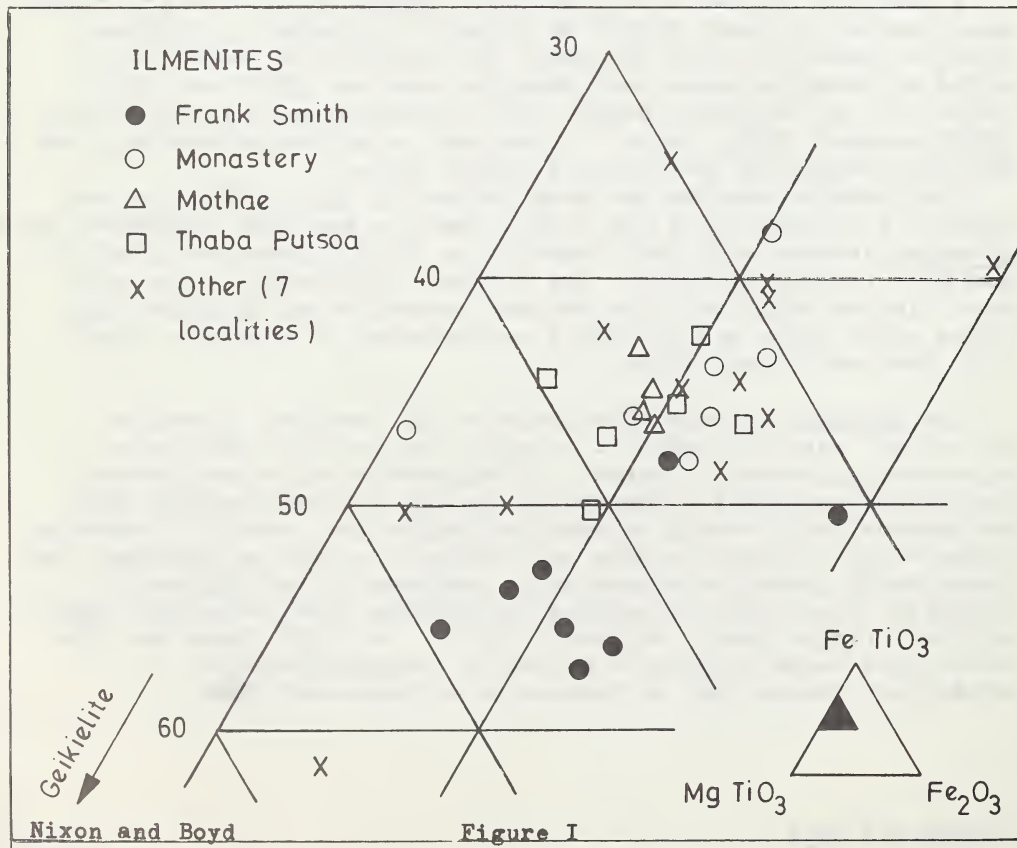


Figure 1

Figure I. Compositions of ilmenites from Frank Smith and other
kimberlites.
References

Boyd, F. R., and Nixon, P. H., 1973 in Lesotho Kimberlites,
p. 254-268, Cape Town, in press.
Cox, K. G., Gurney, J. J. and Harte, B., 1973 in Lesotho
Kimberlites, p. 76-100, Cape Town,
in press.
Haggerty, S., 1973 in Lesotho Kimberlites, p. 149-158, Cape Town
in press.
Nixon, P. H., von Knorring, O and Rooke, J. M., 1963, Amer.
Mineral. 48, 1090-1132.
Weertman, J., 1972, Geol. Soc. Amer. Bull. 83, 3531-3532.

TABLE I ANALYSES OF MINERALS FROM FRANK SMITH KIMBERLITE PIPE

PHN	DISCRETE NODULES							2353C	2353E	
	2381G	2381B	2381F	2381D		2382	2373			
gt	gt	gt	gt	incl	cpx	gt	incl	il	il	
SiO ₂	41.88	40.75	42.27	41.46	54.84	54.43	56.16	41.79	0.10	0.10
TiO ₂	0.86	0.13	0.94	0.72	0.32	0.68	0.21	0.89	49.41	43.67
Al ₂ O ₃	21.83	23.27	19.64	20.85	3.60	7.20	1.01	21.36	1.75	0.35
Cr ₂ O ₃	0.03	0.16	3.36	1.85	0.90	1.29	0.07	0.85	0.72	0.93
Fe ₂ O ₃	—	—	—	—	—	—	—	—	13.94	20.17
FeO	11.37	9.68	7.26	6.33	4.79	4.57	7.64	9.72	21.54	23.81
MnO	0.41	0.29	0.29	0.26	0.13	0.09	0.16	0.30	0.24	0.27
NiO	n.d.	n.d.	n.d.	n.d.	n.d.	n.d.	n.d.	n.d.	0.15	0.15
MgO	19.13	15.58	21.05	21.59	18.88	13.30	32.55	20.93	12.66	8.49
CaO	4.46	9.86	5.16	4.22	13.33	11.48	1.19	3.99	0.04	0.02
Na ₂ O	0.07	0.08	0.03	0.09	2.58	5.36	0.24	0.09	n.d.	n.d.
Totals	100.04	99.74	100.00	99.37	99.37	98.40	99.23	99.92	100.55	97.96
Ca/(Ca+Mg)%	33.7	38.3	2.6							

continued on next page.

Table I (continued)

GRANULAR INTERGROWTHS

PHN	2349		2351A		2351B		2354	
	il	cpx	il	opx	il	opx	il	opx
SiO ₂	0.10	53.41	0.13	55.64	0.09	56.43	0.12	56.82
TiO ₂	49.36	0.35	52.85	0.29	54.08	0.22	52.15	0.29
Al ₂ O ₃	0.59	2.39	0.54	0.92	0.70	1.24	0.49	0.95
Cr ₂ O ₃	0.77	0.32	0.71	0.06	1.18	0.10	0.43	0.02
Fe ₂ O ₃	12.47	—	9.19	—	7.21	—	10.04	—
FeO	25.86	4.77	23.76	7.52	22.93	8.28	24.11	7.68
MnO	0.24	0.11	0.20	0.16	0.25	0.14	0.23	0.16
NiO	0.13	n.d.	0.21	n.d.	0.20	n.d.	0.21	n.d.
MgO	10.24	16.82	13.16	33.63	14.21	32.80	12.59	33.77
CaO	0.02	18.90	0.04	1.08	0.02	0.79	0.04	1.09
Na ₂ O	n.d.	1.84	n.d.	0.21	n.d.	0.29	n.d.	0.27
Totals	99.78	98.91	100.79	99.51	100.87	100.29	100.41	101.05

Ca/(Ca+Mg)% 44.7 2.3 1.7 2.3

LAMELLAR INTERGROWTHS

PHN	2348A		2348B		2367			
	il	cpx	il	cpx	gt	cpx	opx	chr*
SiO ₂	0.11	54.01	0.11	54.58	40.64	54.32	57.87	1.65
TiO ₂	49.96	0.50	48.27	0.42	0.31	0.13	0.05	3.55
Al ₂ O ₃	0.91	2.29	0.75	2.30	16.60	1.93	0.55	7.62
Cr ₂ O ₃	0.74	0.18	0.07	0.01	7.88	2.92	0.39	44.63
Fe ₂ O ₃	12.25	—	14.80	—	—	—	—	7.96
FeO	22.37	4.80	21.73	4.96	7.92	2.48	5.23	22.79
MnO	0.23	0.14	0.24	0.14	0.54	0.14	0.15	0.64
NiO	0.23	n.d.	0.15	n.d.	n.d.	n.d.	n.d.	0.20
MgO	12.45	18.51	12.00	18.22	18.60	16.35	35.30	9.38
CaO	0.03	16.44	0.02	17.49	6.36	18.12	0.42	0.02
Na ₂ O	n.d.	2.11	n.d.	2.21	0.05	3.18	0.12	n.d.
Totals	99.28	98.98	98.14	100.33	98.90	99.57	100.08	98.44

Ca/(Ca+Mg)% 39.0 40.8 44.3 0.8

SUBSOLIDUS MINERAL ASSEMBLAGES IN GARNET-PERIDOTITE AND ECLOGITE COMPOSITIONS

M.J. O'Hara, Grant Institute of Geology, University of Edinburgh

The following direct or implicit identifications have been proposed (O'Hara and Yoder 1967, O'Hara 1968, 1970) linking ultramafic rock types found in kimberlite with source mantle, residual mantle, or high pressure cumulus formed during partial melting and recrystallization events at great depths:-

A. Residua from Partial Melting

I. Garnet-lherzolite (Gnt-cpx-opx-ol) represents (i) source mantle; (ii) source mantle depleted by the earlier stages of partial melting, in which garnet and clinopyroxene are reduced in amount but neither is eliminated; or residual mantle from which (iii) all clinopyroxene or (iv) all clinopyroxene and garnet had been eliminated at the solidus temperature but which have exsolved their present clinopyroxene and some or all of their garnet on subsequent cooling to the sub-continental geotherm. (Some of the garnet and clinopyroxene present in cases I(i) and I(ii) may have exsolved between solidus and geotherm.

II.(i) Garnet-harzburgite (Gnt-opx-ol) or (ii) lherzolite (Cpx-opx-ol) represents residual mantle from an intermediate stage of partial melting or still more residual material in which (iii) all garnet or (iv) all clinopyroxene present has exsolved from orthopyroxene during cooling from the solidus to the geotherm.

III. Harzburgite (Opx-ol) represents residual mantle from a still more advanced stage of partial melting.

IV. Dunite (Ol) represents the residuum after extreme partial melting.

Relative abundances of these materials appear to be I>II>III> IV. Experimental data (Ito and Kennedy 1967) imply that this situation will develop if partial melting temperature rarely exceeds the solidus by more than 50°C, and only exceptionally by more than 200°C, a result readily understood when the latent heat required to produce the liquid is taken into consideration. (The thermal energy which would raise subsolidus peridotite through 100°C will produce c.20% melt from it, without raising the temperature significantly, at the beginning of melting).

These petrographic groupings are correlated in table 1 with the stages of partial melting model proposed by O'Hara (1968, fig 8) and the ranges of residual peridotite composition shown in the partial melting model of O'Hara (1970).

B. Cumulates from the isobaric fractionation of magma at high pressures
If the liquids produced during the processes leading to the creation of the residual mantle compositions undergo crystallization at depth the products may be:-

V. Olivine-poor garnet-wehrlite or garnet-lherzolite representing (i) the total (equilibrium) or near total crystallization product of the liquid produced in partial melting (Cpx>opx) or the subsolidus exsolution products of (ii) olivine-orthopyroxenite or (iii) olivine-garnet-orthopyroxenite precipitated during fractional crystallization of more advanced partial melts.

VI. Olivine-garnet-orthopyroxenites representing either (i) the cumulates formed during fractional crystallization of olivine, garnet and orthopyroxene from the liquid, or (ii) a subsolidus exsolution product of an olivine-orthopyroxene cumulate formed from the liquid.

VII. Olivine (garnet)-websterites representing the cumulates from liquids

Table 1. Source and residual mantle

Category	Low T Petrography	Solidus Petrography	Stage of Partial Melting (O'Hara 1968)	Corresponding residual in model of O'Hara (1970)	Complementary liquid in model O'Hara (1970)
I	(i) ol, opx, gr, cpx	ol, opx, gr, cpx	-	O	
	(ii)	"	stages 1,2	O - O	B
	(iii)	ol, opx, gr	stage 3	O' - O"	B - W
	(iv)	ol, opx	stage 4	O"-olivine	W - X
II	(i) ol, opx, gr	ol, opx, gr	stage 3	O'-O"	B - W
	(ii) ol, opx, cpx	ol, opx, cpx	"	-	B
	(iii) ol, opx, gr	ol, opx	stage 4	O"-olivine	W - X
	(iv) ol, opx, cpx	ol, opx	"	-	Y - Z
III	ol, opx	ol, opx	stage 4	O"-olivine	W - X, Y - Z
IV	ol	ol	stage 5	olivine	X - O, Z - N

fractionating (i) olivine, clinopyroxene and orthopyroxene, or (ii) olivine and orthopyroxene, from which clinopyroxene has later exsolved.

VIII. Dunites representing cumulates from liquids fractionating olivine only.

IX. Garnet-websterites representing early cumulates of garnet and clinopyroxene (in which at the solidus $cpx > gnt$) which have subsequently exsolved both orthopyroxene and garnet. N.B. The models discussed here do not provide for the direct accumulation of this mineral assemblage except as the result of a pressure increase in the liquids.

X. Eclogites representing the most abundant cumulate from the fractional crystallization of the liquids; formed at temperatures below the solidus temperature of the source mantle. At pressures of 25-40 kb solid solution of potential garnet in clinopyroxene at solidus temperatures means (i) that most of the present garnet has exsolved from the pyroxene (O'Hara and Yoder 1967; O'Hara 1969), but (ii) some eclogites may represent the exsolution product of homogeneous clinopyroxene which may precipitate from a magma originally fractionating eclogite, which is subject to a pressure drop.

These relationships are summarised in table 2.

Table 2. Cumulates

Category	Low T Petrography	Solidus or precipitation petrography	Complementary liquids in model (O'Hara 1970)*
V	(i) cpx, gr > opx, ol	cpx, gr, ol	B
	(ii) opx > ol, cpx, gr	(ol), opx	W - X
	(iii) gr > opx, ol, cpx	(ol), opx, gr	W - B
VI	(i) gr > opx > ol	gr, opx, ol	A - B
	(ii) opx > gr > ol	ol, opx	on surface EABD
VII	(i) cpx > opx, ol (gr)	cpx, opx, ol	D - B
	(ii) opx > cpx > ol (gr)	opx, ol	on surface EABD
VIII	ol	ol	-
IX	cpx, opx, gr	cpx, gr	B - U near B
X	(i) cpx \simeq gr	cpx, (gr)	B - U
	(ii) cpx > gr	cpx	inside clinopyroxene liquidus volume as result of pressure drop

*Refers to type of liquid only. Pressure may have changed between partial melting and fractional crystallization events.

Throughout it must be remembered that both low temperature and solidus petrography will be functions of the pressure as well as the bulk composition.

This classification is intended to summarise the implications of recent experimental work and thinking based on materials behaviour. Its application to the interpretation of rare earth element (REE) data will be discussed.

REE are not strongly fractionated between liquid and either olivine or orthopyroxene. Light REE (REE_L) are enriched relative to heavy REE (REE_H) in clinopyroxene; for a given bulk composition the $REE(L/H)$ ratio of coexisting liquid will be correspondingly reduced. REE_H are very strongly enriched in garnet, producing for a corresponding increase in $REE(L/H)$ of a coexisting liquid (for a given bulk composition).

Assuming no relative fractionation of REE between chondrites and source mantle (category I(i)) then $REE^*(L/H)=1$ where REE^* refers to chondrite normalised concentrations. Residual garnet-lherzolites (I(ii)) might display little change in $REE^*(L/H)$ although reduced overall concentrations, and the same would be true to a greater extent of extreme residua (I(iv), II(iii), II(iv), III and IV); the corresponding primary magmas would similarly have $REE^*(L/H) \sim 1$. Rocks developed as residual garnet harzburgites (I(iii), II(i)) would have $REE^*(L/H) < 1$ and the primary magma produced at the same time would have $REE^*(L/H) > 1$. A further partial melting event affecting such residua (after removal of the first liquid) would, however, produce primary magmas with $REE^*(L/H) < 1$, possibly $\ll 1$ if garnet was just eliminated from the residua. Conversely, rocks developed as residual lherzolites (II(ii)) will have $REE^*(L/H) > 1$, and the liquids will have $REE^*(L/H) < 1$ in a first cycle of melting, but in a second partial melting event in which clinopyroxene was eliminated the liquid would have $REE^*(L/H) > 1$.

Primary magmas which undergo fractional crystallization of garnet uncompensated by clinopyroxene removal will develop residual liquids of sharply increased $REE^*(L/H)$ and produce accumulates with $REE^*(L/H) < 1$ (category VI). When both clinopyroxene and garnet are fractionating together the $REE^*(L/H)$ of eclogite extract (categories IX,X) will depend primarily on the coprecipitation ratio of clinopyroxene/garnet, which is a function of pressure and temperature. $REE^*(L/H)$ of eclogite need not differ greatly from 1, and it is not certain at this stage what effect eclogite fractionation might have on $REE^*(L/H)$ of any derivative liquids.

References

Ito, K. and Kennedy, G.C. 1967. Chem. J. Sci. 265, 519-539.
 O'Hara, M.J., 1968. Earth Sci. Rev. 4, 69-133.
 _____ 1969. Geol. Mag. 106, 322-330.
 _____ 1970. Phys. Earth Planet. Int. 3, 236-245.
 _____ and Yoder, H.S., Jr. 1967. Scott. J. Geol. 3, 67-117.

PHASE EQUILIBRIA PRINCIPLES OF PARTIAL MELTING OF GARNET-PERIDOTITE AND FRACTIONATION OF MAGMA PRODUCED

M.J. O'Hara, Grant Institute of Geology, University of Edinburgh.

When the garnet-pyroxene composition 'plane' is a thermal divide (fig 1) garnet-peridotite G begins to melt at a lower temperature than eclogite F with production of liquid B. No eclogite (F-F') can melt incongruently to yield olivine-bearing residua. Most popular prejudices about upper mantle composition fall close to G in a general composition field (four subsolidus phases). Eclogites are 'special' compositions with restricted number of phases best accounted for as residua of partial melting or crystal cumulates. Only initial olivine-bearing mantle compositions such as H could yield eclogite residua on partial melting. Eclogites F-F' can accumulate from liquids B-U. The residual liquids may become strongly undersaturated in silica and have at least some of the properties of kimberlite. The garnet-pyroxene plane is a thermal divide in synthetic and natural systems at high pressures (O'Hara and Yoder 1967; O'Hara 1968)

If the garnet-pyroxene composition plane were not a thermal divide (fig 2) garnet peridotite G and eclogite F-F' might begin to melt at the same temperature with appearance of liquid Q, and olivine, enstatite bearing residua (such as G) might be created from eclogite. The liquid Q would however be hypersthene- or quartz-normative and could only fractionate towards yet more silica saturated compositions, unlike kimberlite, by eclogite fractionation along Q-R. This possible form of the phase equilibria was considered, tested, and rejected by O'Hara and Yoder (1967). The crucial data which would support it (appearance of olivine during partial melting of a bimimetic eclogite which retains that mineralogy to the solidus) have not been produced. Until they are produced, hypotheses which regard eclogite as the source mantle and garnet-peridotite as its residuum after partial melting lack a basis of known materials behaviour.

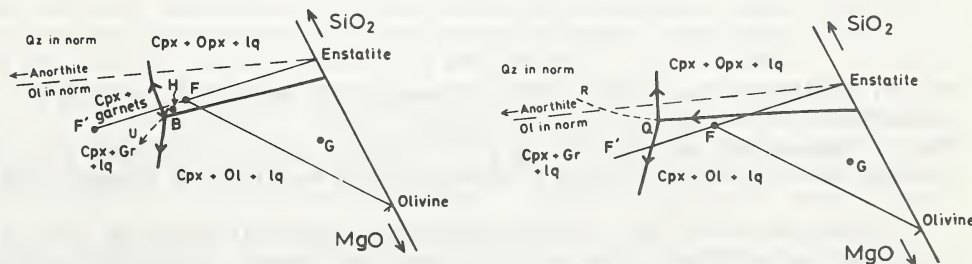


Fig 1. Diopside projection into the part of the system olivine-silica-anorthite showing the form of clinopyroxene-saturated equilibria at some high pressure when the eclogite 'plane' is a thermal divide (Projection method as described by Jamieson 1970).

Fig 2. As fig 1, but drawn for the hypothetical situation where the eclogite plane is not a thermal divide.

Fig 3 shows an isothermal section of the equilibria in fig 1, at the temperature of beginning of melting of the garnet lherzolite assemblage when liquid B appears, to illustrate why the orthopyroxene/olivine ratio will increase in the residua from initial partial melting of a garnet-lherzolite. (See construction lines through G from B, F to find enstatite/olivine ratios after and before melting). By construction it can be shown that the absolute weight per cent of enstatite in the whole liquid-crystal system increases at the beginning of melting (because of the reaction relationship orthopyroxene+liquid = olivine+garnet+clinopyroxene). Further partial melting producing a liquid P, however, causes the orthopyroxene/olivine ratio to decline, as shown in fig 4, an isothermal section drawn for a higher temperature.

The ratio clinopyroxene+garnet/orthopyroxene (fig 4) in the original garnet-lherzolite, G, determines how much partial melting can occur before orthopyroxene is eliminated from the residuum. While orthopyroxene remains, olivine does not increase much in the CIPW norm of the liquid while partial melting proceeds (see fig 1, liquid must lie along olivine-enstatite liquidus interface); once orthopyroxene has been consumed, normative olivine would increase quickly in the further partial melts, but so does the temperature required to produce that liquid.

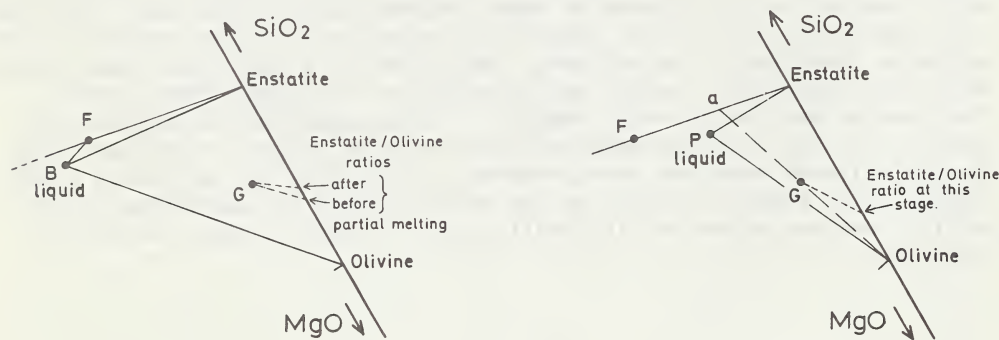


Fig 3. Isothermal section of fig 1, showing the cpx+opx+ol+liquid B assemblage in relation to peridotite G.

Fig 4. Isothermal section of fig 1 at a higher temperature than fig 3, showing the cpx+opx+ol+liquid P assemblage in relation to composition G.

A projection of the olivine-saturated equilibria involved in fig 1, from olivine into the plane of clinopyroxene, orthopyroxene and garnet is shown in fig 5. The critical plane olivine-enstatite-initial liquid B separates garnet-lherzolite compositions such as G, which would yield lherzolite residua in partial melting, from a superficially similar composition, O, which yields garnet-harzburgite residua in partial melting (note light dotted lines showing the isothermal section boundaries at the beginning of melting in fig 5). The position of this critical plane, is pressure dependent (see O'Hara 1970) but the relationship of a garnet lherzolite to this plane is determined essentially by the clinopyroxene/garnet ratio in the rock, or (equally crudely) by the CaO/Al₂O₃ ratio.

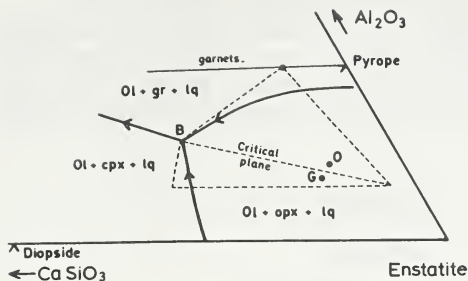


Fig. 5

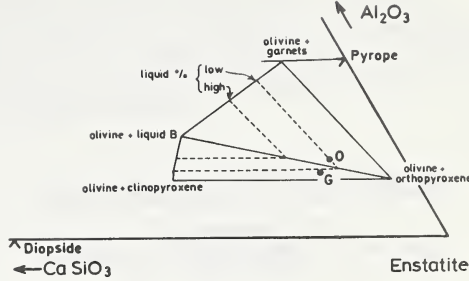


Fig. 6

Fig 6 is a similar projection showing the isothermal section at the beginning of partial melting, contoured with isopleths of equal liquid/pyroxenes \pm garnet ratios produced at the beginning of melting (assuming adequate latent heat). The mineral ratio criteria in the subsolidus or geochemical criteria which govern how much liquid forms are not simple functions, the criteria differ on either side of the critical plane because the isopleths have different orientations. Moreover, the sensitivity of the situation to sampling errors, analytical errors or genuine variations in bulk composition, is different on opposite sides of the critical plane (this is an elementary consideration in quality control of industrial refractories (O'Hara and Biggar 1970) whose performance in service present an analogous situation to that discussed here).

Summarising, what constitutes a significant geochemical or modal measurement and acceptable limits of precision in sampling and analysis in the study of possible upper mantle compositions is itself dependent upon the bulk composition and the nature of the inquiry. When the behaviour of rocks during partial melting is considered, knowledge of the liquidus and solidus relationships is a prerequisite for the choice of meaningful criteria. Whereas the partial melting behaviour of garnet-peridotite is not very sensitive to variations in total SiO_2 or $\text{MgO}+\text{FeO}$ (which dominate the analysis) it is very sensitive to variations in the absolute and relative amounts of CaO , Al_2O_3 and of SiO_2 surplus to that required to form olivine, clinopyroxene and garnet. Simple addition of mineral compositions in a source rock in order to obtain an estimate of possible liquid composition is a defective method when one or more crystalline phases increases in amount as liquid forms. Similarly it is important to pay due regard to these criteria when constructing hypothetical models of upper mantle composition.

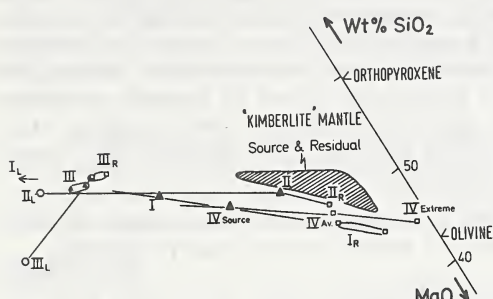
References

- Jamieson, B.G. 1970. *Min. Mag.* 37, 539-554.
- O'Hara, M.J. 1968. *Earth Sci. Rev.* 4, 69-133.
- O'Hara, M.J. 1970. *Phys. Earth. Planet. Int.* 3, 236-245.
- O'Hara, M.J. and Biggar, G.M. 1970. *Trans. Brit. Ceram. Soc.* 69, 243-251.
- O'Hara, M.J. and Yoder, H.S.Jr. 1967. *Scott. J. Geol.* 3, 67-117.

PARAGENESSES OF ULTRAMAFIC NODULES IN BASALTS CONTRASTED WITH THOSE OF NODULES IN KIMBERLITES

M.J. O'Hara, Grant Institute of Geology, University of Edinburgh.

The average composition of ultrabasic nodules in basalts differs slightly but significantly from those of peridotite nodules in kimberlite, the former having persistently higher olivine/orthopyroxene ratios (fig 1) and higher Fe/Mg ratios (fig 2). Nodules in basalt persistently have higher diopside/enstatite ratios also (O'Hara 1970).



SOME UPPER MANTLE MODELS COMPARED

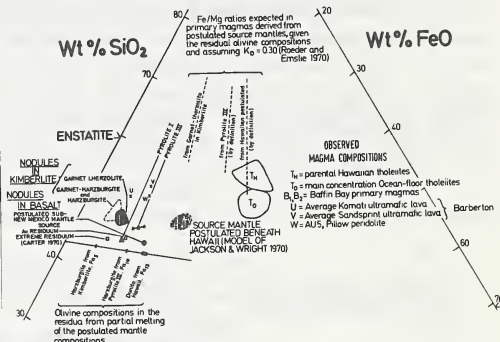


Fig 1. Diopside projection into $\text{CaOAl}_2\text{O}_3\text{-MgO-SiO}_2$ (see O'Hara 1968, Jamieson 1970a for method) showing nodules from kimberlite (shaded field) in relation to nodules from basalt in Hawaii (Jackson and Wright 1970; I, III, III_R=their proposed source mantle; I_R, II_R, III_R=actual nodules, interpreted as residuals of partial melting; I_L, II_L, III_L=their proposed primary magmas) and New Mexico (Carter 1970; IV source=his putative source mantle, IV_{Av}, IV_{Extreme} = his putative average and extreme residual mantle).

Fig 2. MgO-FeO-SiO₂ projection (see Ford *et al* 1972, fig 7) of same data as in fig 1 comparing various nodule compositions from basalt and kimberlite with other upper mantle models and possible or proposed magmas related thereto.

The mineral assemblage of nodules in kimberlites also indicates higher pressures of equilibration (O'Hara 1967, O'Hara *et al* 1971) than does that of nodules in basalt, as well as generally lower temperatures - briefly, nodules from kimberlite appear to have equilibrated at subsolidus temperatures close to those of plausible sub-continental geotherms in the 20-60 kb range whereas nodules in basalt appear to have equilibrated at near solidus temperatures in the less than 25 kb range. The chemical differences prove that the nodules in basalt are not merely kimberlite nodules in a different mineral facies, and prove that they cannot be partial melt residua from kimberlite nodules, NOR VICE VERSA (see geometry of figs 1, 2 and in O'Hara 1970).

If nodules in kimberlite sample upper mantle with little alteration, what then do nodules in basalt represent?

Peridotite nodules from basalts tend to show positive correlation between high Al_2O_3 contents in spinel and pyroxene, high mutual solubility

in the pyroxenes (as judged say by the Ca/Ca+Mg+Fe in the coexisting pyroxenes), and low Mg/Mg+Fe ratios in the minerals. (O'Hara and Mercy 1963, Frechen 1963).

Fig 3A illustrates the solidus, and temperature interval of coexistence of olivine (ol), clinopyroxene (cpx), orthopyroxene (opx), spinel (sp) and liquid (lq) just above the solidus of a natural spinel lherzolite (pressure range c 10-20 kb). Within the solidus to spinelout interval, the Cr/Al ratio in the diminishing amount of spinel increases (because Al is preferentially taken by the liquid). Fig 3B illustrates the variation in Al_2O_3 substitution in the pyroxene with pressure and temperature within and on either side of this interval. Above the solidus, Al_2O_3 substitution decreases sharply with rising temperature due to formation of more and more Al-rich liquid. Fig 3C illustrates the rising mutual solubility of the coexisting pyroxenes, which is little affected by change of pressure. Fig 3D illustrates the way in which Mg/Mg+Fe of the minerals will rise from some near constant level in the solidus once melting has begun (because the liquid formed has low Mg/Mg+Fe).

In each figure the heavy line X-Y illustrates the only type of P-T variation which will produce the observed mineralogical correlations.

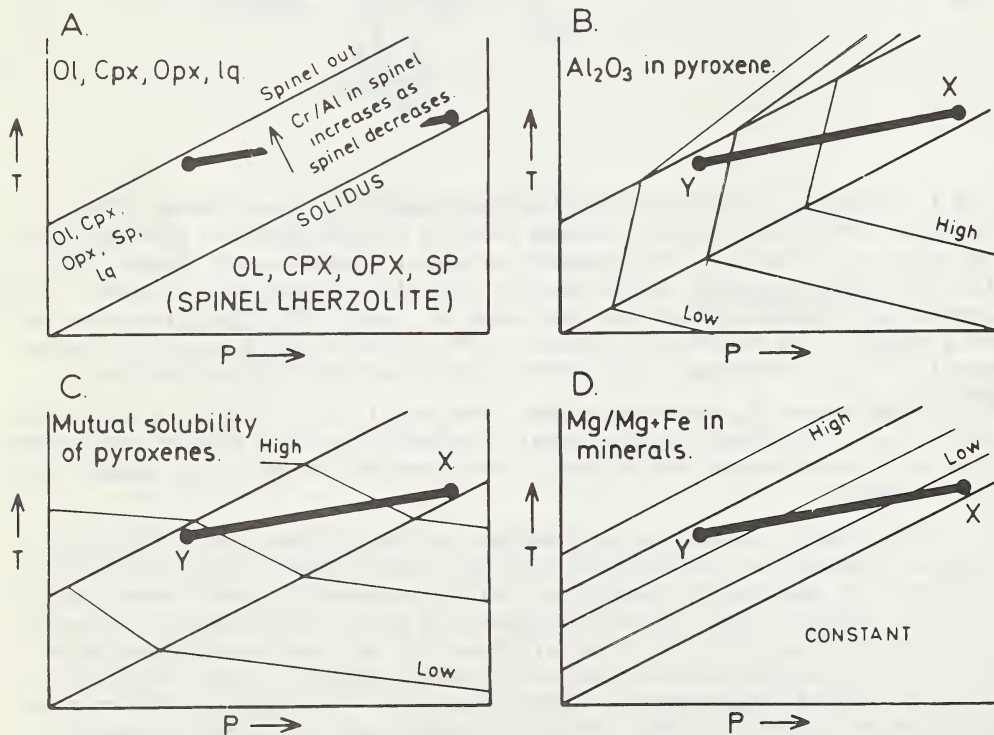


Fig 3. Mineral parageneses in spinel-lherzolite near the solidus. Explanation in the text.

X-Y cannot represent parageneses in an isobaric partial melting sequence. X-Y represents a possible adiabatic decompression path for an ascending basic magma or an ascending peridotite diapir. Because the nodules in question are carried by a basic magma which has manifestly

ascended along such a path and because the existence of peridotite dikes and mantle plumes lacks any direct observational confirmation, the origin of mineral parageneses in these nodules is ascribed to precipitation on the side walls of a conduit through which basic magma was ascending, followed by break-up of the skin and incorporation in the magma during more rapid or violent eruption. Under these conditions polybaric fractional crystallization occurs and high olivine/orthopyroxene and high clinopyroxene/orthopyroxene ratios are expected in the precipitates (O'Hara 1968, Jamieson 1970b).

Nodules in kimberlite, on the other hand, show the positive correlations of Mg/Mg+Fe with increased Cr/Al ratio and depletion of diopside component which is expected to be created in isobaric partial melting processes and these nodules are more acceptable as models of upper mantle composition.

Whatever the choice of interpretation, the chemical and mineralogical differences between peridotite nodules in basalt and kimberlite are real and preclude the bracketing of these two rock types together without due consideration of the reasons for those differences.

References

Carter, J.L. 1970. Geol. Soc. Amer. Bull. 81, 2021-2034.
Ford et al 1972. Proc. 3rd Lunar Sci. Conf. Geochim. Cosmochim. Acta Suppl. 3, 1, 207-229.
Frechen, J. 1963. Neues Jb. Miner. Mh. 205-225.
Jackson, E.D. and Wright, T.L. 1970. J. Petrology 11, 405-430.
Jamieson, B.G. 1970a. Miner. Mag. 37, 537-554.
Jamieson, B.G. 1970b. in Mechanisms of Igneous Intrusion Newall and Rast Geol. J. Spec. Issue No. 2, 165-176.
O'Hara, M.J. 1967. Ultramafic and Related Rocks P.J. Wyllie, J. Wiley, 7-8 and 393-403.
O'Hara, M.J. 1968. Earth Sci. Rev. 4, 69-133
O'Hara, M.J. 1970. Phys. Earth Planet. Int. 3, 236-245.
O'Hara, M.J. and Mercy, E.L.P. 1963. Trans. Roy. Soc. Edinb. 65, 251-314
O'Hara, M.J. et al 1971. Contrib. Mineral. Petrol. 32, 48-68.
Roeder, P.L. and Emslie, R.F. 1970. Contrib. Mineral. Petrol. 29, 275-289

CHEMISTRY AND ASSIGNED ORIGIN OF SOME ULTRAMAFIC NODULES FROM KIMBERLITE
 M.J. O'Hara, M.J. Saunders, Grant Institute of Geology, University of
 Edinburgh, and E.L.P. Mercy, Department of Geology, Lakehead University,
 Ontario.

Table 1 contains new analyses of sixteen peridotites or pyroxenites from S. African kimberlites, grouped according to their postulated origin. Other analyses considered to belong to some of these groups are identified in the table.

A weight per cent plot of other oxides v MgO (after averaging and scaling to 100% water and CO₂ free) is shown in fig 1 (total iron is plotted as FeO). In fig 1 H = average harzburgite, GH = average garnet harzburgite, GLIK = averages of garnet lherzolite (ex table 1 and from Carswell and Dawson 1970) excluding MF most fertile looking garnet lherzolite 1032 (table 1) from Matsoku. A poor linear correlation between MgO and other oxides through these rocks is indicated. Dashed field P includes some possible primary picritic magmas, K, K', S being komatiite and Sandspruit ultramafic lavas (Viljoen and Viljoen 1969a); and B = Baffin Island picrite (Clarke 1970). M = a 'fertile' garnet-lherzolite nodule from Hawaiian basalt (Jackson and Wright 1970). Compositions in field P include known liquid magmas; while B is known to approximate to initial partial melt of garnet lherzolite at 30 kb, the best liquid extract to yield H, GH from GLIK appears to be komatiite, K. MF and M have chemistry of possible liquid extracts. If K, MF, M do represent liquids in equilibrium with olivine and orthopyroxene, the pressure of their derivation must have been much greater than 30 kb (they are high in olivine in the CIPW norm). Field E contains compositions of possible early eclogite extracts during high pressure fractionation (selected from O'Hara *et al* 1973, fig 2). Field T contains the compositions of the parental magmas of Hawaiian tholeiite suites (Macdonald and Katsura 1964). For each major oxide plot, the composition ranges of olivine and pure Mg-Fe orthopyroxene with Mg/Mg+Fe 100-85 are indicated.

Figure 2 illustrates for one pair of oxides how fig 1 might be used to play the currently popular petrogenetic guessing games, using real rock compositions, to obtain 15% primary magma, L_P, from a garnet-lherzolite source mantle, then to fractionate 50% early eclogite (mean composition E) from it, yielding residual liquid L which might still undergo 38.5% extraction of olivine (average Fo_{87.5}) in order to yield an eruptive parental tholeiite magma L_T (maximum enrichment factor for incompatible elements relative to source is ~20). Fe/Mg distribution between liquids and crystals at each step conform to known or plausible equilibrium relationships. (The games may be played for the other oxides as well, and in many other ways; anyone may join in, but subtract points if you have to use rock types not actually found in nature, or find the fit less good when the same calculation is made for the other oxides; stentorian Boanerges have a head start).

None of the commonly erupted magmas seen at the earth's surface can be the primary magma generated during the partial melting events which created the residual mantle types found in kimberlite. Komatiite and related ultramafic lavas, which appear to have been a relatively widespread lava type 3.45×10^9 years ago, might be the complementary liquid extracted when the principal chemical variation between the peridotite was created, constituting evidence for a widespread major thermal, tectonic and chemical upheaval in the upper mantle at that time. This interpretation

Table 1. Analyses of garnetiferous ultrabasic rock from kimberlite

Type	No.	SiO ₂	TiO ₂	Al ₂ O ₃	Cr ₂ O ₃	Fe ₂ O ₃	FeO	MnO	NiO	MgO	CaO	Na ₂ O	K ₂ O	P ₂ O ₅	H ₂ O+	CO ₂	Class (O'Hara 1973) I(i) or V(i)
1.Gnt-Herzolite ¹	1032	45.52	.15	4.83	.58	1.61	10.40	.18	.22	30.34	4.26	.34	.04	.02	1.58		
2. " " 2	11093	45.19	.054	1.52	.39	0.92	4.74	.100	.26	41.8	1.04	.18	.16	.04	3.26	.10	I(i)
3.Gnt-harzburgite 3	A6-10594	43.20	.02	3.13	.37	2.56	3.46	.10	.24	41.98	0.97	.10	.05	.04	3.64		
4. " " 4	11083	45.37	.012	1.29	.42	0.84	4.76	.101	.27	42.5	0.65	.12	.06	.04	3.00	.04	II(i)
5. " " 5	A5-10593	45.49	.080	1.01	.46	1.23	5.02	.106	.29	41.2	0.95	.14	.06	.06	3.13	.14	
6.Harzburgite ³ 3	A11-10586	44.36	.010	1.14	.34	0.62	5.35	.099	.30	44.3	0.53	.08	.06	.08	2.09	.15	
7. " " 3	A13-10587	44.46	.013	0.64	.34	0.98	5.10	.102	.30	43.8	0.67	.11	.06	.04	2.90	.18	
8. " " 3	A14-10588	46.58	.014	1.01	.45	1.20	4.37	.101	.26	40.6	0.77	.20	.20	.07	3.70	.26	III
9. " " 9	11082	45.38	.007	1.18	.36	0.98	4.70	.094	.27	41.9	0.76	.10	.08	.02	3.76	.16	
10. " " 10	11091	45.70	.024	1.19	.38	0.98	4.78	.097	.27	41.6	0.89	.11	.08	.04	2.97	.27	
11.Lherzolite ³ 3	A15-10589	44.77	.55	0.84	.14	1.70	3.99	.10	.27	40.03	1.76	.12	.94	nil	4.07		
12. " " 3	A10-10591	45.23	.06	.57	.35	2.47	3.54	.10	.26	40.70	2.59	.29	.09	.029	3.35		II(iii)
13. " " 11089	41.61	.127	.51	.31	1.42	4.88	.082	.27	44.5	1.39	.21	.14	.03	3.97	.20	or II(iv)	
14. " " 1033	45.14	.06	.48	.14	0.90	7.18	.11	.30	41.78	2.54	.12	.10	.05	1.17			
15.Pyroxenite ³ 1	A17-10597	51.82	.02	2.57	.68	1.84	2.94	.14	.093	25.90	11.04	.83	.12	.043	1.66		
16. " " 1031	51.84	.12	4.18	.44	0.89	6.31	.18	.12	27.00	6.66	.62	.05	.02	0.77		VII(i)	
17. " " 5	1042	51.61	.11	4.24	.57	1.13	6.17	.18	.12	27.65	6.61	.63	.06	.01	0.94		

Notes (1) Garnet and two pyroxenes analysed (O'Hara *et al* 1973). (2) Average used in constructing fig 1 includes analyses of E11, E3 (Nixon *et al* 1963) A3-10596 (Holmes 1936) and KA 64.16 (Ito and Kennedy 1967). (3) Mineral data in O'Hara and Mercy (1963), Mercy and O'Hara (1965). (4) Average used in fig 1 includes A1-10585 (Holmes 1936). (5) 1042 is separate split of same rock as 1032.

supports hypothesis B of Viljoen and Viljoen (1969b).

So far as major element concentrations are concerned, it is possible to choose real rock compositions which permit a partial melting product of garnet-lherzolite to undergo substantial eclogite fractionation, followed by substantial olivine fractionation, in order to yield a residual magma similar to the parental magmas of oceanic island provinces. (Minor and trace elements have not been treated because of contamination problems in the source and residual peridotites).

Eclogite fractionation would have relatively little effect upon the major element composition of primary magmas similar to Baffin Island picrites (at say 30 kb). At higher pressures eclogite extraction will have increasingly dramatic effects, especially upon komatiite-like primary magmas, driving their residual liquids rapidly towards MgO, FeO-rich and CaO, Al_2O_3 -poor compositions.

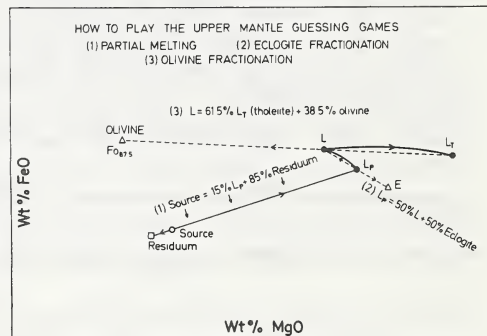
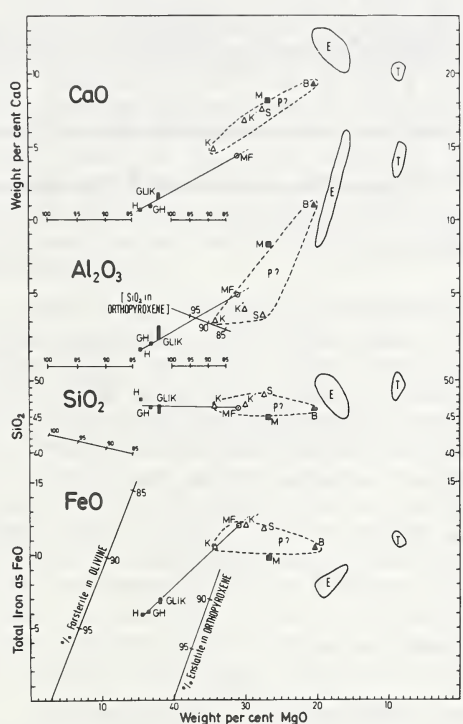


Fig 1. Wt% plot (volatile free) of oxides v MgO. See text.

Fig 2. Example of interpretation of fig 1. See text.

peridotites

Reasons for rejecting the hypothesis that MF represent the true source mantle include (i) scarcity among nodule suites, (ii) predicted relatively slow seismic velocity due to higher Fe/Mg ratio. If, however, material of this type were supposed to exist as source mantle at greater depths than commonly sampled by kimberlite ascending 'plumes' could apparently go some way towards explaining the generation of parental tholeiite as primary magmas in modern volcanic provinces. However, the FeO v MgO balance shown in fig 1 indicates that the common peridotite nodules in kimberlite (or basalt for that matter) could not possibly be residua from such a partial melting process (T , MF and GLIK are not colinear). The hypothesis is in any case unsatisfactory because the tholeiite magmas erupted over alleged mantle plumes in Hawaii and Iceland

have the distinctive compositions, temperatures and phenocryst assemblages associated with liquids which have undergone fractional crystallization at low pressures (Jamieson 1970, O'Hara 1965, 1973b).

References

Carswell, D.A. and Dawson, J.B. 1970. Contr. Mineral. Petrol. 25, 163-184

Clarke, D.B. 1970. Contr. Mineral. Petrol. 25, 203-224

Holmes, A. 1936. Trans. geol. Soc. S. Africa 39, 379-428.

Ito, K. and Kennedy, G.C. 1967. Am. J. Sci. 265, 519-538.

Jackson, E.D. and Wright, T.L. 1970. J. Petrology 11, 405-430.

Jamieson, B.G. 1969. Min. Mag. 37, 537-554.

Macdonald, G.A. and Katsura, T. 1964. J. Petrology 5, 82-133.

Mercy, E.L.P. and O'Hara, M.J. 1965. Norsk geol. Tidsskr. 45, 457-461.

Nixon, P.H. et al 1963. Am. Mineral. 48, 1090-1132.

O'Hara, M.J. 1965. Scott. J. Geol. 1, 19-40.

*O'Hara, M.J. 1973a, this volume (Subsolidus mineral assemblages etc.)

O'Hara, M.J. and Mercy, E.L.P. 1963. Trans. Roy. Soc. Edinb. 65, 251-314.

O'Hara, M.J. et al 1973, this volume (Chemistry of some eclogite nodules from kimberlite).

Viljoen, M.J. and Viljoen, R.P. 1969a. Geol. Soc. S. Africa Spec. Pub. 2 55-85.

and _____ 1969b. Geol. Soc. S. Africa Spec. Pub. 2 275-295.

*O'Hara, M.J. 1973b. Nature 243, 507-508.

CHEMISTRY OF SOME ECLOGITE NODULES FROM KIMBERLITE; ECLOGITE FRACTIONATION
 M.J. O'Hara and M.J. Saunders, Grant Institute of Geology, University of
 Edinburgh, and E.L.P. Mercy, Department of Geology, Lakehead University,
 Ontario.

Eclogite may be a crystal extract from primary magmas differentiating deep within the mantle perhaps on a trend which ultimately leads to kimberlite-like residual fluids (O'Hara and Yoder 1967). The chemistry of eclogites is therefore of fundamental importance. Two technical problems hamper assessment of the data - how far sampling problems affect the apparent results (eclogite hand specimens are generally small samples of coarse grained rocks), and how far contamination influences the chemistry (eclogites, like garnet-peridotites, are poor in many elements which are rich in the kimberlite matrix which encloses them).

Results. Table 1 contains analyses of eclogites (whole rock). Analyses of their pyroxenes (table 2) and garnets (table 3) enable the extent of possible contamination to be assessed. Whole rocks contain more TiO_2 than their constituent major minerals, but the difference could be made up by much less than 0.5% primary rutile which might be missed both during petrographic examination and mineral separation. Some TiO_2 in these eclogites has probably been introduced from the kimberlite. P_2O_5 is uniformly lower in the major minerals than in the bulk rocks; although the discrepancy lies within the range of possible primary apatite presence, some of this P_2O_5 probably represents contamination. The possible effect of contamination and alteration on major oxides can be evaluated from the data presented.

The ratios $Mg/Mg+Fe$ and $Na/Na+Ca$ show wide variations, which are in no way correlated with each other. Clearly, no simple geochemical trend connects all of these rocks. TiO_2 concentrations are moderately low relative to possible ultrabasic and basic magmas, as also are Cr_2O_3 and NiO . The rocks have generally olivine-basaltic major element composition, and their extracation from primary magmas of basaltic character would (obviously) not affect greatly the major_{element} concentrations in the residual liquids. The eclogites are extremely variable in CaO/Al_2O_3 ratio which ranges from 0.4 to 1.0 (in weight per cent) and this is the ratio most affected by sampling error in the pyroxene/garnet ratio. However, the variation among the five Roberts Victor eclogites cannot be ascribed solely to sampling errors. The extracation of eclogite from possible primary partial melts of garnet peridotites will not necessarily produce non-basaltic CaO/Al_2O_3 ratios in the residual liquids.

Clinopyroxene, orthopyroxene and garnet from the garnet websterite and garnet lherzolite from Matsoku are also shown in tables 2 and 3. The lower $Mg/Mg+Fe$ and $Cr/Cr+Al$ ratios of the garnet-lherzolite relative to the garnet websterite, in whole rock (O'Hara et al. 1973) and minerals accords with the interpretation of the garnet lherzolite as a frozen liquid and the garnet websterite as a possible crystal cumulus.

Figures 1 and 2 (projection as in Ford et al. 1972, fig. 7) compare Mg/Fe variations and silica saturation levels in eclogite, peridotite and basalt. Figure 2 shows that it is possible to choose source garnet lherzolite, residual harzburgite, 30 kb primary magmas and early eclogite accumulates such that substantial eclogite fractionation might be followed by substantial olivine fractionation yielding residual tholeiitic magmas without imposing excessively low $Mg/Mg+Fe$ on the residual liquids.

Table 1. Eclogites

	SiO ₂	TiO ₂	Al ₂ O ₃	Cr ₂ O ₃	Fe ₂ O ₃	FeO	MnO	NiO	MgO	CaO	Na ₂ O	K ₂ O
1	42.01	.35	20.30	.058	1.18	11.54	.27	.064	14.14	7.84	0.67	.19
2	44.60	.33	16.93	.078	0.69	11.35	.31	.062	14.10	8.20	1.53	.26
3	46.31	.34	16.67	.082	1.09	9.58	.33	.030	13.75	8.60	2.08	.35
4	46.49	.42	11.94	.39	3.40	8.90	.30	.059	14.52	9.94	1.55	.84
5	48.34	.44	11.90	.12	1.32	9.14	.23	.064	13.51	10.30	2.41	.35
6	43.98	.44	18.33	.118	2.34	10.12	.36	.014	12.32	8.33	1.73	.20
7	45.18	.46	17.06	.15	0.92	11.43	.17	.024	11.92	8.96	2.10	.38
8	45.62	.72	13.45	.036	2.99	9.34	.12	.015	10.23	15.52	1.14	.09
9	45.97	.52	13.26	.043	3.91	9.06	.26	.042	10.51	12.28	0.76	.20
10	44.15	.86	13.54	.022	2.81	8.13	.10	.046	12.37	12.89	0.33	.02

(Eclogite analyses also contain ~ 0.01 - 0.41 P₂O₅ and 0.6-4.5% H₂O)

Table 2. Pyroxenes

	SiO ₂	TiO ₂	Al ₂ O ₃	Cr ₂ O ₃	Fe ₂ O ₃	FeO	MnO	NiO	MgO	CaO	Na ₂ O	K ₂ O	P ₂ O ₅
from (1)	56.62	.37	8.29	0.081	0.00	4.52	.08	.068	11.46	14.06	4.44	-	-
from (2)	54.09	.33	7.22	0.09	1.18	4.16	.13	.050	12.32	14.75	3.90	.17	-
from (3)	55.49	.35	9.04	0.10	1.33	3.00	.083	.040	10.98	13.96	5.19	.18	.052
from (4)	54.05	.24	4.36	0.48	1.73	5.70	.14	.031	14.59	16.32	1.98	.18	.032
from (5)	54.71	.39	6.03	0.15	1.92	4.61	.12	.039	12.54	14.99	4.06	.15	.60
from (6)	52.84	.44	9.79	0.15	1.03	3.81	.093	.023	11.21	13.71	4.46	.16	.011
from (7)	54.03	.42	9.28	0.18	0.71	4.04	.090	.033	10.44	13.67	5.23	.18	.000
from (8)	51.58	.49	7.24	0.029	2.71	3.95	.035	.024	11.68	19.87	1.98	.04	.009
from (10)	52.31	.53	6.23	0.033	2.24	3.56	.046	.012	12.19	19.78	2.49	.03	.085
from 1031	54.66	.14	2.42	0.80	1.13	2.78	.11	.063	16.66	19.50	1.34	.03	.013
from 1032	54.12	.23	2.63	1.43	1.63	3.60	.11	.069	16.26	18.09	1.65	.04	-
from 1031	56.85	.087	0.72	0.15	0.72	6.71	.15	.13	33.28	0.85	0.18	.03	.019
from 1032	56.12	.11	0.95	0.26	1.10	8.40	.086	.13	31.42	1.30	0.22	-	-

Table 3. Garnets

	SiO ₂	TiO ₂	Al ₂ O ₃	Cr ₂ O ₃	Fe ₂ O ₃	FeO	MnO	NiO	MgO	CaO	P ₂ O ₅
from 1	41.24	.29	22.25	.054	.10	14.32	.36	.016	15.17	5.91	.038
from 2	41.06	.28	22.17	.076	.61	15.00	.40	.009	14.67	5.61	.028
from 3	41.03	.27	22.55	.080	.50	14.38	.47	.008	15.32	5.18	.042
from 4	40.74	.33	21.73	.34	.73	16.86	.46	.007	14.44	4.39	.032
from 5	40.58	.35	22.45	.11	.37	16.60	.44	.008	14.58	4.39	.032
from 6	40.61	.39	22.09	.12	.41	15.61	.49	.005	13.14	6.96	.027
from 7	40.64	.34	22.15	.15	.46	16.36	.48	.006	12.89	6.45	.032
from 8	39.58	.24	21.24	.034	1.04	17.84	.46	.004	8.38	11.07	-
from 10	39.93	.06	21.65	.024	.69	19.16	.42	.003	10.96	5.90	.036
from 1031	41.89	.19	22.15	2.00	1.21	9.18	.22	.005	18.51	4.94	.008
from 1032	40.67	.40	19.56	3.97	.06	12.75	.38	.011	17.07	5.18	.014

Key to analyses of eclogites and their minerals

- Eclogite, Roberts Victor mine 11063; garnet $n=1.759$; clinopyroxene $\alpha=1.670$, $\beta=1.679$, $\gamma=1.696$.
- Eclogite, Roberts Victor mine, 11062; garnet $n=1.757$; clinopyroxene $\alpha=1.671$, $\beta=1.681$, $\gamma=1.697$. Garnet partly as blebs in pyroxene. Some interstitial phlogopite and spinel.
- Eclogite, Roberts Victor mine 11060; garnet $n=1.758$; clinopyroxene $\alpha=1.668$, $\beta=1.678$, $\gamma=1.891$; some phlogopite, trace apatite, epidote.
- Eclogite, Roberts Victor mine 11061.
- Eclogite, Roberts Victor mine 11064.
- Eclogite, Jagersfontein 352; garnet $n=1.761$.
- Eclogite, Wesselton.
- Eclogite, Vissers Pipe (No. 8), Tanganyika cf. sample 37079 (O'Hara and Yoder 1967), garnet $n=1.767$; clinopyroxene $\alpha=1.681$, $\beta=1.693$, $\gamma=1.710$.
- Eclogite 509; Shinyanga.
- Eclogite, Matsoku pipe Basutoland.
- 1031 garnet websterite, Matsoku pipe
- 1032 garnet lherzolite, Matsoku pipe (rock analyses in O'Hara et al this vol.)

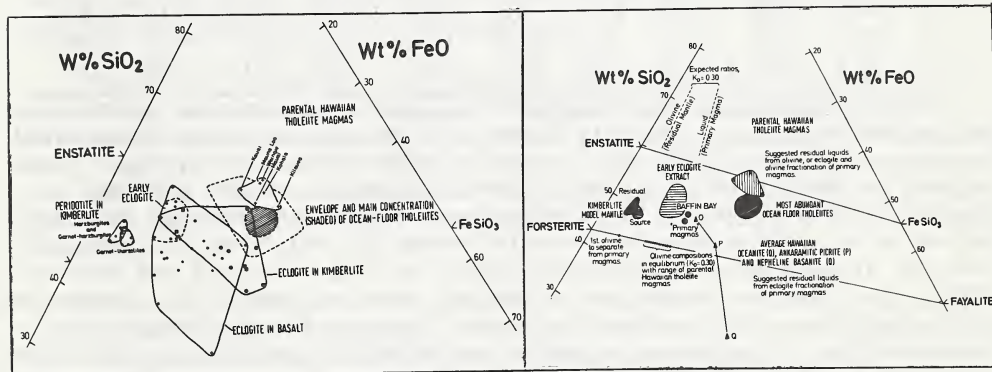


Fig 1

Fig 2

The field indicated 'early eclogites' (fig 1) encloses the compositions of the diopside 42.5%+pyrope 57.5% mixture from A3-10596 which lies close to the possible early eclogite precipitate at 30 kb (O'Hara and Yoder 1967) shown by a cross; and eight eclogites (small filled circles) which have the merits of preserving high temperature, high pressure mineralogy and actually occurring among basalt, from diatremes in Hawaii, Kenya and Australia. Their compositions are listed in table 4. O'Hara (1969) has argued from data projections that rocks such as these probably retain garnet as a separate phase under all subsolidus conditions where the garnet-clinopyroxene assemblage is stable itself and are therefore correctly described as eclogites rather than exsolved clinopyroxenites. The point has been proved experimentally for the specific case of R.392 by Irving and Green (1970) who quote 20% as the minimum amount of garnet seen in their run products.

Table 4. Analyses representing possible early eclogite extracts in fractionation of primary magmas within the upper mantle

SiO ₂	TiO ₂	Al ₂ O ₃	Cr ₂ O ₃	Fe ₂ O ₃	FeO	MnO	NiO	MgO	CaO	Na ₂ O	K ₂ O	P ₂ O ₅
(A) 46.93	0.18	13.82	1.99	1.67	4.62	0.29	0.03	18.54	11.38	0.79	0.01	0.02
(1) 49.26	0.62	8.63	0.31	3.24	5.09	0.17	n.d.	19.40	12.44	0.88	0.06	0.02
(2) 48.46	0.43	7.96	0.54	3.55	4.92	0.17	n.d.	19.96	12.00	1.90	0.19	n.d.
(3) 48.41	0.62	10.41	0.43	2.58	5.61	0.18	n.d.	17.78	12.17	1.24	0.11	0.04
(4) 50.20	0.51	8.37	0.24	1.58	5.72	0.16	0.10	19.00	13.28	0.87	0.02	0.02
(5) 49.52	0.42	9.31	0.35	2.26	5.44	0.16	0.09	17.97	12.90	1.17	0.04	0.03
(6) 45.58	0.80	13.69	0.12	3.76	5.85	0.16	0.06	16.09	11.78	1.27	0.02	0.03
(7) 44.68	0.11	15.79	0.03	3.90	5.50	0.26	n.d.	15.74	10.32	1.22	0.13	0.09
(8) 46.12	0.44	15.05	0.16	1.49	4.87	0.11	-	15.09	14.61	0.82	0.22	0.04

Notes (A) A3-10596 pyrope-diopside mixture (O'Hara and Yoder 1967); (1) - (6) Hawaii, (Macdonald and Katsura 1964, Kuno 1964, Yoder and Tilley 1962, and SAL 6, SAL 24 and SAL 7 from Jackson and Wright 1970); (7) Kenya (Saggesson 1968, no. 9); (8) Australia R392 (Lovering and White 1969).

Table 5

SiO ₂	Al ₂ O ₃	FeO	MgO	CaO	Cr ₂ O ₃	TiO ₂	Na ₂ O	K ₂ O	P ₂ O ₅
(1) 46.2	11.1	10.8	20.2	9.4	0.28	0.77	1.06	0.08	0.09
(2) 46.2	13.9	9.3	16.3	11.9	0.12	0.81	1.29	0.02	0.03
(3) 46.2	8.3	12.3	24.1	6.9	0.44	0.74	0.83	0.14	0.15
(4) 50.0	13.8	12.4	8.5	11.5	0.73	1.23	1.38	0.23	0.25
(5) 50.0	14.1	11.4	8.6	10.4	n.d.	2.53	2.16	0.39	0.26

Table 5 represents the results of a specific calculation in which a possible 30 kb primary magma (1; Clarke 1970 Baffin Bay group II picrite) has extracted from it 50% of an early eclogite in basalt (2; SAL 7 from Jackson and Wright 1970) to yield a putative high pressure residual liquid (3) from which 40% of olivine (mean composition Fo_{87.5}) has been extracted to yield a putative eruptive magma (4) which may be compared with the average Hawaiian parental tholeiite (5); Macdonald and Katsura 1964). All iron was converted to FeO for these calculations. Comparison of the putative eruptive liquid (4) with observed parental magma (5) indicates that if extensive eclogite and olivine fractionation are to be major factors in the evolution of liquids such as (5), either the primary magmas must contain more TiO₂ and Na₂O than (1) or the eclogite must contain less TiO₂ and Na₂O than (2). The calculation, nevertheless, indicates the essential feasibility of such an evolutionary scheme.

References

Clarke, D.B. 1970. Contr. Mineral. Petrology 25, 203-224.
 Ford et al 1972. Proc. 3rd Lunar Sci. Conf. Geochim. Cosmochim. Acta Suppl. 3, 1, 207-229
 Irving, A.J. and Green, D.H. 1970. Phys. Earth Planet. Int. 3, 385-389.
 Jackson, E.D. and Wright, T.L. 1970. J. Petrology 11, 405-430.
 Kuno, H. 1964. Advancing frontiers in Geology and Geophysics 205-220.
 Lovering, J.F. and White, A.J.R. 1969. Contrib. Mineral. Petrology 21, 9-52.
 Macdonald, G.A. and Katsura, E. 1964. J. Petrology 5, 82-133.
 O'Hara, M.J. 1969. Geol. Mag. 106, 322-330.
 O'Hara, M.J. et al 1973 this volume.
 O'Hara, M.J. and Yoder, H.S.Jr. 1967. Scott. J. Geol. 3, 67-117.
 Saggesson, E.P. 1968. Geol. Rdsch. 57, 890-903.
 Yoder, H.S.Jr. and Tilley, C.E. 1962. J. Petrology 3, 342-532.

INCLUSIONS IN DIAMONDS: GARNET LHERZOLITE AND ECLOGITE ASSEMBLAGES.

Martin Prinz

Department of Geology, Institute of Meteoritics, University of New Mexico, Albuquerque, New Mexico, 87131, U.S.A.

D. Vincent Manson

Department of Mineralogy, American Museum of Natural History, New York, N.Y. 10024, U.S.A.

Paul F. Hlava and Klaus Keil

Department of Geology, Institute of Meteoritics, University of New Mexico, Albuquerque, New Mexico, 87131, U.S.A.

Thirty inclusion-bearing diamonds have been studied in order to determine the mineral assemblages and chemical compositions of the inclusions. Inclusions were exposed either by cracking or burning the diamond or studied *in situ* within cut gems. They were analyzed with an electron microprobe, and supplemental data were obtained by optical goniometry and x-ray techniques. Inclusions range in size from $<10\ \mu\text{m}$ to about 1 mm, but are mostly 50-200 μm . Inclusions which are syn-genetic with the formation of the diamond have good crystal faces, but they generally appear to have the morphology of negative crystals of diamond, rather than of their own crystal structure. Thus, garnets, pyroxenes, olivines, and other minerals are dominated by octahedral faces. Sobolev et al. (1972) has reported a similar finding. These crystals which have foreign faces, are termed xenohedral.

Inclusion assemblages fall into two suites, garnet lherzolite (or peridotite) and eclogite. Sobolev (1972) and Meyer and Boyd (1972) have found a similar grouping. Each has compositionally distinct mineralogy and therefore an assemblage can be assigned to one of the suites even when one mineral is present. Thus, the compositional range of assemblages reported here represents portions of assemblages from different diamonds.

Twelve diamonds contained portions of the garnet lherzolite assemblage which consists of garnet, diopside, enstatite, olivine, and chromite. Garnet is burgundy-colored, is pyrope-knorrtingite-rich, with 0.7-9.2% Cr_2O_3 (Table 1). Diopside has 0.11-1.56% Cr_2O_3 and 2.8-4.4% Al_2O_3 . Diopside, in two diamonds, appears to have exsolved enstatite into wholly separate portions of a single crystal. Enstatite (En₈₆₋₉₄) has 0.06-0.28% Cr_2O_3 and 0.09-1.32% Al_2O_3 (Table 2). Olivine (Fo₉₂₋₉₃), commonly present as elongated crystals, has 0.03-0.15% Cr_2O_3 ; the Cr may possibly be present as Cr^{2+} . Chromite has about 66% Cr_2O_3 , 6% Al_2O_3 , and 10% MgO (Table 3).

Eighteen diamonds contained portions of the eclogite assemblage. The essential minerals are garnet and omphacitic pyroxene. Garnets are honey-brown in color and rich in pyrope, grossular, and almandine molecules (Table 1); they contain about 0.2% Na_2O . Omphacitic pyroxenes have 2.7-10.7% Al_2O_3 , 1.4-5.8% Na_2O , and 0.04-0.87% K_2O (Table 2). K_2O contents of 0.62-0.87% were found in numerous crystals within 4 diamonds and are considerably higher than any previously recorded in omphacite; the K_2O is homogeneously distributed and x-ray data shows that no other phase is intergrown. Other primary minerals present in the eclogite assemblage are kyanite (Table 3; reported for the first time in a diamond), olivine (in a rare olivine eclogite assemblage), rutile (Table 3),

phlogopite, and magnetite. The phlogopite is in a polymineralic inclusion, with omphacite and rutile, is low in MgO and high in FeO and TiO_2 (Table 3), and is the first recorded occurrence within a diamond. Magnetite is found in 6 eclogite assemblage diamonds and is a very pure phase (Table 3), except for some inhomogeneously distributed Ni and Co. Crystals are highly porous, and the origin of the porosity is not yet known. Its common occurrence in eclogite assemblage minerals suggests that it is syngenetic, although the oxygen fugacities necessary for its stability remain unknown. Sanidine, a polymorph of silica (possibly coesite), and a membranous material rich in SiO_2 , Al_2O_3 and K_2O are also present in diamonds with eclogite assemblage, but it is not yet clear if they are syngenetic or epigenetic with the origin of the diamond.

Epigenetic minerals found in diamonds are muscovite, amphibole (hornblende, actinolite), sulfide (pentlandite, chalcopyrite), and an altered SiO_2 - Al_2O_3 -FeO phase which may have originally been kyanite.

The following results and conclusions are drawn from this study: (1) Diamonds appear to be a unique window into the upper mantle and provide unaltered samples of a wide compositional range of several rock suites. (2) No mixing of suites has been found within a single diamond. (3) Temperatures of formation of the pyroxenes in garnet lherzolite assemblages are between 1000°C and 1400°C, depending upon whether the present compositions are used or the presumed compositions of the original homogeneous pyroxenes, assuming exsolution. The pressures of formation for the garnet lherzolite assemblages are at least 40 kb, but cannot yet be estimated with existing experimental data. (4) The presence of high (0.6-0.8%) K_2O in omphacitic pyroxene may be highly significant in terms of partial melting models and heat sources in the upper mantle and should be studied experimentally. (5) Some kyanite eclogites are now known to be stable at temperatures and pressures at which diamond is stable. (6) The abundance and variety of inclusions, both monomineralic and polymineralic, within single diamond crystals suggests that a complex history has preceded the formation of the host diamond. This history would appear to precede the formation and emplacement of kimberlite and further study of inclusions in diamonds will reveal some of its details.

References:

Sobolev, N.V., Botkunov, A.I., Bakumenko, I.T., and Sobolev, V.S. (1972) Dokl. Akad. Nauk SSSR. 204, 117-120.
 Sobolev, N.V. (1972). Aust. Nat. Univ. Publ. No. 210, 38 p.
 Meyer, H.O.A. and Boyd, F.R. (1972). Geochim. Cosmochim. Acta 36, 1255-1273.

Table 1. Electron microprobe analyses of garnet inclusions in some diamonds (in weight percent).

Garnet Lherzolite Assemblage			Eclogite Assemblage			
Diamond No.	9	14	1	38	42	27
SiO ₂	41.9	41.8	41.7	40.1	39.3	39.0
TiO ₂	.04	*	.39	.49	.81	1.03
Al ₂ O ₃	17.3	16.3	23.0	22.4	22.1	21.9
Cr ₂ O ₃	9.2	8.3	.70	.06	.18	.03
V ₂ O ₃	.02	.03	.02	.03	.04	.04
+Fe ₂ O ₃	.60	.50	1.00	--	.50	.70
FeO	5.0	8.1	8.3	17.6	18.8	14.9
MnO	.31	.34	.46	.55	.49	.32
MgO	24.3	20.7	20.8	12.1	8.7	6.0
CaO	1.29	3.2	4.2	5.6	9.1	16.2
Na ₂ O	*	.05	.03	.22	.40	.28
K ₂ O	.01	.03	*	.13	.11	.02
Total	99.97	99.35	100.60	99.28	100.53	100.42
+Fe ₂ O ₃	Calculated to balance garnet formula.					

Molecular End Members

Knorringleite	26.0	25.2	2.0	.3	.7	.2
Pyrope	60.2	53.4	71.7	45.1	31.9	22.4
Grossular	1.7	7.6	8.2	16.6	25.4	43.3
Almandine	9.8	11.6	14.5	36.8	39.5	31.5
Andradite	1.6	1.4	2.7	--	1.4	2.0
Spessartite	.6	.7	.9	1.2	1.0	.7

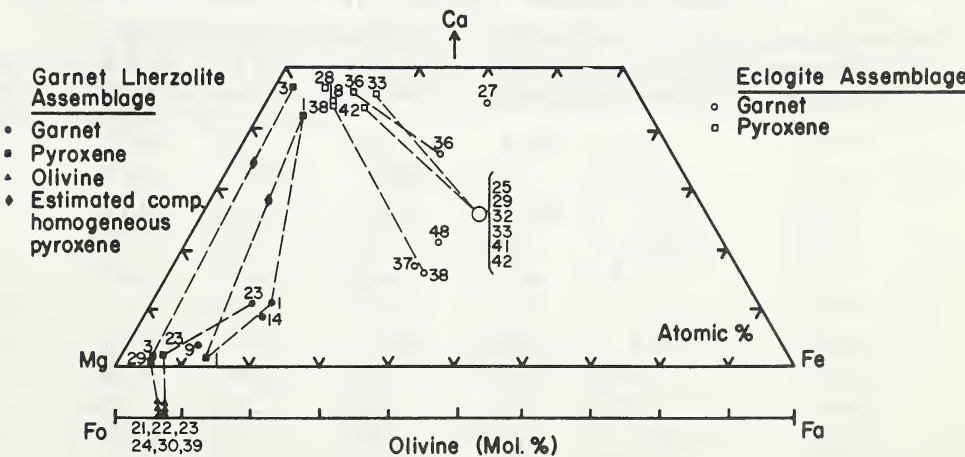


Fig. 1. Ca-Mg-Fe plot of garnet and pyroxene data, and Forsterite-Fayalite (Fo-Fa) plot of olivine data from garnet lherzolite and eclogite inclusion assemblages in diamonds. Dashed lines connect coexisting minerals within a single diamond. Numbers refer to individual diamonds.

Table 2. Electron microprobe analyses of pyroxene inclusions in some diamonds (in weight percent).

Diamond No.	Garnet Lherzolite Assemblage				Eclogite Assemblage	
	3(Cpx)	3(Opx)	1(Cpx)	1(Opx)	38	42
SiO ₂	55.6	58.1	55.5	57.3	55.8	54.7
TiO ₂	.23	.07	.14	.04	.19	.25
Al ₂ O ₃	2.78	.09	4.4	1.32	10.7	7.6
Cr ₂ O ₃	1.56	.11	.28	.06	.13	.13
V ₂ O ₃	.05	.01	.03	*	.09	.05
FeO	1.61	3.9	3.8	8.5	4.1	6.4
NiO	.03	.03	.02	.01	*	*
MnO	.07	.06	.18	.21	.05	.11
MgO	15.6	35.7	15.6	31.4	9.8	10.4
CaO	19.5	.29	17.9	.63	13.3	15.6
Na ₂ O	2.23	.08	1.82	.13	5.8	3.8
K ₂ O	.11	*	.16	.02	.15	.87
Total	99.37	98.44	99.83	99.62	100.11	99.91
Kushiro (1962) End Members						
NaAlSi ₂ O ₆	16.3	.4	13.1	.9	40.9	30.9
CaAl ₂ SiO ₆	.2	.4	3.1	2.3	1.8	.4
CaTiAl ₂ O ₆	.6	--	.4	.1	.5	.7
MgSiO ₃	42.5	88.7	43.2	83.7	26.1	28.2
FeSiO ₃	2.6	9.9	6.2	13.0	6.3	9.9
CaSiO ₃	37.8	.6	34.0	--	24.4	29.9

Table 3. Electron microprobe analyses of selected minerals in some diamonds (in weight percent).

Garnet Lherzolite Assemblage		Eclogite Assemblage				
Diamond No.	4b	51	30	18	18	33
Mineral	Chromite	Kyanite	Rutile	Rutile	Phlogopite	Magnetite
SiO ₂	.11	36.6	.08	.24	36.6	.04
TiO ₂	.32	.13	90.0	96.7	10.8	*
Al ₂ O ₃	5.9	62.1	1.91	1.35	11.8	*
Cr ₂ O ₃	66.2	.02	.17	.34	.35	.09
V ₂ O ₃	.33	n.d.	.20	n.d.	n.d.	.01
Fe ₂ O ₃	--	--	7.2	1.14	--	68.4
FeO	16.1	.30	--	--	12.1	30.8
NiO	.14	n.d.	.21	n.d.	n.d.	.30
MnO	.22	*	.11	.05	.04	.01
MgO	10.0	.04	.07	.01	12.6	*
CaO	.03	.01	.42	.26	.09	.04
Na ₂ O	n.d.	.03	n.d.	n.d.	.10	n.d.
K ₂ O	n.d.	*	n.d.	n.d.	9.6	n.d.
Total	99.35	99.24	100.37	100.09	94.08	99.92
** CoO, 0.23%. Ni and Co variable within crystals.						

DIAMOND-BEARING ECLOGITES

A. M. Reid, NASA Johnson Space Center, Houston, TX 77058; R. W. Brown, Lockheed Electronics Corporation, Houston, TX 77058; J. B. Dawson, Univ. of St. Andrews, Scotland; G. G. Whitfield, c/o Phelps Dodge of Af., Ltd., P.O. Box 106, Kenhardt, Cape, R.S.A.; J.C. Siebert, Cullinan Holdings Ltd, P.O. Olifantsfontein, Transvaal, R.S.A.

Data are presented from a study of garnet and clinopyroxene separates from diamond-bearing eclogites that occur as xenoliths in African kimberlites. Ten garnet-pyroxene pairs, five garnets, and one clinopyroxene have been analyzed by electron microprobe techniques for Si, Ti, Al, Cr, Mn, Fe, Mg, Ca, and Na. A literature survey has also been made to allow comparison with garnet and clinopyroxene compositions in kimberlite eclogites that do not contain diamond.

The scarcity of mineral analyses from diamond-bearing eclogites has not allowed a clear determination of whether diamond-bearing eclogites comprise a chemically or mineralogically unique group. The results reported in this study confirm the conclusion reached by Rickwood and Mathias (1970) that diamond occurs in a wide range of eclogite types. The range of garnet compositions found is comparable to the range reported for kimberlite eclogites with some exceptions. No garnets analyzed in this study have very high Mg contents ($Mg/Mg+Fe > .75$), very high Fe contents ($Mg/Mg+Fe < .6$, as in the Arizona eclogites [Watson, 1967]), or very high Ca contents (grossular > 50 mol. percent as in the grosspydites). High Ca values are common, however, as 11 of the 15 garnets analyzed have between 20 and 40 mol. percent grossular.

The omphacitic pyroxenes also encompass a range in compositions. The range in jadeite substitution is particularly wide with Na_2O contents from under two to over seven weight percent and Al_2O_3 from two to eighteen weight percent.

It is apparent that diamonds are not restricted in occurrence to a single eclogite type and that rocks of varied chemistry must be present in the source region of the African kimberlites, at depths within the stability field of diamond.

GARNET AND SPINEL PERIDOTITE XENOLITHS FROM THE LASHAINE VOLCANO IN NORTHERN TANZANIA

A. M. Reid, NASA Johnson Space Center, Houston, TX 77058; W. I. Ridley, Lunar Science Institute, Houston, TX 77058; C. Donaldson, Lunar Science Institute, Houston, TX 77058; R. W. Brown, Lockheed Electronics Corporation, Houston, TX 77058; and J. B. Dawson, University of St. Andrews, Scotland.

A suite of nine garnet peridotites and eleven spinel (picrochromite) peridotite xenoliths from the Lashaine volcano in northern Tanzania have been studied petrographically and by electron microprobe techniques. The primary assemblages ol+opx+cpx+ga, ol+opx+ga, ol+opx+cpx, ol+opx+ga+sp, ol+opx+cpx+sp, ol+opx+sp, and ol+cpx+sp have been identified. With some exceptions the compositions of primary ol, opx, cpx, ga, and sp are the same in both ga and sp peridotite groups. Olivines are Ni-rich, very low Ca forsterites (Fo92); orthopyroxenes are low Ca, Al, Cr, Ti, Mn enstatites (\sim Wo₁En₉₂Fs₇); clinopyroxenes are low Al, Ti, Mn chrome-diopsides (\sim Wo_{4.4}En₅₂Fs₄, Al₂O₃ two weight percent); garnets are chrome-pyropes (\sim Py₇₅Alm₁₃Gr₁₂); and the spinels are Fe, Al picrochromites (\sim Mg_{0.7}Fe_{0.4}Cr_{1.4}Al_{1.504}).

The primary garnet lherzolite assemblages are stable at \sim 1100°C and 50kb., equivalent to a depth of \sim 150km. Ga and sp coexist in some samples and the ga and sp assemblages apparently have formed at essentially the same P-T conditions from different bulk compositions. The Lashaine spinels are distinct from the highly aluminous variety common in spinel peridotite inclusions in alkali basalts, and the Lashaine spinel peridotites are not the low P equivalents of the garnet peridotites.

Two types of secondary processes are evident in the Lashaine xenoliths.

1. Reaction rims around garnet illustrate the reaction ol+ga \rightarrow Al opx + Al cpx + Al-sp that reflects the transition from ga peridotite to sp peridotite.

2. In several of the ga and sp peridotites there is evidence of partial melting. At some grain boundaries, particularly those involving cpx, local melting has occurred and the melt has quenched to produce the assemblage ol+opx+cpx+sp \pm glass (K-rich) \pm phlogopite. These secondary phases are texturally and compositionally distinct from the primary peridotite phases, and their compositions allow consideration of the nature of the liquids produced by small degrees of partial melting and of the physical environment under which they formed.

MAJOR AND TRACE ELEMENT CHEMISTRY OF GARNET AND SPINEL PERIDOTITES FROM THE LASHAINE VOLCANO, TANZANIA

J. M. Rhodes, Lockheed Electronics Corporation, Houston, TX 77058 and J. B. Dawson, Dept. of Geology, University of St. Andrews, Fife, Scotland

Whole rock analyses, together with determination of the trace elements Rb, Sr, Y, Zr, Nb, Ga, Ni and Cr are reported for twenty, extremely fresh, peridotite xenoliths, together with the host ankaramite and associated carbonatite tuff, from the Lashaine volcano in northern Tanzania. Included for comparison is an analysis of a garnet lherzolite from Matsoku in eastern Lesotho. These xenoliths are inferred to be derived from the garnet peridotite zone of the upper mantle from depths of about 150 km.

The chemical data indicate that two distinct groups of peridotite inclusions have been sampled. One group, the garnet peridotites, is characterized by lower MgO, Mg/Mg+Fe ratios and Ni, and by higher concentrations of SiO₂, Al₂O₃, CaO, K₂O, Cr₂O₃ and lithophile trace elements than the other group, the spinel peridotites. Both groups contain lherzolite and harzburgite variants reflecting internal differences in the CaO/Al₂O₃ ratio. A single inclusion of wehrlite with a markedly lower Mg/Mg+Fe ratio (0.85 versus 0.91-0.93) has a distinctive mineralogy and mineral assemblage.

The mean compositions for the two groups are:

Garnet peridotites: SiO₂ 43.7, TiO₂ 0.07, Al₂O₃ 1.63, total Fe as FeO 6.78, MnO 0.13, MgO 44.5, CaO 1.09, Na₂O 0.11, K₂O 0.09, P₂O₅ 0.06, NiO 0.22, Cr₂O₃ 0.49 wt. percent and Rb 3.6, Sr 14.9, Y 0.9, Zr 4.6, Nb 1.4, Ga 2.8 ppm.

Spinel peridotites: SiO₂ 42.3, TiO₂ 0.06, Al₂O₃ 0.43, total Fe as FeO 7.07, MnO 0.12, MgO 47.7, CaO 0.58, Na₂O 0.07, K₂O 0.03, P₂O₅ 0.02, NiO 0.26, Cr₂O₃ 0.28 wt. percent and Rb 1.7, Sr 11.6, Y 0.6, Zr 3.8, Nb 1.2, Ga 2.2 ppm.

The K₂O and Rb content of the garnet peridotites is higher than is typical for peridotite inclusions but compares closely with the few values published for garnet peridotite inclusions in kimberlite. These high values do not result from contamination, since the rocks are remarkably fresh, and the other trace elements, particularly Nb are too low to be reconciled with appreciable ankaramite contamination. A few samples have unusually high Sr concentrations (>100 ppm) that are unaccompanied by significant increases in other lithophile elements. Most of this Sr is concentrated along grain boundaries and is probably derived from the associated carbonatite.

In comparison with other data available for garnet peridotites, some peridotite inclusions, and inferred mantle compositions, the Lashaine xenoliths appear to be samples of depleted mantle, the garnet peridotites being less depleted than the spinel peridotites. Assuming that the ankaramite host rock is a primary partial melt, complimentary to the depleted peridotite inclusions, then these data can be used to

place limits on the composition of the undepleted upper mantle below the Lashaine volcano.

LITHOPHILE TRACE ELEMENTS IN PERIDOTITE XENOLITHS FROM LASHAINE VOLCANO,
TANZANIA

W. Ian Ridley, Lunar Science Institute, Houston, Texas 77058 and J. B. Dawson, Dept. of Geology, University of St. Andrews, Fife, Scotland.

Large ion lithophile trace elements have been determined in three xenoliths of garnet peridotite and a spinel peridotite, using isotope dilution techniques. The xenoliths occur in an ankaramite lava at Lashaine volcano in N. Tanzania, and they are closely associated with carbonatite. REE, Rb, and Sr have also been determined in pyroxenes and garnets separated from two of the garnet peridotites (BD730, BD738) and in primary phlogopite separated from BD738 using the same techniques as above.

The REE patterns, normalized to chondritic abundances, are of two distinct types. One garnet peridotite, BD730, has a flat, chondrite-like pattern, with about three times chondritic abundances, but with slight depletion in La, Ce, and Nd relative to the heavier rare earths. In this respect it resembles patterns for some oceanic tholeiites. The other two garnet peridotites (BD738, BD776) and the spinel peridotite (BD787) have more fractionated rare earth patterns with Ce/Eu ratios between 2 and 5. The light rare earths have maximum values 3-6 times chondrites but the heavy rare earths are as low as 0.4-0.1 times chondrites. The spinel peridotite shows the smallest concentration of REE as well as low Rb (1 ppm), and Sr (6 ppm). In contrast, BD776 contains 5 ppm Rb and 96 ppm Sr, and BD738 contains 3.8 ppm Rb and 41 ppm Sr.

In two garnet peridotites the separated garnet and chrome-diopside show heavy rare earth and light rare earth enrichment, respectively. However, these minerals in BD738 are approximately twice as enriched in total REE compared to BD730 garnet and clinopyroxene, and are also more enriched in Rb, and Sr. Titanium-rich phlogopite from BD738 contains 4540 ppm Ba, 660 ppm Rb, and 62 ppm Sr. It is enriched in Ba, and Rb but depleted in Sr, relative to phlogopite from Jan Mayen Island, for which a mantle origin has also been proposed. The phlogopite rare earth pattern shows light rare earth enrichment (up to 5.5 times chondrites) relative to heavy rare earths, which have sub-chondritic abundances. The Ce/Eu ratio of approximately 2.5 is within the range of this ratio for some of the xenoliths.

Assuming that the xenoliths represent residual mantle material, then REE distribution coefficients for pyrope-liquid and diopside-liquid allow an estimate of the REE characteristics of possible liquid in equilibrium with the garnet and chrome-diopside in BD730 and BD738. Within each xenolith, both these minerals indicate equilibrium with a melt strongly enriched in light relative to heavy rare earths, but both xenoliths could not have equilibrated with the same melt. BD738 minerals could have equilibrated with a liquid having up to 350 times chondritic abundances of some light rare earths, but these minerals in BD730 would only be in equilibrium with a liquid having approximately 150 times chondritic abundances for these elements. It appears that these two peridotites, and probably BD776 and BD787 show varying degrees of trace element depletion that could have resulted from one or several periods of partial melting.

The liquids theorized to be in equilibrium with BD730, and BD738 have REE patterns that are very similar to ankaramites and some carbonatites. In addition the absolute levels of REE enrichment in the liquid in equilibrium with BD738 minerals are similar to those found in highly alkaline rocks. This suggests that there may be a genetic link between the xenoliths, the host ankaramite, and the closely associated carbonatites i.e. the peridotites are not simply accidental xenoliths of upper mantle material. Although the fractionated rare earth patterns for some of the peridotites, as well as high Rb and Sr, may be the result of intergranular contamination from the host magma, it is equally possible that these features may reflect the presence of intergranular fluid in equilibrium with the high pressure xenolithic minerals (intergranular partial melt).

Trace element data for the peridotite minerals suggests that partial melting involving phlogopite would enrich the melt in Ba, Rb, K, Ti, and this mineral is probably the major source of these elements for very small degrees of partial melting. However whether the phlogopite is totally melted into the liquid phase or remains as a residual phase during small degrees of partial melting will be critical in determining the lithophile trace element content of the resulting magma. It appears probable that for degrees of partial melting greater than 1-3 percent, then melting of chrome diopside and garnet will determine the REE abundances in the melt phase.

MAGNETITE-SERPENTINE-CALCITE DYKES AT PREMIER MINE AND THEIR RELATIONSHIP TO KIMBERLITE AND TO ALKALIC CARBONATITE COMPLEXES

D.N. Robinson, Anglo American Research Laboratories,
P.O. Box 106, Crown Mines, Transvaal.

Carbonate-rich rocks transgressing the multiple kimberlite plug at Premier Mine are of interest for two reasons. Firstly, there has been controversy as to whether they are igneous bodies (e.g. Daly 1925 and Frick 1970) or the result of metasomatic replacement of pre-existing, kimberlite dykes (e.g. Wagner 1914, Williams 1932 and Gerryts 1951). Secondly, should they be igneous bodies they satisfy current definitions of carbonatite (e.g. Heinrich 1966). Thus, their association with kimberlite would be of critical importance in evaluating the relationship between kimberlite and alkali carbonatite complexes.

Two groups of carbonate-rich rocks can be distinguished at Premier Mine. These occur as:

1. Occasional, apparently unconnected magnetite-serpentine-calcite dykes mostly within the so-called Grey Kimberlite of the mine.
2. A system of connected, dyke-like bodies mostly within so-called Black Kimberlite.

1. A MAGNETITE-SERPENTINE-CALCITE DYKE IN GREY KIMBERLITE

The dyke studied is approximately a metre in width and dips steeply. Contacts with adjacent kimberlite are sharp, even where viewed in thin section. The rock is fine-grained at the margins of the dyke but coarsens to medium-grained in the central portions. Calcite constitutes about 55 per cent of the rock and was the first constituent to crystallise. This was followed by magnetite, which accounts for ten per cent of the rock, and then interstitial material apparently consisting of an intimate mixture of poorly crystalline serpentine and gelatinous magnesium hydroxide. A few per cent of the rock consists of ovoid "inclusions", up to a centimetre in length, of various combinations of serpentinous material, magnetite and calcite. The outermost four centimetres of the dyke is peculiar in that carbonate crystals have been pseudomorphosed by serpentine. Small amounts of kimberlite-type minerals recovered from the rock can be adequately accounted for by between one and fifteen per cent assimilation of host rock. The chemistry of the magnetite-serpentine-calcite dyke contrasts with that of associated kimberlite mainly in containing greater amounts of CaO , CO_2 , Fe_2O_3 and P_2O_5 and lesser SiO_2 , MgO , Al_2O_3 and alkalis (Table I).

Consideration of its field relationships and textural characteristics indicates an igneous origin for the magnetite-serpentine-calcite rock.

Megascopic wall rock alteration extends over a width of about twenty centimetres on either side of the dyke. Here, the Grey Kimberlite has been altered from greyish green to dark grey. Instead of exhibiting a turbid matrix as viewed in thin section, this is clear in the altered kimberlite. Talc and tremolite, both of which occur as alteration products of pyroxene in Grey Kimberlite, give way to colourless chlorite whilst biotite, instead of phlogopite, is present in accessory amounts

in the altered rock. The proportions of MgO and H_2O^+ appear to have been enhanced in the altered kimberlite whilst SiO_2 , CaO and alkalis are apparently reduced in amount (Table I). In addition, alteration seems to have resulted in oxidation of some of the ferrous iron present. It should be noted, however, that the abnormally high SiO_2 values quoted for Grey Kimberlite may be a consequence of Waterberg sandstone contamination in the sample analysed.

2. A MAGNETITE-SERPENTINE-CALCITE DYKE IN BLACK KIMBERLITE

The dyke rock is not unlike that described previously. Calcite is less abundant, however, whilst serpentinous material and magnetite are more abundant. Magnetite constitutes thirty per cent of the rock examined. Calcite grains are frequently joined in crooked chains: otherwise the texture of the rock is similar to that of the previous dyke described and, by analogy, is also regarded as igneous. Trace amounts of kimberlite-type minerals occur in the dyke.

Wall rock alteration is intense. In this regard the dyke studied, which is less than five metres wide, grades into unaltered Black Kimberlite through a 35 metre-wide zone of carbonatised kimberlite. Where examined, unaltered Black Kimberlite is a completely serpentised rock without calcite. At twenty metres from the igneous dyke, however, a substantial proportion of the serpentine has been altered to forsterite and phlogopite, and calcite constitutes about fifteen per cent of the rock. Nearer to the igneous dyke calcite becomes progressively more abundant, as do forsterite and magnetite. Kimberlite-type minerals are reduced in amount in carbonatised kimberlite so that the ilmenite content, for example, of samples taken at ten metres and twenty metres, respectively, from the dyke was found to be about twenty per cent of that of Black Kimberlite in each case. A progressive increase in the amounts of CaO and CO_2 and, to a lesser extent, MgO , P_2O_5 and, possibly, MnO and a corresponding decrease in the proportions of SiO_2 , Al_2O_3 , H_2O^+ and alkalis occurs within carbonatised kimberlite as the dyke rock is approached. Relative proportions of TiO_2 , on the other hand, appear to have remained constant (Table I).

It is considered likely that theories of a metasomatic origin for carbonate-rich dykes at Premier Mine may have been influenced by studies made of carbonatised kimberlite rather than actual dyke rock.

The textural characteristics of the magnetite-serpentine-calcite dyke occurring in Grey Kimberlite, in particular, indicate *in situ* crystallisation of the dykes from an essentially liquid magma. Strontium contents of the dykes (Table I) are considerably higher than is usual for sedimentary carbonate, including Transvaal Dolomite (Verwoerd 1967, p.301) and disproves the contention of Daly (1935) that the carbonate of the dykes was derived from Transvaal Dolomite. Since the carbonate-rich dykes are restricted to the kimberlite plug at Premier Mine they have been regarded (e.g. Frick 1970) as representing a phase of the same igneous activity as was responsible for the kimberlite rocks. Such a supposition is in accordance with age determinations made of Premier Mine materials (Allsop, Burger and van Zyl, 1967). The mineralogical and chemical resemblances between the magnetite-serpentine-calcite dykes and matrix material of many kimberlite rocks suggests, furthermore, that they could represent a residual liquid differentiated from a crystallising kimberlite magma. Such

a possibility is supported by experimental results obtained by Franz and Wyllie (1967, p.326).

Whilst the magnetite-serpentine-calcite dykes exhibit many similarities with carbonatite bodies of alkali carbonatite complexes, there are dissimilarities as well. For example, wall rock metasomatism has resulted in basification rather than an introduction of alkalis which tends to negate a direct genetic link between the magnetite-serpentine-calcite dykes and carbonatite of alkali complexes (Le Bas 1973, p.85).

TABLE I
CHEMICAL ANALYSES OF ROCKS STUDIED

	Grey Kimberlite	Altered Kimberlite	Magnetite-serpentine -calcite dyke	Black Kimberlite	Carbonatised Kimberlite 20m	Carbonatised Kimberlite 10m	Magnetite-serpentine -calcite dyke.
SiO ₂	50,3	39,1	16,9	41,0	29,5	30,6	20,8
TiO ₂	0,9	0,8	0,9	2,2	2,1	2,1	1,7
Al ₂ O ₃	3,3	3,8	0,8	2,9	1,6	1,5	0,1
CrO ₃	0,1	0,1	<0,1	0,2	0,2	0,2	<0,1
Fe ₂ O ₃	3,6	4,1	7,0	5,0	6,1	5,1	12,4
FeO	4,4	2,9	3,5	4,3	4,2	6,0	3,2
MnO	0,1	0,3	0,2	0,1	0,2	0,2	0,9
MgO	23,3	36,0	16,6	27,3	32,0	33,0	20,0
CaO	4,2	0,4	26,4	6,0	10,3	11,6	19,3
K ₂ O	0,5	0,2	<0,1	1,2	0,7	0,3	<0,1
Na ₂ O	1,0	<0,1	<0,1	0,7	<0,1	<0,1	<0,1
P ₂ O ₅	0,2	0,1	1,4	0,2	0,2	1,5	0,7
CO ₂	0,3	0,2	19,2	0,2	5,2	4,3	14,6
H ₂ O ⁺	5,0	9,9	5,1	7,5	6,4	1,9	5,4
H ₂ O ⁻	2,8	1,9	0,3	1,1	0,3	0,2	<0,1
Sr	-	79	1218	-	634	767	835

REFERENCES CITED

Allsop H.L., Burger A.J. and van Zyl C. (1967) Earth Planet. Sci. Letts. 3, 161-166.

Daly R.A. (1925) J. Geol. 33, 659-684.

Franz G.W. and Wyllie P.J. (1967) In Ultramafic and Related Rocks. Ed. Wyllie P.J., John Wiley and Sons Inc., New York, 323-326.

Frick C. (1970) D.Sc. thesis (Unpub.), Univ. of Pretoria.

Gerryts E. (1951) Ph.D. thesis (Unpub.), McGill Univ.

Henrich E.Wm (1966) The Geology of Carbonatites. Rand McNally, Chicago.

Le Bas M.J. (1973) Discussion in Jour. Geol. Soc. Lond. 129, 61-85.

Verwoerd W.J. (1967) Handbook G, Geol Surv. S. Afr., Govt. Printer, Pretoria.

Wagner P.A. (1914) Diamond Fields of South Africa, The Transvaal Leader.

Williams A.F. (1932) The Genesis of the Diamond. 1 Ernest Benn Ltd. London.

D/H, $^{13}\text{C}/^{12}\text{C}$ AND $^{18}\text{O}/^{16}\text{O}$ ISOTOPE STUDIES OF MEGACRYST AND MATRIX MINERALS FROM LESOTHO AND SOUTH AFRICAN KIMBERLITES

S.M.F. SHEPPARD* AND J.B. DAWSON**

*Scottish Universities Research and Reactor Centre, East Kilbride, Glasgow, Scotland.

**Dept. of Geology, The University, St. Andrews, Fife, Scotland.

Hydrogen, carbon and oxygen isotope ratios were determined on phlogopite and serpentine megacrysts, unweathered matrix minerals and yellow altered kimberlite from diatremes in Lesotho (Kao, Matsoku) and South Africa (Monastery, New Elands, Wesselton) and dykes and a sill in Lesotho (Kaunyane) and South Africa (Benfontein, Du Plessis, Premier, Wesselton). In this study we try to (1) set limits on the variability of the D/H and C-13/C-12 ratios of deep-seated hydrogen and carbon, and (2) determine the extent and temperature of any isotopic exchange among the minerals of kimberlite and the country rocks and their associated formation waters.

Isotopic Analyses and Results

Well established analytical methods were used to extract hydrogen, carbon and oxygen quantitatively from minerals after removal of all absorbed or interlayer water at temperatures up to 200°C. Our overall analytical precision is better than ± 0.2 per mil for O-18/O-16 and C-13/C-12, and $\pm 2-3$ per mil for D/H. The majority of our results are presented in Figs. 1 and 2.

Discussion

The hydrogen and oxygen isotope data for the hydrous minerals can be divided into three distinct groups (Fig. 1). Except for the yellow kimberlite from the altered margin of the Benfontein sill (S 437) which plots close to the kaolinite line, none of our Group A and B samples have undergone hydrogen and oxygen isotopic exchange in a low temperature ($< 50^\circ\text{C}$) surface or near-surface environment. Similarly all the carbonate data of Fig. 2 support this conclusion except, notably, S437.

All phlogopite megacrysts plot within the Group A field. These are 20 per mil or more enriched in D relative to the Group B serpentine megacrysts and the serpentine - mica matrix including samples from the same hand specimen (Monastery, Wesselton). Glimmerite samples plot within the Group A field. With no evidence to the contrary, Group A data support the proposal that isotopically deep-seated hydrogen is probably in the range - 40 to - 70 per mil and variable from one locality to another (Sheppard and Epstein, 1970)

Most Group B samples coexist with carbonates. These carbonates are enriched, in general, in O-18 relative to the primary igneous carbonatite field (Fig. 2). Group B matrix and serpentine minerals are depleted in O-18 relative to "normal" ultramafic rocks (5.4 to 6.6‰, Taylor, 1968) even when corrected for their O-18 rich carbonate content ($< 12\%$ by weight). If we assume that O-18 values were originally "normal"

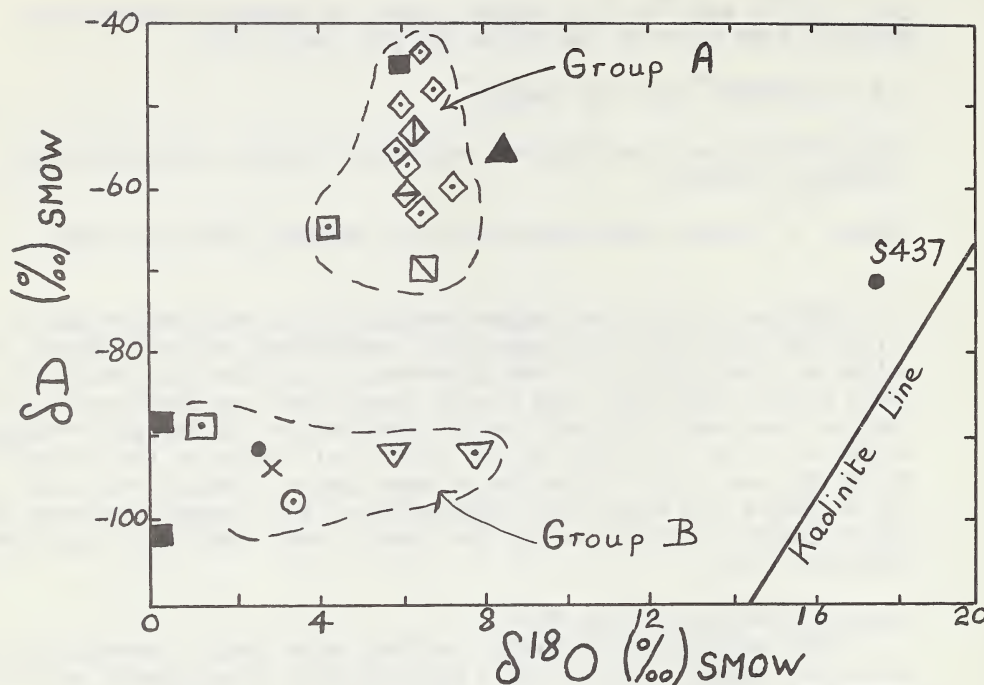


Fig. 1. The $\delta^{18}\text{O}$ vs δD diagram for hydrous minerals from kimberlites from the present study and Sheppard and Epstein (1970). Also plotted is the average δD value for uncontaminated volcanic gases (as water) from Surtsey, Iceland of Arnason and Sigurgeirsson (1968) combined with an assumed $\delta^{18}\text{O}$ value for magmatic water. The kaolinite line of Savin and Epstein (1970), representing the isotopic variation shown by kaolinites from surface weathering environments, is given for reference. Locality symbols are: ∇ Bachelor Lake, \bullet Benfontein, \odot Du Plessis, \diamond Dutoitspan, \blacksquare Panna, \diamond Phoenix, \diamond Central and Eastern United States, \blacksquare Wesselton, \blacktriangle Surtsey. *All Group A minerals are biotite-phlogopite megacrysts including glimmerites (Dutoitspan, Wesselton) from diatremes. Group B minerals include serpentine megacrysts (Monastery) and serpentine and/or mica from the kimberlite matrix of a sill, dykes and fragmental kimberlite. Group B $\delta^{18}\text{O}$ are carbonate free "whole rock" values. Group B Wesselton samples are δD values only. Benfontein S437 is yellow altered kimberlite. * \times Kaunyane, \square Monastery.

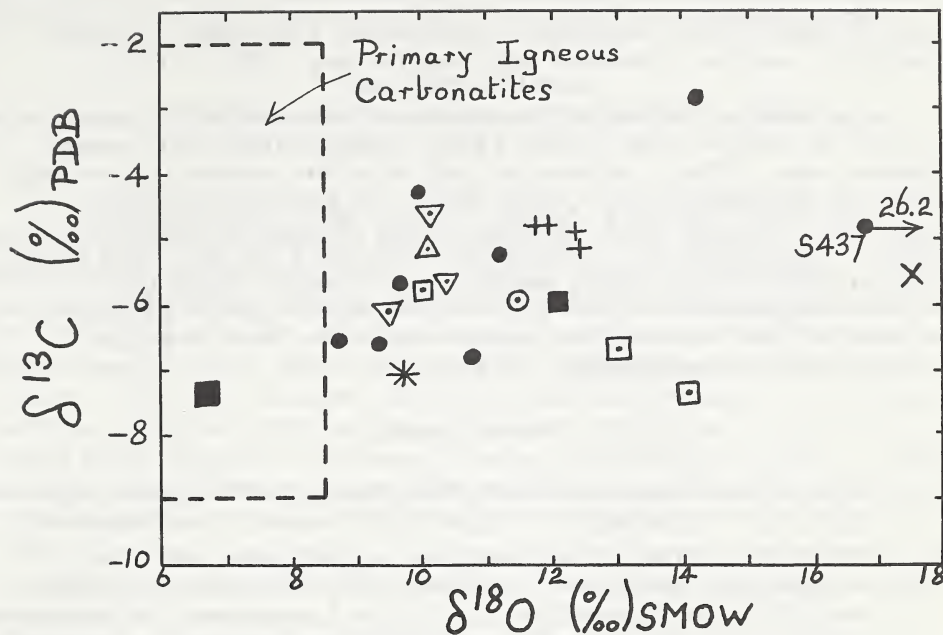


Fig 2. Plot of $\delta^{18}\text{O}$ vs $\delta^{13}\text{C}$ for calcites and dolomites from kimberlites from the present study and Dawson and Hawthorne (1973) compared with the probable field for primary igneous carbonatites (Sheppard and Dawson, 1973). Locality symbols are the same as Fig. 1 except Δ Matsoku, $*$ New Elands, + Premier. The carbonates come from (1) the matrix of a massive black dyke (Wesselton), fragmental kimberlite, a sill and dykes, (2) carbonatite dyke in kimberlite (Premier), (3) carbonated granulite xenoliths (Monastery), and (4) yellow altered kimberlite (S 437).

then low temperature exchange between carbonate and serpentine-mica matrix is a necessary, but, in general, insufficient process to account for these data. Either loss of O-18 rich material, such as a CO_2 rich fluid, or exchange with a low O-18 reservoir, such as meteoric water, is required.

Assuming that the carbonate - serpentine-mica matrix minerals are approximately in equilibrium, then the observed 8 to 14 ‰ fractionations imply temperatures on the order of 150° to 75° C (Wenner and Taylor, 1973; O'Neil et al., 1969). At these temperatures, water in equilibrium with Group B assemblages are isotopically similar to meteoric waters with δD on the order of -40‰ and the O-isotope composition of the matrix is essentially controlled by the ground water reservoir.

A specific and more detailed interpretation of Group B samples and their O-18 data must await more refined studies because of the complexity of the mineralogy and observation of magmatic sedimentation

and flowage differentiation phenomena for some of these specific samples (Dawson and Hawthorne, 1970, 1973).

C-isotope ratios of carbonates are variable both within a single kimberlite (e.g. Benfontein) and among themselves. Their values are within the range for primary igneous carbonatites. This range is similar to that observed for diamonds (Craig, 1953; Vinogradov et al., 1965). Although the carbon isotope data do not conflict with a genetic relation among these carbon sources, a direct comparison may not be valid since the O-isotope ratios of the carbonates appear to have been modified during the post-magmatic processes.

Conclusions

1. The D/H ratios of phlogopite megacrysts (Group A) from 10 different kimberlites are from -40 to -70 per mil.
2. The D/H ratios of serpentine megacrysts and the serpentine-mica matrix (Group B) are 20‰ or more depleted in D relative to Group A, and may be depleted in O-18 by up to 4-5‰ relative to "normal" ultramafic values. Coexisting carbonates tend to be O-18 rich relative to primary igneous values.
3. Calcite-serpentine "isotopic temperatures" for Group B are 75° - 150°C.
4. Group B minerals including carbonates have been isotopically modified assuming "normal" initial O-18/O-16 ratios by either the loss of O-18 rich material (e.g. CO_2) or exchange with low O-18 meteoric waters at $T > 75^\circ\text{C}$.

References

Arnason, B., and Sigurgeirsson, T., 1968, *Geochim. et Cosmochim. Acta* 32, 807.

Craig, H., 1953, *Geochim. et Cosmochim. Acta*, 3, 53.

Dawson, J. B., and Hawthorne, J. B., 1970, *Bull. Volcan.*, 34, 740. 1973, *Jl. Geol. Soc. London*, 129, 61.

O'Neil, J. R., Clayton, R. N., and Mayeda, T.K., 1969, *J. Chem. Phys.*, 51, 5547.

Sheppard, S. M. F., and Dawson, J. B., 1973, *Fortschr. Miner.*, 50, 128.

Sheppard, S. M. F., and Epstein, S., 1970, *Earth Planet. Sci. Lett.*, 9, 232.

Taylor, H. P., Jr., 1968, *Contr. Mineral. Petrol.* 19, 1.

Vinogradov, A. P., Kropotova, O. I., and Ustinov, V. I., 1965, *Geochem. Int.*, 2, 495.

Wenner, D. B., and Taylor, H.P., Jr., 1973, *Amer. J. Sci.*, 273, 207.

GEOCHEMISTRY OF ULTRAMAFIC INCLUSIONS FROM SALT LAKE CRATER, HAWAII AND FROM SOUTH AFRICAN KIMBERLITES

Nobumichi Shimizu

Department of Terrestrial Magnetism, Carnegie Inst., Washington,
Washington, D. C. U. S. A.

The ultramafic inclusions of Salt Lake Crater are among the best-documented suites of rocks of this kind (Kuno, 1969; Kuno & Aoki, 1970). Clinopyroxenes separated from 17 samples of spinel lherzolites, olivine eclogites and eclogites (garnet pyroxenites) were analyzed by isotope dilution for K, Rb, Cs, Sr, and Ba abundances because in lherzolitic and eclogitic assemblages, these elements are most concentrated in clinopyroxene. The trace element variations of clinopyroxenes are considered here in connection with the major element variations in order to understand trace element chemistry in terms of petrologic models. These rocks show wide variations in Mg/Fe ratio and other oxide components vary in a systematic manner with respect to this ratio. The Mg/Fe ratio should be a good indicator of the upper mantle processes such as partial melting or fractional crystallization. Therefore, the trace element contents of clinopyroxenes are plotted against whole-rock Mg/Fe ratio to see if there are any correlations between them (Fig. 1). In lherzolites and olivine eclogites, K, Rb and Cs decrease and Sr increases with increasing Mg/Fe ratio. On the contrary, for eclogites (or garnet pyroxenites) the systematics are rather poor, but they tend to be depleted in these elements relative to the other groups of rocks. It is noticeable that even in sub-ppb level, a trace element (Cs in olivine eclogites) behaves systematically with major elements, indicating that the contamination from the enclosing magma, if any, has been very minor.

Assuming that these rocks represent solid phases which were once equilibrated with liquid either as residues or cumulates, the trace element variations shown in Fig. 1 may be explained by the partition relations of these elements between clinopyroxene and liquid. An important feature in this context is the increase of Sr with increasing Mg/Fe ratio observed in lherzolites and olivine eclogites. If Mg/Fe ratio represents the degree of partial melting or stage of fractional crystallization, the increase of Sr is interpreted as either 1) Sr was more enriched in the residual pyroxene left after larger degree of partial melting or 2) Sr was more enriched in the pyroxene crystallized in the earlier stage of crystallization. These interpretations require that Sr is partitioned into pyroxene relative to liquid. However, this is quite unlikely in the light of data on Sr partitioning (Philpotts & Schnetzler, 1970; Shimizu & Akitomo, 1971). This strongly indicates that the present mineralogy is a recrystallized assemblage and at the time of primary solid-liquid equilibrium there must have been a phase in which Sr was preferentially partitioned. In addition, this phase must have been stable only at higher temperature and have disappeared during the subsolidus recrystallization. A possible candidate for this phase from the trace element point

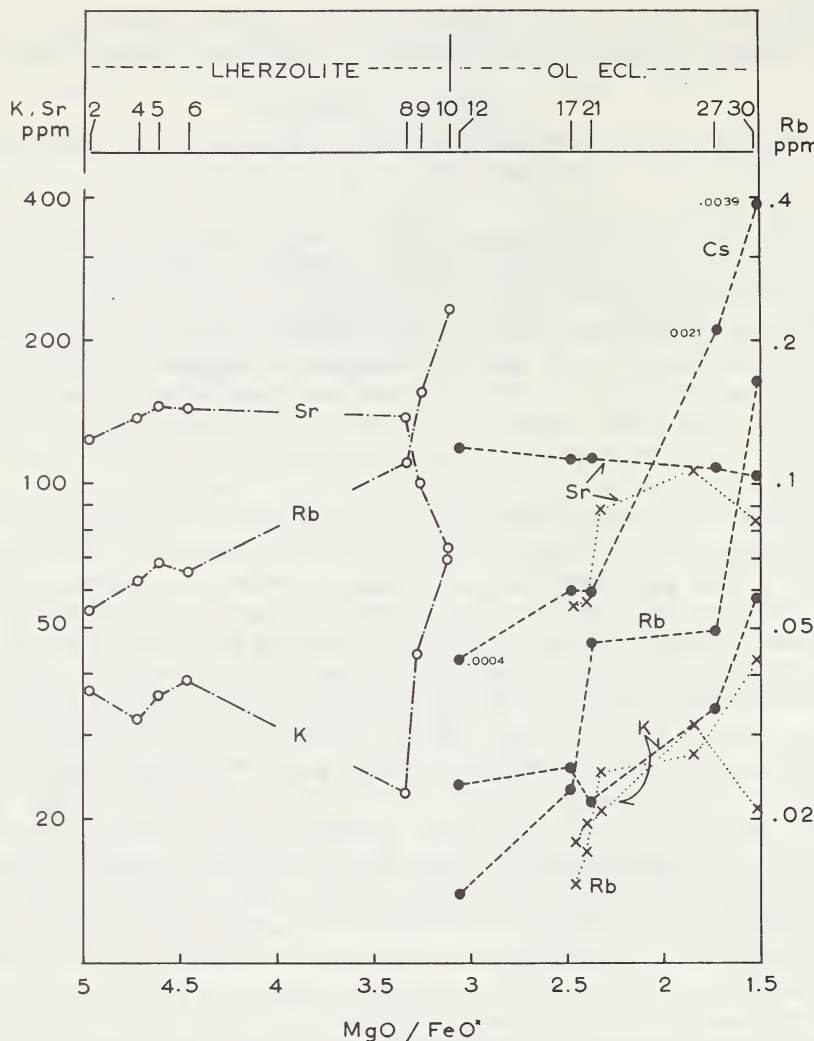


Fig. 1 Trace element variations of clinopyroxenes with respect to whole-rock $MgO/\Sigma FeO$. Open circles tied with broken lines: lherzolites; solid circles with dashed lines: olivine eclogites; xs with dotted lines: eclogites.

of view is plagioclase because Sr is strongly partitioned into plagioclase relative to liquid (Philpotts & Schnetzler, 1970). The problem is then if this is plausible in the light of phase petrology, since plagioclase is stable only at relatively low pressures and thus puts limitations on the conditions at which these rocks were equilibrated with liquid. There is no way to estimate the P and T of the primary equilibrium, but assuming that the subsequent recrystallization took place by isobaric cooling, the estimated P and T for the re-equilibrium should be close to the stability limit of plagioclase-bearing assemblages in lherzolitic and olivine eclogitic composi-

tions. The P and T were then estimated for lherzolites from major element compositions of pyroxenes in the same manner as discussed by Boyd (1973). The temperature was estimated from the diopside composition on the Di-En solvus using the data by Davis & Boyd (1966), and pressure from alumina content of enstatite using the data by MacGregor (1973). The estimated conditions (10-13 kb, 950-1050°C) are close to the stability limit of plagioclase in lherzolitic composition (Green & Hibberson, 1970) and therefore it seems likely that lherzolites were equilibrated with liquid in the presence of plagioclase and during cooling they crossed the boundary and recrystallized as spinel lherzolite assemblage. The liquid in equilibrium with those rocks may well be tholeiitic rather than alkalic judging from the pressure. Note that the trace element content of the liquid cannot readily be estimated from the pyroxene data, since this is not a primary phase. The same argument appears to hold true for olivine eclogites. Although the olivine eclogites are of intermediate nature between basalt and lherzolite in major elements, the olivine-garnet-pyroxene assemblage may be stable at the conditions given above because of the excess olivine component and higher anorthite content of normative plagioclase of olivine eclogites compared with olivine tholeiite B studied by Green & Ringwood (1967). In contrast to these two groups of rocks, trace elements of eclogitic pyroxenes appear to be consistent with an argument given by Green (1966) that the eclogites were originally monomineralic clinopyroxene crystallized on the liquidus of alkali basalt at 13-18 kb which later exsolved garnet, because when the partition coefficients of these elements between clinopyroxene and liquid obtained at high pressures (Shimizu, in prep.) are applied to the pyroxenes, we obtain trace element contents of the liquid in equilibrium (8000-10000 ppm K; 10-40 ppm Rb; ~800 ppm Sr), which are quite reasonable for alkalic basalt.

For a better understanding of upper mantle processes in a possibly different situation from that of Salt Lake Crater, these trace elements were analyzed in clinopyroxenes separated from kimberlite inclusions. They include four garnet lherzolites with sheared structure (sheared nodules), three granular garnet lherzolites, one discrete nodule of diopside single crystal, and another discrete nodule of diopside-ilmenite lamellar intergrowth. These samples appear to be separated into two groups in terms of absolute as well as relative abundances of trace elements, one consisting of the sheared and discrete nodules characterized by high K/Rb (2000-22000), K/Cs (100000-300000) K/Ba (50-1100) and K/Sr (1.5-4.5), and almost constant Sr (around 90 ppm), while the other being the granular nodules characterized by normal K/Rb and K/Cs, low K/Sr (0.5-0.2) and high Sr (200-500 ppm). Figure 2 shows K-Rb relations. Particularly the anomalously high K/Rb in the sheared nodules and high Sr in the granular ones are extremely hard to reconcile with any pyroxene-silicate melt relationships. Sr^{87}/Sr^{86} ratios of most of these pyroxenes are in the range of 0.7027-0.7038, indicating that crustal contamination, if any, is insignificant. These peculiar trace element characteristics suggest that some secondary processes in the mantle, which are not yet understood, have altered the primary features in the pyroxenes. The second-

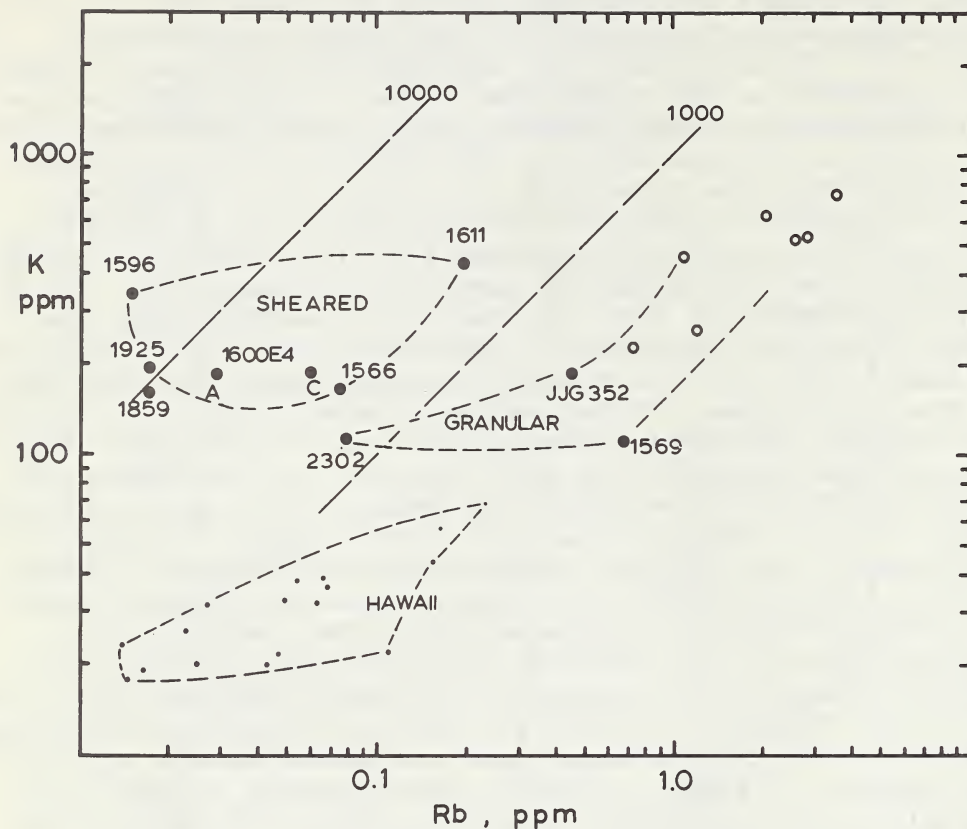


Fig. 2. K-Rb relations of clinopyroxenes from kimberlite inclusions. Solid circles with numbers: present study; open circles: data from literature; dots: clinopyroxenes from Hawaiian inclusions.

ary processes may include reaction between carbonate rich kimberlite magma and/or that between some fluid from which secondary phlogopite was formed.

References

Boyd, F. R. (1973) *Geochim. Cosmochim. Acta*, in press.
 Davis, B. T. C. & Boyd, F. R. (1966) *J. Geophys. Res.* 71, 3567.
 Green, D. H. (1966) *Earth Planet. Sci. Lett.*, 1, 414.
 Green, D. H. & Hibberson, W. (1970) *Lithos*, 3, 209.
 Green, D. H. & Ringwood, A. E. (1967) *Geochim. Cosmoch. Acta*, 31, 767.
 Kuno, H. (1969) *Geol. Soc. Am. Mem.*, 115, 189.
 Kuno, H. & Aoki, K. (1970) *Phys. Earth Planet. Int.*, 3, 273.
 MacGregor, I. D. (1973) *Am. Mineral.*, in press.
 Philpotts, J. A. & Schnetzler, C. C. (1970) *Geochim. Cosmoch. Acta*, 34, 307.
 Shimizu, N. & Akimoto, S. (1971) *Earth Planet. Sci. Lett.*, 13, 134.

SULPHIDE-OXIDE AND SILICATE-OXIDE INTERGROWTHS IN XENOLITHS
OF UPPER-MANTLE PERIDOTITE

J. V. Smith ⁽¹⁾, J. B. Dawson ⁽²⁾, and F. I. Bishop ⁽¹⁾

(1) Dept. of the Geophysical Sciences, University of Chicago, Chicago, Illinois 60637, U.S.A.

(2) Dept. of Geology, University of St. Andrews, Scotland.

Pentlandite-magnetite intergrowths occur as globules, altered to various degrees in a nodule of spinel lherzolite (BD1197) from the De Beers mine. The freshest intergrowth consists of (i) pentlandite free of magnetite, and (ii) pentlandite-magnetite intergrowth. The phases were identified by single-crystal X-ray study and found not to be crystallographically orientated. Electron microprobe analysis gave: pentlandite Fe 26.6 - 27.7, Co 0.8, Ni 37.5 - 40.5, S 32.6 - 33.8; magnetite Fe 67.5, Ni 1.0, S 0.1 wt.%. The intergrowth might result either from (i) a eutectic in the Fe-Ni-S-O system (ii) oxidation of a pentlandite-pyrrhotite precursor (iii) exsolution of an oxide-sulphide single-phase. Possibly (i) is preferred tentatively, but the others cannot be ruled out without further studies. Coexisting silicates are olivine ($_{94}$), orthopyroxene (not analysed), Cr-diopsidite (Na_2O 2.9, Al_2O_3 1.0, Cr_2O_3 4.6, FeO 1.6, CaO 19.1, MgO 16.1), secondary phlogopite (TiO_2 0.16, Cr_2O_3 0.76, FeO 2.0, MgO 26.5, NiO 0.25). The coexisting spinel is a picrochromite (SiO_2 0.10, TiO_2 0.27, Al_2O_3 2.55, Cr_2O_3 68.7, FeO 16.6, MnO 0.30, MgO 12.5, NiO 0.12 wt.%).

Intergrowth textures resembling fingerprints occur between chromite on the one hand and olivine, orthopyroxene, diopsidite and chromic pargasitic hornblende on the other hand. The dactylic chromite may be intergrown with just a single silicate or more than one silicate. The intergrowths tend to occur at multiple junctions but some occur in thin section apparently totally enclosed in a single silicate grain. The silicate of the intergrowth frequently occurs in thin section with parallel optical extinction to a neighbouring grain of the same type of silicate (often the silicate is seen to be physically continuous). Some intergrowths involve several silicate grains, and some intergrowths appear to be completely independent. A sequence of textures can be traced from euhedral isolated chromite grains, through irregular graphic intergrowths with silicates, to fine-scale vermicular intergrowths.

Electron-microprobe analyses of the following intergrowths revealed essentially similar compositions for euhedral and intergrowth chromites and for the silicates both inside and outside the symplectites: chromite-orthopyroxene (spinel harzburgite, Newlands Mine); chromite orthopyroxene and chromite-diopside (spinel lherzolite, Bultfontein Mine); chromite-chromic pargasitic hornblende (spinel amphibole harzburgite, Monastery Mine). Actually very slight differences in the composition of some intergrowth silicates do occur. The main bulk-rock orthopyroxene in the Bultfontein specimen contains more CaO (0.6 - 0.8 wt.%) and Al_2O_3 (2.6 - 2.9 wt.%) than the intergrowth orthopyroxene (0.3 - 0.4 and 2.1 - 2.3), consistent with adjustment to a lower T and P of the latter, and in the amphibole harzburgite the intergrowth amphibole contains very slightly higher amounts of chromium. The composition of the olivines, orthopyroxenes and clinopyroxenes in the investigated xenoliths is similar to that of these phases in other upper-mantle peridotite, though the amphibole differs from other upper-mantle pargasites in being more potassic; in this aspect it lies intermediate between the pargasites and the potassic richterite reported from the Wesselton Mine (Table 1).

Earlier models for these fingerprint textures involved (i) replacement (HOLMES, 1936) and (ii) reaction between original garnet and chromian diopside to form pargasite and chromite (BOYD, 1971). We suggest that at least some intergrowths form by simultaneous crystallization, possibly as a result of pressure-induced recrystallization of original chromite and surrounding silicate. Others might involve simultaneous crystallization of primary phases.

A symplectite of euhedral olivine and euhedral chromite occurs in a spinel lherzolite from Lashaine volcano. A resemblance to coronas around garnets might imply breakdown of an earlier phase of bulk composition XY_2O_4 , perhaps of spinel structure.

References

BOYD, F.R. Carnegie Inst. Washington Yr. Bk. 70, 138-142, 1971.

ERLANK, A. J. and FINGER, L. W. Carnegie Inst. Washington Yr. Bk. 68, 320-324, 1970.

HOLMES, A. Trans. Geol. Soc. S.Africa. 39, 379-428, 1936.

VARNE, R. Contr. Min. Petr. 27, 45-51, 1970.

TABLE 1

	1	2	3	4
SiO ₂	44.73	45.5	54.3	44.2 - 44.8
TiO ₂	0.29	<0.01	0.59	0.00- 0.01
Al ₂ O ₃	12.58	11.1	1.24	11.0 - 11.2
Cr ₂ O ₃	2.43	1.67	0.06	2.07- 2.34
Fe ₂ O ₃	1.10	n.d.	n.d.	n.d.
FeO	2.37	3.18*	4.30	2.68- 2.75*
MnO	0.11	0.06	0.07	0.18- 0.19
MgO	19.17	20.0	21.2	20.1 - 20.5
NiO	n.d.	0.10	n.d.	0.34- 0.37
CaO	10.95	10.6	7.12	10.7 - 11.3
Na ₂ O	3.84	3.79	3.25	3.16- 3.31
K ₂ O	0.43	0.60	4.72	1.33- 1.35

* Total iron reported as FeO

1. Chromic pargasite in lherzolite xenolith, Kirsh Volcano Aden (VARNE, 1970).
2. Pargasite in amphibole/spinel symplectite, in harzburgite, Wesselton Mine (BOYD, 1971).
3. Average of 3 analyses of potassic richterites in mica-pyroxenite xenolith, Wesselton Mine (ERLANK, 1970).
4. Range of composition of chromic pargasitic hornblende, both intergrown with spinel and isolated grains in harzburgite BD 1368, Monastery Mine.

THE DISTRIBUTION OF SOME TRANSITION ELEMENTS
BETWEEN COEXISTING MINERAL PHASES IN NODULES
FROM SOUTH AFRICAN KIMBERLITES.

P. SUDDABY, DEPT., OF GEOLOGY, IMPERIAL COLLEGE,
LONDON.

Most models for the composition of the upper mantle have emphasised the importance of the phases olivine, clinopyroxene, orthopyroxene and garnet, which in different combinations give rise to the suites of peridotitic and eclogitic nodules found in Kimberlites. As Boyd (1970) indicated, although the geological literature contains a number of analyses of these rock types and of individual minerals, there are very few analyses of all the coexisting minerals from individual nodules and therefore little may be deduced about the partitioning of elements between these phases.

The co-existing minerals from a number of peridotite and eclogite nodules from various South African localities have therefore been analysed using the electron microprobe. Most of the analysed nodules are from the well known 'Williams' (1932) collection but others are from the British Museum (Natural History). Many of the nodules are remarkable for the chemical homogeneity of their minerals both within grains and from grain to grain and these are taken to represent equilibrium assemblages.

The partitioning of iron, manganese and nickel relative to magnesium is shown to decrease in the following ways:-

Fe/Mg	Garnet > Olivine > Enstatite > Diopside
Mn/Mg	Garnet >> Enstatite >? Diopside > Olivine
Ni/Mg	Olivine > Enstatite > Garnet

The abundance of chromium decreases in the order Garnet, Diopside, Enstatite, Olivine.

The partition coefficients for chromium $K_{\text{CR}}^{\text{GNT-OPX}}$, $K_{\text{CR}}^{\text{GNT-CPX}}$ and $K_{\text{CR}}^{\text{CPX-OPX}}$ lie in the ranges 10-16, 1.3-2.9 and 5.0-9.2 respectively.

On the basis of the limited data available these figures appear to have a bimodal distribution. The detection of small quantities of chromium in the olivines of some nodules confirms the work of Sobolev (1972) who suggests that this indicates low fO_2 by the presence of the Cr^{2+} ion.

All the phlogopite that has been analysed so far contains less chromium than the coexisting clinopyroxene and it is suggested that this indicates a secondary origin even when the textural evidence is uncertain.

In the specimens so far analysed it has not been possible to detect potassium in the diopside as has been reported by Sobolev (1972) and Boyd (1970) from other localities.

References:-

Boyd (1970) Papers from the GEOPHYSICAL LABORATORY No1572
Sobolev (1972) Abstracts of the 24th IGC, Section 2.

ISOTOPE GEOCHEMISTRY AND PETROLOGY OF THE AFRICAN CARBONATITES

Kanenori Suwa*, Shinya Oana*, Hideki Wada* and Susumu Osaki**

*Department of Earth Sciences, Faculty of Science,
Nagoya University, Nagoya, Japan

** Department of Chemistry, Faculty of Science,
Kyushu University, Fukuoka, Japan

Many carbonatite bodies were emplaced in the African continent since Precambrian period.

Measurements of oxygen and carbon isotopes of the various kinds of the African carbonatites were performed to elucidate the conditions of formation of the carbonatites, and to elucidate the variation of the isotope ratios in rocks which have been affected by late-magmatic hydrothermal and deuterian processes, and to come to firm conclusions about the ultimate origin of the carbonatite.

The carbonatite bodies examined are Precambrian Phalaborwa and Premier carbonatites, Mesozoic Spitskop and Mbeya carbonatites, Tertiary Homa Mountain carbonatites and Recent Oldoinyo Lengai carbonatite.

The results of oxygen and carbon isotope analyses are expressed as the per mil deviation of the $^{18}\text{O}/^{16}\text{O}$ and $^{13}\text{C}/^{12}\text{C}$ ratios from the ratios in SMOW and PDB standards, respectively.

(1) Precambrian Phalaborwa carbonatite:

The Phalaborwa carbonatite is located near the north-east border of South Africa, and is Middle Precambrian (2060 m. y.) in age.

The carbonatite occurs in the centre of the Phalaborwa Igneous Complex, mainly composed of diopside-pyroxenite.

The two principal types of carbonatite are an older banded s_bvite and a younger transgressive s_bvite. There is no clean-cut division between the older s_bvite and phoscorite. The younger s_bvite forms a well-defined but irregular intrusion in the central part of the pipe as well as a series of narrow dikes or offshoots.

Four calcite samples from the carbonatites were analysed.

Older s_bvite shows $\delta^{18}\text{O}$: 8.05‰, $\delta^{13}\text{C}$: -4.28‰.

Younger s_bvites show $\delta^{18}\text{O}$: 8.10 ~ 10.24‰, $\delta^{13}\text{C}$: -3.10 ~ -3.94‰.

The field of oxygen and carbon isotope ratios of the Phalaborwa carbonatite, especially of older carbonatite, coincides with that of primary igneous carbonatites.

(2) Precambrian Premier carbonatite :

The Premier carbonatite (Premier Diamond Mine) is located near Pretoria in South Africa, and is Middle Precambrian (1750 ± 100 m. y.) in age.

The Premier Mine kimberlites are extraordinarily rich in calcium carbonate, and the kimberlites have been named according to the predominant matrix colour : Grey, brown, black, green, orange, pale grey, fawn and blue kimberlites.

The main carbonatite dike mass intruded the centre of the Black kimberlite. The carbonatite dike consists essentially of anhedral grains of calcite, fine-grained granular magnetite and some interstitial serpentine. The Black kimberlite consists of very dark, almost black, aphanitic rather uniform material, in which occurs ilmenite, serpentinized phenocrysts of olivine and, less commonly, garnets and chrome-diopside.

Carbonatized varieties of Black kimberlite, named "Pale Piebald" and "Dark Piebald", occur in the kimberlite surrounding the carbonatite dikes.

Three calcite samples from the carbonatite, "Pale Piebald" and Black kimberlite were analysed : $\delta^{18}\text{O}$: $12.44 \sim 13.29\text{\textperthousand}$
 $\delta^{13}\text{C}$: $-5.99 \sim -6.97\text{\textperthousand}$.

Of considerable interest are these data that the Premier carbonatite in kimberlite pipe shows strong similarities with the primary hydrothermal calcite (Calcite I) formed at about 360°C at the Providencia, Mexico (Rye, 1966).

This calciferous dikes described by Daly (1925) cannot be regarded as true carbonatite. They were probably formed by replacement of a kimberlite variety already rich in CaCO_3 .

(3) Mesozoic Spitskop carbonatite :

The Spitskop carbonatite is located in north-eastern part of South Africa, and is to be believed as a late-Karoo age.

The Spitskop Alkaline Complex is mainly of ijolite intruded by two great foyaite ring-dikes and by a central plug of carbonatite.

Four varieties of carbonatite have been distinguished (Verwoerd, 1966) :

(a) White s b vitite occurs presumably continuous, outer zone on all sides of the plug.

(b) Grey dolomite-s b vitite is intermediate in position as well as composition between the white s b vitite and beforsite.

(c) Beforsite forms the bulk of the Spitskop carbonatite.

(d) Apatite-rich carbonatite occurs in beforsite as well as in dolomite-s b vitite along three concentric horizons.

Nine calcite, ankerite and dolomite samples were analysed. Calcites in dolomite-s b vitite show $\delta^{18}\text{O}$: $11.71 \sim 12.30\text{\textperthousand}$, ankerites in beforsite and apatite-rich beforsite show $\delta^{18}\text{O}$: $16.54 \sim 17.54\text{\textperthousand}$ and $\delta^{13}\text{C}$: $-1.96 \sim -2.49\text{\textperthousand}$, later stage calcite and

dolomite show $\delta^{18}\text{O}$: 17.50 and 18.35 ‰, and $\delta^{13}\text{C}$: -2.34 and -1.99 ‰, respectively.

Spitskop carbonatite shows a slight deviation from that of primary igneous carbonatites. The Spitskop carbonatite is regarded as a pipe-like body of which the composition was modified after emplacement by circulating fluids in several stages marked by progressive enrichment in magnesium and iron.

The isotope fractionation among coexisting minerals in later stage carbonate vein indicates $320^\circ\text{C} \sim 660^\circ\text{C}$.

(4) Mesozoic Mbeya carbonatite:

The Mbeya carbonatite is located near the south-west border of Tanzania, and is Cretaceous in age.

Fifty two calcite and dolomite samples were analysed.

Calcite and dolomite samples from unaltered carbonatites lie in a small field low in $\delta^{18}\text{O}$ (5.9 ~ 7.7 ‰) and low in $\delta^{13}\text{C}$ (-3.6 ~ -5.3 ‰), this field coincides with that of primary igneous carbonatites. Carbonates coexisting with abundant metal oxides become enriched in $\delta^{18}\text{O}$ (Suwa, et al., 1969).

The fractionation factors of oxygen and carbon isotopes between the coexisting calcites and dolomites in the carbonatites range from 0.07 to 0.64 ‰ and from 0.20 to 0.59 ‰, respectively, suggesting that the carbonates crystallized at temperatures $800^\circ\text{C} \sim 380^\circ\text{C}$ and $>700^\circ\text{C} \sim 380^\circ\text{C}$, respectively.

(5) Tertiary Homa Mountain carbonatites:

The Homa Mountain carbonatite is located near the north-eastern coast of Lake Victoria, and is Miocene in age.

Commencing with the first intrusion of ijolite suite, the following five main types of carbonatite are thought to be the sequence of intrusions and extrusions at Homa Mountain (Clarke, 1968).

C 1 : Coarse-grained sōvites

C 2 : Medium-grained alvikites

C 3 : Purple rhomb carbonatites

C 4 : Ferruginous carbonatites

C 5 : Carbonated melilitites

Twenty eight calcite samples from the carbonatites and related rocks were analysed.

The field of oxygen (7.99 ~ 9.16 ‰) and carbon (-5.12 ~ -4.17 ‰) isotope ratios of unaltered sōvite (C 1) samples coincides with that of primary igneous carbonatites.

Calcite samples in carbonatites (C 2, C 3, C 4, C 5) and their related rocks are enriched in ^{18}O (8.10 ~ 29.11 ‰), and these are altered and/or formed in relation to one or more cycles of younger hydrothermal activity, brecciation and mixing accompanied by explosive activity, and weathering.

(6) Recent Oldoinyo Lengai carbonatite :

Oldoinyo Lengai is an active volcano in northern Tanzania and yielded lavas of high alkali carbonatite in its 1960 and 1961 eruptions (Dawson, 1962 a, b).

Five sodium carbonate samples collected by J. B. Dawson in 1960 were analysed.

The sample, ground to minus 200 mesh, is dissolved in 0.04 mole/l NaOH solution and immediately CaCl_2 is added to the solution in order to precipitate CaCO_3 . This CaCO_3 is used for isotopic analysis.

Sodium carbonate lava is deliquescent and is easily affected in air. Unaltered samples, inner part of the specimen, show $\delta^{18}\text{O}$: 6.17 ~ 6.37 ‰, $\delta^{13}\text{C}$: -10.22 ~ -9.65 ‰.

The lower value of $\delta^{13}\text{C}$ in the sodium carbonate lava is due to the violent explosion of CO_2 gas having heavy carbon during vulcanicity and thereby carbon remaining in the form of sodium carbonate becomes lighter. At temperature between 300° C and 800° C, carbon in CaCO_3 coexisting with CO_2 gas is lighter than carbon in the CO_2 gas as 2 ~ 3 ‰ (Bottinga, 1968).

References

Bottinga, Y. (1968) : J. Phys. Chem., vol. 72, 800 - 808.

Clarke, M. C. G. (1968) : Ph. D. Thesis (Manuscript), Univ. Leicester, 1 - 291.

Daly, R. A. (1925) : J. Geol., vol. 33, 659 - 684.

Dawson, J. B. (1962 a) : Nature, vol. 195, 1075 - 1076.

Dawson, J. B. (1962 b) : Bull. Volcanol., vol. 24, 349 - 387.

Rye, R. O. (1966) : Econ. Geol., vol. 61, 1399 - 1427.

Suwa, K., Osaki, S., Oana, S., Shiida, I., and Miyakawa, K. (1969) : J. Earth Sci., Nagoya Univ., vol. 17, 125 - 168.

Verwoerd, W. J. (1966) : Ann. Univ. Stellenbosch, vol. 41, ser. A, No. 2, 115 - 233.

PETROLOGY OF PERIDOTITE NODULES FROM THE NDONYUO
OLNCHORO, SAMBURU DISTRICT, CENTRAL KENYA

Kanenori Suwa*, Yasuhisa Yusa* and Nobutaka Kishida**

*Department of Earth Sciences, Faculty of Science,
Nagoya University, Nagoya, Japan

**Africa Natural Resources Development Company,
Nairobi, Kenya

The sodic alkaline volcanic rocks were extruded in enormous volumes repeatedly from Miocene times onwards in Kenya, eastern Uganda and northern Tanzania. The Miocene and Pliocene basaltic volcanism was closely controlled by the developing rift valley.

Around the Ndonyuo Olnchoro, $37^{\circ}46'E$, $1^{\circ}22'N$, there occurs Pliocene olivine nephelinite, in which many ejected blocks of a suite of ultramafic nodules are enclosed. This is the first detailed paper of the peridotite nodules in the Gregory Rift Valley of Kenya.

Petrochemistry:

Chemical composition and norms of the olivine nephelinite are shown in Table 1. It belongs to Group C of Mantle norm.

The peridotite nodules are divisible into two groups.

Table 1. Chemical composition and norms of the host rock(Olivine nephelinite)

	No.14	C.I.P.W.Norm			Mantle Norm
SiO ₂	38.59				
TiO ₂	2.62	an	1.36		NaFeSi ₂ O ₆ 20.20
Al ₂ O ₃	9.20	lc	8.73	28.64	NaAlSi ₂ O ₆ 12.34
Cr ₂ O ₃	0.16	ne	18.55	sal	CaTiAl ₂ O ₆ 7.73
Fe ₂ O ₃	8.52				CaAl ₂ SiO ₆ 5.75
FeO	8.23	wo	18.79		CaSiO ₃ 15.50
MnO	0.22	di	en	14.84	MgSiO ₃ 9.82
NiO	0.01		fs	1.83	FeSiO ₃ 4.70
CaO	10.88	ol	fo	12.39	Mg ₂ SiO ₄ 15.71
MgO	13.06		fa	1.68	Fe ₂ SiO ₄ 8.25
Na ₂ O	4.05	cs	0.35	fem	Total 100.00
K ₂ O	1.88	mt	12.36		
P ₂ O ₅	0.99	cm	2.46		
H ₂ O(+)	1.65	il	4.98		
H ₂ O(-)	0.24	ap	2.35		
Total	100.30				

The first group contains rocks consisting of varying combinations of magnesian olivine, orthopyroxene, and small amount of chromian spinel and clinopyroxene. Harzburgite and lherzolite belong to the first group and occupy about 90 per cent of the peridotite nodules by volume. The other group of ultramafic nodules comprises of websterite consisting of orthopyroxene, clinopyroxene and small amount of chromian spinel and occupies about 10 per cent of the nodules by volume.

Chemical compositions of the peridotite nodules are shown in Table 2.

The continental lherzolite such as those of Ndonyuo Olnchoro ($MgO/\Sigma FeO=7.63\sim 6.96$) and Lashaine, northern Tanzania ($MgO/\Sigma FeO=6.97\sim 5.49$) (Dawson et al, 1970) show a tendency to have higher $MgO/\Sigma FeO$ and therefore to be more enriched in the higher melting components, than the oceanic lherzolites. This might imply that the continental upper mantle has been more depleted of the material that formed the crust.

The nodules from kimberlite are higher in $MgO/\Sigma FeO$ ($7.65\sim 5.36$) than most lherzolite nodules from basalts ($6.57\sim 2.28$). Of considerable interest is the fact that the $MgO/\Sigma FeO$ ratios ($7.63\sim 5.49$) of the lherzolite nodules from Ndonyuo Olnchoro and Lashaine fall within the limit of variation of nodules from kimberlite.

Table 2. Chemical composition of the peridotite nodules

	Harzburgite		Lherzolite		Websterite
	No.17	No.18	No.13	No.16	No.12
SiO_2	43.16	43.28	43.16	40.59	52.24
TiO_2	0.01	0.01	tr	tr	tr
Al_2O_3	1.79	1.61	1.47	0.92	2.14
Cr_2O_3	0.04	0.23	0.29	0.41	3.42
Fe_2O_3	2.07	1.60	2.55	3.83	2.95
FeO	4.61	4.74	4.31	3.59	5.39
MnO	0.21	0.19	0.18	0.16	0.35
NiO	0.18	0.17	0.15	0.20	0.08
MgO	46.57	47.14	46.57	48.99	30.08
CaO	0.28	0.33	0.49	0.39	2.58
Na_2O	0.04	0.33	0.07	0.12	0.09
K_2O	0.02	0.01	0.06	0.02	0.07
P_2O_5	0.06	tr	0.05	0.07	0.03
$H_2O(+)$	0.61	0.75	0.81	0.38	1.12
$H_2O(-)$	0.04	0.04	0.05	0.03	0.02
Total	99.69	100.13	100.21	99.70	100.56
$MgO/\Sigma FeO$	7.20	7.63	7.05	6.96	3.74

The variation trends of some oxides in websterite-pyroxenite nodules including the websterite nodule from Ndonyuo Olnchoro are different from those in the lherzolite nodules (Kuno and Aoki, 1970). These two types of nodules are of different origin, as is also suggested by the difference in pyroxene compositions. The websterite-pyroxenite variation is very similar to the eclogite variation, suggesting their similar origin. There may be a petrogenetical relationship between the eclogite nodule from Chunya Hill, southern Kenya (Saggerson, 1968) and the websterite nodule from Ndonyuo Olnchoro.

Mineralogy:

Nineteen olivines, twenty two orthopyroxenes, three clinopyroxenes and eighteen spinels from the harzburgite and lherzolite nodules and seven orthopyroxenes, three clinopyroxenes and four spinels from the websterite nodule are analysed with an EPMA chiefly, and only FeO is analysed by wet method.

The contents of forsterite molecule of olivines from harzburgite and lherzolite nodules are homogeneous (Fo 92.8~91.9) from rock to rock, from grain to grain, and even in the grain.

The ratios of $Mg:Fe^{2+}:Ca$ of orthopyroxenes from harzburgite and lherzolite nodules are homogeneous (91.9:7.1:1.0~92.7:6.5:0.8), and those of orthopyroxenes from websterite nodule are also homogeneous (89.4:9.7:0.8~89.7:9.5:0.8). Al_2O_3 contents of orthopyroxenes are 1.86~2.94 wt% for the harzburgite and lherzolite nodules and are 3.12~3.27 wt% for the websterite nodule. Cr_2O_3 contents of orthopyroxenes are 0.41~0.51 wt% for all peridotite nodules.

The ratios of $Mg:Fe^{2+}:Ca$ of clinopyroxenes from lherzolite nodules are 53.3:4.0:42.6~57.3:3.9:38.8, and those of clinopyroxenes from websterite nodule are 48.9:2.7:48.4~49.2:2.7:48.1. Al_2O_3 contents of clinopyroxenes are 1.84~3.03 wt% for lherzolite nodules and are 3.19~3.43 wt% for websterite nodule. Cr_2O_3 contents of clinopyroxenes are 0.96~1.07 wt% for lherzolite nodules and are 0.75~0.80 wt% for websterite nodule.

The Al_2O_3 contents and $Ca/Ca + Mg$ ratios of the clinopyroxenes from lherzolite nodules indicate more affinities with those in mantle-derived rocks rather than with peridotites derived by accumulation from a basaltic melt.

Various methods are used to estimate the temperature of formation of the olivine-pyroxene assemblage within the rock, these methods being $Fe^{2+}:Mg$ partition between coexisting pyroxenes (Bartholomé, 1962; Kretz, 1963), $Fe^{2+}:Mg$ partition between olivine and orthopyroxene (Bartholomé, 1962). For harzburgite and lherzolite equilibrium temperatures are more than 1500°C and for websterite these are 500°~620°C.

Using the phase relations $\text{CaMgSi}_2\text{O}_6 - \text{Mg}_2\text{Si}_2\text{O}_6$ at 30kb (Davis and Boyd, 1966), temperatures $1060^\circ \sim 1190^\circ\text{C}$ for lherzolites and 880°C for websterite are obtained. The temperature and pressure of formation obtained by plotting the clinopyroxene and compositions on the grid drawn up by O'Hara(1967) are $1210^\circ\text{C}/36\text{kb} \sim 1340^\circ\text{C}/38\text{kb}$ for the lherzolites.

However, no garnet is found in the peridotite nodules from Ndonyuo Olnchoro. Symplektites of chromian spinel and orthopyroxene are found in the peridotite nodules. Chemistry of chromian spinel is not so homogeneous from rock to rock and from grain to grain. The symplektites may be derived from the original garnet according to the reaction forsterite + pyrope \rightarrow 4 enstatite + spinel. From the present compositions of forsterite, enstatite and spinel in harzburgite, the composition of garnet is inferred to be pyrope molecule $55 \sim 60\%$, knorringite molecule $30 \sim 35\%$, almandine molecule 10% and andradite molecule 1%.

References

Barthlomé, P.(1962) : Petrologic Studies, 1-20. Geol. Soc. Am.

Dawson, J.B., Powell, D.G. and Reid, A.M. (1970) : J. Petrology, vol.11, 519-548.

Davis, B.T.C. and Boyd, F.R. (1966) : J. Geophys. Res. vol.71, 3567-3576.

Kretz, R. (1963) : J. Geol., vol.71, 773-785.

Kuno, H. and Aoki, K. (1970) : Phys. Earth Planet. Interiors, vol.3, 273-301. North-Holland, Amsterdam.

O'Hara, M.J. (1967) : Ultramafic and related rocks, 393-403. John Wiley, New York.

Saggesson, E.P. (1968) : Geol. Rund., vol.57, 890-903.

KIMBERLITES OF THE SUPERIOR PROVINCE, CANADIAN SHIELD

K. D. Watson, Department of Geology,
University of California, Los Angeles, U.S.A.

Kimberlites occur in the following places in the Superior Structural Province of the Canadian Shield: Gauthier, Keith, and Michaud Townships in Ontario and Lesueur Township in Quebec. All are narrow post-orogenic dikes. They consist of olivine and altered olivine, phlogopite, calcite and/or dolomite, magnesian ilmenite, titaniferous magnetite, perovskite, clinopyroxene, apatite, and serpentine (Tables 1,2). Some contain xenoliths of igneous and metamorphic rock and rounded megacrysts of olivine, phlogopite, ilmenite, pyrope, and chromite (Table 3).

Carbonate minerals are abundant and in some samples exceed 50 percent. Although carbonate in kimberlite at some localities is considered to be a product of weathering, this cannot be so in the Superior Province occurrences. There, the bedrock is glacially scoured and the specimens are from a mine and drill holes far beneath the surface. Moreover, in Lesueur Township, it has been shown that no relationship exists between depth of intersection and amount of calcite present.

The alternative possibility that the calcite in the Lesueur kimberlite is a product of hydrothermal alteration derived from a source distinctly younger than the kimberlite may be ruled out since carbonates are either absent, or essentially so, from all the other rocks and ores of the area. Consequently, one may conclude that the carbonates in the kimberlite of Lesueur Township, and probably of Keith and Gauthier Townships as well, are a product of the kimberlite magma itself. Except for a little carbonate-facies iron formation, the Abitibi belt, unlike a large part of the adjacent Grenville Province, lacks carbonate sedimentary rocks. Hence, there is no sound reason for postulating that in the Abitibi belt, the kimberlite magma obtained its carbonate by reaction with limestone or dolomite.

The calcite in the kimberlite of Lesueur Township has an average Sr (87/86) ratio of 0.7040 ± 0.0001 and an average Sr content of approximately 4000 p.p.m. (Brookins and Watson, 1969, p. 370-371). These values match those of most carbonates and differ from those of most sedimentary carbonates.

Some of the calcite and dolomite in the Superior Province kimberlites has formed by partial replacement of olivine and phlogopite. Most of the carbonate, however, shows no evidence whatever of a secondary origin. On the contrary, it occurs as medium- to fine-grained anhedral grains which are sharply molded against or completely enclosing euhedral crystals of olivine, phlogopite, magnetite, perovskite, clinopyroxene, and apatite in a manner indicating strongly that it is a late-crystallizing primary mineral.

One of the kimberlite dikes in Lesueur Township has narrow margins consisting mainly of calcite. Veinlets which are composed of calcite containing occasional crystals of

phlogopite and altered olivine, project from these dike margins. The rhyolitic country rock adjacent to the veinlets and dike margins has been replaced by fine-grained riebeckite. This alteration is comparable, albeit on a small scale, to the fenitization that commonly is associated with margins of carbonatites.

Chemically, these kimberlites are ultrabasic rocks, which compared to other ultrabasics, have unusually high contents of K_2O , CaO , CO_2 , TiO_2 , P_2O_5 , Al_2O_3 , and H_2O ; low Mg/Fe ratios; and high K/Na and Fe^{3+}/Fe^{2+} ratios (Table 4). Their trace element content is similar to that of other kimberlites (Table 5).

The Abitibi orogenic belt consists of Archean volcanic and sedimentary rocks which were last deformed, metamorphosed and intruded by granite principally during the Kenoran orogeny, about 2500 million years ago (Goodwin and Ridler, 1970; McGlynn, 1970). Only two of the kimberlites in the Abitibi belt have been dated radiometrically. The one in Lesueur Township, based upon the K-Ar ratio in phlogopite, is 1100 m.y. (Neohelikian). This kimberlite is matched closely in age by several post-orogenic carbonatite and alkaline complexes of the Superior Province. The kimberlite of Gauthier Township has a K-Ar age obtained from phlogopite, of 151 ± 8 m.y. (Upper Jurassic) (Lee and Lawrence, 1968, p. 1).

The geological evidence, textural relationships, Sr content, Sr isotopic ratios, and local fenitization are consistent with a primary carbonatitic origin for the calcite and dolomite present in the kimberlites of the Superior Province. It seems likely that the kimberlite was intruded as an accumulation of rounded megacrysts and euhedral phenocrysts transported by highly fluid carbonatitic liquid from which calcite and/or dolomite, along with lesser amounts of other phases such as perovskite and apatite subsequently crystallized.

Brookins, D.G., and Watson, K.D., 1969, *Jour. Geol.*, 77, 367-371.
Dawson, J.B., 1967, *in Ultramafic and Related Rocks*: John Wiley and Sons, 269-278.

Goodwin, A.M., and Ridler, R.H., 1970, *in Basins and Geosynclines of the Canadian Shield*: *Geol. Surv. Can.*, Paper 70-40, 1-30.

Lee, H.A., and Lawrence, D.E., 1968, *Geol. Surv. Can.*, Paper 68-22, 16 p.

McGlynn, J.C., 1970, *in Geology and Economic Minerals of Canada*: *Geol. Surv. Can.*, Econ. Geol. Rept. No. 1, 54-71.

Satterly, J., 1949, *Ont. Dept. Mines, Ann. Rept.*, 57, pt. 4, 27 p.

Watson, K.D., 1967, *in Ultramafic and Related Rocks*: John Wiley and Sons, 312-323.

Table 3. Megacrysts in Kimberlite from Superior Province
(Maximum size, mm)

	Gauthier	Keith	Lesueur	Michaud
Olivine	x (12)	x (18)	x (20)	x (5)
Phlogopite	x (2)	---	x (10)	x (2.5)
Ilmenite	---	x (1)	x (7)	---
Pyrope	x (2)	---	---	x (2.5)
Chromite	x (1)	---	---	---

Table 1. Mineralogical Composition of Kimberlite from Superior Province (Percentage by volume)

	1	2	3	4	5	6	7	8	9	10
Olivine & altered olivine	31	41	41	29	27	14	48	45	38	41
Phlogopite	25	25	27	24	20	28	9	21	20	26
Carbonate minerals*	--	20	20	39	39	38	18	13	20	17
Calcite & serpentine †	35	--	--	--	--	--	--	--	7	--
Ilmenite	--	2	2	1	7	10	7	4	--	3
Magnetite	15	4	4	6	6	12	6	5	5	4
Chromite	15	0.4	0.3	--	--	--	--	--	--	--
Perovskite	4	0.4	0.3	1	2	1	3	7	1	3
Clinopyroxene	tr	2	2	0.1	--	--	--	0.2	6	1
Apatite	tr	0.2	0.3	0.1	3	6	0.1	0.2	2	4
Serpentine & chlorite	--	3	2	--	2	3	3	4	1	1
Pyrite	--	2	1	--	--	--	--	--	--	--
Pyrrhotite	tr	--	--	--	--	--	--	--	--	--
Pyrope	tr	--	--	--	--	--	--	--	--	--

*Dolomite and minor magnesite in Nos. 2 and 3; calcite in Nos. 4-10.

†Includes some fine olivine and phlogopite in No. 1; may be pseudomorphic after melilite in No. 9.

1/ Gauthier Township, Ontario (Lee & Lawrence, 1968, p. 4); 2 and 3. Keith Township, Ontario; 4-10. Lesueur Township, Quebec.

Table 2. Microprobe Analyses of Opaque Oxides in Kimberlite from Lesueur Township

	1	2	3	4	5	6	7	8	9	10
TiO ₂	44.0	56.7	52.4	46.2	53.3	27.1	38.5	20.4	5.8	
Al ₂ O ₃	0.4	0.1	0.8	--	0.3	--	2.5	2.3	0.2	
Cr ₂ O ₃	0.5	0.3	1.1	0.7	0.8	0.2	5.4	2.5	0.1	
FeO*	48.0	33.8	35.5	42.0	27.3	64.7	36.5	59.4	92.2	
MnO	0.3	0.3	0.2	--	0.5	0.2	0.5	0.8	0.2	
MgO	6.7	8.1	10.2	10.8	18.2	7.5	16.2	14.9	1.3	
Total	99.9	99.3	100.2	99.7	100.4	99.7	99.6	100.3	99.8	

*Total iron expressed as FeO
1, 2, 3, 4, and 5. Magnesian ilmenite; 6. Magnesian ulvöspinel; exsolution lamella in magnesian ilmenite No. 3; 7 and 8. Magnesian ulvöspinel; exsolution lamellae in magnesian ilmenite No. 5; 9. Titaniferous magnetite.

Table 4. Chemical Analyses of Kimberlite from Superior Province

	1	2	3	4	5	6
SiO ₂	32.7	33.2	27.23	22.86	22.74	24.15
TiO ₂	2.1	2.1	2.42	2.98	5.86	6.46
Al ₂ O ₃	3.2	3.2	4.80	3.78	3.09	2.58
Fe ₂ O ₃	3.9	4.1	2.57	4.79	8.47	7.67
FeO	5.8	5.8	7.05	5.32	7.54	8.36
MnO	0.2	0.2	0.21	0.17	0.21	0.16
MgO	31.5	31.6	15.63	14.58	23.83	24.03
CaO	8.1	8.3	16.02	22.24	11.82	10.27
Na ₂ O	0.5	0.4	0.45	0.33	0.27	0.25
K ₂ O	2.0	2.0	2.81	1.52	0.94	1.02
H ₂ O+	3.4	3.7	0.32	3.42	6.22	4.98
H ₂ O-	---	---	0.18	1.65	0.76	0.90
P ₂ O ₅	0.4	0.4	1.03	1.32	0.68	0.23
CO ₂	5.1	5.0	18.6	14.84	7.24	9.02
S	n.d.	n.d.	0.05	n.d.	n.d.	n.d.

1 & 2. Gauthier Township, Ontario (Lee & Lawrence, 1968, p.10).

3. Keith Township, Ontario; W.H.Herdsman, analyst; 4-6. Lesueur Township, Quebec; correspond to samples 4, 7, and 8 in Table 1 (Watson, 1967, p.318).

Table 5. Minor Element Content of Kimberlite (p.p.m.)

	1	2	3	4	5	6
Cr	1500	1600	600	1440	1000	2000
Ni	1100	1100	920	1140	1200	2000
Co	78	78	37	77	50	200
Rb	n.d.	n.d.	n.d.	21	250	2
Ba	1900	2000	1600	740	1000	1
Sr	710	760	960	445	600	1
Y	---	---	n.d.	46	40	---
Zr	250	250	450	445	190	30
Nb	220	210	100	240	200	1
La	150	150	80	370	n.d.	---

1 & 2. Gauthier Township, Ontario (Lee & Lawrence, 1968, p.12);

3. Keith Township, Ontario; W.H.Herdsman, analyst;

4. Basutoland; average of 14 (Dawson, 1967, p.273);

5. South West Africa; average of four, except Y which is average of two (Dawson, 1967, p.273, after Janse, 1964);

6. Ultrabasic rocks (Dawson, 1967, p.273);

n.d. - not determined.

SOME TRACE ELEMENTS IN RUTILE FROM ECLOGITES AND THEIR IMPLICATIONS

A.J.R. WHITE La Trobe University, Melbourne, Australia.

S. R. TAYLOR Australian National University, Canberra, Australia.

A study of paragenesis and compositions of rutiles in eclogites has been made in order to assess the model of partial melting of eclogite to produce andesitic rocks in subduction zones.

Rutile appears as an accessory phase in almost all eclogites because there is no other phase capable of accommodating titanium. The high pressure of omphacite formation favours the entry of aluminium into 6-fold rather than 4-fold co-ordination (THOMPSON, 1947) and formation of the titanium-bearing pyroxene component $\text{CaTiAl}_2\text{O}_6$ is precluded under these conditions. Iron may enter the omphacitic pyroxene as $\text{CaFeSi}_2\text{O}_6$ and/or $\text{NaFe}^{3+}\text{Si}_2\text{O}_6$ depending on the oxidation state. Pyrope-almandine garnets are also low in titanium. This means that unless amphibole or mica is present as a primary Ti-bearing mineral, rutile occurs as a separate phase.

Rutiles from three eclogites have been studied. Two (New Guinea 295, Tasmania EC30) are from amphibolite terrains and a third (California EC84) is from a blue schist terrain. Rutile from the New Guinea eclogite (295) was analyzed for Cu, Ni, Sc and V by optical emission spectroscopy. V was found to be high (365 ppm) but the other elements were not detected.

The specimens were analyzed for Zr, Hf, Sn, W, Mo, Y and the rare earth elements using a spark source mass spectrometer (method of TAYLOR, 1971). The results are shown in Table 1.

Table 1 Some trace elements in rutiles from eclogites

	295 New Guinea	EC20 Tasmania	EC84 California
Zr	689	910	168
Hf	17.5	17.7	7.8
Zr/Hf	39	51	22
Nb	261	>300	228
Zr/Nb	2.64	<3.0	0.74
Sn	38.6	17.9	5.5
W	12.5	8.2	1.6
Mo	33	10.2	nd*
Y	0.44	1.24	15.2
U	4.2	.48	nd*
Th	0.05	.34	nd*
Th/U	.01	.71	nd*

* nd = not detected.

All values in ppm

There is a large but systematic variation of these elements between samples. For instance, Sn, W and Mo all decrease as Zr decreases. This systematic variation is probably a reflection of their variation in abundance in the type of basalt metamorphosed. The New Guinea eclogite was probably derived from an alkali basalt whereas the Californian eclogite was probably from an ocean-floor basalt.

As expected from previous studies on terrestrial and extraterrestrial rutiles, the eclogite rutiles are high in Zr and Nb. Hafnium is also high and the Zr/Hf ratios are much the same as those of basalts. On the other hand Nb is high relative to Zr, the Zr/Nb ratios of rutiles being about an order of magnitude less than those of basalts.

The quadrivalent elements, Sn, W and Mo are also enriched in rutiles possibly by as much as an order of magnitude over basalt abundance.

Rare earth elements are low and could not be quantitatively determined because of interference effects, but there is clearly an enrichment in light relative to heavy rare earth elements. In two samples the low Y values tend to confirm this suggested rare earth pattern.

Uranium is unexpectedly high and thorium very low in the New Guinea sample. This is not so in the other two samples although both elements are sufficiently high in rutile from the Tasmanian eclogite to indicate a Th/U ratio of less than one. Basalts have a ratio greater than one.

It has been suggested that andesites and related rocks of island arcs are produced by partial melting of basaltic rocks in subduction zones (GREEN and RINGWOOD, 1968). The residue of this process is eclogite. It is assumed in the following discussion that the subduced and partially melted basalt is oceanfloor tholeiite. GREEN and RINGWOOD (1968) have shown that major element compositions of near liquidus pyroxenes and garnets produced from basaltic material under high pressure are consistent with the residual eclogite hypothesis.

Subduction zone rocks of all types including island arc tholeiites, high-Al basalts and andesites are all characterized by very low Ti contents. These low titanium values can be explained if rutile is a minor phase in the eclogite residuum (GILL, 1972). The low abundances in these rocks of several other elements that can be concentrated in rutile are also explained if refractory rutile occurs in residual eclogite. For example, Zr is less abundant in arc tholeiites than in ocean floor basalts, and andesites have similar average Zr contents to ocean floor basalts (Table 2).

In contrast Nb is lower by at least a factor of two in subduction zone rocks: this is explained by the very low Zr/Nb ratios found in all the rutiles of eclogites.

Zr/Hf ratios are not discernibly different in ocean floor basalts and andesites. This is compatible with the fact that the Zr/Hf ratios in rutiles are similar to those in basalts and andesites.

Insufficient data are available on Sn, W and Mo, in basalts and andesites. Because of their high values in rutiles we predict that they will be low in andesites. The increase in Th/U ratios of subduction zone volcanics relative to those of ocean floor basalts (Table 2), could be enhanced by the presence of rutile in the residuum since rutile takes up U preferentially to Th.

Table 2 Average values of selected trace elements in ocean floor tholeiites and subduction zone volcanic rocks

	Ocean floor Tholeiites	Island Arc Tholeiites	Andesites
SiO ₂ (% : Typical values)	48-50	48-53	55-60
TiO ₂	1.50	0.80	0.45
Zr (ppm)	95	46	96
Nb "	7	~0.5	4
Zr/Nb	13	-	24
Hf (ppm)	2.4	-	2.5
Zr/Hf	40	-	38
Sn (ppm)	1-2	-	0.4
U	0.1	0.27	0.52
Th	0.15	0.49	1.31
Th/U	1.5	1.8	2.5

Data from BROOKS (1970), CANN (1971), CHAPPELL and WHITE (unpublished) GILL (1972), HAMAGUCHI and KURODA (1969), TAYLOR and WHITE (1966).

It is concluded that Ti, Zr, Nb and possibly Sn, W, Mo abundances in subduction zone rocks such as andesites can be qualitatively explained using the model of andesite magma genesis by partial melting of ocean floor tholeiite.

REFERENCES

BROOKS, C.K. (1970) Geochim. Cosmochim. Acta. 34, 411-416.

CANN, J.R. (1970) Earth and Planet. Sci. Letts. 10, 7-11.

GILL, J.B. (1972) Ph.D. thesis Aust. Nat. Univ. (unpublished)

GREEN, T.H. and RINGWOOD, A.E. (1968) Contr. Mineral. and Petrol. 18, 105-162.

HAMMAGUCHI, H. and KURODA, R. (1969) Handbook of Geochemistry, Springer Verlag, Berlin.

TAYLOR, S.R. (1971) Geochim. Cosmochim. Acta. 35, 1187-96.

TAYLOR, S.R. and WHITE, A.J.R. (1966) Bull. Volcanol. 29, 177-194.

THOMPSON, J.B. (1947) Geol. Soc. Amer. Bull. (abstr.) 58, 1232.

THE PETROLOGY AND MINERALOGY OF ECLOGITE XENOLITHS
FROM THE ROBERTS VICTOR KIMBERLITE

G.G. Whitfield,
P.O. Box 106,
Kenhardt. Cape.

The Roberts Victor kimberlite is well known for its abundant eclogite xenoliths, twenty-five of which have been examined by the author. The ellipsoidal or discoidal xenoliths often display a rudimentary layering, are medium to coarse-grained and show a variable mozaic-like fabric. Four primary eclogite-mineral assemblages have been recognised, namely, the basic garnet-clinopyroxene assemblage (21 xenoliths) with additions of kyanite (2 xenoliths), kyanite-corundum, and diamond (one xenolith each). Primary rutile and sulphides are common trace constituents.

On petrographic grounds a broad distinction can be made between three groups characterised by the following general features:

Group I: garnets dark reddish to brown, bright and clear, tend to be rounded to elongated, occasionally subhedral, clinopyroxene dark green, only partially altered (10 specimens).

Group II: garnets pale orange to pink, turbid and fractured, tend to be rounded to irregular or angular, rarely subhedral; clinopyroxene pale green, extensively altered (12 specimens).

Group III: garnets bright orange, clear, rounded to irregular; clinopyroxene completely altered; kyanite always present (3 specimens).

The amount of garnet present varies tremendously, ranging from 14% to 74%, but showing a bimodal distribution with maxima at 45% and 65%. These two maxima show some correlation with the Group I and Group II eclogites respectively. In several specimens the garnet has been largely altered to secondary fine-grained micaceous material. Kyanite ranges between 3,3% to 9,0%.

Normally the xenoliths are extensively altered and also show distinct signs of undergoing tectonic deformation before incorporation into the kimberlite. Careful microscopic examination also reveals that almost every eclogite displays evidence of partial melting of the clinopyroxene (and possibly also the garnet) with the formation of secondary amphibole, feldspar crystallites and zeolite, usually in a vitreous matrix. This unusual feature is interpreted as resulting from the incongruent melting of the primary constituents on a sudden relief of pressure and while at a considerable depth. This probably took place at the time of kimberlite emplacement.

Chemical analyses of nine selected xenoliths show their variable composition; two specimens are alkalic, the remainder being tholeiitic. They are all undersaturated and three

are nepheline normative. Complete melting of these rocks would not produce typical basaltic liquids but rather liquids of picritic character. This clearly indicates that the eclogite xenoliths do not represent isochemically transformed gabbroic material.

The garnets, which are distinct from those found in peridotite xenoliths, are pink, orange or brown. The majority of garnet compositions, estimated from refractive index and unit cell size, ranges from 40% to 60% pyrope with an appreciable content of almandine and grossularite. Four analysed garnets also show a significant andradite but negligible uvarovite content. Garnets from the kyanite eclogites are pyrope-poor and grossularite-rich. On the basis of estimated garnet compositions two fairly distinct groupings can be made (but with several widely scattered compositions) which show some correlation to the Group I and II eclogites, the former being slightly richer in the pyrope and grossularite end-members. The bulk of the garnet compositions are typical of those from eclogites belonging to high-grade metamorphic complexes and are not at all similar to those from kimberlites or ultra-basic rocks. Their pyrope content suggests formation at lower pressures than typical kimberlitic or peridotitic garnets.

Chemical analyses of two pure blue-green clinopyroxene (omphacite) separates reveals its jadeite-rich nature and its clear distinction from chrome diopside. The omphacite has invariably been altered by a process of incongruent melting and is therefore not normally suitable for conventional chemical analyses. Kyanite, found in three xenoliths, occurs as bright blue platey grains and is in no way different to that from high-grade regionally metamorphosed rocks. The minor amount of corundum seen in one kyanite eclogite may be of secondary origin. Diamond is the only other constituent of significance and occurs both as colourless, well-formed crystals and as blackish granular aggregates of diamond and graphite. In general diamonds found in eclogites probably formed under conditions similar to those diamonds found in kimberlite. The question of diamond formation in natural silicate systems is still unanswered but conditions need not necessarily be as severe as often thought.

In general eclogites occur in five petrologically distinct environments, namely, lenses in ultramafic masses, masses associated with high-grade metamorphic complexes, lenses in Alpine-type orogenic zones, inclusions in alkali basalts and finally as inclusions in kimberlites. It is clear that the name eclogite can refer to a number of distinct garnet-pyroxene rocks of differing origin. Numerous origins have been suggested for those found in kimberlite. They have been considered to be samples of an eclogitic upper mantle, to be cognate with the kimberlite, to represent accidentally incorporated crustal eclogite from high-grade metamorphic complexes, or to originate from eclogite lenses within an ultrabasic upper mantle.

Normally kimberlites are extremely poor in eclogite xenoliths. The abundant eclogite xenoliths in the Roberts Victor kimberlite indicates that this pipe cannot be considered

typical. This suggests that these xenoliths are probably not related to the kimberlite genesis. The Roberts Victor eclogites are of variable mineralogical and chemical composition and their constituent minerals are in no way similar to those of kimberlite or its peridotite xenoliths. Garnet compositions are very similar to garnets from eclogites typical of high-grade gneissic complexes.

From this study it has been concluded that: 1. The Roberts Victor eclogites are not cognate with the kimberlite host and are probably in no way related to it. The possibility of the eclogites representing a high pressure cumulate of a fractioning liquid, which would also produce a residual kimberlitic liquid, appears highly improbable. 2. Their origin, as material from a primary eclogite upper mantle, cannot, in the light of present day ultrabasic upper mantle concepts, be supported, neither can the hypothesis that they are samples of simple eclogite segregations derived purely from the partial melting of primary garnet lherzolite. 3. Their source is most probably from within the upper mantle or lower crust where pockets of heterogeneous, partly fractionated basaltic magma have been trapped and solidified within an eclogite-stable region. Samples of this material have been fortuitously brought to surface by the ascending kimberlite intrusion. 4. The fact that the Roberts Victor eclogites are very similar to eclogite from regionally metamorphosed complexes suggests that a possible source, for at least some of the material, is within some high-grade metamorphic zone hidden beneath the sedimentary cover of the Roberts Victor area.

THE PETROLOGY AND MINERALOGY OF PERIDOTITE XENOLITHS
FROM THE BULTFONTEIN, WESSELTON, DUTOITSPAN AND
ROBERTS VICTOR KIMBERLITES

G.G. Whitfield,
P.O. Box 106,
Kenhardt. Cape. R.S.A.

Forty-two well-rounded peridotite xenoliths, found in the abovementioned kimberlite diatremes, have been studied by conventional petrological and mineralogical techniques. Quantitative data is presented and their origin and occurrence in kimberlite explained.

Petrographically the xenoliths can be divided into three main groups, namely, garnet peridotite (twenty-four xenoliths comprising sixteen lherzolites and eight harzburgites), spinel peridotite (eleven xenoliths comprising six lherzolites and five harzburgites) and highly altered or granulated peridotite of essentially dunitic composition (seven xenoliths). Macroscopically and in thin section the garnet and spinel peridotites are virtually identical, both being relatively fresh, phanerocrystalline, medium to coarse-grained, allotriomorphic aggregates of olivine and orthopyroxene with possible minor or trace amounts of wine-red garnet, bright green clinopyroxene, phlogopite, black chrome spinel, and rarely traces of graphite and sulphides. Several specimens contain both garnet and spinel, with one phase present in a trace amount. Most of the xenoliths display microscopic features consistent with a notable degree of tectonic deformation, and in cases, recrystallisation, clearly indicating that at some stage, before incorporation into the kimberlite magma, the peridotites were tectonically disturbed.

The average modal composition of the garnet peridotites is 65% olivine, 29% orthopyroxene, 0,7% clinopyroxene, 4,6% garnet and 1,0% phlogopite while the garnet peridotite xenoliths most closely approaching suggested compositions of the upper mantle consists of 65% olivine, 22% orthopyroxene, 5,0% clinopyroxene, 5,9% garnet and 1,2% phlogopite. The average modal composition of the spinel peridotites is 72% olivine, 25% orthopyroxene, 0,1% clinopyroxene, 0,4% spinel and 2,2% phlogopite.

Chemical analyses of nine garnet peridotites and four spinel peridotites reveal that the specimens are more or less identical, all being undersaturated, olivine-normative rocks of tholeiitic character and typical ultrabasic composition. No significant variations are apparent and the small differences can be explained by variations in the modal composition.

The olivine composition, determined by X-ray and optical methods, ranges from Fo₉₁ to Fo₉₄, and is confirmed by chemical analyses of five pure separates; nickel is always present in a minor amount. The olivine shows some serpentinisation and normally displays uneven optical extinction, deformation lamellae and marginal granulation or distinct recrystallisation, indicating intensive tectonic deformation.

Orthopyroxene compositions, estimated from optical properties, range from En₈₈ to En₉₁, and are supported by chemical analyses of five pure separates. The orthopyroxene from the garnet peridotites are deficient in aluminium and calcium compared with that from spinel peridotite, indicating formation under higher pressure conditions. Chrome is an important minor constituent. In thin section uneven optical extinction is typical and kink bands and bent crystals are common, similarly indicating tectonic deformation.

The bright green clinopyroxene (chrome diopside) has not been studied in detail but a chemical analysis of one pure separate shows it to consist mainly of diopside with appreciable amounts of enstatite and jadeite in solid solution. From chemical calculations it is estimated that the analysed chrome diopside formed at a depth of 125 kilometres.

The vividly coloured garnets fall into a small compositional range rich in the pyrope end-member but also containing almandine, andradite, uvarovite, plus minor grossularite and spessartite. The average three end-member garnet composition, estimated from refractive index and unit cell size is 73% pyrope, 14% almandine and 13% andradite/uvarovite. Partial chemical analyses of four pure separates indicate the essential reliability of the estimated compositions. The garnets are typical of those found in kimberlites and orogenic dunites and serpentinites; their pyrope-rich composition points to formation at very high pressures.

Phlogopite is, in certain cases, undoubtedly of primary origin, especially so when exhibiting gross deformation structures. The presence of a primary potassium and water-bearing phase, also capable of providing radiogenic heat, in rocks of probable upper mantle origin is of considerable petrogenic significance.

Basically three main theories have been used to account for the peridotite xenoliths in kimberlite; these are firstly as accidentally included fragments of high-grade crustal peridotite; secondly as a segregated or accumulated co-magmatic phase of the kimberlite; thirdly as fragments of upper mantle material. This study shows that texturally, mineralogically and chemically the peridotites are remarkable similar. Variations in both the mineral assemblage and individual mineral compositions can be explained by formation under varying temperature/pressure conditions and by a process of partial melting and depletion in certain constituents. A comparison of peridotite xenoliths from other kimberlites, on a world-wide scale, likewise reveals their essential similarity to those described above. It must be concluded that all such xenoliths are derived from one source of relatively constant mineralogical and chemical composition, and of universal extent. Present day thinking points to an upper mantle of peridotitic composition as being the most likely source.

The following major conclusions are made:- 1. The xenoliths represent upper mantle material carried to near surface by a volatile-rich, rapid moving kimberlite magma originating from depths of at least 125 kilometres. 2. The xenoliths do not represent primary upper mantle material but

rather portions which have undergone significant tectonic activity and varying degrees of partial melting with resultant depletion of the more easily fused constituents such as garnet, chrome diopside and phlogopite. The completely recrystallised dunitic xenoliths possibly represent the end product of this trend. 3. The spinel peridotites differ from the garnet peridotites in that they formed at a shallower depth in the upper mantle and generally show slightly more partial melting. A minor transitional zone probably exists between the two groups. 4. Evidence indicates that the xenoliths are not cognate with the kimberlite. It is highly unlikely that kimberlite magmas of variable composition could produce, by any process, a suite of such uniform and wide-spread rocks. 5. Kimberlites are generated within the garnet peridotite (phlogopite-bearing?) of the upper mantle and much of the fragmentary material in kimberlite is probably derived from comminution of incorporated peridotite. No diamonds however have ever been found in true peridotite xenoliths.

Al-AUGITE AND Cr-DIOPSIDE ULTRAMAFIC XENOLITHS IN BASALTIC ROCKS FROM
WESTERN UNITED STATES: STRUCTURAL AND TEXTURAL RELATIONSHIPS.

H.G. Wilshire and J.W. Shervais, U.S. Geological Survey, Menlo Park, Ca.

Common ultramafic xenoliths in basalts from the western United States are divisible into Al-augite and Cr-diopside groups (Table 1). The Al-augite group is characterized by black Al, Fe, Ti-rich clinopyroxene, Fe-rich olivine and orthopyroxene, and Al-rich spinel. The Cr-diopside group is characterized by green Cr, Mg-rich clinopyroxene and spinel and by Mg-rich olivine and orthopyroxene. Both groups have a wide range of subtypes (Fig. 1), but augite-rich types dominate the Al-augite group and lherzolites dominate the Cr-diopside group. These two groups are of world-wide occurrence (Forbes and Kuno, 1965); in the United States, as elsewhere (Kuno, 1969), members of the Cr-diopside group are dominant.

Pyroxene-rich members of the Al-augite group are typically irregularly interleaved with olivine-rich members. Where contacts are sharp, branching and intersecting augite-rich bands isolate angular fragments of the olivine-rich rocks (Fig. 2). Gradational contacts result from granular disaggregation of the olivine-rich rock. The textures of the augite-rich bands appear, with a few exceptions, to be igneous (hypidiomorphic granular), but they are not cumulus textures as is widely held (e.g., Frechen, 1963; White, 1966; Carter, 1970; Kutolin and Frolova, 1970). Poorly developed unmixing and reaction textures are widespread but not abundant. Cataclastic textures are locally well developed, and a few augite-rich members of the group are extensively recrystallized. Textures of olivine-rich members of the group are metamorphic; visibly foliated or lineated fabrics occur, but granoblastic recrystallization textures predominate.

The structures and textures of members of the Al-augite group indicate that the augite-rich rocks are dikes and veins, and that the olivine-rich rocks are their metamorphic wall rocks. The wall rocks have been modified in places by extraction of melt, in others by saturation with the melt phase, and generally by reaction with melt producing the more iron-rich compositions that identify the group. The veins have been modified by reaction with the wall rocks and by vein-forming processes. These structural, textural, and compositional relationships are like those in some alpine peridotites (Dickey, 1970; Boudier and Nicolas, 1972).

The general lack of deformation and recrystallization of the dike rocks and isotopic similarity (Steuber and Murthy, 1966) to the basaltic magma that brought them to the surface suggest that most of the Al-augite pyroxenites are cognate. This conclusion is strengthened by the generally poor development of unmixing and reaction textures which, in the absence of recrystallization, indicate that the rocks have had little opportunity to equilibrate at subsolvus temperatures. Accordingly, we postulate that xenoliths of the Al-augite ultramafic group are complex mixtures of dikes and reacted wall rock derived from the source areas of the basalts that brought them to the surface.

The Cr-diopside ultramafic group also consists of pyroxene-rich units interleaved with olivine-rich units but differs from the Al-augite group in that the lithologic layering is normally plane parallel and all members have dominantly metamorphic textures (Table 1). However, at some localities, especially well represented by San Carlos, Arizona, intersecting and branching diopside-rich layers are found. Dunitic zones (see

Boudier and Nicolas, 1972) also occur adjacent to some diopside-rich bands and large, deformed pyroxene grains with unmixing textures that have survived recrystallization attest to a former high temperature history. The textures of these rocks (deformed diopside with coarse enstatite exsolution lamellae surrounded by granoblastic intergrowths of diopside and enstatite) are nearly identical to those of clinopyroxenite vein networks in some alpine peridotites. The intersecting and branching pyroxene-rich bands in lherzolite inclusions from San Carlos could represent pieces of similar vein networks, but generally both the original structures and textures have been largely eradicated by solid flow and recrystallization.

The similarities of structure and texture of xenoliths in the Al-augite group to the relict structures and textures of xenoliths in the Cr-diopside group are sufficient to support the hypothesis that both originated in the same way. That is, that the pyroxene-rich members are veins formed by crystallization in the mantle of partial melts that failed to escape to volcanic conduits and the olivine-rich host rocks of the pyroxene-rich bands are the wall rock of such veins modified in varying degrees by extraction or addition of melt and by reaction. The Al-augite series appears generally to be cognate with basalt that carries the xenoliths, whereas the extensive exsolution, deformation, and recrystallization of rocks in the Cr-diopside group indicate that they represent older episodes of melting. These relationships are illustrated in figure 3.

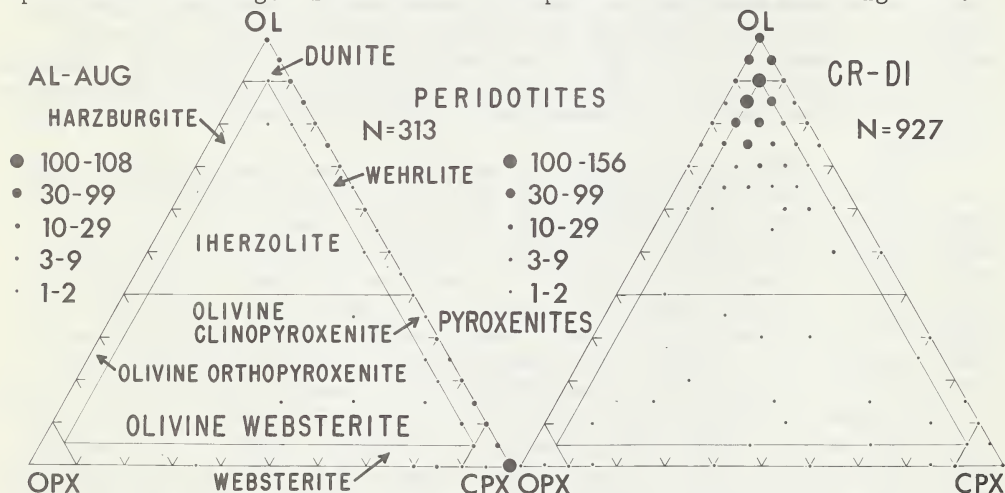


Fig. 1. Triangular plots showing distribution of lithologies in Al-augite and Cr-diopside ultramafic groups. Boundaries and names follow IUGS recommendations.

References

Boudier, F. and Nicolas, A., 1972: Bull. Suisse Mineral. Petrogr., v. 52/1, p. 39-56. Carter J.L., 1970: Geol. Soc. America Bull., v. 81, p. 2021-2034. Dickey, J.S., Jr., 1970: Min. Soc. America Spec. Pub. 3, p. 33-49. Forbes, R.B. and Kuno, H., 1965: Proc. 22d Internat'l. Geol. Congr., Upper Mantle Symp., New Delhi (1964), p. 161-179. Frechen, J., 1963, N. Jahrb. f. Mineral., Nos. 9-10, p. 205-224. Kuno, H., 1969, in *The earth's crust and upper mantle* (ed. P.J. Hart): Amer. Geophys. Union, Geophys. Mono 13,

p. 507-513. Kutolin, V.A. and Frolova, V.M., 1970: Contr. Mineral. Petrol. v. 29, p. 163-179. Steuber, A.M. and Murthy, V.M., 1966: Geochim. Cosmochim. Acta, v. 30, p. 1243-1259. White, R.W., 1966: Contr. Mineral. Petrol. v. 12, p. 245-314.

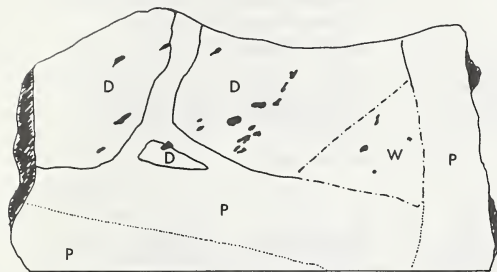


Fig. 2. Sketch of xenolith showing branching and intersecting Al-augite pyroxenite veins (P) in dunite (D). Black areas denote spinel. Note dunite inclusion in pyroxenite. Vein on right is coarser-grained than the vein it cuts; bottom vein is more spinel-rich below dotted line. Wehrlite (W) has gradational contacts with all adjacent lithologies.

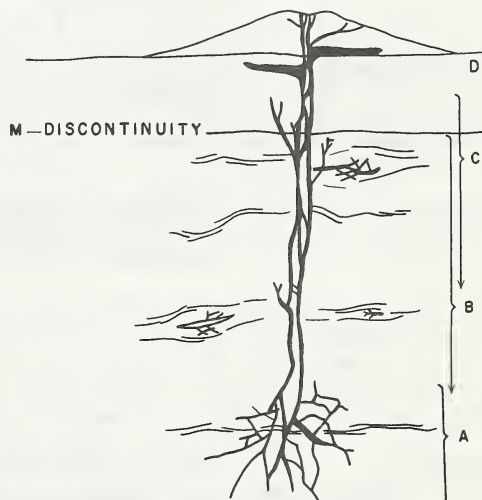


Fig. 3. Schematic diagram illustrating possible relationships of cognate Al-augite pyroxenite and Cr-diopside ultramafic groups. A. Mantle source zone; anastomosing feeders to main conduits. Al-augite ultramafic xenoliths with complex vein networks represent earlier melts and wall rock from this and higher zones. B. Gneissic mantle material composed of penetratively deformed Cr-diopside peridotites. Augen preserve parts of former complex vein networks. Depending on depth in mantle, these may belong to the Cr-diopside, garnetiferous, or feldspathic ultramafic groups. C. Offshoot veins from the main conduits penetrate crustal and mantle rock that was not involved in the youngest melting episode. Xenoliths from this horizon include veins in peridotite of the Cr-diopside and feldspathic ultramafic groups. D. Sill injections in upper crust and within contemporaneous volcanic pile yield cumulate differentiates that form locally important members of xenolith suites.

Table 1. Principal Features of Al-augite and Cr-diopside Ultramafic Groups^{1/}

	<u>Cr-diopside Group</u>	<u>Al-augite Group</u>																																																																						
<u>Rock Types</u>	LHERZOLITE; dunite; olivine websterite; websterite; wehrlite; olivine clinopyroxenite; harzburgite; clino-pyroxenite; [olivine orthopyroxenite]; [orthopyroxenite]	OLIVINE CLINOPYROXENITE; WEHRLITE; CLINOPYROXENITE; dunite; lherzolite; [olivine websterite]; [websterite]																																																																						
<u>Structures</u>																																																																								
A. Layering and cross-cutting	COMMONLY CONCORDANT SOLID FLOW LAYERS; branching but not cross-cutting	COMMONLY BRANCHING AND CROSS-CUTTING IGNEOUS LAYERS; pyroxene-rich dikes cross foliation of olivine-rich wall rock																																																																						
B. Inclusions	Olivine-rich inclusions in pyroxene-rich rocks	OLIVINE-RICH INCLUSIONS IN PYROXENE-RICH ROCKS																																																																						
C. Grain orientation	Common	Uncommon																																																																						
<u>Textures</u>	TECTONITE TEXTURES; RE-CRYSTALLIZATION TEXTURES; unmixing textures	<u>Pyroxene-rich rocks:</u> IGNEOUS VEIN TEXTURES; unmixing textures; re-crystallization textures; reaction textures; cumulus textures; cataclastic textures <u>Olivine-rich rocks:</u> RECRYSTALLIZATION TEXTURES; tectonite textures																																																																						
<u>Mineralogy</u>																																																																								
A. Relative abundance	OLIVINE; ORTHOPYROXENE; clinopyroxene; spinel; pargasite; phlogopite	CLINOPYROXENE; OLIVINE; spinel; orthopyroxene; kaersutite; Ti-phlogopite																																																																						
B. Composition ^{2/}	<table> <thead> <tr> <th></th> <th>Cpx</th> <th>Opx</th> <th>O1</th> <th>Sp</th> </tr> </thead> <tbody> <tr> <td>Ca</td> <td>45.1</td> <td></td> <td></td> <td>Fe 8.1</td> </tr> <tr> <td>Mg</td> <td>49.3</td> <td>89.6</td> <td>86.8</td> <td>Al 61.3</td> </tr> <tr> <td>Fe</td> <td>5.6</td> <td>10.4</td> <td>12.2</td> <td>Cr 30.6</td> </tr> <tr> <td>Al</td> <td>5.5</td> <td>4.7</td> <td></td> <td></td> </tr> <tr> <td>Cr</td> <td>.84</td> <td></td> <td></td> <td></td> </tr> <tr> <td>Ti</td> <td>.56</td> <td></td> <td></td> <td></td> </tr> </tbody> </table>		Cpx	Opx	O1	Sp	Ca	45.1			Fe 8.1	Mg	49.3	89.6	86.8	Al 61.3	Fe	5.6	10.4	12.2	Cr 30.6	Al	5.5	4.7			Cr	.84				Ti	.56				<table> <thead> <tr> <th></th> <th>Cpx</th> <th>Opx</th> <th>O1</th> <th>Sp</th> </tr> </thead> <tbody> <tr> <td>Ca</td> <td>46.0</td> <td></td> <td></td> <td>Fe 7.4</td> </tr> <tr> <td>Mg</td> <td>46.4</td> <td>86.6</td> <td>81.8</td> <td>Al 88.6</td> </tr> <tr> <td>Fe</td> <td>7.8</td> <td>13.4</td> <td>18.5</td> <td>Cr 4.0</td> </tr> <tr> <td>Al</td> <td>7.7</td> <td>4.7</td> <td></td> <td></td> </tr> <tr> <td>Cr</td> <td>.23</td> <td></td> <td></td> <td></td> </tr> <tr> <td>Ti</td> <td>1.28</td> <td></td> <td></td> <td></td> </tr> </tbody> </table>		Cpx	Opx	O1	Sp	Ca	46.0			Fe 7.4	Mg	46.4	86.6	81.8	Al 88.6	Fe	7.8	13.4	18.5	Cr 4.0	Al	7.7	4.7			Cr	.23				Ti	1.28			
	Cpx	Opx	O1	Sp																																																																				
Ca	45.1			Fe 8.1																																																																				
Mg	49.3	89.6	86.8	Al 61.3																																																																				
Fe	5.6	10.4	12.2	Cr 30.6																																																																				
Al	5.5	4.7																																																																						
Cr	.84																																																																							
Ti	.56																																																																							
	Cpx	Opx	O1	Sp																																																																				
Ca	46.0			Fe 7.4																																																																				
Mg	46.4	86.6	81.8	Al 88.6																																																																				
Fe	7.8	13.4	18.5	Cr 4.0																																																																				
Al	7.7	4.7																																																																						
Cr	.23																																																																							
Ti	1.28																																																																							

^{1/} All upper case indicates important or dominant feature or rock type; lower case indicates feature or rock type present but subordinate; lower case in brackets indicates rare feature or rock type.

^{2/} Compositions above line are normalized At.% and represent averages of 15 or more analyses in each of 12 samples. Compositions below line are wt.% oxides.

PHYSICAL MODELING OF DIATREME EMPLACEMENT

T. S. Woolsey, Physical Sciences Div., Lincoln Land Community College, Springfield, Illinois 62703

M. E. McCallum, and S. A. Schumm, Department of Earth Resources, Colorado State Univ., Ft. Collins, Colo. 80521

Fluidization or mobilization of particulate materials by upward moving high velocity gas is the mechanism suggested by most field investigators for emplacement of diatremes and development of associated structures. A series of experiments was conducted with small scale models utilizing fluidization techniques similar to those developed by chemical engineers for industrial applications. These experiments generated a number of structural and textural features that are similar to features observed in diatremes.

Containers were constructed in various cylindrical, parallel plate, and box-like configurations. The cylindrical containers were 20 cm high and ranged in diameter from 7 to 15 cm. Parallel plate containers were 4 cm thick, 35 cm high and both 21 and 100 cm wide. The two box containers used were 30 x 30 cm and 90 x 90 cm in plan and 17 cm deep. Some model containers were designed for sectioning while others were constructed with plexiglass walls to allow direct observation of developing features.

Gas was supplied to the base of the containers via a 2 cm diameter screened orifice and allowed to pass upward through the contents and out the top which was open to the atmosphere. Gas used in all experiments was compressed air from a large volume source piped to the models through a pressure regulator and float-type flow meter.

Particulate mixtures used ranged from clay-size (powdered kaolinite) to 0.5 cm gravel. Materials were arranged in layers that varied in experiments from layers of different particle sizes to homogeneous mixtures in which contrasting colors served as marker horizons. A few experiments utilized layers of different size particles in dipping beds or with bed pinch-outs. Surface crusts and subsurface layers of poorly consolidated silt were used to study the effects of fluidization on low-strength, highly friable materials.

Most experiments were characterized by the early development of surface doming and, where a cohesive or semi-consolidated surface layer was present, associated ring and radial fractures. A rapid upward propagation of intricate subsurface fracture patterns was generated with increasing gas pressures during tests with cohesive materials, and subsurface gas-filled cavities with arched roofs formed in many of the scale simulations. Fluidized

circulation cells developed below these voids and slowly moved upward to the surface by stoping (Fig. 1A). Multiple vertically aligned voids were observed simultaneously in several cases. In some tests where particularly explosive blowout occurred, formerly horizontal beds in the surrounding strata were deformed into compressional folds. When gas flow was terminated prior to breaching of the surface by the circulation cell, some subsidence of overlying beds was observed. This might suggest that some cryptovolcanic features exhibiting circular subsidence structure and an absence of volcanic material may be the result of diatremes that never reached the surface.

Conduits were typically funnel-shaped, widening toward the surface, and eruption usually produced a maar type crater with a diameter several times that of the lower part of the conduit. Such configuration resembles diatremes that have been revealed to considerable depth, such as the Kimberley Pipe in S. Africa, and is similar to shapes derived through theoretical calculation by McGetchin (1968). Subsidence in the models occurred concentric to the mobilization conduit, and surface blocks were transported down along pipe margins. Blocks and slabs of highly friable, low strength materials subsided in the fluidized convection cells, but they showed little attrition unless circulated many times (Fig. 1B).

In a few experiments, a slow bubbling surface eruption was accompanied by an air-fall size sorting and bedding of particulate matter. Such bedding was most notable when mixtures of 0.25 mm sand and 200 mesh marble dust (finer than 0.074 mm) were used. The bedded material was carried down the pipe by slow marginal subsidence concurrent with central eruption (Fig. 1C). Final disposition closely approximates numerous field conditions, where moderately to steeply dipping bedded tuffs occur deep in pipes and are cross-cut by central zones of unbedded breccia (e.g., Cloos, 1941; Hearn, 1968). Crude segregations of unbedded pipe materials were noted in several experiments, the finest particulate mixtures found toward pipe centers and coarse aggregates near the margins. Spheroidal pellets possibly analogous to the pelletal lapilli described by Rust (1937) and Hearn (1968) were formed by accretion of clay-size particles on larger grains during bubbling fluidization.

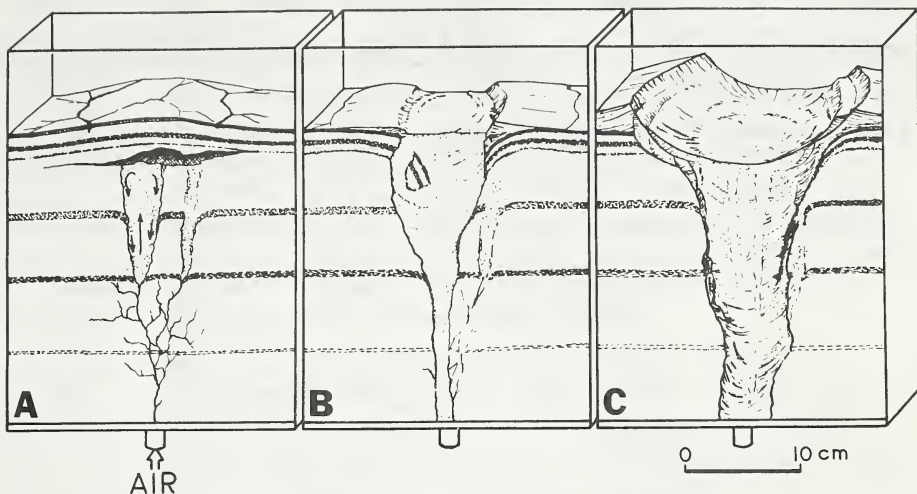


Fig. 1. Diagrammatic series showing principle features developed in model diatremes.

A. Compressed air entering base of container propagates fractures in cohesive clay or marble dust mixture. Two subsurface fluidized circulation cells develop below void produced by fracture and uplift of upper layers. Doming of the surface with ring and radial fractures results from uplift.

B. Breakthrough to surface occurred above main fluidization cell and smaller cell has become inactive. Surface layers display inward dip on right and detachment and descent of a surface slab on left. A cone of bedded ejecta has begun forming.

C. Continued bubbling circulation has built a larger bedded ejecta cone with rotational slumping into crater. Smears and slices of adjacent strata have descended along pipe margins. Bedded ejecta is carried downward during continued bubbling fluidization accentuating saucer-like form by drag along the pipe walls. Faint channelways may be seen where higher velocity upward moving gas has cleared out fines. Minor dog-leg offset may be related to variation in competency of beds.

References Cited

Cloos, H., 1941, Geol. Rundschau, 32, 709-800.

Hearn, B. C., 1968, Science, 159, 622-625.

McGetchin, T. R., 1968, Calif. Inst. Tech., unpub. Ph.D. thesis, 405p.

Rust, G. W., 1937, Jour. Geol., 45, 48-75.

RELATIONSHIP OF MELILITE-BEARING ROCKS TO KIMBERLITE: THE SYSTEM AKERMANITE - CO_2

H. S. Yoder, Jr., Geophysical Laboratory, Washington, D.C., U.S.A.

The notion that kimberlite is genetically related to melilite "basalt", attributed to H. C. Lewis (1897), was revived after olivine melilitite was discovered in close association with a kimberlite brecchia (Ukhanov, 1963). Reports of melilite in kimberlite have been rare and then the identification of the mineral was dubious or based on the interpretation of alleged pseudomorphs. Both CO_2 and H_2O play an important role in kimberlite groundmass (olivine + phlogopite + calcite); however, akermanite (Ak), the principal component of melilite, was found to be stable only at water pressures below 10.2 kbar (Yoder, 1968). Because the stability field of phlogopite enlarges with CO_2 , akermanite was investigated in the presence of CO_2 .

Two mixtures having the composition $2\text{CaO}:\text{MgO}:2\text{SiO}_2:\text{CO}_2$ (= Ak + CO_2) and $3\text{CaO}:\text{MgO}:2\text{SiO}_2:2\text{CO}_2$ (= Merwinite + 2CO_2) were studied up to 10 kbar total pressure at temperatures from 950° to 1475°C . The results of the first composition run in gas-media, high-pressure apparatus for times up to 1 week are presented in Fig. 1.

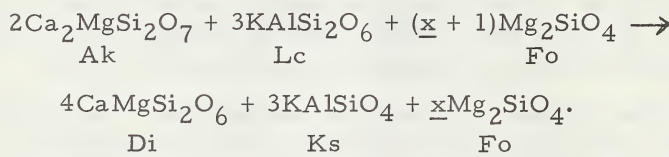
The maximum stability limit of akermanite in the presence of excess CO_2 was found to be 6.1 kbar. At relatively lower temperatures and below that pressure, akermanite reacts with CO_2 to form diopside (Di) + calcite (Ct). The reaction takes place through a range of temperatures because of possible solid solutions in dolomite in calcite, akermanite in diopside, and a variety of solid solutions in akermanite. The reaction curve, extended through the measurements of Walter (1963), terminates at its junction with the breakdown curve of akermanite \rightarrow wollastonite + monticellite (Yoder, 1968) near 685°C at a pressure less than 100 bars. The appearance of diopside in the Ak + CO_2 composition is due primarily to the solution of additional components in the gas phase (G).

The melting of akermanite in the presence of CO_2 appears to be congruent and produces liquids which quench to a clear glass. The lowering of the melting curve relative to the anhydrous melting curve of Kushiro (1964) is believed to be due to the solubility of CO_2 in the liquid. The melting of Di + Ct also yields a clear, homogeneous glass without quench products. It is concluded that carbonatite is not necessarily a product of immiscibility from all ultrabasic compositions. New preliminary data on the melting of calcite cleavage blocks in the absence of excess CO_2 and the melting of diopside in the presence of CO_2 (Eggler, 1973) are given in Fig. 2.

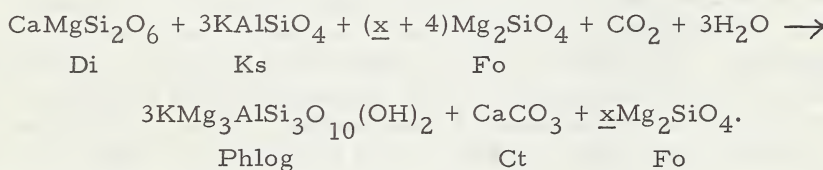
The restriction of akermanite to relatively low pressures in the presence of excess CO_2 is evident in Fig. 1. In the absence of free CO_2 , the assemblage Ak + Di + Ct, related to the alnoites, is stable

and would persist until the breakdown of Ak itself at about 15 kbar. Inclusion of the soda melilite component may extend this range to higher pressures; however, the minerals in natural melilite-bearing rocks were shown to react at high pressures to form pyroxenites in the absence of water and CO_2 (Tilley and Yoder, 1968). Similar behavior would be expected in the absence of the additional phase calcite. It is not uncommon to see veins of calcite crossing pyroxenites without the formation of melilite. If kimberlite is derived from the mantle, then melilite-bearing rocks are not likely sources.

Melilite is commonly associated with leucite (Lc), kalsilite (Ks), and phlogopite (Phlog). Olivine melilite leucitite (ugandite) is probably related to olivine kalsilite pyroxenite (mafurite) by the reaction:



Diopside + kalsilite occurs with melilite in metamorphosed sedimentary blocks at Brome Mountain, Quebec (Philpotts, Pattison, and Fox, 1967), and at Hendriksplaats, Bushveld (Willemse and Bensch, 1964). It is important to note that the three phases akermanite, monticellite, and leucite, which commonly occur together, all break down at relatively low pressures. Addition of CO_2 and H_2O to different proportions of the above products yields the kimberlite groundmass assemblage:



It appears that there is some support for the suggestion that a magma having melilite affinities could be transformed into kimberlite with the aid of suitable volatiles. Loss of volatiles in transit or crystallization at low pressure would yield a melilite-bearing assemblage within the upper crust.

From the relations exhibited in Fig. 1 and the equations listed immediately above, it would seem that clinopyroxene ought to be a common residual phase in kimberlite. It is in fact a rare phase and then may be derived in part from fragmented xenoliths incorporated in the kimberlite. The large array of intermediate rocks that do contain clinopyroxene, melilite, and the major phases in the groundmass of kimberlite are usually described as alnoite.

The results presented in Fig. 1 are also of importance to the metamorphism of carbonaceous rocks. The reaction $\text{Di} + \text{Ct} \rightarrow$

Ak + CO₂ is Bowen's (1940) step 8 in the metamorphism of a siliceous dolomite. Because of the exceptionally high temperatures involved where the CO₂ pressure is the total pressure, it would appear that the reaction runs in nature at very low partial pressures of CO₂.

References

Baker, E. H. (1962) J. Chem. Soc. London, Part I, 464-470.

Bowen, N. L. (1940) Jour. Geol. 48, 225-274.

Eggler, D. H. (1973) Carnegie Inst. Wash. Year Book 72 (in press).

Kushiro, I. (1964) Carnegie Inst. Wash. Year Book 63, 84-86.

Lewis, H. C. (1897) Papers and Notes on the Genesis and Matrix of the Diamond, T. G. Bonney, ed., Longmans, Green and Co., 72 p.

Philpotts, A. R., E. F. Pattison, and J. S. Fox (1967) Nature 214, 1322-1323.

Tilley, C. E., and H. S. Yoder (1968) Carnegie Inst. Wash. Year Book 66, 457-460.

Ukhanov, A. V. (1963) Dokl. Akad. Nauk. SSSR, 153, 923-925.

Walter, L. S. (1963) Am. Jour. Sci., 261, 488-500.

Willemse, J., and J. J. Bench (1964) Trans. Geol. Soc. So. Africa, 67, 1-87.

Wyllie, P. J., and O. F. Tuttle (1960) Jour. Petrology, 1, 1-46.

Yoder, H. S. (1968) Carnegie Inst. Wash. Year Book 66, 471-477.

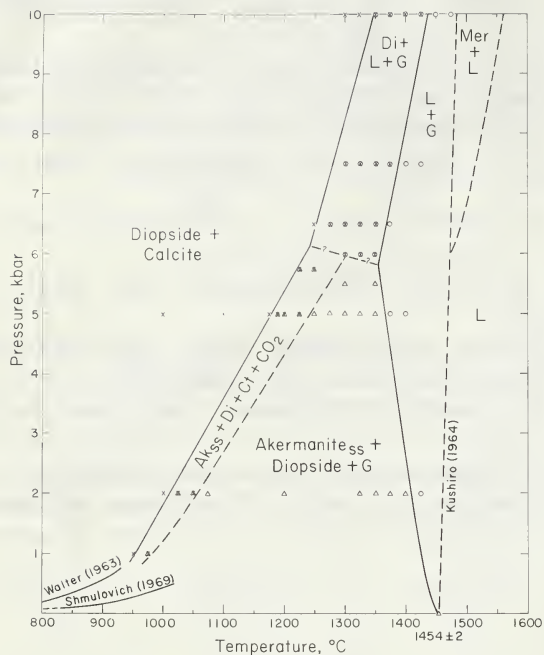


Fig. 1. Pressure-temperature diagram illustrating new results for akermanite- CO_2 using the diopside + calcite (1:1 mole) composition. Short-dash curves represent an extrapolation to low pressures of the melting data of Kushiro (1964) for akermanite.

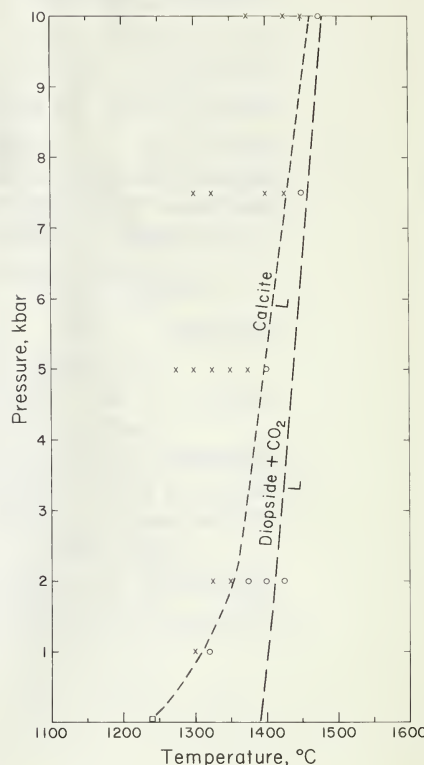


Fig. 2. Preliminary pressure-temperature curve for the melting of calcite cleavage blocks. Invariant point (square) from Baker (1962) and 1-kbar bracket from Wyllie and Tuttle (1960). The melting of calcite is compared with that of diopside in the presence of an excess of CO_2 (Eggler, 1973). Calcite may melt at slightly lower temperatures in the presence of excess CO_2 .

QE 462 K5 162 1973
INTERNATIONAL CONFERENCE ON
KIMBERLITES 1973 UNIVERSITY OF
CAPE TOWN 39207990 SCI



000002548964

Date Due

DUE CAM APR 30 '80	RECEIVED CAM	NOV 03 '81
DUE CAM SEP 15 '81	OCT 26 '81	RECEIVED
DUE 15 SEP '81	OCT 26	RECEIVED
DUE CAM APR 30 '80	JAN 25 '88	RECEIVED
DUE CAM APR 30 '80	JAN 16	RECEIVED
JUN 19 '81	FEB 12 '88	RECEIVED
DUE CAM SEP 15 '80	FEB 23	RECEIVED
AUG 14 '81	DEC 11 '88	RECEIVED
DUE CAM FEB 21 '86		
FEB 21 '86	DEC 17	RECEIVED
JUN 19 '81	DEC 17	RECEIVED
APR 17 '81	JAN 28	RECEIVED
DUE CAM APR 30 '87	AUG 30 '90	RECEIVED
CARREL, LOAN	AUG 29	RECEIVED
JAN 22	OCT 23 '90	RECEIVED
DUE CAM	NOV 07 '90	
DUE CAM FEB 05 '87	OCT 30	RECEIVED
DUE CAM FEB 17 '87	FEB 25	RECEIVED
	MAR 27 1992	
FEB 12	MAR 19	RECEIVED
	APR 30 1993	

DATE DUE SLIP

JAN 29	RETUR
MAR 30	1993
MAR 29	RETURN
APR 20	1993
DEL 01	1993
DEC 05	RETURN

QE 462 K5 I62 1973
International Conference on
Kimberlites, University of Cape
Town, 1973.

0109999X SCI

